TECTONICS, SEDIMENTATION AND MAGMATISM OF THE CANTERBURY BASIN, NEW ZEALAND

by

ANDREA BARRIER

A dissertation submitted in partial fulfilment of the requirements for the Degree of DOCTOR OF PHILOSOPHY IN GEOLOGY

APRIL 2019

Table of Contents

List of figures

List of tables

Acknowledgements

I would like to thank the technician staff of the UC Geology Departments for their services and their constant good mood: Cathy, Chris, Sacha and Sarah, I am thankful for the help with field-gear preparation and the lab inductions. Matt and Anekant, thank for the help with drone acquisition at Cave Stream and Castlepoint. Thanks as well for showing me how to use a drone. Thanks to Rob, for the thin section preparation. A huge thanks to John Southward for the IT support you gave me during this PhD. Thanks a lot for your reactivity and enthusiasm when a problem was popping-up on my screen. I cannot remember an issue that you could not fix! Thanks a lot to Janet and Rebekah for all the help you gave me. I have asked many times for your assistance and you have always helped me with a lot of good mood.

I would like to thank Jonathan Davidson and Paul Ashwell for the two Glen's of Tekoa fieldtrips where I demonstrated, it was good fun and good geology! Thanks to Alex Nichols for all our discussions, staff club sessions and all the Westport fieldtrips we did, they were all great moments! Thanks to Catherine Reid for her support as head of the department and for the help I received when I was looking for outcrops to sample the Oamaru Limestone. Many thanks to Jarg Pettinga and his precious dusty-library and for our numerous discussions. Many thanks to John Bradshaw for sharing decades of expertise on Zealandia geology with me and always being open to discussions and giving your point of view on my research, I really appreciated that. Thanks to Harry Jol, a vising professor from the University Wisconsin Eau-Clair, for the interesting discussions on active sedimentary processes and for introducing me to GPR methods. I would like to thank the Mason Trust for all the funding that allowed me to attend numerous conferences and participate to numerous fieldtrips and fieldworks.

During this PhD thesis I have discussed with several geologist about New Zealand geology. They shared with me their knowledge and participated in building-up my understanding of Zealandia Geology. I would like to thank Carlos, Mac and Mark, for all the discussions that brought me knowledge about New Zealand petroleum industry. Thanks a lot to Jane Newman for all the help on measuring VR and VRF on my coal samples, for sharing your enormous knowledge on organic matter and for introducing me to Nova software. Unfortunately, I did not have enough time to finish this part of my PhD. I hope in the future to have time to finish working on this subject. Enormous thanks to Ewan Fordyce and Marcus Richards from the Otago University for sharing your knowledge of the local geology and paleontology of the North Otago and South Canterbury. The fieldtrip that you organised was a great opportunity for me to learn and see more about the Oligocene geology of the region. Thanks to Brad Field for helping me finding information on the Canterbury Basin geology in the early stage of my PhD. I would like to thank Andy Tulloch, for taking me inboard of his paper on south Zealandia basement and for the interesting discussions, we had on this subject. A huge thanks to Nick Mortimer for always showing interest and kindness in our discussions on Zealandia Geology. Thanks a lot for inviting me to Dunedin for a seminar at the Otago University and for the fieldtrip that followed where we explored the Otago basement lithologies. I would like to thank Steve Blank for our discussions on basement reflectors and the rift structure. Thanks to Jean-Michel Gaulier, with whom discussions about the Canterbury Basin geology sparked my thinking about under-filled rift basins. I huge thanks to Tusar Sahoo from GNS, for all the help you gave me and the numerous discussion we had during my PhD.

Huge thanks to Julien Bailleul, Frank Chanier, Pierre Malie, Geoffroy Mahieux and Barbara Claussman for taking me on board during three fieldwork missions in the East Coast Basin. It was amazing to be able to catch up with you on the other side of the world three times and to be able to learn about the East Coast sedimentology and tectonic.

Being in New Zealand, I was far away from many dear friends and geologist colleagues, but I have still managed to keep in touch with you, and I have succeeded in bothering you with many geology related questions. Thanks a lot to Antoine Auzemery for taking the time answering questions related to geodynamic, sandbox modelling and helping me with the use of G-Plate software. Thanks a lot Camille Martinez for taking the time to look at my data when I was working on basement reflectors. Thanks to Anta Sarr and Boris Gailleton for discussions about glacial processes when this subject crossed my mind for the Canterbury Basin. Huge thanks to Victorien for sharing your knowledge on quantitative seismic stratigraphy and the western Australian sedimentary basins and for the epic trip to the Cape Town Conference we both attended!

Big thanks to all my friends from France that came to visit me in New Zealand. Thanks Antoine, Alex, Flo, Pauline and Alexis for coming here, it was great to show you around and to feed you to the sand-flies!

Staying for more than three years in the same country also means that you get to see dear friends leaving to go back in their home country. A special thanks to Alexis, Thomas, Federico and Anthonin with whom I shared a year of great fun and crazy adventures! I have missed you guys after you all left!

I want to thank three students that helped me during my PhD project. First, Callum Cleary, that was supposed to help me with fieldwork to collect mudstone samples throughout the Canterbury Basin. We did one fieldwork in the Waipara River, then I got injured, and you had to do it on your own. You did a great job in running many porosity measurements and I am thankful for that. I want to thank Nicolas De Williencourt and Vincent Laville, two French trainees from UniLaSalle, which travelled to the other side of the world for a 3 months internship. You did a great job here and the data you produced helped me to have a clearer vision of some aspect of the geology of the basin. Thanks a lot!

Over these three years of PhD I have meet numerous other post-grad students here in the department with whom we shared friendship, good and bad moments of the PhD life, good times at the GSNZ conferences and a few beers the staff club/shilling club. Thanks to all of you! Special thanks to Elodie and Gilles for your presence in the department and the time spent with you outside from UC! A special thanks to Narges Kahjavi for the great interaction we had and for taking me into the field in the Hanmer Basin! Thanks to Mrinmoy, Rinze, Sam, Priscila and Gabriel, Marcos and Hanfei, students I have been sharing office with or who were working on similar stuff as me. We had good scientific and social interactions, it was great to work by your sides!

Big thanks to you Cassandre for all our moments traveling, hiking, tramping around New Zealand! You have managed to find a job in Kaikoura 200 km from where I lived, quite unbelievable! Thanks as well to Marion and Freddy who arrived at the same time as Cass and tagged along to most of our adventures.

Soon after arriving in New Zealand, I met five people that I will remember for a long time. Alan, my workmate with whom I shared various offices for nearly 3 years. Thanks for all the great discussions and great moments we had and thanks for pushing me into looking at volcanoes in seismic reflection. This PhD would not have been the same without you! Astrid and Gabby, you are amongst the first persons I have met in New Zealand and I will always be grateful for all the moment we have spent together in and outside UC. Elizabeth and Stan, with you I discovered most of New Zealand's outdoor, we crossed a many saddles, reached a several summits and had a lot of fun together. It was great to spend few years with both of you, and I know that we will meet again somewhere!

I want to thank my family both in France and Italy for their constant support despite the long distance that was separating us and for the numerous parcels containing French and Italian goods you sent me.

I took the decision to travel 19 000 km and spend more than three years in Christchurch to do my PhD but despite the distance (hard to be further away from each other) you have always supported me. Thanks to you my beloved Mylene, for supporting me and for joining me in New Zealand for the last 6 months of my PhD.

Finally, I would like to thank my PhD supervisory team Kari Bassett, Greg Browne and Andy Nicol for their valuable support and guidance over these past three years. Kari, thanks for your constant enthusiasm during our numerous discussions after which I would always leave with numerous new ideas in mind. Thanks as well for the several fieldtrips on the West Coast, it was great to learn about the geology of another sedimentary basin. Greg, thanks for sharing your knowledge on the Canterbury Basin and Zealandia geology. Your enlightened opinion and dedication meant a lot to me. I am grateful for the time spent with you on the field, too bad I have not had the chance to do a fieldtrip in the Taranaki Basin with you! Finally, an enormous thanks to Andy, I have learnt a huge amount by working with you. You have always encouraged me to take initiatives, to attend conferences, fieldtrips and fieldworks. You gave me a lot of autonomy but have always step-forward to bring a valuable contribution and your wisdom to this PhD project. I believe Geology is about transmitting knowledge and skills to others and I believe the three of you did a great job!

Abstract

This PhD investigates the tectonics, sedimentation and magmatism of the Canterbury Basin. Unlike the emergent part of Zealandia continent, the offshore Canterbury Basin has not been deformed by Cenozoic plate boundary movements and represents a rare opportunity to conduct detailed analysis of the mid- Cretaceous rifting (~110 Ma to ~85 Ma) and the Late Cretaceous to Paleogene drift sequences. The results help improve understanding of the regional processes that led to the breakup of eastern Gondwana and the far-field effects of Cenozoic plate boundary deformation.

The Canterbury Basin initiated in the mid-Cretaceous (~110 Ma) as a rift system. Syn-rift sedimentation was characterised by under-filled depocenters, where early syn-rift sedimentation was dominated by short drainage systems sourced from within the basin to produce alluvial fans along fault scarps inter-fingered with axial braided river or lake deposits. The predominance of local drainage systems coupled with a low supply of sediment into the Canterbury Basin during the Late Cretaceous may partly account for the under-filling of rift depocenters. Post rift latest Cretaceous and Paleogene, pelagic sediments draped and buried most of the earlier-formed horsts, with complete burial being achieved ~60 Myr after the onset of faulting. Despite filling of the rift structures, many of the geomorphological features of the contemporary Canterbury Basin were also present in the Late Cretaceous including, the Chatham Rise and the topographic hinterland west of the basin. The timing of the Cretaceous-Paleogene marine transgression and the degree of preservation of rift structures in the Canterbury Basin, differs from that in northern Zealandia (e.g., Taranaki Basin). These differences may reflect the relative tectonic quiescence in the offshore Canterbury Basin post ~85 Ma and the ongoing influence of subduction beneath northern Zealandia in the Late Cretaceous and Eocene.

A total of 346 faults were analysed, with maximum displacements ranging from <0.1 to 2.8 seconds two way time. Results of the structural interpretation of the rifting show that the Canterbury Basin was stretched in three directions forming three sets of synchronous normal faults. The parallelism the three sets of rift faults and future spreading centres suggests that the multi-directional extension in the Canterbury Basin records the early stages of Gondwana breakup. The plate tectonic forces responsible for Gondwana breakup probably commenced soon after the cessation of subduction (e.g., < 5 Myr), and ~20 Myr before breakup. With the onset of breakup extension was focused along the spreading centres and multi-directional stretching of Zealandia ceased or continued at much diminished rates.

The geometries of rift fill in seismic reflection lines has been quantified using the ratio of syn-rift strata thickness to syn-rift fault throw (here referred to as the Sediment Fill Ratio - SFR). Measurements from seven sedimentary basins globally (including the Canterbury Basin), permits recognition of four types of rift basins: (1) starved ($SFR \leq 0.2$), (2) under-filled ($0.2 < SFR \leq 0.9$), (3) balanced-filled ($0.9 < SFR \leq 1.1$), and (4) over-filled ($SFR > 1.1$). The degree of syn-rift basin fill at the cessation of faulting varies with fault size across the same basin and between different rift basins for the same fault size. Small faults are more often characterized by balanced or over-filled geometries because they have low displacement rates and are located in the hangingwall of larger faults (e.g., >1 seconds TwT throw) where sedimentation rates are locally high. Rift systems dominated by large faults, such as the Canterbury Basin, tend to be under-filled, and require sediment supply from outside the rift system to become over-filled.

The offshore Canterbury Basin provides a new perspective on Early Oligocene erosion that occurred between 29 and 32 Ma throughout the basin. Seismic reflection data permits mapping of erosive channels that incised the shelf and slope of the Canterbury Basin during

the Early Oligocene. Similar channels are inferred onshore and offer an explanation for thickness variations of Oligocene limestones at a time when the rates of deformation were inferred to be low. Channelisation initiated due to a sea-level fall associated with uplift west of the Canterbury Basin that potentially reflects the onset of Cenozoic plate boundary deformation. The drainage system set-up during the Early Oligocene displays similar trends to the present day hydrographic pattern, which suggests that the first-order topographic elements of the eastern South Island may be 30 Myr in age or older.

Seismic reflection data in the offshore Canterbury Basin has enabled us to identify 185 buried magmatic structures, some of which were previously unknown, ranging in age from mid-Cretaceous to Pleistocene. Buried volcanic edifices of <1 to 20 km diameter have been mapped and are grouped into five geomorphological and chronological categories. 1. Monogenetic to polygenetic volcanoes up to 5 km diameter within the Cretaceous syn-rift succession. 2. Large volcanic complexes with diameters >10 km within the post-breakup Late Cretaceous succession. 3. Monogenetic to polygenetic volcanoes of Paleocene to Middle Miocene age. 4. Large Miocene composite volcanoes of >10 km diameter formed in association with present-day Banks and Otago peninsulas. 5. Eruptive centers along the Chatham Rise that erupted during the Late Neogene. The continuous volcanic activity of the Canterbury Basin from the Late Cretaceous rifting to the Late Neogene was accompanied by widespread sill intrusion but did not resolve batholiths or plutons which, if present, are at depths of >10 km depth. This study increases the total known surface area of volcanoes in the Canterbury Basin by 300%, and suggests that across Zealandia, more volcanoes can be expected to exist of varying ages.

CHAPTER 1) Introduction

This PhD thesis examines the tectonic, sedimentological, paleogeographic and magmatic evolution of the Canterbury Basin from its inception in the mid-Cretaceous (~110 Ma) to the formation of the present plate boundary in the Miocene. The results have implications for the geological history of the basin and the wider Zealandia region **(Mortimer, 2017)**. The Canterbury Basin lies on the East Coast of the South Island, New Zealand, outside the main zone of Cenozoic plate-boundary deformation (Figs 1.1 and 1.2, **Field and Browne, 1989)**. In the offshore basin the low tectonic Cenozoic strains, the almost continuous sedimentation since the mid-Cretaceous, the thick basin succession (~3-8 km) and the extensive seismic reflection dataset provide a high quality record of the basin history.

The present study builds on the results of many previous publications, both on the Canterbury Basin and the Zealandia region. The literature highlight a long and tectonically complex basin history commencing with long-lived subduction from the Permian to the Early Cretaceous along the eastern Gondwana margin (Laird, 1993; Laird and Bradshaw, 2004; Mortimer *et al.*, 2014). Subduction was largely responsible for the configuration of basement terranes which underpin much of New Zealand's geology. During the mid-Cretaceous, contraction gave way to extension which affected much of Zealandia (Fig. 1.2). The phase of widespread stretching created several rift basins immediately prior to Gondwana breakup. From the breakup of the Gondwana continental crust at about 83 Ma, Zealandia started to drift away from Antarctica and Australia.

Cretaceous rifting initiated the formation of nineteen sedimentary basins throughout Zealandia (King *et al*, 1999). The strata in these sedimentary basins records the rifting event and the post-rift tectono-sedimentary evolution of Zealandia, which is key to understanding better the history of past geological events (Figs. 1.3 and 1.4). Some of these sedimentary basins were deformed and eroded during the Late Eocene to Early Miocene and younger formation of the present plate boundary (Figs. 1.2 and 1.3 - King *et al.*, 1999), making it difficult to unravel the earlier geological history. The onshore Canterbury Basin experienced tectonic deformation during the Cenozoic (Fig. 1.2), however, the intensity of deformation decreases towards the east, with offshore parts of the basin neither experiencing significant contractional or strike slip deformation during the Cenozoic (Field and Browne, 1989). Offshore Canterbury Basin therefore represents an opportunity to observe un-deformed Late Mesozoic to Cenozoic strata that illuminate some of the uncertainties of the Zealandia rift to drift evolution.

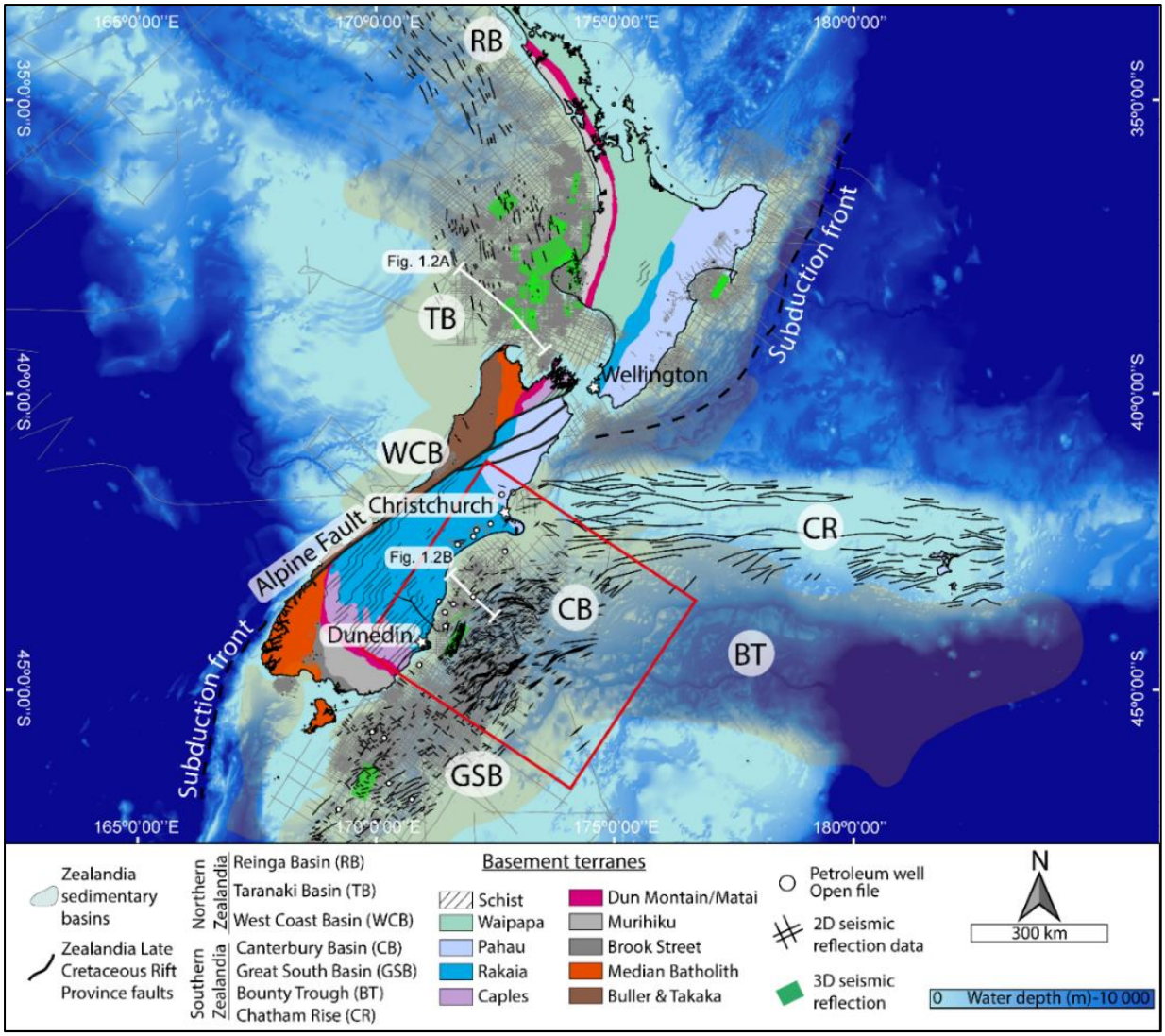

Figure.1.1 Present-day map of Zealandia showing rift structures and basement terranes adapted from Mortimer (2004), Arnot & Bland (2016) and Sahoo & Bland (2017). Red square indicates the field area, while the Alpine fault and subduction thrusts represent the main Cenozoic plate boundary

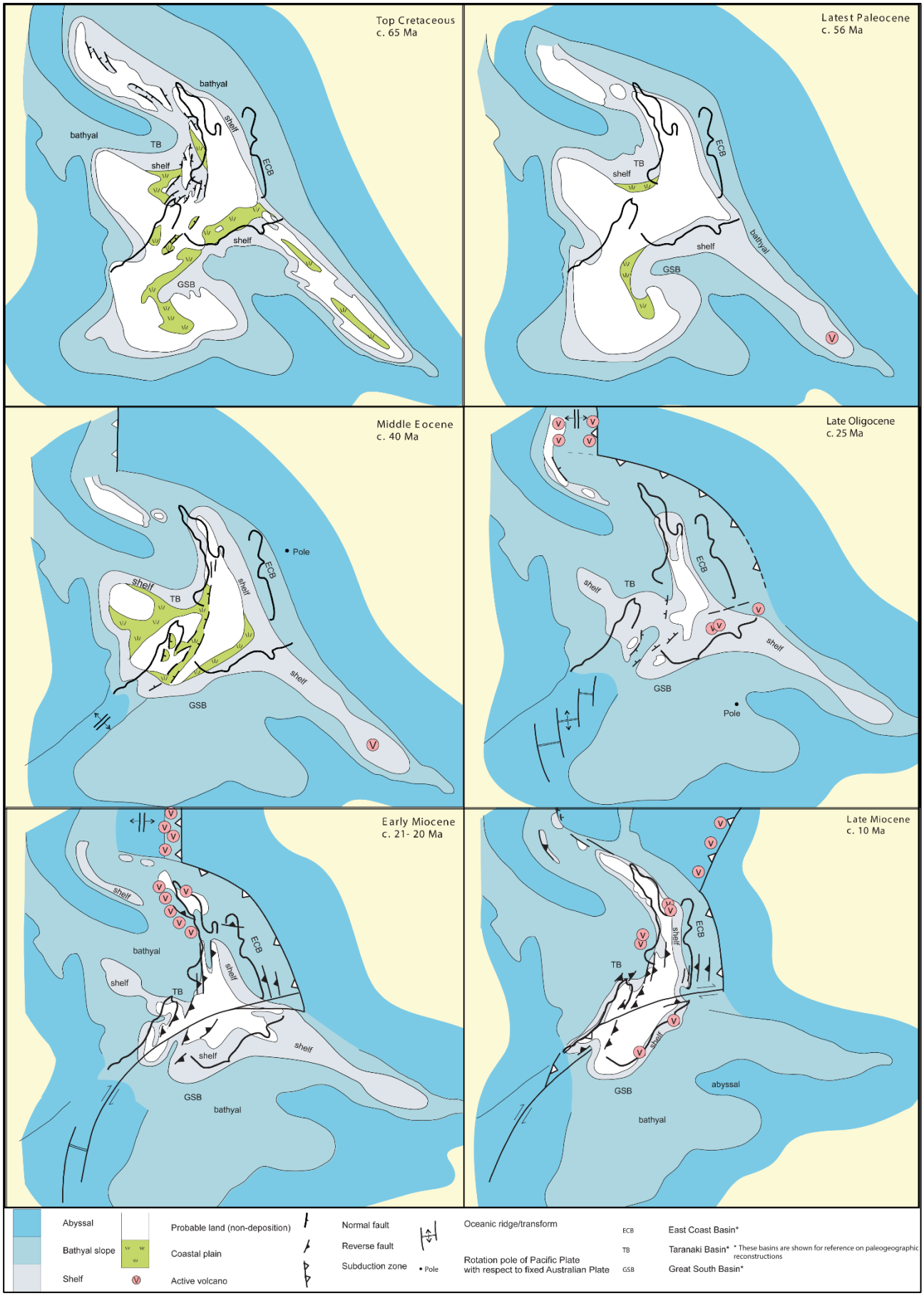

Figure 1.2 Zealandia Geological palaeographic and geodynamic evolution after King et al., 1999

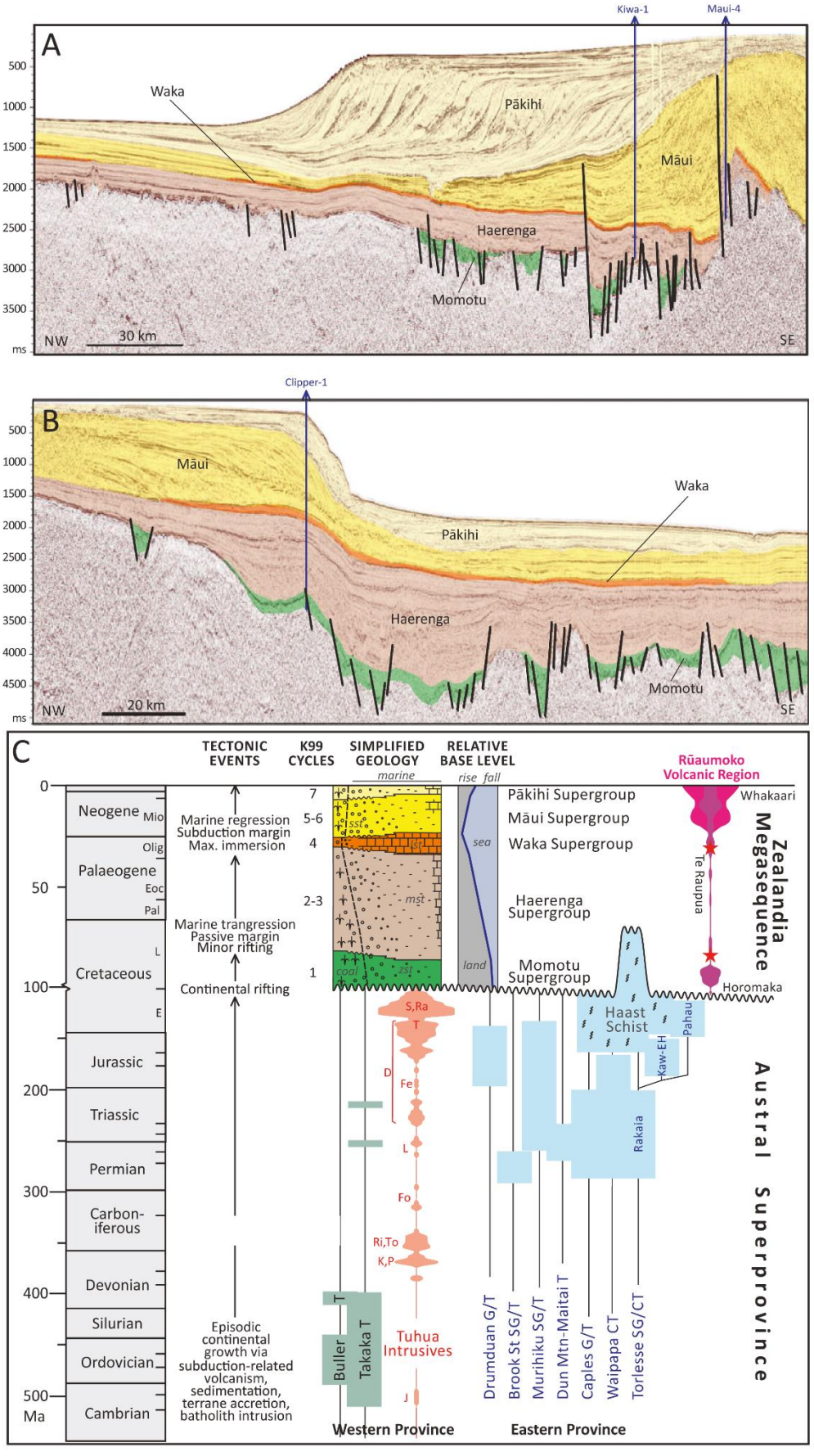

Figure 1.3 Seismic reflection profiles across the (A) Taranaki Basin, (B) Canterbury Basin and (C) Megasequence chart of Zealandia (Mortimer et al., 2014). See Figure 1.1 for seismic profiles location.

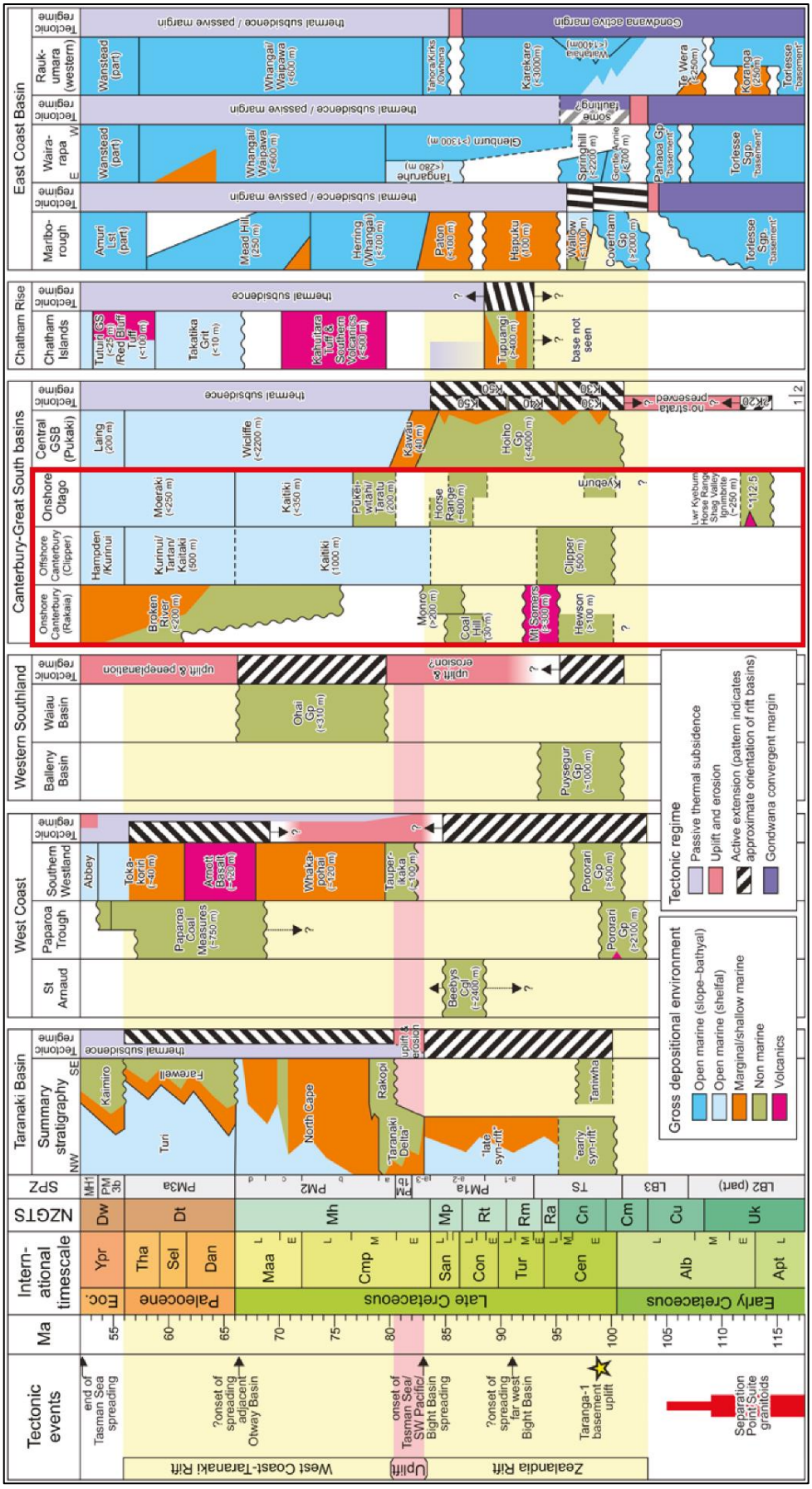

Figure 1.4 Stratigraphic chart of Zealandia Late Cretaceous rift basins (Strogen et al., 2017). The red square indicates the present study area.

I.1. Questions and Aims of The PhD Project

Although the rift evolution of the Canterbury Basin has been studied for more than four decades (Field and Browne, 1989; Browne *et al.*, 2012; Jongens *et al.*, 2012; Sahoo *et al.*, 2014, 2015; Shoup and Cozens, 2015, Higgs *et al.*, 2019), no recent work has integrated data from open file petroleum industry seismic reflection lines and exploration wells to constrain the rift and post-rift structural evolution of the basin and its impact on the sediment fill. In this PhD we utilise these data to address five main questions, with each the focus of a thesis chapter. These questions are:

(1) What information does the Late Cretaceous-Eocene sedimentary fill of the Canterbury Basin provide on the tectonic and paleogeographic evolution of the basin and its surrounding landmass (Chapter 2)?

(2) What processes controlled the multi-directional stretching of the Canterbury Basin (Chapter 3)?

(3) How to quantify syn-rift sediment fill in rift basins after rift cessation (Chapter 4)?

(4) What mechanisms triggered Early Oligocene channels incision of the Canterbury Basin shelf and slope (Chapter 5)?

(5) What was the evolution of the magmatic activity in the offshore Canterbury Basin (Chapter 6)?

This PhD research project has adopted a multi-disciplinary approach, combining seismic reflection lines, exploration and scientific wells, outcrop, tectonic, sedimentology, volcanology, structural, seismic geomorphology and seismic facies analysis to constrain the structure, sedimentology and volcanism of the Canterbury Basin. The new structural and sedimentological research in this thesis provides the following outputs: 1) a seismic facies analysis of the Late Cretaceous to Eocene seismic reflector package to assess the sediment distribution across the Canterbury Basin and improved understanding of the evolution of Zealandia landmass (Chapter 2), 2) new isochron structural maps for several key intervals from the Late Cretaceous to the Eocene that add details to our understanding of the geometry, kinematics, timing and plate boundary origin of the rift system (Chapter 3), 3) a new method for quantifying syn-rift basin sediment fill by calculating the ratio between vertical fault displacement and syn-rift depocenter thickness (Chapter 4), 4) a new paleogeographic reconstruction of the Early Oligocene of the Canterbury Basin integrating onshore-offshore data to propose a mechanism for the formation of Early Oligocene erosive channels affecting the shelf and slope of the Canterbury Basin (Chapter 5), and 5) maps of magmatic occurrences in the onshore and offshore Canterbury Basin (Chapter 6).

1.2. Tectonic History of The Canterbury Basin

The chapters and their associated geological questions straddle different time periods of the Canterbury Basin geological history from the Mid Cretaceous (~110 Ma) to the Miocene (~20 Ma). Over this period of time, Zealandia and the Canterbury Basin experienced four main phases of tectonic deformation which are summarized below:

1.2.1 Phase 1: Eastern Gondwana Subduction

New Zealand's basement rocks formed during the accretion of an arc-trench system related to the subduction of the oceanic crust beneath eastern Gondwana from the Permian to Early Cretaceous (McKinnon, 1984; Coney *et al.*, 1990; Floettmanet *et al.*, 1993; Mortimer 2004; Mortimer *et al.*, 2014). Basement rocks record the complex geological evolution of continuous accretion with terranes of variable thicknesses and origin.

The cessation of the subduction system has been proposed to have started along Chatham Rise at around 105 Ma, following Zealandia's collision with the Hikurangi Plateau (Laird and Bradshaw, 2004; Davy, 2014). Recent evidence suggests that the plateau partially subducted beneath the Chatham Rise and the South Island (Reyners *et al.*, 2017). Mesozoic subduction west of the present day Alpine Fault has also been inferred from the Pounamu Terrane, which is located in the Southern Alps and forms enigmatic turbiditic metasediments deposited over an oceanic floor (Cooper and Ireland, 2015; Cooper *et al.*, 2018; Cooper and Palin, 2018). Subduction associated with accretion of the Pounamu Terrane may have been active until at least 80 Ma, however, the timing of the end of Gondwana subduction system beneath New Zealand and its extent remain controversial.

Basement rocks in the Canterbury Basin mainly belong to the Torlesse Composite Terrane which represents the accretionary prism of Gondwana subduction system (Fig., 1.1 - MacKinmon, 1984; Mortimer, 2004; Mortimer *et al.*, 2014). The Torlesse Composite Terrane can be divided into three terranes, the Caples, Rakaia and Pahau terranes, and the exhumed prism represented by the Otago Schists. The Torlesse Composite Terrane facies comprises meta-sediments, pumpellyites meta-arkoses and argillites. Rare coal rich units are also present in this basement terrane (e.g. Wakaepa Formation and Clent Hill Group) (Oliver and Keene, 1989; Rattenbury *et al.*, 2006; Forsyth *et al.*, 2008). Localized and poorly understood basement igneous rocks, including gabbro and granitoids, have been found in offshore wells (Sahoo *et al.*, 2015; Blanke, 2015; Higgs *et al.*, 2019). Generally, the Caples, Rakaia and Pahau terranes beneath the Canterbury Basin have been subject to low grade metamorphism of zeolite to phrenite/pumpellyite facies (Mortimer, 2004). The part of the prism comprising Caples and Rakaia terranes was metamorphosed to pumpellyite-actinolite and was already partially exhumed by around 110 Ma (Mortimer, 2004). The maximum degree of metamorphism of the Torlesse Terrane is observed within the Southern Alps immediately east of the Alpine Fault and west of the Canterbury Basin, where these rocks reached amphibolite facies (Mortimer, 2004). In summary, the basement of the Canterbury Basin comprises metasediments of the Torlesse Composite Terrane formed during Gondwana accretion with a complex structural fabric controlled by contractional tectonics and a diverse petrology.

In this PhD thesis, several questions relating to the basement geology of the Canterbury Basin are raised and answered:

- Did the basement lithology and structure influence syn- to post-rift tectonic and sedimentation? (Chapter 2-3)
- When did subduction below Gondwana cease and was it ever synchronous with the onset of rifting? (Chapter 2-3)
- What are the lithologies, geometries and extent of the basement rocks in the offshore Canterbury Basin? (Chapter 3)

1.2.2 Phase 2: Rifting and Eastern Gondwana Breakup

A widespread rift province across Zealandia records extension prior to, and during, eastern Gondwana breakup during the mid-Cretaceous. The mid-Cretaceous period does not correspond to an official term of the international geological timescale, however it is often used in New Zealand geology and refers to the end of the Early Cretaceous to the beginning of the Late Cretaceous (~110 to ~83 Ma) (e.g., Crampton et al., 2004). According to previous authors, the onset of rifting varies from 114 ±2 Ma to 105 Ma (Fig. 1.2- Tulloch et al., 2009; Adams et al., 2017; Strogen et al., 2017). This spread in the age of the onset of rifting can be explained by the different dating methods used (and their uncertainties) and the variety of rocks dated. Palynology ages for syn-rift sediments do not come from the deepest part of rift depocenters where the strata are the oldest (Fig. 1.4 - Strogen et al., 2017 and references therein). Detrital zircon U-Pb ages for silicic tuff horizons suggest that the oldest ages for the rift sequence are 112.5±0.2 to 114±2 Ma but these dates may also not be sampled from the deepest parts of the basin (Fig. 1.4 - Tulloch et al., 2009; Adams et al., 2017). However, it is not clear whether the tuff beds were deposited within, or below, syn-rift growth strata and the timing of faulting relative to formation of the tuff is equivocal (Bishop et al., 1976; Mitchell et al., 2009). The dating of the rapid cooling of metamorphic rocks within metamorphic core complexes return ages of 92 to 89 Ma depending on their location (Spell et al., 2000; Kula et al., 2007), but represent ages for deep processes and may not record the age of rifting at the surface. In the Canterbury Basin, information from mid-Cretaceous outcrops onshore provide little information about the time of rifting due to widespread erosion.

Seismic reflection data allows continuous imaging of rift structures and their infill in the offshore Canterbury Basin (Fig. 1.3). Fault patterns during the middle to Late Cretaceous rifting suggest at least three different structural domains (Field and Browne, 1989; Jongens *et al.*, 2012; Sahoo *et al.*, 2014). These are; the North Otago domain with NW-SE striking faults, the Clipper domain with NE-SW faults and the Chatham Rise domain with E-W faults. Onshore rift fault geometry is poorly constrained due to the tectonic overprint of Miocene-Recent deformation and to the poor preservation of mid-Cretaceous syn-rift outcrops. Nevertheless, some outcrops and onshore seismic reflection profiles show evidence of NE-SW and E-W rift faults during the Late Cretaceous (Nicol, 1993; Browne *et al.* 2012; Jongens *et al.*, 2012).

Syn-rift deposits in the Canterbury Basin include an up-ward fining non-marine succession comprising alluvial fan to fluvial plain conglomerate, sandstone, siltstone, mudstone and coal that developed in rift half-grabens, overlain by a marine transgression (Figs. 1.3, 1.4 and 1.5 - Browne and Field, 1985; Field and Browne, 1986, 1989; Andrew *et al*., 1987; Browne, 2003; Mitchell *et al.*, 2009). These strata are contained in 500-6000 m thick fault-controlled depocenters in the following locations: Kyeburn, Horse Range, Hewson, Mid Waipara and Clipper (Fig. 1.4 - Bishop *et al.*, 1976; Field and Browne, 1989; Nicol, 1993). During mid-Cretaceous extension, the Canterbury Basin experienced volcanic activity (Mount Somers Volcanic Group, Adams and Oliver, 1979; Oliver, 1984; Barley, 1988; Smith and Cole, 1997; Tappenden, 2003; Van der Meer *et al.*, 2017). The geochemistry of the Mount Somers Volcanic Group suggests subduction influenced volcanism (Van der Meer *et al.*, 2017). Such volcanic activity could also have extended offshore.

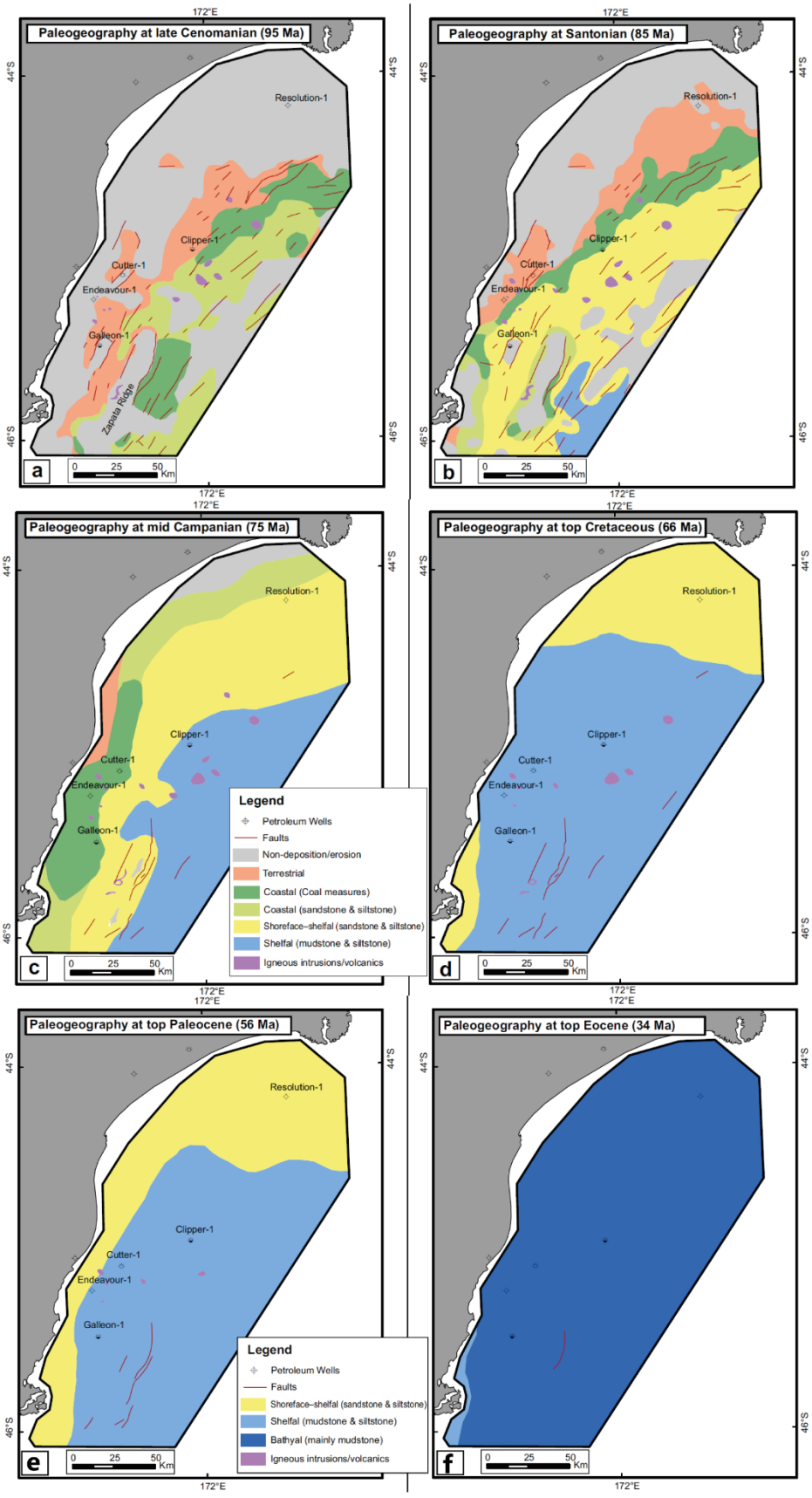

Figure 1.5 Paleogeographic reconstruction of the Canterbury Basin for (a) Late Cenomanian (95 Ma); (b) Santonian (85 Ma), (c) Mid-Campanian (75 Ma); (d) top Cretaceous (66 Ma); (e) Paleocene (56 Ma); (f) Eocene (34 Ma) (Sahoo et al., 2015).

This PhD thesis addresses several questions that relate to the rifting of the Canterbury Basin and its syn-rift sedimentary fill to understand better the geological evolution of Zealandia immediately prior to Gondwana breakup:

- When did rifting start? (Chapter 2)
- What was the sediment fill in the Canterbury Basin during the rifting? (Chapter 2 and 4)
- Why are there different orientations of rift faults in the Canterbury Basin? (Chapter 3)
- Are the different sets of rift faults coeval or did they form at different times? (Chapter 3)
- Was the displacement along rift faults purely dip-slip or did some faults accommodate a component of strike-slip? (Chapter 3)
- What was the mechanism driving extension of the Canterbury Basin and did this mechanism operate across the rest of Zealandia Late Cretaceous Rift Province? (Chapter 3)
- Was there any volcanic activity in offshore parts of the basin analogous with the volcanic rocks in the onshore basin? (Chapter 6)

I also answer more generic and process related questions, including:

- How can we quantify syn-rift basin sediment fill? (Chapter 4)
- What processes can lead to the under filling of a rift basin? (Chapter 2-4)
- What mechanisms can result in the formation of multiple sets of coeval rift faults during continental breakup? (Chapter 3)

1.2.3 Phase 3: Zealandia Drifting

From around 83 Ma, the Canterbury Basin entered a tectonically quiescence phase dominated by thermal and load subsidence and the infill of the paleo-rift topography during a second order marine transgression (Field and Browne, 1989). The drift phase commenced with the breakup of eastern Gondwana along the Australian-North Zealandia and the Western Antarctica-South Zealandia ridges. The localisation of extension relocated to the newly formed spreading centres (Fig. 1.2).

The latest Late Cretaceous to Eocene is generally considered to represent a post-rift quiescence during which small normal fault displacements (<50 m) occurred on some faults in the Canterbury Basin (Field and Browne, 1989). Sedimentation records a second order marine transgression during this post-rift stage. The depositional environments range from fluvial to tidally influenced paralic to upper bathyal water depth (Field and Browne, 1989; Sahoo *et al.*, 2015) with the coast line moving westward with time as the Zealandia landmass submerged (Figs. 1.2, 1.4 and 1.5 - Field and Browne, 1989).

During the Oligocene, the Canterbury Basin strata were dominated by carbonate deposits (like many basins in Zealandia) corresponding to the time of maximum flooding in the Canterbury Basin (Figs. 1.2, 1.4 and 1.5 - King *et al.*, 1999). Today, Early Oligocene limestone Amuri Limestone displays an important thickness variability. At some locations, the stratigraphic successions display a complete erosion of the Amuri Limestone while in others, it is overlain by an Early Oligocene erosional surface namely the Marshall Unconformity (Carter and Landis, 1972; Finlay, 1980; Carter *et al.*, 1982; Field, 1985; Lewis *et al.*, 1992;

Fulthorpe, 1996; Lever, 2007). This unconformity represents one of the most controversial and enigmatic stratigraphic features of New Zealand geology. Offshore, it is suggested that erosive channels incised the top of the Eocene-Oligocene interval (Sahoo *et al.*, 2015).

Despite a quiescence tectonic phase, volcanic activity was still present in the Canterbury Basin from the Late Cretaceous to the Oligocene as suggested by the numerous outcrops onshore. Widespread volcanic activity extends offshore were magmatic activity has been described (BP Shell Todd, 1984; Blanke, 2013).

The structural and sedimentological analysis in this PhD thesis identifies new elements of the post-rift Late Cretaceous-Eocene infilling of the paleo-rift structures as well as the Oligocene paleogeographic evolution of the Canterbury Basin and its magmatic occurrences. The data and analysis in this thesis contribute to addressing questions about the Canterbury Basin and Zealandia post-rift Late Cretaceous to Oligocene drift phase of basin evolution. These questions are:

- What was the evolution of the sediment fill in the Canterbury Basin after cessation of rifting? (Chapter 2)
- What triggered the increase in sedimentation rate in the Canterbury Basin during the Eocene? (Chapter 2)
- Did Zealandia rift basins have a similar Late Cretaceous syn- to post-rift evolution? (Chapter 2)
- What was the evolution of Zealandia landmass during the Late Cretaceous-Eocene? (Chapter 2)
- Why is the onshore Oligocene post-rift sedimentation so discontinuous? (Chapter 5)
- What do the Early Oligocene erosive channels indicate about Zealandia landmass evolution? (Chapter 5)
- How similar are Late Cretaceous-Oligocene paleo-channels and Recent channel and what does this tell us about the age of the first-order Zealandia landforms (Chapter 2 and 5)?
- How much volcanic activity occurred in the offshore Canterbury Basin and what processes produced it (Chapter 6)?

1.2.4 Phase 4: Formation of The Present-day Plate Boundary

Contractional deformation affected onshore parts of the Canterbury Basin, from the Miocene onwards, and records the development of the Cenozoic plate boundary (e.g., Alpine Fault and the associated uplift) through the South Island. New faults formed with northeast strikes and pre-existing faults were inverted or reactivated with strike-slip movement (Fig. 1.2 - Field and Browne, 1989; King *et al.*, 1999). Uplift in the central South Island resulted in increased erosion and large volumes of sediments were deposited in offshore Canterbury Basin during the Neogene-Quaternary (Wellman, 1979; Browne and Naish, 2003; Marsaglia *et al.*, 2017). In the Canterbury Basin, a rejuvenation of the volcanic activity occurred during the Miocene with two main eruptive centres that persist in the present-day landscape: Banks and Otago peninsulas (e.g., Coombs *et al.*, 1986; Field and Browne, 1989; Hampton and Cole, 2009). Offshore, the sedimentary record of Miocene uplift has been presented in Lu *et al* (2003) and Lu and Fulthorpe (2004) but does not integrate the most recent seismic reflection data.

In this thesis I examine only the Miocene to Recent volcanic occurrences in offshore Canterbury Basin to finish the topic of post-rift volcanic activity. I address the following question:

- Was the Canterbury Basin Miocene volcanic activity mostly centred around Banks and Otago peninsulas or was it more widespread? (Chapter 6)

1.3. Previous Work and Thesis Scientific Contribution

Even though the Canterbury Basin is not a mature petroleum basin, many aspects of its geology such as structural, sedimentology, and volcanology have been studied for several decades by numerous geologists from New Zealand and overseas. This PhD builds on the work published over the previous decades. We have summarized in **Table 1.1** the previous work that have most influenced research in this PhD**.**

Table 1.1 Table summarizing the main authors that have influenced this PhD research project.

Authors	Year	Main topic
Browne and Field	1985	Stratigraphy of North Canterbury region
Field and Browne	1986	Stratigraphy of South Canterbury region
Andrew et al.	1987	Stratigraphy of Central Canterbury region
Field and Browne	1989	Summary of the stratigraphy, paleoenvironment and structural evolution of the Canterbury Basin
Schioler and Raine et al.	2011	Well biostratigraphy constraining top horizon for seismic interpretation
Sahoo & Bland	2017	Isochron and paleoenviroment maps of the Canterbury Basin
Strogen et al.	2017	Geodynamic reconstructions of Zealandia Rift phase
Tulloch et al	2009	U-Pb dating of syn-rift sequence
Adams et al	2017	U-Pb dating of syn-rift sequence
Cooper and Ireland	2015	Pounamu Terrane
Cooper et al	2018	Pounamu Terrane
Cooper and Palin	2018	Pounamu Terrane
Mortimer	2004	Basement terranes
Mortimer et al	2014	High Level stratigraphic scheme of New Zealand
Lever	2007	Regional analysis of the Marshall Unconformity across the South Island

By investigating the most recent seismic reflection data and combining it with previous research, the PhD complements the geological knowledge of the Canterbury Basin. It assesses the tectonic, sedimentary and magmatic evolution of the Canterbury Basin during both rift and post-rift periods. At a larger scale it is helpful for paleogeographic and geodynamic reconstruction of Zealandia from the Late Cretaceous to the Oligocene.

1.4. Data and Methods

The Oil and Gas Industry in New Zealand played a major role in understanding the geological evolution of Zealandia. Since the beginning of the 20th century, the Oil and Gas Industry acquired numerous seismic reflection surveys, drilled exploration wells, and compiled numerous geological reports unlocking sub-surface geometries and improving our knowledge of Zealandia geological evolution (e.g. BP, Shell, Todd, 1984; ExxonMobil, 2010; Constable and Kirk, 2010; Beckman, 2012; Blanke, 2013, 2015; Plampton, 2018). New Zealand Petroleum and Mineral (NZPM), a branch of the Ministry of Business, Innovation and Employment, has been building up a petroleum exploration data base since the mid-20th (https://www.nzpam.govt.nz/maps-geoscience/exploration-database/). More recently, they compiled petroleum exploration data packs that feature open file seismic and well data with interpretation projects and technical reports (https://www.nzpam.govt.nz/maps-geoscience/petroleum-datapack/). The data packs contain 24 000 km^2 of 3D seismic data and 4 750 000 line kilometre of 2D seismic lines tied to over 1044 wells. These data represent a unique resource with which to study New Zealand sedimentary basins in detail.

This PhD research project primarily used petroleum industry data to conduct a detailed seismic interpretation of the Canterbury Basin. I have utilised ~26 000 line kilometre of open-file 2D seismic reflection lines and one 3D seismic reflection survey provided by NZPM (for details see https://data.nzpam.govt.nz) issued as part of the New Zealand Government 2015 to 2018 Data Packs. Seismic data quality and coverage is variable, with seismic surveys acquired between 1966 and 2014. Most coverage comes from nearshore with fewer lines available towards the east. The data acquired post-2006 and the older data reprocessed post-2006 have a quality that ranges from good to very good. Seismic data pre-2006 that has not been re-processed is usually of poor to medium quality. Seismic data has been tied to five petroleum exploration wells in the Canterbury Basin and to the most recent biostratigraphic ages established for those wells (Schiøler and Raine, 2011). From the wells, six horizons have been interpreted according to the GNS Science "K" and "P" seismic horizon naming convention (Table 1.2- Strogen and King, 2014).

Table 1.2 Table summarizing the horizon nomenclature used in this PhD thesis.

Color code	Horizon Name	GNS Science nomenclature (Strogen & King, 2014)	Age (Ma)	NZ Stage	International Stage	Horizon mapped
	Sea Bed	seabed	0	Recent	Recent	yes
	Top Pliocene	N70	2.4	Mangapanian	Piacenzian	no
	Top Late Miocene	N60	5.3	Kapitean	Messinian	no
	Top Middle Miocene	N40	11.6	Waiauan	Serravallian	no
	Top Lower Miocene	N30	16	Altonian	Burdigalian	no
	Top Oligocene	N00	23	Waitakian	Chattian	no
	Top Eocene	P50	34	Runangan	Priabonian	yes
	Top Paleocene	P10	56	Teurian	Thanetian	yes
	Top Late Cretaceous post-rift	P00	66	upper Haumurian	Maastrichtian	yes
	Intra Late Cretaceous post-rift	K90	78	lower Haumurian	intra Campanian	yes
	Top Late Cretaceous syn-rift	K80	84.5±1.5	Piripuan	Santonian	yes
	Top Basement	basement	110±5	Urutawan to Korangan	Aptian-Albian	yes

The seismic interpretation was completed using Kingdom Suite software. Maps were generated from numerous raster and shape file data using ArcGis software. Geological data was sourced from © GNS Science 2014, topographic data from LINZ Data Service, and bathymetric data was licensed under NIWA Open Data Licence v1.0.v.

I have used different techniques to address the different aspects of the research project:

Chapter 2 uses seismic facies analysis and mapping of sedimentary geometries to understand the Late Cretaceous to Eocene evolution of the distribution of sediments across the offshore Canterbury Basin. The results were combined with information from the literature to propose an explanation for the under-filling of the Canterbury Basin and to analyse the evolution of Zealandia landmass from the Late Cretaceous to the Eocene.

Chapter 3 combines the structural interpretation with the key horizon isochron grids to generate structural maps. Fault throws and lengths have been measured for different key horizons and stored in an ArcGis database. I then exported the data to generate graphs to analyse rift fault kinematics. The maps and observations were finally combined with the literature to reconstruct the position of the Canterbury Basin within the Eastern Gondwana margin during the Late Cretaceous rifting period and propose a new model to explain the breakup of eastern Gondwana.

The chapter 4 uses the top basement and top syn-rift (K80) as the primary horizons (Table 1.2). For each set of rift faults intersecting a seismic profile, two values were measured in second TwT, (1) the rift fault throw and (2) the depocenter thickness adjacent to corresponding rift fault. These data were then stored in an ArcGis project and exported into Excel spreadsheets to generate graphs. The results from the Canterbury Basin was then compared to data from other rift basins where pre- syn- and post-rift sequences were clearly identified.

Chapter 5 focuses on the Oligocene. Offshore, the top Eocene horizon (P50) was used to track the Early Oligocene erosion that formed numerous erosive channels. Onshore over 110 measured stratigraphic sections were used in order to map complete or partial erosion of Early Oligocene limestones. These stratigraphic sections were sourced from work done by GNS Science in the late 1980's (Browne and Field, 1985; Field and Browne, 1986; Andrew *et al.*, 1987; Field and Browne, 1989), sections reviewed by Fulthorpe *et al.*, (1996), Lever (2007), Fordyce *et al.* (2009) and Fordyce and Richards (2016) and from onshore petroleum exploration wells (Schiøler and Raine, 2011). Onshore and offshore datasets were then combined to propose new paleogeographic maps of the Canterbury Basin during the Early Oligocene. Finally, I compared the orientation of the Early Oligocene drainage system with the present day drainage pattern of the East Coast of the South Island of New Zealand to highlight the similarity of their trends.

Chapter 6 uses both seismic reflection data tied to offshore wells and the six key horizons to map the extent of volcanic and intrusive features in the offshore Canterbury Basin. This mapping was combined with onshore mapping of volcanic rocks (Mortimer *et al.*, 2017) and a magnetic map (FrOG Tech, 2011) to propose five maps of magmatic occurrences across the Canterbury Basin from the Late Cretaceous rifting to the Miocene-Recent time interval as well as three maps at Zealandia scale.

I.5. Thesis Structure

The thesis starts by analysing the evolution of the syn- to post-rift sedimentary infill of the Canterbury Basin (Chapter 2). This gives information on the onset and cessation of the rifting and on the evolution of the landmass surrounding the Canterbury Basin. Chapter 3 analyses the structure and the timing of the rifting, from its onset during the Mid Cretaceous until the Eocene. Having defined the onset and cessation of the rift activity in Chapter 2, it is possible to compare the timing and kinematics of the different sets of rift faults formed during extension. Chapter 2 and 3 highlight the overall lack of sediment filling the accommodation created by extension and therefore at the end of the rifting, the Canterbury Basin was under-filled which impacted on sediment distribution and the evolution of the paleogeography for a protracted period of time. These observations lead us to propose (Chapter 4) a new method for quantifying rift sediment fill at the cessation of rifting using the Sediment Fill Ratio. The results are compared to other rift basins which suggest that overall, rift basins display important variations in syn-rift sediment fill compared to the amount of accommodation created during rifting.

Having constrained both the syn- to post-rift structural and sedimentary evolution of the Canterbury Basin, the PhD thesis then looks at the passive drift phase that cumulates in the Oligocene (Chapter 5). The Early Oligocene is a key time for understanding the changing tectonic regime from post-rift quiescence to contraction and plate boundary development across Zealandia. The results identify connectivity between onshore and offshore Early Oligocene through corridors of erosion that formed a submarine paleo-drainage system flowing towards the south-east. This drainage system, affecting the top of the Early Oligocene Amuri Limestone, was potentially generated by tectonic uplift west of the Canterbury Basin and could relate to tectonic movement along the present-day plate boundary that triggered a sea-level fall at around 32 Ma in the Canterbury Basin. In addition, the mapping of erosive channels suggests that the Early Oligocene drainage pattern display a very similar trend to present-day drainage. This shows that despite the important tectonic movement in the Canterbury Basin since the formation of the Southern Alps, the hydrographic pattern did not change significantly. The last findings presented in this PhD relates to the mapping of buried volcanoes across the Canterbury Basin which increases the surface area of known volcanoes in the Canterbury Basin by 300%. This adds to the catalogue of New Zealand magmatic occurrences showing the potential for more buried volcanoes in other sedimentary basins of Zealandia (Chapter 6).

This PhD Thesis is written as a series of five journal articles, resulting in a certain degree of repetition in the introduction and geological setting of each of the five chapters. At the time of thesis submission none of the chapters had been submitted for publication. Chapter 2 will be submitted to the *Journal of Sedimentary Research*. It focuses on the analysis of the sedimentary infill of the under filled Canterbury Basin combining seismic facies analysis with outcrop data and proposes reasons for the under filling of the Canterbury Basin. Chapter 3 will be submitted to *Tectonics* as it focusses on basin scale tectonic analysis of the faults of a rift system in order to understand regional processes driving extension of the eastern Gondwana margin. Chapter 4 will be submitted to *Geology* as it proposes a new approach to quantify the sediment fill of a rift basin and discusses generic geological processes. Chapter 5 will be submitted to the journal *Marine Geology* as it shows combination of offshore seismic reflection data with onshore outcrop data helps understanding the sedimentary and tectonic processes of the Canterbury Basin. Chapter 6 will be submitted to the *New Zealand Journal of Geology and Geophysics* as it proposes to update the Late Cretaceous to Recent mapping of offshore magmatic occurrences in the Canterbury Basin. This work is important in order to develop a

bigger picture of the magmatic evolution of Zealandia and will encourage further similar work in other offshore sedimentary basins of Zealand.

The details of the key findings covered in each of the chapters are summarized below:

- **Chapter 2:** The sedimentary fill of a Cretaceous under-filled rift basin, insights into the evolution of its surrounding landmass, Canterbury, New Zealand.

The Canterbury Basin initiated in the mid-Cretaceous (~110 Ma) as a rift system prior to the breakup of eastern Gondwana at ~85 Ma. Basin-fill architecture was controlled by rifting with basin and range topography produced by normal faulting persisting until its complete burial and draping during the Paleocene to Eocene. During the syn-rift and post-rift phases the interplay of rift structures and sedimentation impacted sedimentary records giving insights into the evolution of the Canterbury Basin and wider Zealandia landmass. Syn-rift sedimentation was characterised by under-filled depocenters where early syn-rift sedimentation was dominated by short drainage systems sourced within the basin and producing alluvial fans along fault scarps inter-fingering with axial braided river or lake deposits. The predominance of local drainage systems coupled with a low supply of sediment into the Canterbury Basin during the Late Cretaceous may partly account for rift depocenter under-filling at this time. In the post rift latest Cretaceous and Paleogene, pelagic sedimentation draped and buried most of the earlier-formed horsts, with complete burial being achieved in up to 60 Myr. Despite filling of the rift structures, many of the geomorphological features of the contemporary Canterbury Basin were also present in the Late Cretaceous including, the Chatham Rise and the topographic hinterland west of the basin. The timing of the progression of the marine transgression and the degree of preservation of rift structures in the Canterbury Basin differs from that in northern Zealandia (e.g., Taranaki Basin). These differences may reflect the relative tectonic quiescence in the offshore Canterbury Basin post ~85 Ma and the ongoing influence of subduction beneath northern Zealandia in the Late Cretaceous and Eocene.

- **Chapter 3:** Multi-directional extension in New Zealand's Canterbury Basin prior to Cretaceous breakup of eastern Gondwana.

The Canterbury Basin in eastern Gondwana was deformed by rift faults from ~110 to ~85 Ma with trends of NE-SW, E-W and NW-SE. Analysis of 2D and 3D seismic reflection lines tied to wells indicates that these three fault sets have primarily normal fault geometries and displacements. Displacements accrued synchronously on each fault set with N-S and NW-SE extension dominating along the Chatham Rise and in the southern Canterbury Basin, respectively. Each of the three fault sets are parallel to spreading centres that primarily define the present margins of Zealandia, with NE-SW trending faults in the southern basin being parallel to the mid-ocean ridge separating southern Zealandia and western Antarctica. The parallelism between spreading centres and rift faulting suggests that multi-directional extension in the Canterbury Basin records the early stages of Gondwana breakup. Faulting in the Canterbury Basin indicates that the plate tectonic forces responsible for Gondwana breakup commenced 10s of millions of years before breakup either soon after the cessation of subduction (e.g., < 5 Myr) or during the transition from subduction to rifting from ~110 to 105 Ma. With the onset of breakup, extension was focused along the spreading centres and multi-directional stretching of Zealandia ceased or continued at much diminished rates. Canterbury Basin multidirectional stretching differs from triple junction examples in that it was surrounded by multiple future spreading centres which vary in trend. In the Canterbury Basin case, the

initial phase of Gondwana breakup appears to have been characterised by minor (<20%) extension while we speculate that it was significantly more than across the Canterbury Basin crust between spreading centres. With the onset of seafloor spreading, extension was focused along the spreading centres, and distributed stretching of Zealandia ceased or continued at much diminished rates.

- **Chapter 4:** Relation between syn-rift sediment fill and normal-fault throw at the cessation of rifting.

This chapter examines how best to quantify basin under-filling and the fault attributes that contribute to under-filling. We quantify the geometries of rift fill in seismic reflection lines using the ratio of syn-rift strata thickness to syn-rift fault throw (here referred to as the Sediment Fill Ratio - SFR). Measurements from the Canterbury Basin are compared to six other basins The Sediment Fill permits recognition of four types of rift basins: (1) starved ($SFR \leq 0.1$), (2) under-filled ($0.1 < SFR \leq 0.9$), (3) balanced-filled ($0.9 < SFR \leq 1.1$), and (4) over-filled ($SFR > 1.1$). The degree of syn-rift basin fill at the cessation of faulting varies with fault size across the same basin and between different rift basins for the same fault size. A negative non-linear relationship between fault displacement and SFR is observed in rift basins sampled. Small faults are more often characterized by balanced or over-filled geometries because they have low displacement rates and are located in the hangingwall of larger faults (e.g., >1 seconds TwT throw) where sedimentation rates are locally high. Rift systems dominated by large faults, such as the Canterbury Basin, tend to be under-filled, and require sediment supply from outside the rift system to become over-filled.

- **Chapter 5:** Early Oligocene marine canyon-channel systems: implications for paleogeography and tectonics in the Canterbury Basin, New Zealand.

The Oligocene is a time of maximum submersion of the Zealandia landmass; it coincides with changes in oceanographic currents as well as with the inception of the Cenozoic plate boundary through New Zealand. Offshore wells and seismic reflection lines in the Canterbury Basin reveal condensed Oligocene strata (<150 m thick), which were eroded by mid-Oligocene (~32-29 Ma) channels 1-10 km wide, 15-90 km long and up to ~200 milliseconds two-way-time deep. Onshore, corridors of complete erosion of the Early Oligocene Amuri Limestone, overlain by younger Oligocene and Miocene strata have been mapped using measured sections from the published literature and offshore seismic reflection data. The synchronicity, similar trends, and comparable morphology of onshore and offshore channels suggest that they may have formed part of the same erosive system. We propose that a sea-level fall at ~32 Ma initiated the development of this drainage system with erosive channels converging towards canyons in the deeper water offshore. The drainage was active for up to 17 Ma, flowing both towards the south-east into the present-day Bounty Trough and the north-east into the Pegasus Basin. The temporal (millions of years) and the spatial (hundreds of metres) scales of the sea-level fall are larger than would be expected for eustatic processes and we suggest that regional tectonic uplift may have played an important role in channel formation. The channel orientations and their eastward gradients together with the Oligocene sedimentary facies observed in outcrop, suggest that the axis of uplift (and maximum topography) was primarily west of the Canterbury Basin. Tectonic shortening that collectively affected the western North Island – Marlborough Sounds – western Otago high may have produced uplift and eastward

flowing Early Oligocene channels in the Canterbury Basin. The orientations, geometries, and locations of Early Oligocene drainage is similar to present day systems, suggesting they have persisted as physiographic entities for at least 30 Myr, throughout Late Cenozoic plate tectonic deformation.

- **Chapter 6:** Identification and morphology of buried volcanoes from the Canterbury Basin, New Zealand.

Seismic reflection data in the offshore Canterbury Basin has enabled us to identify buried magmatic structures, ranging in age from mid-Cretaceous to Pleistocene. Buried volcanic edifices of <1 to 20 km diameter have been mapped and are grouped into five geomorphological and chronological categories. 1. Monogenetic to polygenetic volcanoes up to 5 km diameter within the Cretaceous syn-rift succession. 2. Large polygenic volcanic complexes with diameters >10 km within the post-breakup Late Cretaceous succession. 3. Monogenetic volcanoes of Paleocene to Middle Miocene age. 4. Large Miocene polygenetic volcanoes of >10 km diameter formed in association with present-day Banks and Otago peninsulas. 5. Monogenetic eruptive centers along the Chatham Rise that erupted during the Late Neogene. Widespread sill intrusion exists but did not resolve batholiths or plutons which, if present, are at depths of >10 km depth. Volcanic activity resulted in three main volumes of erupted magma, respectively 10's, 100's and 1000's km^3 during Cenozoic post-rift, Late Cretaceous syn-rift and both Late Cretaceous post-rift and Middle to Late Miocene times. This study increases the total known surface area of volcanoes in the Canterbury Basin by 300%, and suggests that across Zealandia, more volcanoes can be expected to exist.

1. References

ADAMS, C. & OLIVER, P. (1979) Potassium-Argon Dating of Mt Somers Volcanics, South Island, New Zealand: Limitations in Dating Mesozoic Volcanic Rocks. New Zealand Journal of Geology and Geophysics, 22, 455-463 pp.

ADAMS, C.J., CAMPBELL, H.J., MORTIMER, N. & GRIFFIN, W.L. (2017) Perspectives on Cretaceous Gondwana Breakup from Detrital Zircon Provenance of Southern Zealandia Sandstones. Geological Magazine, 154, 661-682 pp.

ANDREW, P.B., FIELD, B.D., BROWNE, G.H., MCLENNAN, J.M., (1987) Lithostratigraphic Nomenclature for the Upper Cretaceous and Tertiary Sequence of Central Canterbury, New Zealand. New Zealand geological Survey record, 24, 40p.

ARNOT, M.J., BLAND, K.J., COMPILERS (2016) Atlas of Petroleum Prospectivity, Northwest Province: Arcgis Geodatabase and Technical Report. GNS Science Data Series, 23b, 34p +31p ArcGIS geodatabase +35p ArcGIS projects.

BARLEY, M.E., WEAVER, S.D. & DE LAETER, J.R. (1988) Strontium Isotope Composition and Geochronology of Intermediate—Silicic Volcanics, Mt Somers and Banks Peninsula, New Zealand. New Zealand Journal of Geology and Geophysics, 31, 197-206 pp.

BECKMAN, D.W. (2012) Final Interpretation Report for Acb11, Offshore Canterbury, New Zealand. Ministry of Economic Development Petroleum Report Series, PR4492, 50p.

BLANKE, S.J. (2013) "Saucer Sills" of the Offshore Canterbury Basin. Advantage NZ Petroleum Conference, Auckland.

BLANKE, S.J. (2015) Caravel-1: Lessons Learned in the Deepwater Canterbury Basin. International Conference and Exhibition, Melbourne, Australia 13-16 September 2015.

BP, SHELL & TODD (1984) Interpretation and Prospectivity of Ppl 38203 Canterbury Basin New Zealand. New Zealand Geological Survey Library, Unpublished Petroleum Report, Ministry of Economic Development, New Zealand. PR1046.

BROWNE, G.H. (2003) Sedimentological Database for the Offshore Canterbury Basin, New Zealand. Unpublished data on CD. GNS Science, Lower Hutt.

BROWNE, G.H. & NAISH, T.R. (2003) Facies Development and Sequence Architecture of a Late Quaternary Fluvial-Marine Transition, Canterbury Plains and Shelf, New Zealand: Implications for Forced Regressive Deposits. Sedimentary Geology, 158, 57-86 pp.

BROWNE, G.H., FIELD, B.D., BARRELL, D.J.A., JONGENS, R., BASSETT, K.N. & WOOD, R.A. (2012) The Geological Setting of the Darfield and Christchurch Earthquakes. New Zealand Journal of Geology and Geophysics, 55, 193-197 pp.

BROWNE, G.H., FIELD, B.D. (1985) The Lithostratigraphy of Late Cretaceous to Early Pleistocene Rocks of Northern Canterbury, New Zealand. New Zealand Geological Survey Record, 6, 63p.

CARTER, R.M. & LANDIS, C.A. (1972) Correlative Oligocene Unconformities in Southern Australasia. Nature Physical Science, 237, 12p.

CARTER, R.M., LINDQVIST, J.K. & NORRIS, R.J. (1982) Oligocene Unconformities and Nodular Phosphate — Hardground Horizons in Western Southland and Northern West Coast. Journal of the Royal Society of New Zealand, 12, 11-41 pp.

CONEY, P.J., EDWARDS, A., HINE, R., MORRISON, F. & WINDRIM, D. (1990) The Regional Tectonics of the Tasman Orogenic System, Eastern Australia. Journal of Structural Geology, 12, 519-543 pp.

COOMBS, D.S., CAS, R., KAWACHI, Y., LANDIS, C., MCDONOUGH, W. & REAY, A. (1986) Cenozoic Volcanism in North, East and Central Otago. Royal Society of New Zealand Bulletin, 23, 278-312 pp.

COOPER, A., PRICE, R. & REAY, A. (2018) Geochemistry and Origin of a Mesozoic Ophiolite: The Pounamu Ultramafics, Westland, New Zealand. New Zealand Journal of Geology and Geophysics, 61, 1-17 pp.

COOPER, A.F. & IRELAND, T.R. (2015) The Pounamu Terrane, a New Cretaceous Exotic Terrane within the Alpine Schist, New Zealand; Tectonically Emplaced, Deformed and Metamorphosed During Collision of the Lip Hikurangi Plateau with Zealandia. Gondwana Research, 27, 1255-1269 pp.

COOPER, A.F. & PALIN, J.M. (2018) Two-Sided Accretion and Polyphase Metamorphism in the Haast Schist Belt, New Zealand: Constraints from Detrital Zircon Geochronology. Bulletin, 130, 1501-1518 pp.

COOPER, R., AGTERBERG, F.P., ALLOWAY, B., BEU, A., CAMPBELL, H., CRAMPTON, J.S., CROUCH, E., CRUNDWELL, M., GRAHAM, I.J., HOLLIS, C., JONES, C., KAMP, P., MILDENHALL, D.C., MORGANS, H., NAISH, T.R., RAINE, J.I., RONCAGLIA, L., SADLER, P.M., SCHIØLER, P. & WILSON, G. (2004) The New Zealand Geological Timescale. 22, 284p.

CRAMPTON, J.S.H., C.J.; RAINE, J.I.; RONCAGLIA, L.; SCHIOLER, P.; STRONG, C.P.; WILSON, G.J. (2004) Cretaceous (Taitai, Clarence, Raukumara and Mata Series). In: The New Zealand Geological Timescale (Ed. Cooper, R.A.) Institute of Geological & Nuclear Sciences monograph, 22, 102-122 pp.

DAVY, B. (2014) Rotation and Offset of the Gondwana Convergent Margin in the New Zealand Region Following Cretaceous Jamming of Hikurangi Plateau Large Igneous Province Subduction. Tectonics, 33, 1577-1595 pp.

EXXONMOBIL (2010) Great South Basin 3d/2d Seismic Interpretation Report, Pep 50117. PR4233, 37p.

FIELD, B.D. (1985) Stratigraphic Drillholes at Charteris Bay, Lyttelton Harbour, Christchurch, New Zealand Geological Survey, Dept. of Scientific and Industrial Research. New Zealand Geological, Survey. SL11.

FIELD, B.D. & BROWNE, G.H. (1989) Cretaceous and Cenozoic Sedimentary Basins and Geological Evolution of the Canterbury Region, South Island, New Zealand. Institute of Geological & Nuclear Sciences monograph, 2, 94p.

FIELD, B.D., BROWNE, G.H. (1986) Lithostratigraphy of Cretaceous and Tertiary Rocks, Southern Canterbury, New Zealand. New Zealand Geological Survey basin studies, 14, 55p.

FINDLAY, R.H. (1980) The Marshall Paraconformity (Note). New Zealand Journal of Geology and Geophysics, 23, 125-133 pp.

FLOOTTMANN, T., GIBSON, G.M. & KLEINSCHMIDT, G. (1993) Structural Continuity of the Ross and Delamerian Orogens of Antarctica and Australia Along the Margin of the Paleo-Pacific. Geology, 21, 319-322 pp.

FORDYCE, R.E. (2006) New Light on New Zealand Mesozoic Reptiles. Geological Society of New Zealand Newsletter, 140, 6-15 pp.

FORDYCE, R.E. & RICHARDS, M.D. (2016) Fossils and Strata of Central and North Otago-Waitaki Valley. In: Field Trip Guide Volume, Geosciences 2016 Conference. Smillie, R. (compiler). 28 November - 1 December 2016, Wanaka, New Zealand. Geoscience Society of New Zealand Miscellaneous Publication 145B.

FORSYTH, P.J., BARRELL, D.J.A. & JONGENS, R. (2008) Geology of the Christchurch Area : Scale 1:250,000. Lower Hutt: Gns Science. Institute of Geological & Nuclear Sciences 1:250,000 Geological Map 16. 67p + 1 Folded Map.

FULTHORPE, C.S., CARTER, R.M., MILLER, K.G. & WILSON, J. (1996) Marshall Paraconformity: A Mid-Oligocene Record of Inception of the Antarctic Circumpolar Current and Coeval Glacio-Eustatic Lowstand? Marine and Petroleum Geology, 13, 61-77 pp.

HAMPTON, S. & COLE, J. (2009) Lyttelton Volcano, Banks Peninsula, New Zealand: Primary Volcanic Landforms and Eruptive Centre Identification. Geomorphology, 104, 284-298 pp.

HIGGS, K.E., BROWNE, G.H. & SAHOO, T.R. (2019) Reservoir Characterisation of Syn-Rift and Post-Rift Sandstones in Frontier Basins: An Example from the Cretaceous of Canterbury and Great South Basins, New Zealand. Marine and Petroleum Geology, 101, 1-29 pp.

JONGENS, R., BARRELL, D.J.A., CAMPBELL, J.K. & PETTINGA, J.R. (2012) Faulting and Folding beneath the Canterbury Plains Identified Prior to the 2010 Emergence of the Greendale Fault. New Zealand Journal of Geology and Geophysics, 55, 169-176 pp.

KING, P.R., NAISH, T.R., BROWNE, G.H., FIELD, B.D. & EDBROOKE, S.W. (1999) Cretaceous to Recent Sedimentary Patterns in New Zealand. Institute of Geological and Nuclear Sciences Folio Series 1, 35p.

KIRK, R. & CONSTABLE, R.M. (2010) Seismic Facies Mapping & Paleogeographic Interpretation from Seismic Sequence Straitigraphy. Ministry of Economic Development New Zealand Unpublished Petroleum Report, PR4347, 212p.

KULA, J., TULLOCH, A., SPELL, T.L. & WELLS, M.L. (2007) Two-Stage Rifting of Zealandia-Australia-Antarctica: Evidence from 40ar/39ar Thermochronometry of the Sisters Shear Zone, Stewart Island, New Zealand. Geology, 35, 411-414 pp.

LAIRD, M.G. (1993) Cretaceous Continental Rifts: New Zealand Region. In: Sedimentary basins of the world. South Pacific sedimentary basins (Ed. Ballance, P.E.), Elsevier Science Publisher 2, 37-49 pp.

LAIRD, M.G. & BRADSHAW, J.D. (2004) The Breakup of a Long-Term Relationship: The Cretaceous Separation of New Zealand from Gondwana. Gondwana Research, 7, 273-286 pp.

LEVER, H. (2007) Review of Unconformities in the Late Eocene to Early Miocene Successions of the South Island, New Zealand: Ages, Correlations, and Causes. New Zealand Journal of Geology and Geophysics, 50, 245-261 pp.

LEWIS, D.W. (1992) Anatomy of an Unconformity on Mid-Oligocene Amuri Limestone, Canterbury, New Zealand. New Zealand Journal of Geology and Geophysics, 35, 463-475 pp.

LU, H., FULTHORPE, C.S. & MANN, P. (2003) Three-Dimensional Architecture of Shelf-Building Sediment Drifts in the Offshore Canterbury Basin, New Zealand. Marine Geology, 193, 19-47 pp.

LU, H. & FULTHORPE, C.S. (2004) Controls on Sequence Stratigraphy of a Middle Miocene–Holocene, Current-Swept, Passive Margin: Offshore Canterbury Basin, New Zealand. GSA Bulletin, 116, 1345-1366 pp.

MACKINNON, T.C. (1984) Origin of the Torlesse Terrane and Coeval Rocks, South Island, New Zealand: Discussion and Reply: Reply. GSA Bulletin, 95, 981p.

MARSAGLIA, K.M., BROWNE, G.H., GEORGE, S.C., KEMP, D.B., JAEGER, J.M., CARSON, D. & RICHAUD, M. (2017) The Transformation of Sediment into Rock: Insights from Iodp Site U1352, Canterbury Basin, New Zealand. Journal of Sedimentary Research, 87, 272-287 pp.

MITCHELL, M., CRAW, D., LANDIS, C.A. & FREW, R. (2009) Stratigraphy, Provenance, and Diagenesis of the Cretaceous Horse Range Formation, East Otago, New Zealand. New Zealand Journal of Geology and Geophysics, 52, 171-183 pp.

MORTIMER, N. (2004) New Zealand's Geological Foundations. Gondwana Research, 7, 261-272 pp.

MORTIMER, N., RATTENBURY, M.S., KING, P.R., BLAND, K.J., BARRELL, D.J.A., BACHE, F., BEGG, J.G., CAMPBELL, H.J., COX, S.C., CRAMPTON, J.S., EDBROOKE, S.W., FORSYTH, P.J., JOHNSTON, M.R., JONGENS, R., LEE, J.M., LEONARD, G.S., RAINE, J.I., SKINNER, D.N.B., TIMM, C., TOWNSEND, D.B., TULLOCH, A.J., TURNBULL, I.M. & TURNBULL, R.E. (2014) High-Level Stratigraphic Scheme for New Zealand Rocks. New Zealand Journal of Geology and Geophysics, 57, 402-419 pp.

MORTIMER, N., CAMPBELL, H.J., TULLOCH, A.J., KING, P.R., STAGPOOLE, V.M., WOOD, R.A., RATTENBURY, M.S., SUTHERLAND, R., ADAMS, C.J., COLLOT, J. & SETON, M. (2017a) Zealandia: Earth's Hidden Continent. GSA Today, 27, 27-35 pp.

MORTIMER, N., GANS, P.B., MEFFRE, S., MARTIN, C.E., SETON, M., WILLIAMS, S., TURNBULL, R.E., QUILTY, P.G., MICKLETHWAITE, S., TIMM, C., SUTHERLAND, R., BACHE, F., COLLOT, J., MAURIZOT, P., ROUILLARD, P. & ROLLET, N. (2017b) Regional Volcanism of Northern Zealandia: Post-Gondwana Breakup Magmatism on an Extended, Submerged Continent. Geological Society, London, Special Publications, 463, SP463. 469p.

NICOL, A. (1993) Haumurian (C. 66–80 Ma) Half-Graben Development and Deformation, Mid Waipara, North Canterbury, New Zealand. New Zealand Journal of Geology and Geophysics, 36, 127-130 pp.

OLIVER, P.J. (1984) The Mid-Cretaceous Volcanic Rocks of Rakaia Gorge and Malvern Hills Area, Canterbury. New Zealand Geological Survey Record, 3, 86-91 pp.

OLIVER, P.J. & KEENE, H.W. (1989) Sheet K36 Ac & Part Sheet K35 Mount Somers. Geological Map of New Zealand 1:50 000. Map (One Sheet) and Notes. Wellington, New Zealand. Department of Scientific and Industrial Research.

PLAMPTON, W. (2018) Geometry and Distribution of Latest Cretaceous / Paleocene Turbidites and Their Prospectivity, Great South Basin, Offshore Se New Zealand. Poster presentation at PESGB SEAPEX Asia Pacific E&P Conference, Olympia Exhibition Centre, London, 27th – 28th June 2018.

RAINE, J.I., BEU, A.G., BOYES, A.F., CAMPBELL, H.J., COOPER, R.A., CRAMPTON, J.S., CRUNDWELL, M.P., HOLLIS, C.J., MORGANS, H.E.G. & MORTIMER, N. (2015) New Zealand Geological Timescale Nzgt 2015. New Zealand Journal of Geology and Geophysics, 58, 398-403 pp.

RATTENBURY, M.S., TOWNSEND, D.B. & JOHNSTON, M.R. (2006) Geology of the Kaikoura Area : Scale 1:250,000 Geological Map. . Lower Hutt: GNS Science. Institute of Geological & Nuclear Sciences 1:250,000 geological map, 13, 70 p. + 71 folded map.

REYNERS, M., EBERHART-PHILLIPS, D., UPTON, P. & GUBBINS, D. (2017) Three-Dimensional Imaging of Impact of a Large Igneous Province with a Subduction Zone. Earth and Planetary Science Letters, 460, 143-151 pp.

SAHOO, T.R., KING, P.R., BLAND, K.J., STROGEN, D.P., SYKES, R. & BACHE, F. (2014) Tectono-Sedimentary Evolution and Source Rock Distribution of the Mid to Late Cretaceous Succession in Great South Basin, New Zealand. APPEA Journal, 54, 259-274 pp.

SAHOO, T.R., KROEGER, K.F., THRASHER, G., MUNDAY, S., MINGARD, H., COZENS, N. & HILL, M. (2015) Facies Distribution and Impact on Petroleum Migration in the Canterbury Basin , New Zealand. In: Eastern Australian Basins Symposium 2015: Publication of Proceedings. Petroleum Exploration Society of Australia, Perth, WA, 187-202 pp.

SAHOO, T.R., BLAND, K. J.,COMPILERS (2017) Atlas of Petroleum Prospectivity, Southeast Province: Arcgis Geodatabase and Technical Report. GNS Science Data Series, 23c, 50p + 51p ArcGIS geodatabase + 55p ArcGIS projects.

SCHIØLER, P.R., RAINE, J.I., COMPILERS (2011) Revised Biostratigraphy and Well Correlation, Canterbury Basin, New Zealand. GNS Science Consultancy Report 2011/12, PR4365, 142p.

SHOUP, R.C. & COZENS, N. (2016) Explorers from New Zealand: Application of Modern and Ancient Depositional Environments to Construct Paleo Depositional Environment Maps of the Canterbury and Great South Rift Basins. AAPG Search and Discovery Article, 107p.

SMITH, T. & COLE, J. (1997) Somers Ignimbrite Formation: Cretaceous High-Grade Ignimbrites from South Island, New Zealand. Journal of volcanology and geothermal research, 75, 39-57 pp.

SPELL, T.L., MCDOUGALL, I. & TULLOCH, A.J. (2000) Thermochronologic Constraints on the Breakup of the Pacific Gondwana Margin: The Paparoa Metamorphic Core Complex, South Island, New Zealand. Tectonics, 19, 433-451 pp.

STROGEN, D.P., SEEBECK, H., NICOL, A. & KING, P.R. (2017) Two-Phase Cretaceous – Paleocene Rifting in the Taranaki Basin Region, New Zealand; Implications for Gondwana Breakup. Journal of the Geological Society, 174, 929-946 pp.

STROGEN, D.P., KING, P.R. (2014) A New Zealandia-Wide Seismic Horizon Naming Scheme. GNS Science Report, 2014/34, 20p.

TAPPENDEN, V.E. (2003) Magmatic Response to the Evolving New Zealand Margin of Gondwana During the Mid-Late Cretaceous. PhD thesis, University of Canterbury, 376p.

TULLOCH, A.J., RAMEZANI, J., MORTIMER, N., MORTENSEN, J., VAN DEN BOGAARD, P. & MAAS, R. (2009) Cretaceous Felsic Volcanism in New Zealand and Lord Howe Rise (Zealandia) as a Precursor to Final Gondwana Breakup. Geological Society, London, Special Publications, 321, 89-118 pp.

VAN DER MEER, Q.H.A., WAIGHT, T.E., SCOTT, J.M. & MÜNKER, C. (2017) Variable Sources for Cretaceous to Recent Himu and Himu-Like Intraplate Magmatism in New Zealand. Earth and Planetary Science Letters, 469, 27-41 pp.

WELLMAN, H.W. (1979) An Uplift Map for the South Island of New Zealand and a Model for Uplift of the Southern Alps. In: The Origin of the Southern Alps (Eds. Walcott, R.I. & Cresswell, M.M.), . Royal Society of New Zealand Bulletin, 18, 13-20 pp.

CHAPTER 2) THE SEDIMENTARY FILL OF A CRETACEOUS UNDER-FILLED RIFT BASIN, INSIGHTS INTO THE EVOLUTION OF ITS SURROUNDING LANDMASS, CANTERBURY, NEW ZEALAND.

A. Barrier[1], G. H. Browne[2], A. Nicol[1] and K. Bassett[1]

[1] University of Canterbury, Department of Geological Science, Christchurch, New Zealand.

[2]GNS Science, PO Box 30368, Lower Hutt, New Zealand.

2. Abstract

The Canterbury Basin initiated in the mid-Cretaceous (~110 Ma) as a rift system, prior to the breakup of eastern Gondwana at ~85 Ma. Basin-fill architecture was controlled by rifting, with the basin and range topography produced by normal faulting, persisting until its complete burial and draping during the Paleocene to Eocene. During the syn-rift and post-rift phases, the interplay of rift structures and sedimentation impacted the sedimentary record giving insights into the evolution of the Canterbury Basin and wider Zealandia landmass. Syn-rift sedimentation was characterised by under-filled depocenters, where early syn-rift sedimentation was dominated by short drainage systems sourced from within the basin to produce alluvial fans along fault scarps inter-fingered with axial braided river or lake deposits. The predominance of local drainage systems coupled with a low supply of sediment into the Canterbury Basin during the Late Cretaceous may partly account for the under-filling of rift depocenter at this time. In the post rift latest Cretaceous and Paleogene, pelagic sedimentation draped and buried most of the earlier-formed horsts, with complete burial being achieved within 60 Myr. Despite filling of the rift structures, many of the geomorphological features of the contemporary Canterbury Basin were also present in the Late Cretaceous including, the Chatham Rise and the topographic hinterland west of the basin. The timing of the progression of the marine transgression and the degree of preservation of rift structures in the Canterbury Basin, differs from that in northern Zealandia (e.g., Taranaki Basin). These differences may reflect the relative tectonic quiescence in the offshore Canterbury Basin post ~85 Ma and the ongoing influence of subduction beneath northern Zealandia in the Late Cretaceous and Eocene.

2.1. Introduction

Continental rift basins are structurally controlled depocenters, characterised by continent-scale stretching. Crustal thinning along plate boundaries or intraplate tectonic sutures typically occurs over timescales of millions of years, and can generate subsidence of >10 km (Davison and Underhill, 2012). After an initial phase of extension, strain hardening of the lithosphere can increase due to the influence of cold continental mantle and rifting ultimately ceases. Alternatively, rift activity may cease due to continental breakup and the onset of spreading associated with the creation of oceanic crust. Sedimentary infill of rift basins reflects the tectonic controls and provides important data for understanding the timing and kinematics of faulting, as well as continent-scale tectonics (Lambiase and Morley, 1999; Gawthorpe and Leeder, 2000; Whitjack *et al.*, 2002, Davison and Underhill, 2012).

Large-scale continental rift basins are typically divided into syn- and post-rift sedimentary phases (e.g. Eriksson *et al*., 1994; Schlische *et al.*, 2003). During the syn-rift phase, tectonics and climate are the two main controls on sedimentation (Lambiaise and Morley, 1999). The transition to the post-rift phase is marked by a significant decrease of the rift activity, typically to a more passive margin drift period. Post-rifting thermal subsidence dominates, which controls the depositional slope and the accommodation space that is ultimately filled with sediments (Lambiaise and Morley, 1999).

We focus on the content, geometries and origin of sediments deposited in under-filled syn-rift basins, and the insights that these sediments provide for the evolution of the landmass surrounding the rift system. The term "Under-filled" is often used to describe the sedimentary fill of foreland basins (Allen *et al*., 1986; Sinclair, 1997), and here we use it to describe rift basins where the rate of subsidence far exceeds sediment supply in the hanging wall of normal faults (Ravnås and Steel, 1998; see chapter 4 of this thesis for further details). For these rift basins, the accommodation space generated by faulting is not filled during rifting, as complete basin filling is often only achieved by post-rift sedimentation. As a consequence, the duration of basin infilling exceeds that of the faulting. The interplay of rift structures and syn- to post-rift sedimentation in such under-filled rift basins can control the sediment distribution and its evolution for tens of millions of years. Rift basins and their infill can host important mineral and petroleum potential. Therefore, studying the sediment distribution in under-filled rift basins from syn- to post-rift phases can help improve understanding of the tectonic and sedimentological processes in these basins, and their impact on the formation of key resources such as minerals and petroleum (Harding, 1984; Lambiase and Morley, 1999; Mann *et al.*, 2003; Davison and Underhill, 2012). The analysis of under-filled rift basins may also provide insights into the geological evolution of the surrounding landmass.

In this paper we study basin filling of the Canterbury Basin in offshore New Zealand, using seismic reflection and well data (Fig. 2.1). These data permit analysis of the interplay between rift faulting and the distribution of the sediment fill for a rift system, in which 80% of rift faults with throws > 1 second Two-way-Time (TwT) are associated with under-filled depocenters (see chapter 4 of this thesis for further details). Under-filling of rift basins impacts both syn- and post-rift sedimentation, therefore both are considered in this chapter. We analyse the geometry and seismic character of strata from the onset of rifting in the mid-Cretaceous (~110 Ma) to eventual burial in the Eocene (~34 Ma). The implications of under-filling for the evolution of the New Zealand landmass, and the factors that lead to the under filling of the Canterbury Basin, are examined. The results have implications for other basins in Zealandia and elsewhere, and for Zealandia paleogeography during the Cretaceous to Eocene.

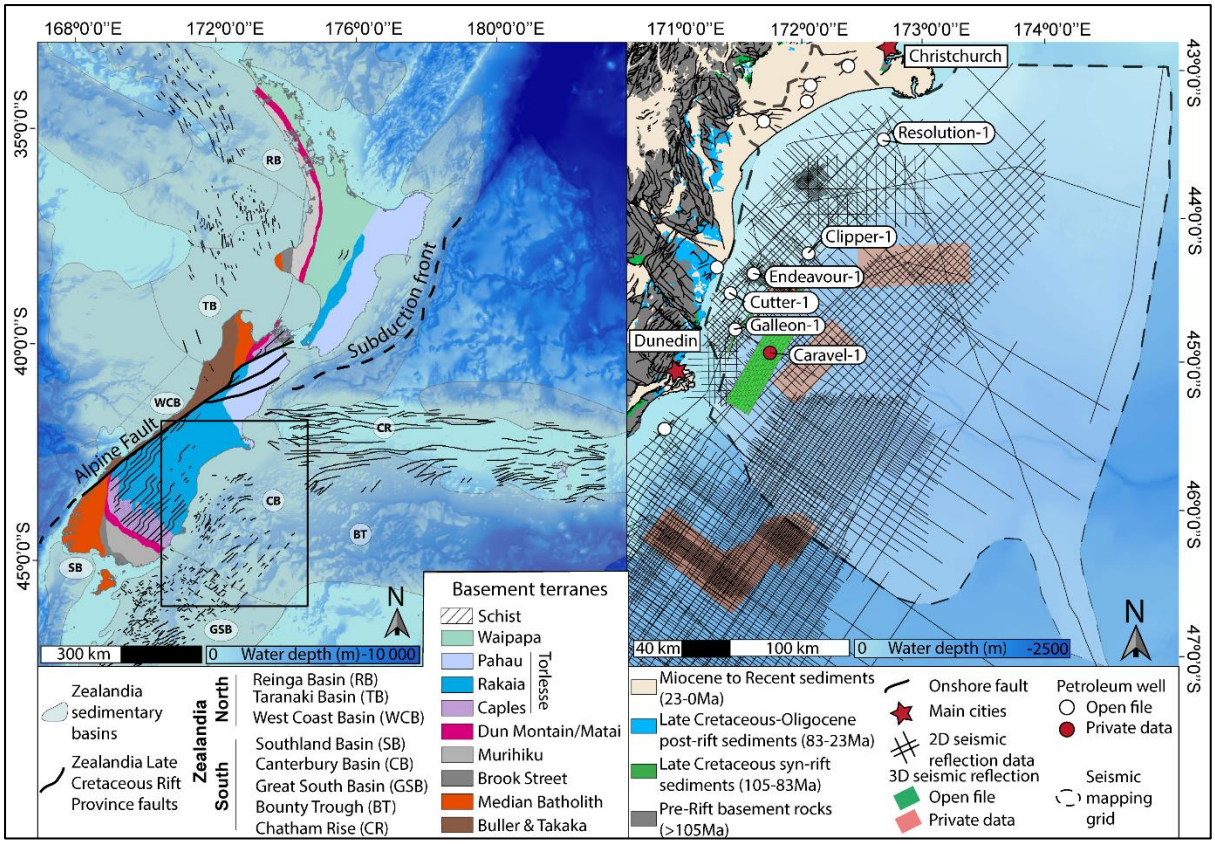

Figure 2.1(A) New Zealand basemap showing onshore basement terranes, offshore Late Cretaceous faults and associated sedimentary basins (adapted from Mortimer, 2004; Rift faults, Arnot & Bland, 2016; Sahoo & Bland, 2017). (B) Canterbury Basin dataset showing the locations of syn-rift outcrops, seismic reflection and well data. Bathymetric data licensed under NIWA Open Data Licence v1.0.v.

2.2. Geological Setting of the Canterbury Basin

The Canterbury Basin is one of the nineteen main sedimentary basins located in the continental crust of Zealandia, the largely submerged continent that underlies New Zealand (Mortimer and Campbell, 2014; Mortimer *et al.*, 2017). The basin is located on the eastern South Island of New Zealand and is primarily located offshore. The boundaries of the basin are defined by the Chatham Rise, Southern Alps, Bounty Trough and Great South Basin (Fig. 2.1). The basin contains strata up to 8 km thick that range in age from ~110 Ma to present and rest on Mesozoic terranes which accreted in eastern Gondwana during the Permian to Early Cretaceous (Fig. 2.1, Field and Browne, 1989; Wood and Herzer, 1993; Laird and Bradshaw, 2004; Davy, 2014; Sahoo and Bland, 2017). For the purposes of this paper, basin stratigraphy has been divided into three main parts; (1) the Cretaceous rift sequence, (2) post breakup quiescence, and (3) convergent margin. The strata in each of these stratigraphic intervals are briefly outlined below.

2.2.1 Cretaceous Rifting (~110 to 85 Ma)

The Canterbury Basin formed during rifting and breakup of the eastern Gondwana margin in the Late Cretaceous between ~110-85 Ma (Fig. 2.2 - Field and Browne, 1989; King et al., 1999; Laird and Bradshaw, 2004; Strogen et al., 2017). Cretaceous rifting post-dated a prolonged period of Permian to Early Cretaceous subduction and accretion during a time when many of the terranes that comprise of the basement of Zealandia were assembled (Fig. 2.2 - Carter, 1988; Laird, 1993; Mortimer et al., 1999; Mortimer, 2004; Mortimer et al., 2014). The age of rifting has a degree of uncertainty due in part to a lack of wells that penetrate the rift successions of Zealandia, and to limited biostratigraphic resolution (for discussion see Crampton et al., 2004; Schiøler and Raine, 2011; Strogen et al., 2017; Crampton et al., 2019). The oldest ages for Cretaceous rocks of the Canterbury Basin are 112.5±0.2 Ma (Tulloch et al., 2009) to 114±2 Ma (Adams et al., 2017) based on detrital zircon U-Pb ages for silicic tuff horizons (Fig. 2.1 and 2.2). However, it is not well acknowledged if these are growth strata that constrain the timing of rifting. The oldest biostratigraphically dated sediments in the Canterbury Basin (from palynology) are ~103 to 100 Ma based on the work of Adams and Raine (1988) in the Kyeburn Formation. However, these paleontological samples are often not the deepest or the oldest stratigraphically in either outcrop or wells.

Ages assigned to the end of rifting range between 86 Ma (Higgs et al., 2019) and 83 Ma (Adams et al., 2017; Strogen et al., 2017). In the Canterbury Basin, the age of rift cessation is constrained by the oldest dated post-breakup sediments (from palynology) at Clipper-1 (Schiøler and Raine, 2011). However, at this location, the syn-rift/post-breakup transition is preceded by a 10 Myr hiatus of erosion or non- deposition from ~93 to 83 Ma.

The age of onset of rifting is estimated to be 110±5 Ma (for the purposes of this paper referred to as ~110 Ma) and the age of cessation of the rifting to be 84.5±1.5 Ma (we use ~85 Ma for this paper) given the above caveats. The period of rifting therefore persisted for between 19 to 32 Myr, potentially longer than the 5-20 Myr usually referred to in the international literature for the duration of rifting (e.g. Davidson and Underhill, 2012).

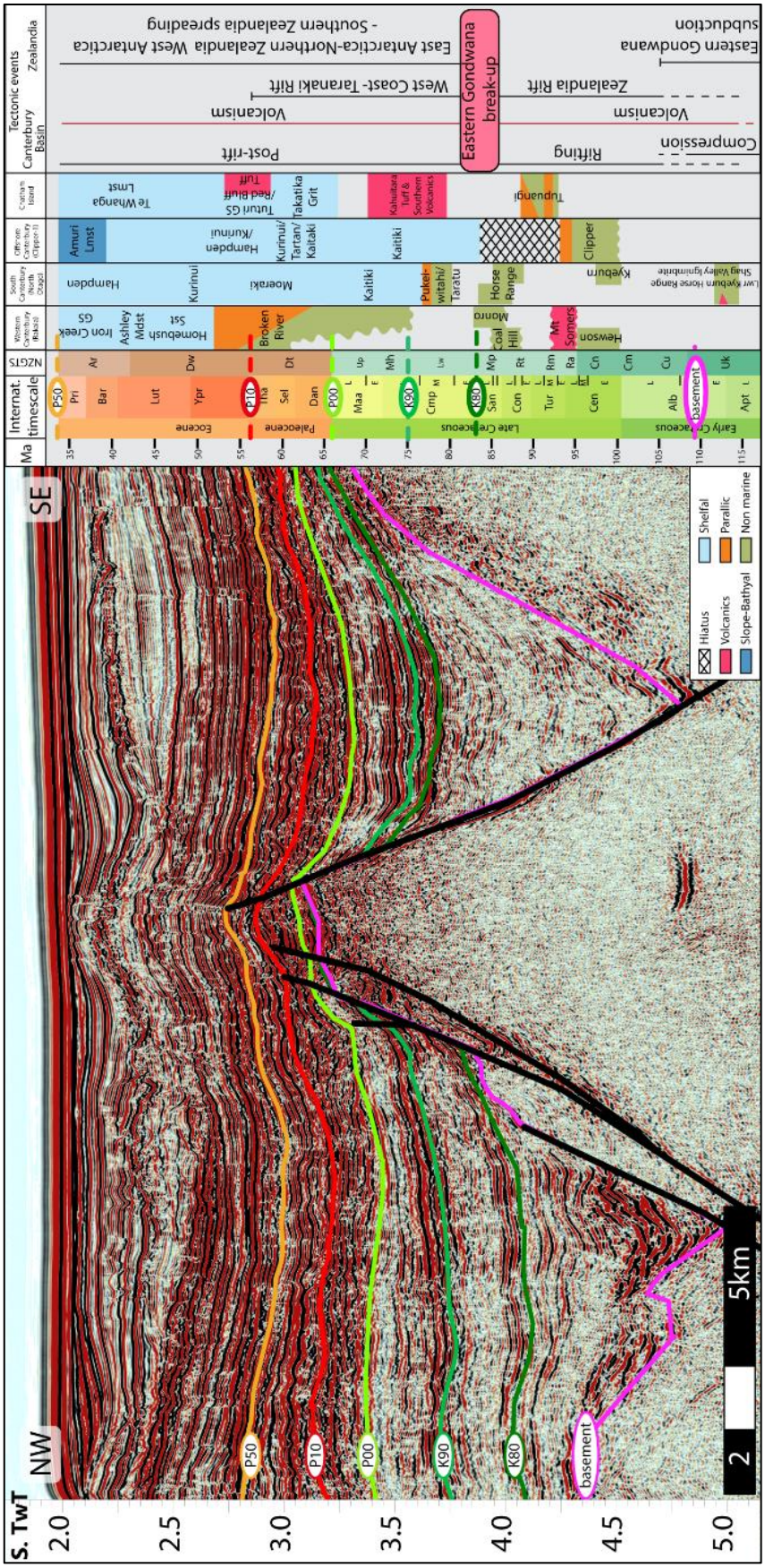

Figure 2.2 Seismic reflection profile CARINA-25 showing rift geometries and seismic horizons mapped offshore Canterbury Basin. Onshore to offshore stratigraphy and depositional environment evolution of the Canterbury Basin with the main tectonic event of the Canterbury Basin and Zealandia. See Figure 2.4 for location.

Initially, syn-rift sedimentation occurred in a continental setting when Zealandia was at a high southern latitude between 70-85° S. Over time the basin experienced an increase in marine influence and the hanging walls of the largest faults became fully marine during rifting. The paleoclimate during rifting was wet with cool mean annual temperatures of ~10°C (Pole, 1995; Parish et al., 1998). Such a climate would likely have provided abundant precipitation suitable for the existence of river systems (Browne and Reay, 1993) and is consistent with locally abundant plant macrofossils in Cretaceous fluvial sediments across Zealandia during this time (Kennedy, 2003; Pole and Philippe, 2010). For example, in the Clipper-1 well, 479.5 m of syn-rift braided river sediments were penetrated and comprise the Clipper Formation (Browne, 2003; Schiøler and Raine, 2011; Higgs et al., 2019). Onshore equivalents include the Kyeburn, Horse Range, Henley Breccia and Hewson Conglomerate formations, syn-rift formations that display upward fining non-marine successions, comprising alluvial fan to fluvial conglomerate, sandstone, siltstone, mudstone, and coal, overlain by marine transgressive sediments (Fig. 2.2 - Browne and Field, 1985; Field and Browne, 1986, 1989; Andrew et al., 1987; Mitchell et al., 2009; Higgs et al., 2019). Recently, syn-rift lacustrine siltstone have been described within the Kyeburn Formation indicating that the extensional setting also favoured the development of lakes in the Canterbury Basin (Raine et al., 2018). The onshore syn-rift succession in the Canterbury Basin reaches a maximum thickness of 3950m (±150m) along the Waihemo Fault in North Otago region (Bishop et al., 1976; Field and Browne, 1989, Mitchell et al., 2009). At Clipper-1 well, the top of the syn-rift is overlain by outer-shelf post-rift strata (83-75 Ma), which suggest erosion and/or a hiatus in sedimentation of up to 10 Myr between the syn-rift and post-breakup succession (Fig. 2.2 - Schiøler and Raine, 2011).

2.2.2 Post Breakup Quiescence (~85 to 23 Ma)

The post-rift passive phase of sedimentation records a widespread transgression by shoreline facies concluding in maximum inundation during the Early Oligocene (Field and Browne, 1989; Lever, 2007). During this transgression the uplifted footwalls of rift faults were progressively buried, with burial being completed largely by Eocene time. Following breakup, Zealandia drifted northward to reach a latitude of 45-60°S during the Late Cretaceous to Eocene when a temperate (Late Cretaceous) to sub-tropical (Eocene) climate existed (Pocknall, 1989; Kennedy, 2003; Vajda and Raine, 2003; Browne et al., 2008; Kennedy et al., 2014; Hollis et al., 2014, 2015). Outcrop and well data of post-breakup Late Cretaceous strata comprise widespread fluvial to tidally influenced paralic facies of the Taratu, Broken River, and Pukeiwitahi formations, and shelf sandstone-siltstone-mudstone of the Conway and Katiki formations (Field and Browne, 1989; Higgs et al., 2019). With time these facies transgressed progressively from east to west, associated with an overall deepening of the basin (Fig. 2.2 - Browne and Field, 1985; Field and Browne, 1986, 1989; Andrew et al., 1987). By the end of Eocene- Early Oligocene time, the coastline had migrated to its most westerly extent and fine-grained carbonate sedimentation predominated throughout the area, with localised shallow and cold-water bryozoan-molluscan-brachiopod dominated carbonate build-ups developing over paleo-topographic highs (Field and Browne, 1989; Lever, 2007; Thompson et al., 2014).

2.2.3 Miocene to Recent Convergent Margin (~23 Ma to Recent)

The increase in plate convergence rates and possible initiation of the Alpine Fault during the Oligocene and Early Miocene triggered uplift, erosion, and marine regression throughout the majority of New Zealand, including the Canterbury Basin (Mortimer et al., 2014). The Miocene is dominated by an increase in sediment supply from topography to the west of the basin, generated by uplift in the central South Island manifest as the Southern Alps (Wellman, 1979; Browne and Naish, 2003; Marsaglia et al., 2017). Large volumes of sediment deposited in the offshore Canterbury Basin during the Neogene-Quaternary are recorded by drift deposits and prograding foresets which show the eastward migration through time of the shelf break, and burial of the older succession (Browne and Naish, 2003; Lu et al., 2003, 2005; Lu and Fulthorpe, 2004)

2.3. Methods

To map the thicknesses and lateral geometries of the main stratigraphic units in the offshore Canterbury Basin, we have utilised open-file 2D seismic reflection and one 3D seismic volume provided by New Zealand Petroleum and Minerals (NZP&M; for details see https://data.nzpam.govt.nz), issued as part of the New Zealand Government 2015 to 2018 Data Pack (Figs. 2.1 and 2.3). Seismic data quality and coverage is variable, with seismic surveys acquired between 1966 to 2014 and fewer lines available in the east of the study area. The data acquired post-2006 and the older data reprocessed post-2006 have a quality that ranges from good to very good. Seismic data pre-2006, that has not been processed, is usually of poor to medium quality.

Seismic data has been tied to five petroleum exploration wells in the area and ages assigned to reflectors using the most recent biostratigraphic ages established for those wells (Schiøler and Raine, 2011). Clipper-1 well provides some age control for older strata, while the Endeavour-1, Galleon-1, Resolution-1 and Cutter-1 wells constrain the age of the younger post-rift period. From the wells, six horizons have been interpreted using ~26 000 line-kilometres of seismic data, according to the GNS Science "K" and "P" seismic horizon naming convention (Strogen and King, 2014). The horizons were assigned an age, based on the New Zealand Geological Time Scale (Cooper *et al.*, 2004; Raine *et al.*, 2015) and from the international geological time scale (Table 2.1). The top of the Late Cretaceous syn-rift sequence was only drilled in the Clipper-1 well, where it is defined by the intra Late Cretaceous K80 horizon which is ~85 Ma in age. The K80 horizon coincides with the onset of the breakup of south Zealandia and western Antarctica and marks the cessation of significant normal displacements and rifting (i.e. >50 ms) across the Canterbury Basin (Fig. 2.2).

The resulting main rift sub-basin and structural highs have been named using the nomenclature from the literature and this study (see Fig. 2.4). Three new names have been given to three main rift structures using Māori word of cultural significance. These Māori word were selected in consultation with Nā Nekerangi Paul, Māori Liaison Librarian at the University of Canterbury. The Puke Intra-basin High name is derived from Puke, which corresponds to a mound (Best, 1926). Here, the Puke intra-basin High forms a mound several

kilometres wide in-between two of the main rift faults of the basin (i.e., the east-dipping Caravel fault and the Taiepa Nui Fault). The Taiepa Nui name is derived from Taiepa, which correspond to a wall or a fence (Pōtatau, 1991) and Nui for vastness or greatness (Orange, 1998). Indeed, the Taiepa Nui High and associated fault represent the more distinctive (largest fault throw) and pervasive rift structure recognised in the Canterbury Basin. Finally, Tawhiti name characterise an object that is distant or far away (Grey, 1928). The Tawhiti basin and High represent the most eastward rift structures recognised in the Canterbury Basin. The main rift faults across the Canterbury Basin are named accordingly to the horst and depocenters they separate.

Table 2.1 Seismic horizon nomenclature used in this paper following GNS nomenclature (Strogen and King, 2014).

Color code	Horizon Name	GNS Science nomenclature (Strogen & King, 2014)	Age (Ma)	NZ Stage	International Stage	Mapped
	Top Eocene	P50	34	Runangan	Priabonian	yes
	Top Paleocene	P10	56	Teurian	Thanetian	yes
	Top Late Cretaceous post-rift	P00	66	upper Haumurian	Maastrichtian	yes
	Intra Late Cretaceous post-rift	K90	78	lower Haumurian	intra Campanian	yes
	Top Late Cretaceous syn-rift	K80	84.5±1.5	Piripuan	Santonian	yes
	Top Basement	basement	110±5	Urutawan to Korangan	Aptian-Albian	yes

From the six horizons mapped in seismic reflection lines, four isochron grids have been generated for the syn-rift interval (top basement to K80), the post-rift Late Cretaceous interval (K80 to P00), the Paleocene (P00 to P10) interval, and Eocene (P10 to P50) interval. The isochron grids constrain the evolution of the geometries and locations of depocenters during the syn- and post-rift phases. Using the top basement isochron map in depth for the Canterbury and Great South basins published by Sahoo and Bland (2017), we generate a drainage model showing where fluvial systems may have flowed and water accumulated during the early stages of basin formation (~110-100 Ma). The modelling was achieved using Hydro Terrain Processing Tool of ArcGIS software, enabling potential areas for lake development to be identified and comparison of fluvial drainage patterns in the Canterbury and Great South basins.

For this study, we constrain the onset and cessation of rifting using the geometries of seismic reflectors, together with the ages from graben sedimentary infill and intercalated extrusive igneous rocks outcropping onshore (Tulloch *et al.*, 2009; Adams *et al.*, 2017) (Fig. 2.2). Two seismic reflector geometries have been used to differentiate syn-rift and post-rift seismic intervals (Fig. 2.2). (1) Syn-rift reflector packages show growth strata geometries along rift faults and onlap of reflectors towards the hinge of the half graben. (2) Post-rift reflectors drape paleo-fault scarps and horst blocks, with parallel reflector geometries from the hinge to the centre of the graben. Seismic facies have been tied to petroleum exploration wells and correlated to onshore outcrops from the Canterbury Basin and other New Zealand sedimentary basins of similar age (Table 2.1 and. Fig 2.3). Clinoform geometries formed across the post-rift reflectors were characterised using their width and length dimensions (in metres) and their height in seconds two-way travel time (TwT). Parameters were then used to classify clinoforms following Patruno and Helland-Hansen (2018).

Table 2.2 Table of the seismic facies identified offshore Canterbury Basin.

	Environment	Amplitude	Lateral continuity	Geometry/structural position	Seismic image	New Zealand analogues
Syn-rift	**Lacustrine mudstone (A)**	Low- to medium-amplitude	Relatively continuous	Sub-parallel to chaotic In the axis of half-graben	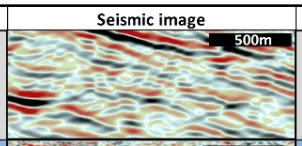	Kyeburn fm. (Canterbury Basin) Waiomo gr. (West Coast Basin)
	Braided fluvial system (B)	Medium- to high-amplitude	Relatively discontunuous	Sub-parallel Over the edge of half graben	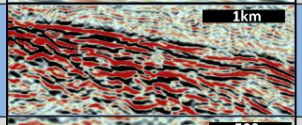	Keyburn and Horse Range fm. (Canterbury Basin)
	Mouth bar (C)	High-amplitude	Relatively discontinuous	Channel fill, wedge In the axis of the half-graben	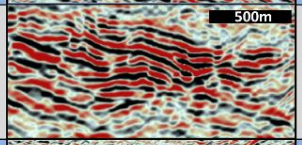	Rawanui Mb. (West Coast Basin)
	Alluvial fan to fan delta (D)	Low-, medium- to high- amplitude	Discontinuous to relatively continuous	Chaotic, deeping, wedge Along rift fault	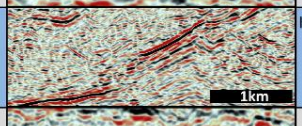	Keyburn and Horse Range fm. (Canterbury Basin) Rawanui Mb. (West Coast Basin)
	Paralic to deeper marine (E)	Low- to medium-amplitude	Relatively continuous	Sub-parallel In the depocenter	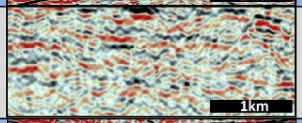	e.g. Pukeiwitahi fm. Waipara fm. (Canterbury Basin)
submersion	**Alluvial fan or fan delta stream flow dominated (F)**	Medium- to high-amplitude	Relatively continuous	Dipping, wedge Along rift fault	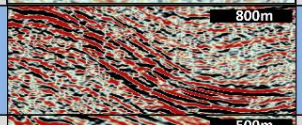	No analogues
	Alluvial fan or fan delta debris flow dominated (G)	Low- to medium-amplitude	Discontinuous	Chaotic, dipping, wedge Along rift fault	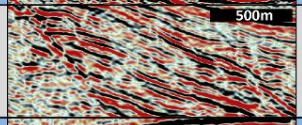	No post -rift analogues
	Gilbert delta (H)	Medium- to high-amplitude	Continuous to discontinuous	Sigmoid On top of rift structural high and adjacent to rift faults	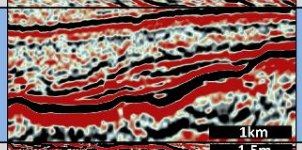	No analogues
Post-rift	**Accretionary shelf-edge clinoforms (I)**	Medium- to high-amplitude	Relatively continuous to discontinuous	Parallel to chaotic Aligned over several tens of kilometers	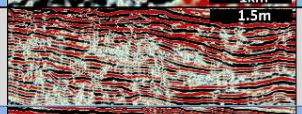	Seismic facies and wells in Great South Basin (ExxonMobil, 2010; Sahoo *et al.*, 2014)
	Draping shelf-edge clinoforms (J)	Low- to medium-amplitude	Continuous to discontinuous (due to polygonal faulting)	Oblique tangential (tens of kilometers) Parallel Chaotic (due to polygonal faulting)		Drilled by exploration wells (Clipper-1; Galleon-1; Caravel-1)
draping	**Pelagic basin floor (K)**	Medium- to high-amplitude	Relatively continuous to discontinuous	Sub-parallel, wavy to chaotic At the toe of the ramp	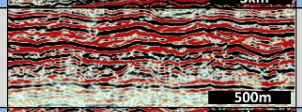	No analogues
	Deep water fan (L)	Medium- to high-amplitude	Continuous to discontinous	Mounded Bi directional downlaps Channel on top of mound At the toe of the ramp	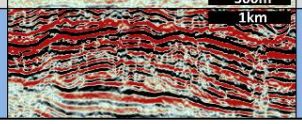	Seismic facies and wells in Great South Basin (ExxonMobil, 2010; Sahoo *et al.*, 2014)

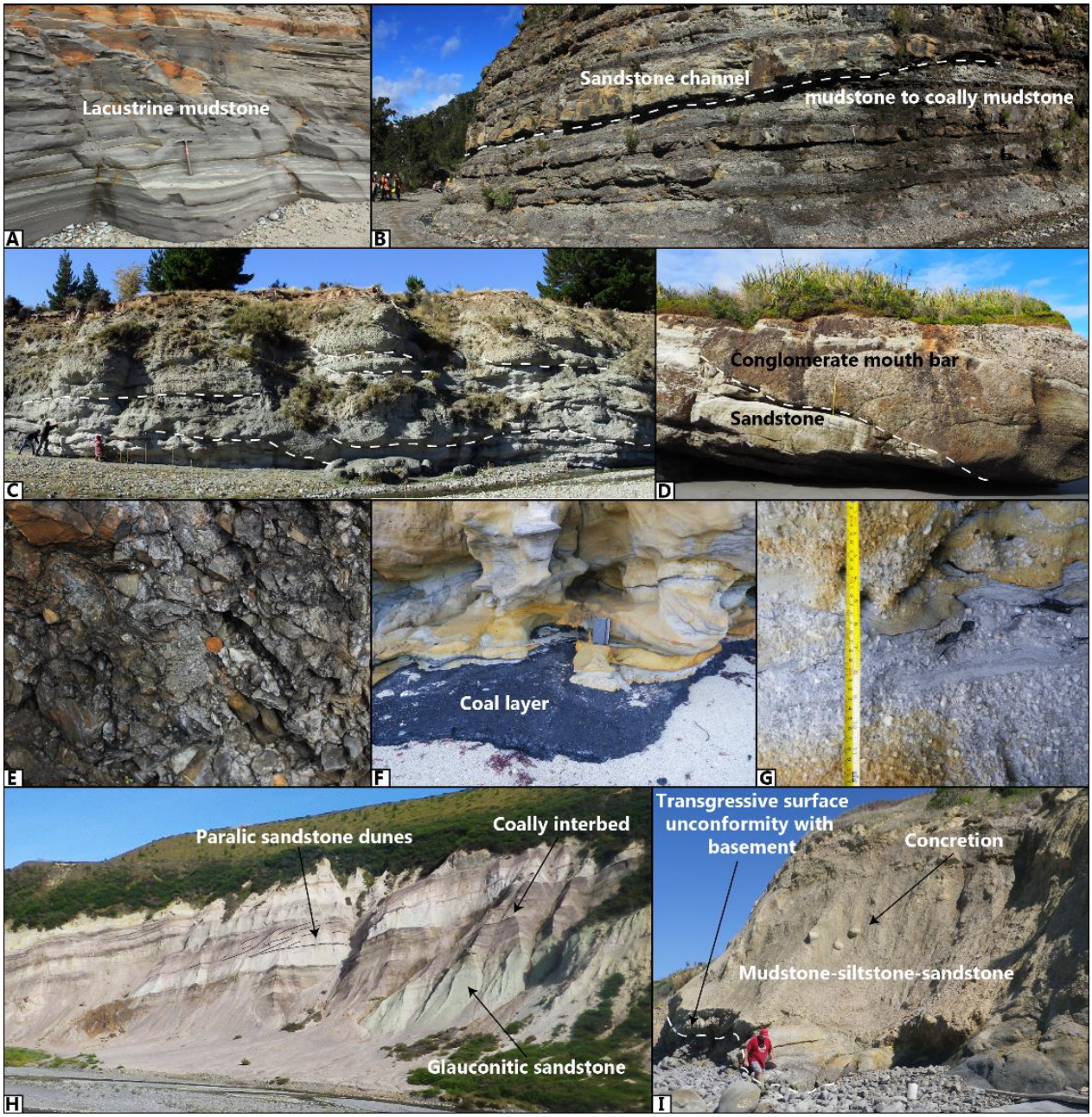

Figure 2.3 Late Cretaceous outcrops of seismic analogues of the Canterbury Basin sediment fill from the Canterbury and West Coast basins: (A) Syn-rift lacustrine mudstone of the Paparoa Formation (West Coast Basin). (B) Syn-rift meandering fluvial sandstone, mudstone and coal alternating from the Paparoa Formation (Spring Creek Mine, West Coast). (C) Syn-rift fluvial conglomerate channel fill, sandstone, mudstone and coal from the Kyeburn Formation (Canterbury Basin). (D) Syn-rift conglomerate mouth bar, Paparoa Formation (West Coast Basin). (E) Syn-rift alluvial fan of the Hawks Crag Breccia Formation (West Coast Basin). (F) Syn-rift paralic sandstone and coal seam from the Pukeiwitahi Formation (Canterbury Basin). (G) Zoom on the coarse paralic sandstone of the Pukeiwitahi Formation. (H) Post-rift paralic sandstone and coal seam of the Broken River Formation (Canterbury Basin). (I) Post-rift shelf mudstone, siltstone to sandstone of the Conway Formation (Canterbury Basin).

2.4. First Order Basin Geometry

The Canterbury Basin rifting created three main depocenters; the Clipper-Galleon-Caravel, Taiepa Nui and the Tawhiti depocenters, which are separated either by horsts or intra basin highs (Figs. 2.4, 2.5 and 2.6).

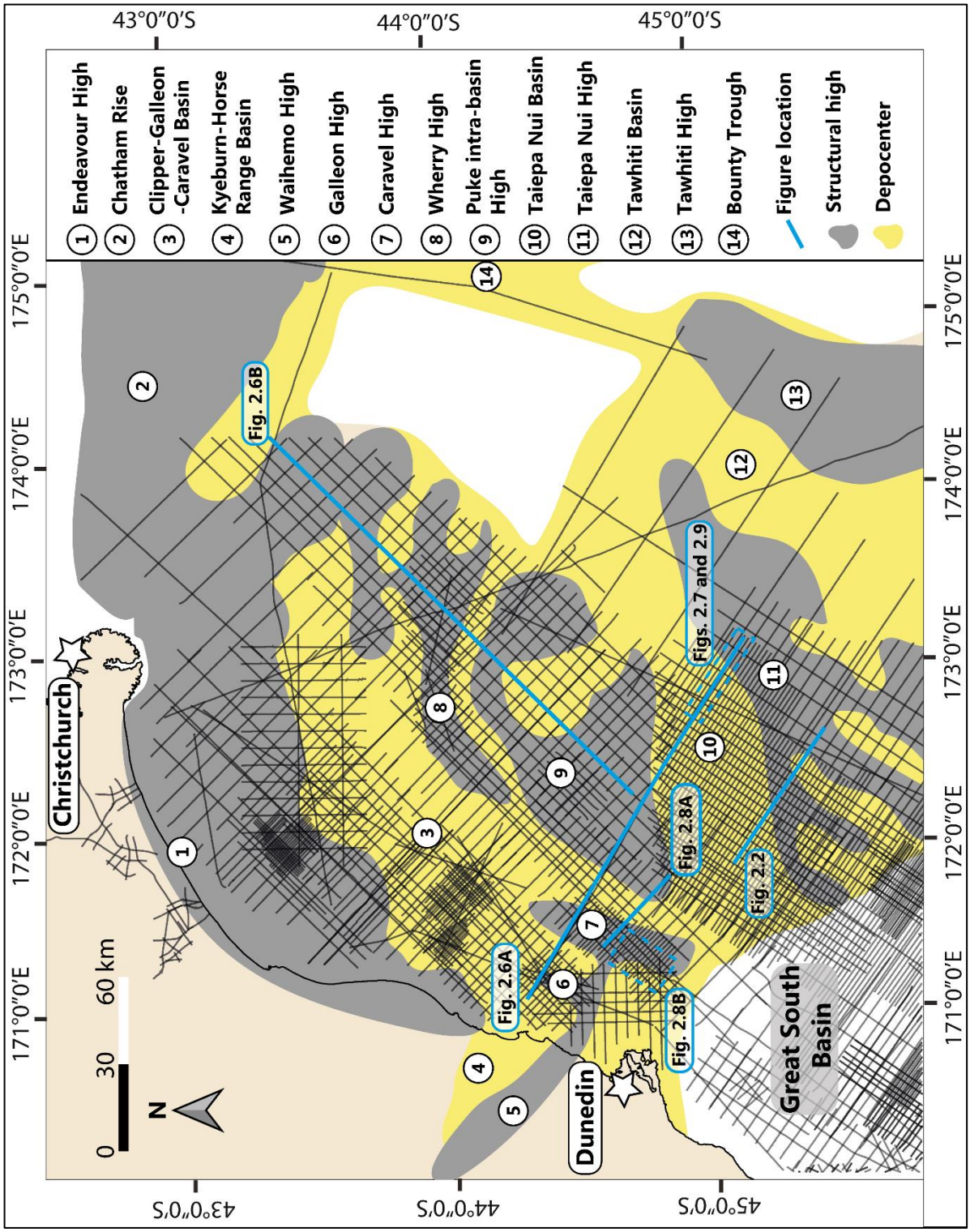

Figure 2.4 Simplified map of rift structural highs and sub-basins nomenclature with location of figures. Rift nomenclature is mostly derived from Field and Browne (1989) and Sahoo et al. (2015). Name 8-13 have been introduced in this thesis. The fault separating a rift basin and horst is named accordingly to thereof.

The Clipper-Galleon-Caravel depocenter is oriented NE-SW to E-W and ~12 000 km^2 in size. It is bounded to the north by the Chatham Rise, to the north-west by the Endeavour High, to the east by the Puke intra-basin High and the Wherry E-W horst. The north-eastern extent of this basin is not covered by seismic reflection data and may extend eastward to the Bounty Trough.

The south-western extent Clipper-Galleon-Caravel depocenter is bounded by the Waihemo Fault but is not well imaged by seismic reflection profiles offshore. The maximum sediment accumulation in the Clipper-Galleon-Caravel depocenter is around 1.2 second TwT adjacent to the Caravel High rift fault. The Taiepa Nui depocenter (the second main basin) is located in the central southern offshore Canterbury Basin, oriented NE-SW and ~ 12 000 km^2 in size. It is bounded to the north-west by the Puke intra-basin high and to the south-east by the Taiepa Nui Horst. Its south-western extent is contiguous with the Great South Basin while its north-eastern extent is not covered by available seismic reflection data and may continue towards the Bounty Trough. The maximum sediment accumulation in the Taiepa Nui depocenter is around 1.7 second TwT adjacent to the Taiepa Nui High border fault. The Tawhiti depocenter, (the third of the main basins, is located in the south-eastern offshore Canterbury Basin and oriented NE-SW. It is poorly covered by seismic reflection data and covers an area of 8 000 km^2. It is bounded to the north-west and south-east by the Taiepa Nui and Tawhiti horsts. The maximum sediment accumulation in the Tawhiti Depocenter is around 0.8 second TwT. These basins are separated by a number of horst blocks. The Puke intra-basin High is up to 80 km wide, oriented NE-SW to E-W, and developed between the Caravel and Wherry highs. Horst blocks width ranges from 6 to 20 km for the Caravel, Galleon or Wherry highs. The faults bounding these highs have vertical displacements of 1-2.8 seconds TwT.

2.5. Basin Sedimentation

2.5.1 Syn-rift (~110 to ~85 Ma)

Syn-rift sedimentation occurred between ~110 and 85 Ma during the initial phase of basin filling. During the syn-rift interval, deposition primarily occurred within grabens produced by normal faulting, along rift bounding faults (Figs. 2.4A and 2.5).

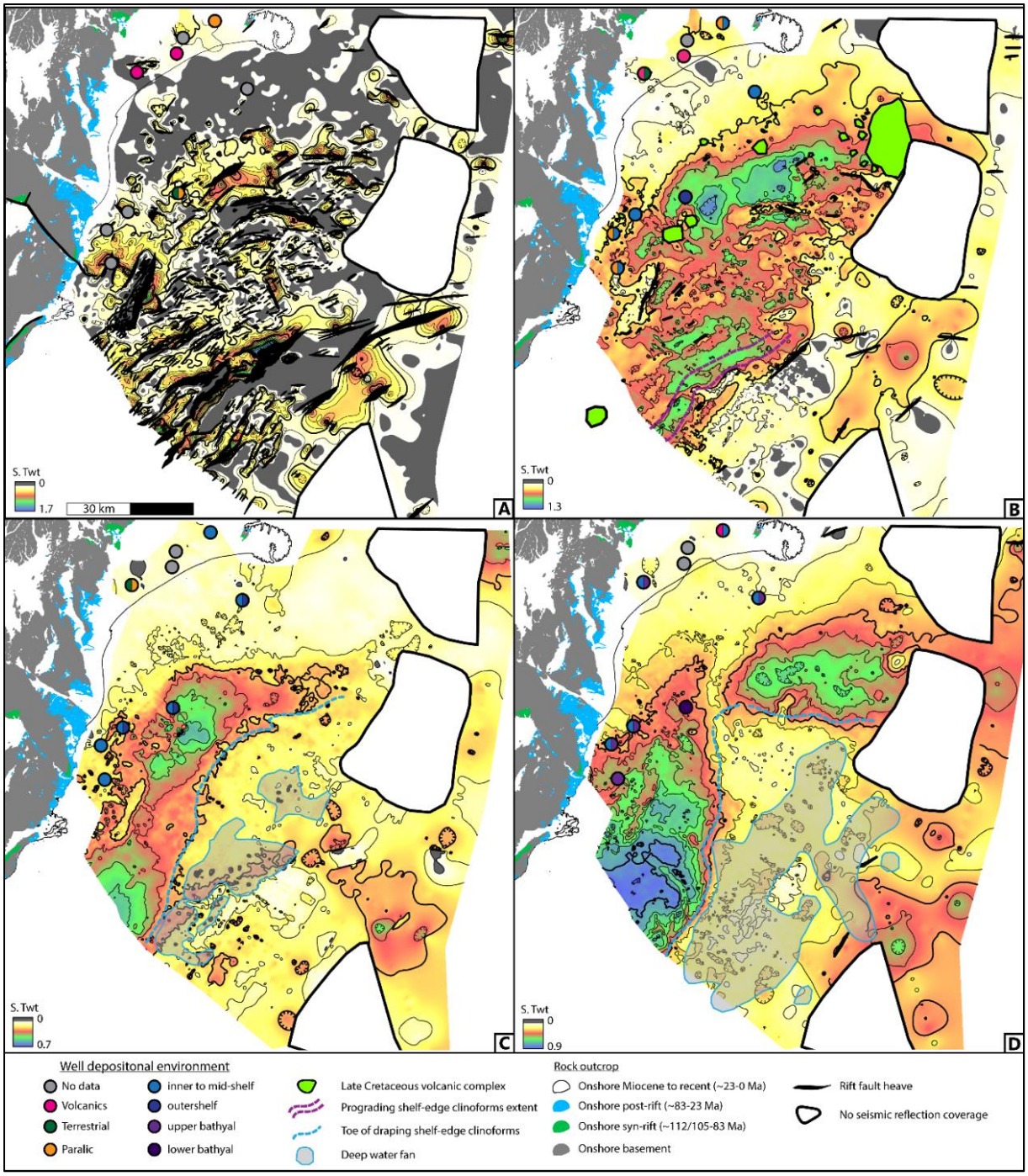

Figure 2.5 Structural isochron maps generated from seismic horizons for (A) Late Cretaceous syn-rift, (B) Late Cretaceous post-rift, (C) Paleocene post-rift and (D) Eocene post-rift. Isochron structural maps show the evolution of the depositional environment for each wells of the Canterbury Basin. See Appendix 3 for individual maps.

2.5.1.1 Sediment Thickness Distribution

The under-filled nature of the Canterbury Basin impacts the geometry of both syn- and post-rift strata. Rift strata in the immediate hanging wall of rift faults can reach up to 1.8 second TwT thickness, however, these thicknesses decrease away from the primary fault over kilometre distances, with sediment condensed or absent on the intra-basin highs (Figs. 2.4 and 2.5). Numerous faults located over basin highs are not covered by thick strata (e.g., >0.5 second TwT). This implies that not many rift faults cross-cut syn-rift strata and therefore their faulting history is barely recorded by sediments. In this case, the under-filling of the rift basin impacts the petroleum potential of syn-rift strata due to the absence of syn-rift fault block traps. Some half-grabens located on structural highs, such as above the Taiepa Nui High, display syn-rift infill of up to 1.4 second TwT while others have little or no infill.

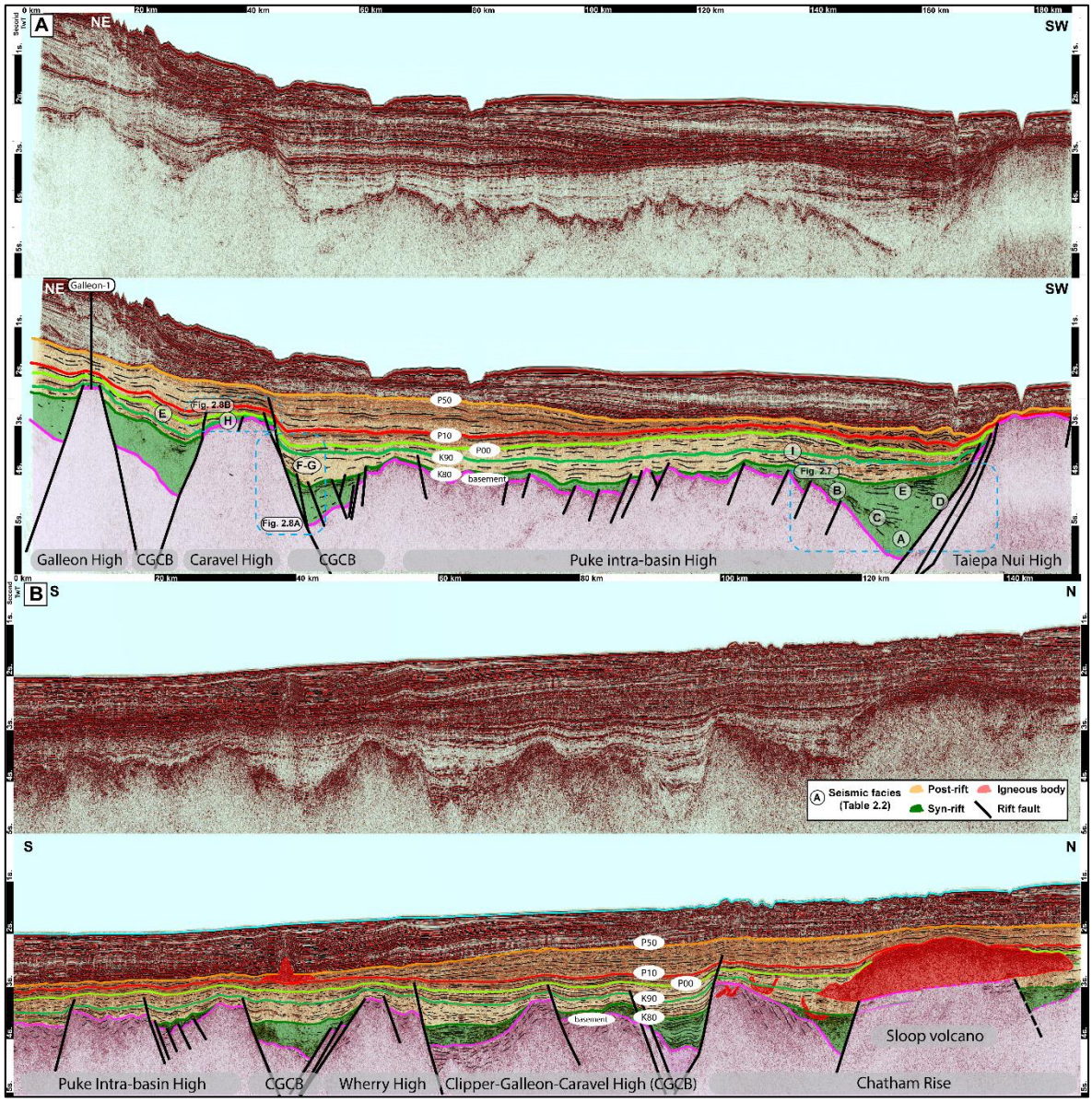

Figure 2.6 Composite seismic profiles offshore Canterbury Basin showing the rift structures and infill geometries across the basin. (A) NW-SE composite section located in the South offshore Canterbury Basin. (B) N-S composite section. Figure and seismic facies locations are indicated on the composite sections. See Figure 2.4 for location. See Table 2.2 for seismic facies.

2.5.1.2 Seismic Facies Identification and Interpretation

Five different seismic facies have been observed in the syn-rift interval (Figs. 2.5, 2.6A and Table 2.2). Seismic facies (A) displays relatively continuous and sub-parallel low- to medium-amplitude seismic reflectors located in the axis of the half-graben. We interpret these seismic facies to correspond to lacustrine rocks forming parallel and continuous strata deposited in the axial portions of the half-graben. Towards the edge of half-grabens, seismic facies (B) comprises relatively discontinuous and sub-parallel medium- to high-amplitude reflectors. Seismic facies (B) is inferred to correspond to braided fluvial systems or deltas that drain from the hinge of the depocenter towards seismic facies (A) in axial parts of the depocenter. The discontinuous pattern of seismic facies (B) could reflect the high heterogeneity of braided fluvial or delta facies while the high-amplitude could correspond to coal seams present in these strata similar to onshore outcrops (Figs. 2.3 and 2.6A).

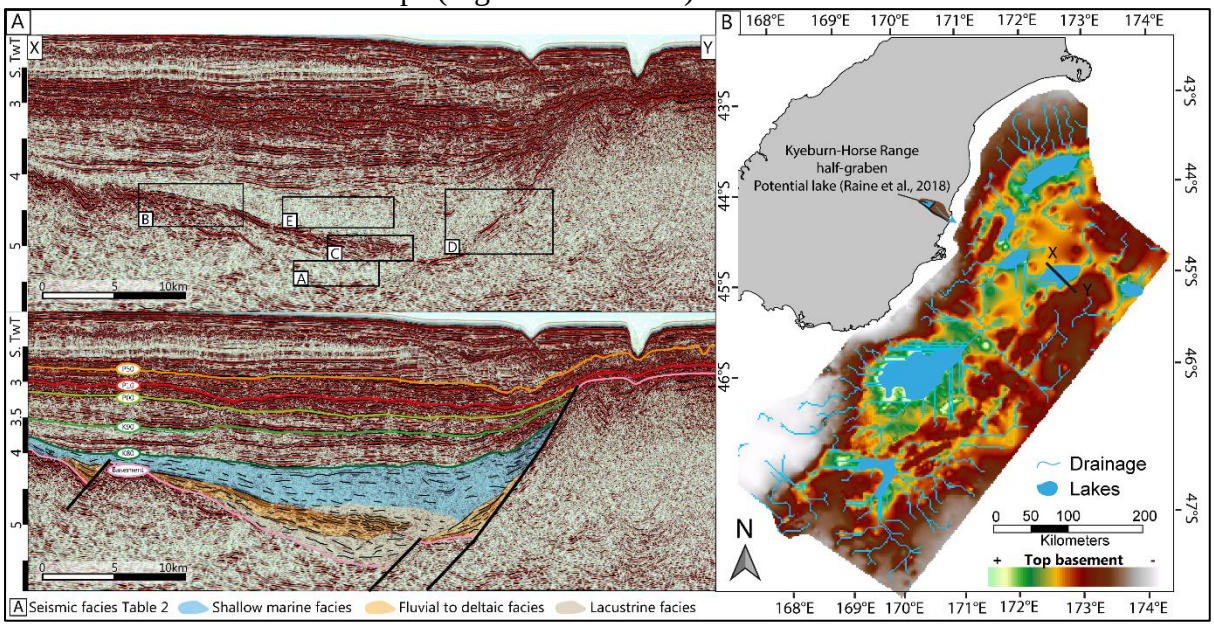

Figure 2.7 Seismic reflection profile across the Taiepa Nui Basin and High illustrating syn-rift seismic facies filling the Taiepa Nui Basin (Left panel). Results of the modelling of drainage on the top basement isochron from Sahoo and Bland (2017) (Right panel). See Figure 2.4 for location.

Seismic facies (B) also grade laterally into seismic facies (C), which is characterised by relatively discontinuous high-amplitudes reflectors, displaying channel fill and wedge geometries. The wedge geometries of seismic facies (C) may represent progradational mouth bar systems of the fluvial/delta system of seismic facies (B) as they entered into seismic facies (A). Seismic facies (D) occurs along fault scarps and comprises relatively continuous low- to high-amplitude reflectors with wedge shaped geometry dipping towards the central portion of the depocenter. Seismic facies (D) downlap from the fault scarp and are inferred to correspond to alluvial fans or fan deltas forming along the fault scarp, flowing into either braided rivers (seismic facies B) or into lacustrine areas (seismic facies A).

The fluvial-lacustrine system represented by seismic facies A to D is overlain by seismic facies (E), covering the whole depocenter and characterized by continuous and sub-parallel low- to medium-amplitude reflectors. Seismic facies (E) covers the largest area of all the seismic facies with continuous deposition across the half-graben. Seismic facies E is interpreted to correspond to paralic-shallow marine or deep-water facies, depending on the location and the extent of the transgression. Seismic facies A to E are imaged on seismic

reflection profile BT10-09M100 (Fig. 2.6A), which is interpreted to display a variation of syn-rift sediment fill from lacustrine to mixed fluvial and deltaic environment settings, to ultimately marine deposition.

As no well has drilled the axis of a half-grabens, the interpretation of these seismic facies remains speculative. However, several data support our interpretations. Indeed, onshore outcrops and Clipper-1 well data indicate the presence of axial and transverse drainage, with braided fluvial systems and alluvial fan to fan delta facies (Schioler and Raine, 2011). Lacustrine siltstone within the Kyeburn-Horse Range half-graben indicates that lakes developed in the Canterbury Basin during rifting (Raine et al., 2018). In addition, similar seismic facies have also been inferred in the Late Cretaceous Great South Basin further south, although again they have not been penetrated by exploration wells (Kirk and Constable, 2010; Sahoo et al, 2014).

2.5.1.3 Formation of Accommodation vs. Sediment Supply

The degree of connectivity and under-filling of grabens is dependent on the relative rates of fault displacement and sedimentation. For the Canterbury Basin, the amount of fault displacement exceeded the rate of sediment infilling of the rift basins at least during their early development. Displacement rate and sedimentation rate (compacted) have been approximated for the Canterbury Basin from measurements of faults with vertical displacements >2 seconds (TwT) converted to depth. Maximum vertical displacement of ~5.2 km occurs along the Taiepa Nui bounding fault (Figs. 2.4, 2.5A, 2.6A and 2.7A) with an average displacement rate of 0.16-0.23 $mm.y^{-1}$ for a 19-32 Myr duration of rifting. Maximum thickness along the Taiepa Nui depocenter (Figs. 2.4, 2.5A, 2.6A and 2.7A) was ~3.4 km with a sedimentation rate (compacted) of 0.11-0.15 $mm.y^{-1}$ for the 19-32 Myr rifting periods. Using the Kyeburn-Horse Range onshore depocenter thickness of 5.5 to 6 km (Figs. 2.4 and 2.7 - Bishop et al., 1976; Mitchell et al., 2009) as an analogue, the syn-rift sedimentation rate along the Waihemo Fault ranges from 0.17 to 0.27 $mm.y^{-1}$ for a 19-32 Myr time interval. These examples constitute the highest rates in the Canterbury Basin region and indicate that fault displacement rates typically were far greater than sedimentation rates.

Comparing minimum and maximum sedimentation rate values from the Waihemo (0.17 $mm.y^{-1}$ to 0.27 $mm.y^{-1}$) and the Taiepa Nui depocenters (0.11 $mm.y^{-1}$ to 0.15 $mm.y^{-1}$), the onshore Waihemo measurements suggest greater sedimentation rate in the current onshore regions, which could be explained by their location closer to the sediment source in the west. The formation of accommodation space during rifting along the Taiepa Nui rift fault was ~1.5 times greater than the corresponding sedimentation rate (Figs. 2.5 and 2.6) and reinforce the notion that the availability of sediments was not enough to keep up with the space created during rifting and is the prime reason for the under-filled nature of the Canterbury Basin.

2.5.2 Late Cretaceous Post-rift Burial (~85 to 66 Ma)

The Late Cretaceous post-rift burial phase of sedimentation occurred from ~85 to 66 Ma, and is dominated by regional subsidence associated with east to west marine transgression. Although the faults were predominantly inactive from ~85-66 Ma, first-order basin topography during this time interval was primarily formed by normal-fault displacements in the syn-rift phase. Structural highs and basins impacted the sedimentation for a protracted period of time, controlling paleo-bathymetry and the sediment distribution. The resulting structural highs in the immediate footwalls of normal faults persisted in the basin topography for at least 30 Myr, with the topography being progressively filled and buried by post-rift sediments.

2.5.2.1 Sediment Thickness Distribution

The Late Cretaceous post-rift isochron map (Fig. 2.5B) shows that the topography generated by faulting continued to influence sediment thickness in the offshore Canterbury Basin. The thickest post-rift Late Cretaceous depocenters corresponded to the broad position of syn-rift depocenters, whereas the thinnest strata were deposited above paleo-horst structures (Fig. 2.5B and 2.6). The thickest Late Cretaceous post-rift strata are located in the Clipper Basin area where ~1.3 second TwT of sediments accumulated (Fig. 2.5B). However, over the Clipper Basin, seismic data is sparse and resolution is poor which hampers seismic interpretation (Fig. 2.4). By the end of the Late Cretaceous, most of the rift structural highs were covered by sediments except in the south eastern offshore where the Taiepa Nui structural high was devoid of sediments and remained a bathymetric high. Large polygenic composite volcanoes of >10 km diameter that formed paleo-highs in the Late Cretaceous post-rift sequence were not draped by sediment at the end of the Late Cretaceous. Towards the north to northwest of the basin, the Chatham Rise and the Endeavour High, a possible rift-faulted structural high (Field and Browne, 1989), formed a ~100 km long structural highs oriented E-W and NE-SW, respectively, that was onlapped by post-rift Late Cretaceous reflectors (Fig. 3).

2.5.2.2 Seismic Facies Identification and Interpretation

Along inactive fault scarps, sedimentary wedges downlap onto growth strata, onlap the fault scarp, and pinch out basin-ward (Fig. 2.8A and Table 2.2). They can be divided into two groups with distinctive seismic facies. The first seismic facies (F) corresponds to relatively continuous medium- to high-amplitude reflectors while a second type (G) display chaotic low- to medium-amplitude reflectors. Seismic facies (F) and (G) are thought to represent sheet-flood dominated, and debris-flow dominated strata (Fig. 2.8A and Table 2.2 - e.g., Blair and McPherson, 1994) as they both correspond to reflector packages downlapping from a fault scarp. Seismic facies (F) and (G) differ in their internal architecture. Seismic facies (F) displays relatively continuous internal reflections which could correspond to deposits transported by fluid gravity flows forming a bedded internal organisation (e.g., sheet-floods. Blair and McPherson, 1994). Whereas, seismic facies (G) is more chaotic and could correspond to the poor sorting and mixing of sediment gravity flows deposits (e.g., rock falls, rocks slides, debris flows; Blair and McPherson, 1994). The stacking of these two processes formed sedimentary wedge geometries, typically developing along inactive fault scarps. The rift fault bounding the

Caravel Horst on its eastern side, shows one such sedimentary wedge extending ~10 km from the footwall of the fault, over an area of ~390 km^2. A transverse drainage system was active during the Late Cretaceous post-breakup phase, as rift structures still dominate the paleo-landscape, providing a source for sediments in adjacent depocenters. These sedimentary wedges can either be interpreted as alluvial fans which flowed into a river, or a fan delta in situations where they flowed into lakes or the sea.

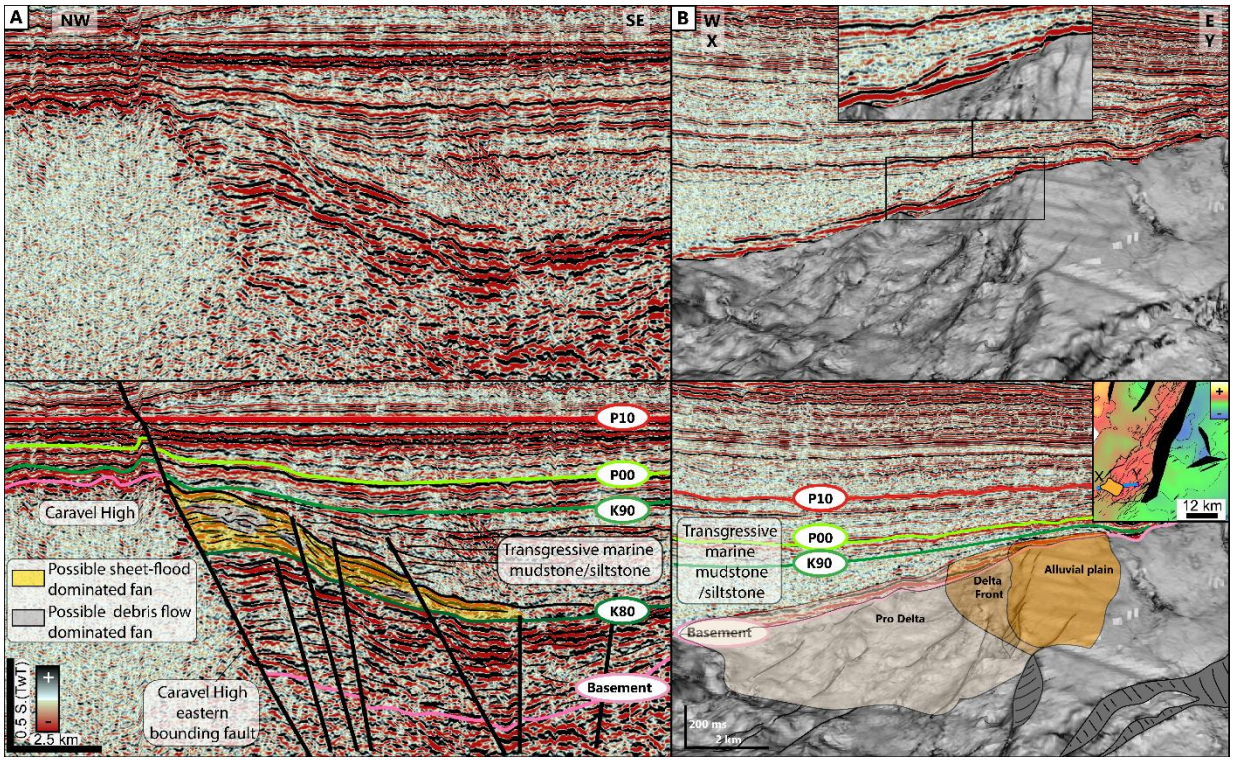

Figure 2.8(A) Seismic reflection profile flatten on top Paleocene horizon, showing post-rift alluvial fan or fan delta developing along a paleo-fault scarp. (B) Seismic reflection profile showing delta on the top of the Caravel High and top basement grid with dip of maximum similarity attribute showing fault affecting the top basement. See Figure 2.4 for location.

Structural highs often have a flat top geometry which we infer to represent sub-aerial/marine planation and erosion. Both types are consistent with sediments being generated from these topographic highs (Fig. 2.6). The Waka 3D seismic survey over the Caravel High shows 5 km long sigmoid reflector geometries of seismic facies (H) with topset, foreset, and bottomset geometries. They are up to 2 km wide and around 0.1 second TwT thick (Fig. 2.8B). Seismic facies (H) is onlapped by post-rift strata equivalent to seismic facies (E) that exist in most of the offshore Canterbury Basin and were drilled at Clipper-1, Cutter-1, Endeavour-1, and Resolution-1 wells. Seismic facies (H) could correspond to accretionary delta scale clinoforms of ~32 km^2 size for which, topset, foreset, and bottomset could represent the alluvial plain, delta front, and pro-delta facies of a prograding delta complex respectively (Fig. 2.8B and Table 2.2, Patruno and Helland-Hansen, 2018). This delta developed along a normal fault with ~100 ms TwT of throw which formed a steep slope over a few kilometres across a previously active normal-fault scarp (Fig. 2.8B). Such sedimentary systems characterised by a high-angle sedimentary slope over short distances may represent Gilbert fan deltas (e.g., Colella, 1988). Throughout the basin, such deltas were subsequently onlapped and overlain by marine transgressive facies (seismic facies E) that progressively buried the rift structural highs (Table 2.2 and Fig. 2.8B). These deltas highlight the presence of a local source for sediments

toping structural highs during the Late Cretaceous and is consistent with petrographic studies that suggest local sources of sediment were common (Higgs et al., 2019).

Towards the south-east of the study area, medium- to low-amplitude, relatively continuous and sigmoidal seismic reflectors (Seismic facies I) are present for ~120 km along the western margin of the Taiepa Nui Basin (Table 2.2 and Fig. 2.6). Seismic facies (I) form up to 10 km wide and 0.3 second TwT high sigmoids, and here are interpreted to represent accretionary shelf-edge clinoforms (Fig. 2.5B - Patruno and Hansen-Hallen, 2018).

2.5.3 Paleocene-Eocene Post breakup Rift Structures Draping (66- 34 Ma)

Paleocene to Eocene (66-34 Ma) strata drape and bury remnant structural highs that impacted the paleobathymetry until the Late Paleocene. Sedimentation records progressive increases in water depth with draping of structural highs at least partly due to differential compaction of the sedimentary succession.

2.5.3.1 Sediment Thickness Distribution

The Paleocene isochron map (Fig. 2.5C) shows that the majority of the rift structural highs of the basin were covered with sediments by the end of the Paleocene. The largest Paleocene sediment accumulation (~0.4±0.1 second TwT thick, 45±10 km wide and 300 km long) straddles the present-day coastline along the NE-SW trending Clipper Basin, and rotates into an E-W trend along the northern edge of the basin (Fig. 2.5C). However, a drastic thickness reduction of the Paleocene reflectors package from ~0.4 to 0.2 second TwT is observed east from the Caravel High (Figs. 2.5C and 2.6A). Over the Caravel High, the Paleocene section appears to be even more condensed comprising ~0.1 second TwT of Paleocene reflectors (Figs. 2.5C and 2.6A). In the southeast of the Canterbury Basin, the Tawhiti Basin contains a ~0.5 s TwT thickness of Paleocene strata at its depocenter. The thinnest accumulations of Paleocene reflectors are <0.1 s TwT and are observed above buried rift structural highs or Late Cretaceous volcanic edifices (Figs. 2.5C and 2.6).

The Eocene isochron map shows that only the Galleon, Caravel, and Taiepa Nui highs affected the sediment distribution during the Eocene (Figs. 2.5D and 2.6). The thickest Eocene sediment accumulation has a similar location to the Paleocene depocenter but is wider (~52±10 km wide), thicker (~0.8±0.1 second TwT), longer (430 km) and extends further to the east in the northern section of the offshore Canterbury Basin (Figs. 2.5D and 2.6). Unlike for Paleocene time, the Eocene accumulation east of the Caravel High, does not display a thickness reduction. At the inflexion point of the thick accumulation of Eocene strata, the top Eocene horizon is affected by Oligocene erosion which reduced the thickness of the Eocene reflectors (Fig. 2.5D - Sahoo *et al*., 2015a). The thickness of Eocene strata in the south-eastern part of the basin was influenced by the NE-SW structural depression along the Taiepa Nui High where the thickness of the Eocene reflector reaches up to 0.4 second TwT (Figs. 2.5D and 2.6). The Taiepa Nui High was sediment starved in the Late Cretaceous to Eocene with only 0.2 second TwT of strata on the high which is similar to the 0.3 second TwT thickness of post-Eocene strata (Figs. 2.5D and 2.6). Similar to the Paleocene strata, the Tawhiti Basin displays the thickest accumulation of sediments in the south-eastern Canterbury Basin.

2.5.3.2 Seismic Facies Identification and Interpretation

The Paleocene reflector package displays a ~100 km wide and ~0.6 second TwT thick draping sigmoid geometry, downlapping towards the south-east which is characterised by seismic facies (J) (Table 2.2 and Fig. 2.6). Seismic facies (J) displays continuous low- to medium-amplitude seismic reflectors dipping towards the south-east and are partially affected by polygonal faulting (Fig 2.6 - Sahoo et al., 2015). The polygonal faulting is widespread throughout the Paleocene and Eocene, most likely reflecting the fine-grained nature of the sediments (Sahoo et al., 2015). Seismic facies (J) corresponds to the development of draping shelf-edge clinoforms that graded eastward into more distal facies. By the Paleocene, seismic facies (J) developed towards the south-east along a NE-SW axis ~200 km long.

More distally, towards south-eastern parts of the basin, seismic facies (K) and (L) can be observed (Table 2.2, Figs. 2.6 and 2.9). Seismic facies (K) comprises of a condensed interval of relatively continuous to discontinuous medium- to high-amplitude seismic reflectors with parallel to chaotic geometry. Seismic facies (K) passes laterally to seismic facies (L) which is characterised by bi-directional downlapping reflectors, forming a mound shape with medium- to high-amplitude reflectors that filled the Taiepa Nui Basin. The top of the mounds display channel geometries of unknown orientation due to the poor resolution and spacing of the seismic reflection lines. Located at the toe of the draping shelf-edge clinoforms, seismic facies (K) could correspond to a pelagic basin floor. Seismic facies (K) passes laterally to seismic facies (L) that has been interpreted in the literature as both toe-of-slope fans and more laterally extensive basin floor fans in cross section (Mitchum *et al.*, 1985; Bally, 1987; Feeley *et al.*, 1990). These deep-water sediments have not previously been recognised in the Canterbury Basin, though similar Paleocene deep-water fan deposits were interpreted in the Great South Basin by Plampton (2018) and in slightly younger intervals by ExxonMobil (2010), Kirk and Constable (2010) and Sahoo *et al.*, (2014). The distal part of the basin was characterized by a NE-SW depression along the Taiepa Nui high formed by differential compaction between horst and depocenters creating depressions filled by deep-water sediments of seismic facies (L) (Figs. 2.5C and 2.6). Thickness variations of the draping shelf-edge clinoforms and the formation of a depression where deep water fans accumulated are consistent with differential compaction of the basin fill across the highs.

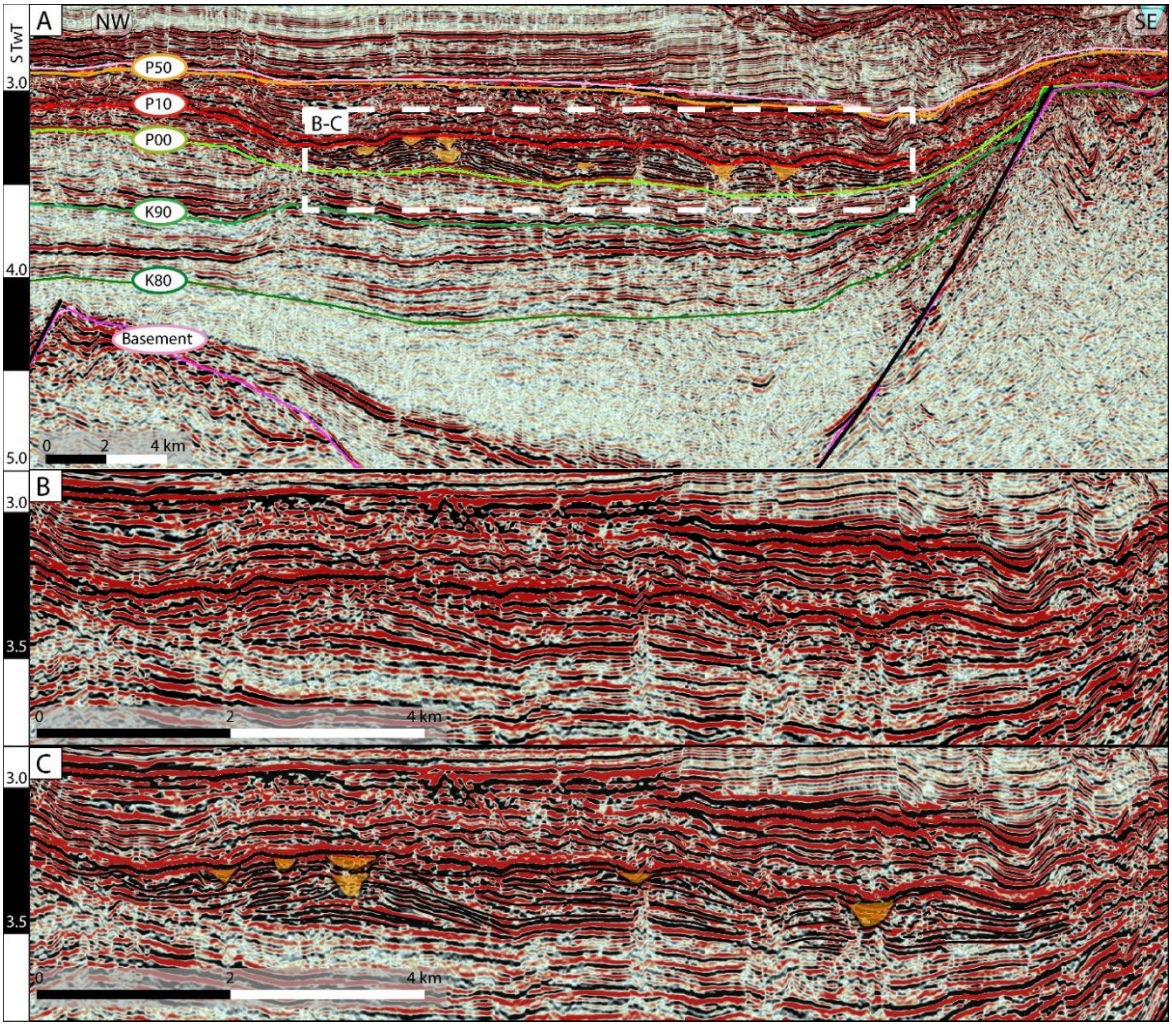

Figure 2.9 Seismic reflection profile across the Taiepa Nui Basin showing Paleocene deep-water fan seismic facies. See Figure 2.4 for location

The three seismic facies observed in the Paleocene (J, K, and L) are also present in the Eocene (Figs. 2.6 and 2.9). Seismic reflection profiles striking NW-SE and N-S show Eocene shelf-edge draping clinoforms of seismic facies (J) pinching out towards the basin (Figs. 2.5D and 2.6). These clinoforms are ~100 km wide but their height is up to 0.9 second TwT, ~0.3 s TwT thicker than the Paleocene clinoforms. Eocene clinoforms extended further east and south into the offshore Canterbury Basin than Paleocene strata. The clinoforms may record an increase in sediment supply to the basin in the Late Eocene (see section 6.3 for further discussion).

2.6. Paleogeographic Evolution

2.6.1 Syn-rift Basin and Range Topography

Syn-rift sedimentation records initial fluvial to lacustrine environments followed by regional marine transgression. The modelling of a drainage system pattern using the top basement isochron map of Sahoo and Bland (2017), shows that the primary paleoflow direction of fluvial systems was likely west to east into the Canterbury Basin. Within the Canterbury Basin the majority of the under-filled depocenters were disconnected and principally fed by short drainage systems from local structural highs. The paleo-drainage modelling suggest five main potential lacustrine accumulations, surrounded by fluvial systems at the margins of these depocenters (Fig. 2.7B). The modelling is supported by the onshore Kyeburn-Horse Range half-graben where lacustrine setting occurred and may have drained towards the SE (Raine et al., 2018). By analogy, outcrops and drill core from the Greymouth Basin on the West Coast of New Zealand's South Island, show mid and Late Cretaceous alluvial fan and fan deltas facies forming adjacent to faulted margins, transitioning into lacustrine units within the central portions of depocenters (Fig. 2.3A, B and D - Laird, 1995; Maitra and Bassett, 2017).

Turonian-Cenomanian tidally influenced shallow marine sediments (Browne, 2003) drilled at Clipper-1 indicate that by ~93 Ma, the sea must have already reached the western offshore Canterbury Basin, and is consistent with the paleogeographic maps presented by Sahoo et al. (2015). The depocenter became increasingly connected to the sea as marine transgression progressed, allowing for the up-sequence transition from paralic, shallow marine to deep-water sedimentation (Fig. 2.4). By contrast, some of the larger structural highs (e.g., associated with > 1 km fault displacement) may have remained above sea level. Half-grabens located on the tops of these highs must be filled with a continental succession due to their elevated topographic position, with respect to the rest of the basin (e.g. Taiepa Nui High, Fig. 2.5).

2.6.2 Late Cretaceous Post-Rift Submersion

The Late Cretaceous post-rift interval is characterised by progressive transgression of the rift structural highs. After the onset of Gondwana breakup at ~85 Ma, rift structural highs remained physiographic features that were slowly topped by post-rift sediments until the end of the Eocene (~34 Ma). The evolution of the depositional environments at exploration wells and onshore outcrops indicate a progressive east to west migrating shoreline during this transgression during the Late Cretaceous (Fig. 2.5).

By the start of the Campanian time (~84 Ma), most of the fans formed along inactive normal-fault scarps were being transgressed, and with time, deltas emanating from the top of horsts were also becoming submerged by marine transgression. Many of the horsts were probably subjected to wave reworking in high-energy littoral settings, before being submerged below wave base, where they were buried by extensive pelagic sediments (Figs. 5 and 7B). Because the marine transgression progressed from east to west, the over topping of western horsts was later than over horsts in the east of the Canterbury Basin. Indeed, the extreme western part of the basin received only a thin veneer of sediment from Late Cretaceous to Eocene time, and conversely, the eastern offshore horsts maybe have been submerged rapidly

to allow thick siliciclastic sedimentation on structural highs. The above statement is valid for faults with similar and sufficiently large fault throw to form a persistent horst structure (e.g, >1.5 second TwT).

The eastward increase of Late Cretaceous water depths is consistent with the presence of prograding shelf edge deltas with associated shelf-slope-basin floor transitions in the Canterbury Basin (Figs. 2.5B and 2.6). Upstream from the seismic facies (J) sigmoids, the Canterbury Basin comprises of a shelf with either submerged or emergent structural highs. Downstream, the clinoforms prograded towards the depression formed by the Taiepa Nuit High where they are interpreted to suggest the presence of a basin floor between the toe of the sigmoids and local rift-related highs which were not buried. Although, no basin floor fan geometries are observed on the 2D seismic reflection lines in the deeper basin, they have been recognised in a high-resolution 3D seismic survey in the Great South Basin (Plampton, 2018).

2.6.3 Paleocene to Eocene Draping Shelf-edge Clinoforms Development

The Paleocene to Eocene depositional environment was predominately marine with local variation in water depths being mainly controlled by topography generated during rifting and draped by post-rift sediments. On a regional scale Paleocene to Eocene strata record a westward progression of the marine transgression associated with development of a shelf edge. Paleocene strata in the south-eastern offshore Canterbury Basin correspond to discrete deep-water fans. This contrast with Late Cretaceous strata of the same area where deep water fans may have accumulated, but do not correspond to discrete features recognisable on seismic data. Eocene deep-water fans are observed over a larger area and are thicker than their Paleocene equivalents (Figs. 2.5D and 2.9). The increase in thickness and lateral extent of shelf-edge clinoforms from the Paleocene to the Eocene could indicates a change in sediment supply, a reduction of the accommodation to the west towards the hinterland, or the creation of accommodation space in the basin. These mechanisms may reflect tectonic uplift in the western part of the basin, or a greater amount of subsidence in the distal part of the basin due to thermal and loading subsidence. Shelf-edge clinoforms are also observed along the southern edge of the Chatham Rise and indicate the presence of land in this area during the Eocene as inferred by Wood *et al (*1989). To the south-east, the geometries of post-Eocene reflectors across the top of the Taiepa Nui High indicate that it remained a physiographic feature on the seabed after the high was buried during the Eocene (Figs. 2.5 and 2.6).

2.7. Discussion

2.7.1 Rift Under-filling

The syn-rift sediment thickness was variable in the different Late Cretaceous rift basins of Zealandia. The Canterbury Basin, received less sediment for a given fault throw than the Great South or Taranaki basins for example (Fig 2.10 - Arnot and Bland, 2016; Sahoo and Bland, 2017) and reinforce the notion that the Canterbury Basin was not promoting sediment accumulation compared to other rift basins across Zealandia.

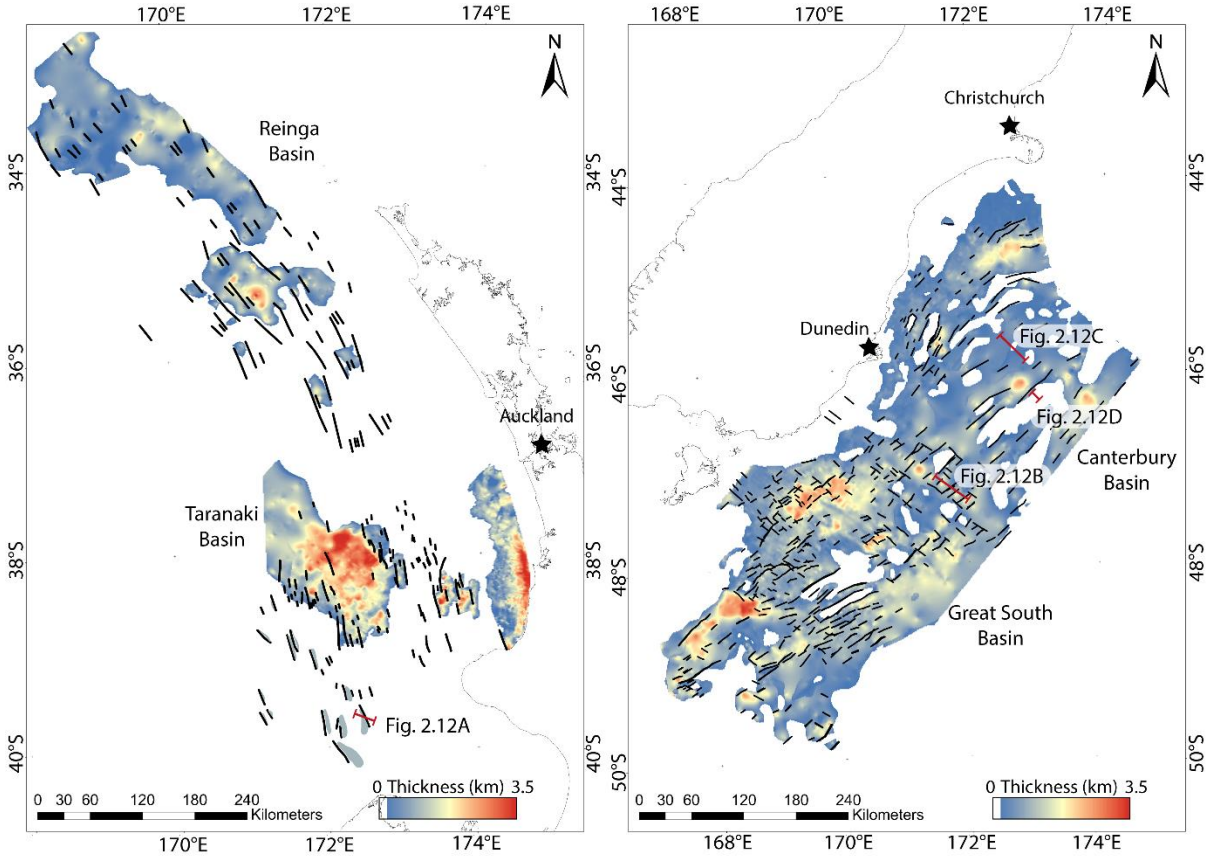

Figure 2.10 Isochron maps of syn-rift Late Cretaceous strata in the offshore Taranaki-Reinga, northern Zealandia and Canterbury-Great South basins, southern Zealandia (data from Arnot & Bland, 2016; Sahoo & Bland, 2017).

Depocenters created by large normal-fault displacements (e.g., >1 km) within the Canterbury Basin were under-filled during the syn-rift phase of basin history. For these basins, the rates of sedimentation were not sufficiently high to fill the available space created by fault displacement on basin-bounding faults. Sediment thickness varies considerably in the different depocenters mapped within the study area. Sediment feeding into the Canterbury Basin was likely sourced from local sources such as fault scarps and associated topography (as suggested by Higgs et al., 2019), or long-travelled routes via fluvial transport from the wider Gondwana landmass (as suggested by Mitchell et al., 2009). We think the volume of sediment supplied to the rift basin was likely controlled by several factors such as climate, topography, the geometry of the drainage system, sediment transport distances, and whether the sediment was transported or alternatively broken down to silts or clay during transport (i.e., sediment competence).

Below we considered how each of these factors could have contributed to a low sediment supply.

2.7.1.1 Climate

This portion of Zealandia during the mid-Cretaceous was at a high southern latitude of 85-70°S (Fig. 2.11B) implying important seasonal variation in light (daylight and night-time darkness) as well as climate, with an average temperature ~10°C under a wet polar climate (Pole, 1995; Parrish et al., 1998; Fordyce, 2006; Pole and Philippe, 2010). Under these climatic factors southern Zealandia was most likely able to support a diverse vegetation as is indeed indicated from the macrofossil and palynological record (Daniel et al., 1988; Schiøler and Raine, 2011; Raine et al., 2018). It is reasonable therefore to assume given the above, that weathering and erosion were prominent and able to provide sediment supply to depocenters, and thus the climate should have been conducive to providing sufficient sediment to fill the basin.

2.7.1.2 Topography and Transport Distance

Although we are not able to quantify topographic elevation, the paleo-topography of the Gondwana landmass making up the hinterland would likely have had considerable relief created during the preceding Late Jurassic-Early Cretaceous subduction and forearc phases (Fig. 2.11A – e.g., Laird and Bradshaw, 2004; Mortimer et al., 2014).

A major drainage divide has been suggested through Zealandia by different authors (e.g., Tulloch et al., 2006; Adams et al., 2017) between Reinga-Taranaki-East Coast-Canterbury basins on one side and the West Coast-Great South basins on the other. The inferred topographic divide was approximately located along the Median Batholith and some have described it as a Cretaceous "Cordillera Zealandia" mountain range (Fig. 2.11B – Tulloch et al., 2006). Such a topographic divide would have seen basins in the east (including Canterbury) receiving sediment from the west. Basins near to this divide, for example, the West Coast, Taranaki and Great South basins, were filled with sediment from nearby topographically elevated basement source regions of Median Batholith, Rahu Suite granitoids and the Paleozoic Buller Terrane of the Western Province (Adams et al., 2017; Higgs and King, 2018; Higgs et al., 2019). Canterbury Basin was more distant to these sediment-forming basement terranes than the West Coast, Taranaki and Great South basins. In general, the presence of a topographic divide would increase the sediment supply, but because Canterbury was a location distant to this topographic divide, the supply of sediment would likely have been less than those basins located in a more proximal setting adjacent to the topography (e.g., Great South Basin). On the northern margin of the Canterbury Basin, the Hikurangi Plateau formed a broad submerged zone with no substantial landmass present and together with the largely subdued Chatham Rise, were unlikely to provide a lot of sediment into the Canterbury Basin (Fig. 2.11).

Sediment provenance analysis of Zealandia rift basins indicate that during rifting, sediments were not sourced from the interior of eastern Gondwana landmass (Adams et al., 2017). Adams et al. (2017) proposed that uplift during the rifting along the future spreading centre would have cut any river system drainage coming from the interior of eastern Gondwana, therefore, most

of the sediment catchment was local to Zealandia (Fig. 2.11B). Petrographic work by Higgs et al. (2019) show that most of the sediment deposited during the syn-rift period were derived from local basement source lithologies (Torlesse Composite Terrane and schists for the Canterbury Basin as opposed to Median Batholith and schists for the adjacent Great South Basin, Fig. 2.11). These petrographic conclusions support the detrital zircon ages of Adams et al. (2017), that indicate the Canterbury Basin was furthest from the Zealandia highlands, with the least diversity of sediment source compared to other basins of Zealandia (Fig. 2.11B).

We have modelled the drainage system for the Canterbury-Great South basins during the Late Cretaceous (Fig. 6B) and it suggests that both axial and transverse drainage systems could have existed. However, transverse and short sedimentary systems with small catchment areas coming from adjacent structural highs are thought to have dominated, consistent with the work of Higgs et al. (2019), while axial long-distance transports (over ~100 km) have been interpreted for the onshore Kyeburn-Horse Range Formation may also have existed (Mitchell et al., 2009). Modelling supports a paleo-drainage system converging towards what would have corresponded to lakes in central portions of the basin especially during the early phase of the rifting. These lacustrine areas appear to be larger in the Great South Basin further south, where the drainage patterns are modelled to be longer and also display larger catchment areas (Fig. 6B). The under-filled nature of the Canterbury Basin and the dominance of short-drainage systems could indicate that a substantial sediment input from outside of the rift basins would be required to completely fill the accommodation created by rifting.

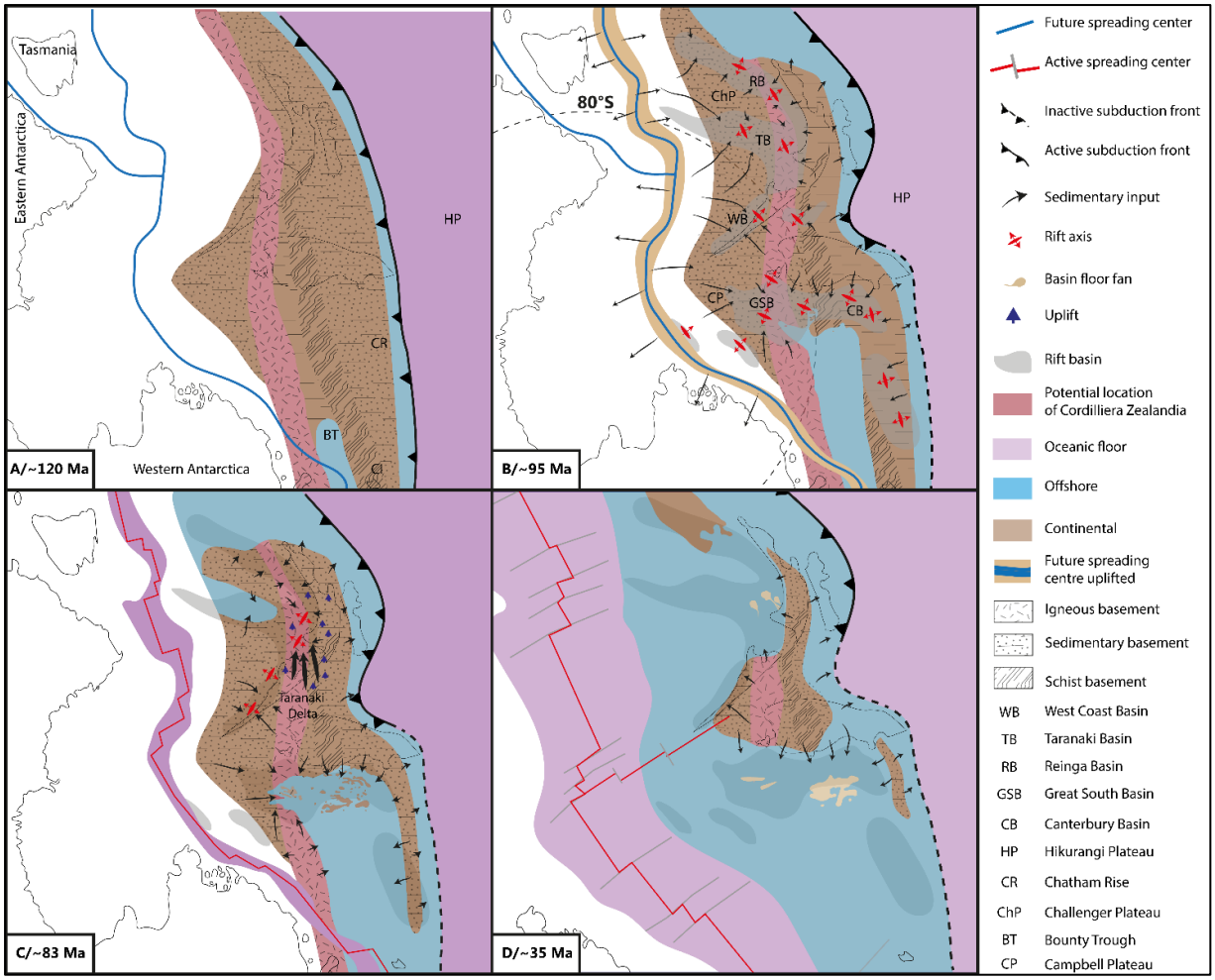

Figure 2.11 Zealandia geodynamic and paleogeographic reconstruction showing the evolution of the landmass surrounding the rift basins and associated sediment input as well as the evolution of the marine transgression (modified from Nicol et al., 2007; Arnot and Bland, 2016; Adams et al., 2017; Sahoo and Bland, 2017; Strogen et al., 2017; Mortimer, 2018). A) Geodynamic reconstruction before the onset of the Zealandia rifting, B) during eastern Gondwana breakup, C) after eastern Gondwana breakup, D) during the Eocene.

2.7.1.3 Sediment Competence

The bulk of the sediment that contributed to the filling of the Canterbury Basin was derived from the lithic-rich greywacke and schist metasediments of the Eastern Province (Higgs et al. 2019). These basement terranes would have contributed a combination of hard and resistant medium- to fine-grained quartz which would erode to produce sand grains, and an abundance of less resistant lithics, micas, and feldspar that ultimately break-down to mud. The greywacke contains secondary mineral such as zeolite and prehnite-pumpellyite, and the schist chlorite (Bishop and Turnbull, 1996), that are not resistant to weathering and transport and would also break down to muds. Mud has the ability to be transported great distances, and may have been retained in suspension and therefore not be retained within the confines of the Canterbury Basin. Other rift basins of Zealandia however, had more igneous sediment source areas (from the Tuhua Intrusives - Karamea, Darren and Separation Point batholiths) in their catchments, that would produce a higher proportion of sand-forming quartz than the greywacke and schist dominated basement source rocks of the Canterbury Basin. It is possible therefore, that the basement rocks of the Canterbury Basin produced less sand or coarse-grained detrital material to fill the depocenters, relative to the basement lithologies in similar aged basins

elsewhere in Zealandia. We think the majority of sediment produced was fine-grained, and may have been transported and deposited outside of the Canterbury Basin thus contributing to the under-filled nature of the Canterbury Basin.

2.7.2 Post Breakup Landmass Evolution

After breakup of eastern Gondwana at ~85 Ma, Zealandia drifted away from Australia and Antarctica, forming an isolated landmass feeding sediment into the eastern and northern basins of Zealandia. The paleo-latitude decreased as Zealandia moved northward with generally an increasing paleo-temperatures from the Late Cretaceous into the Tertiary (Pocknall, 1989; Kennedy, 2003; Vajda and Raine, 2003; Browne *et al.*, 2008; Kennedy *et al*., 2014; Hollis *et al.*, 2014, 2015). Immediately post breakup, during the Late Cretaceous, it appears that the Canterbury Basin received less sediment than the Great South and the northern basins of Zealandia (Arnot and Bland, 2016; Sahoo and Bland, 2017). At the beginning of the post breakup phase (i.e. ~83 to 80 Ma) the Taranaki Delta, which represents shelf edge clinoform progradations, was developing in northern basins due to an increase in erosion in the region (Fig. 2.11C - Strogen *et al.*, 2017). Strogen *et al*. (2017) has related the increase in sediment influx to a brief period (~3 Ma) of uplift and erosion, following the breakup of Eastern Gondwana at ~83 Ma. This erosion was mostly directed towards the northern basins instead of being equally distributed between the north and south regions, as no such sediment input is recognised in any of the southern basins. However, in the Canterbury Basin, intra Late Cretaceous post-rift prograding shelf-edge clinoforms, observed towards the south-east, could correspond to a similar progradational event of smaller extent and magnitude. It developed towards the south-east throughout the entire Late Cretaceous post-rift as opposed to only after breakup (e.g. Taranaki Delta), and could be referred to as the Canterbury Basin Late Cretaceous Prograding Complex. However, this interpretation is only based on seismic facies analysis and is yet to be proven by exploration wells.

Marine transgression proceeded more rapidly in the Canterbury Basin and Great South Basin compared to the Reinga-Taranaki basins during the Late Cretaceous to Eocene (Figs. 2.11C and 2.11D). Active extension continued until the Late Paleocene in northern Zealandia rift basins, creating space to accommodate sediment and the marine transgression (Strogen *et al*., 2017). By contrast, the Canterbury Basin and Great South Basin were undergoing a quiescent phase from ~85 Ma with formation of accommodation space mostly driven by thermal and load subsidence.

The Eocene marks the onset of extension in the Emerald-West Coast basins and to compression and inversion in the Taranaki-Reinga basins (Fig. 2.11D - King, 2000; Stagpoole and Nicol, 2008; Reilly *et al.*, 2015). The regional scale effects of these tectonic activities in the Eocene could have had some impact on the Canterbury Basin, where we observe an eastward progradation of a shelf-edge clinoform system and increase in sedimentation rates.

2.7.3 Differences of Late Cretaceous Regional Uplift Between Northern and Southern Zealandia

Comparing the remnants of the Gondwana rift phase of the Taranaki Basin (Strogen *et al.*, 2017) with the buried geometries of the rifting of the Canterbury and Great-South basins, we can observe two different states of preservation for the coeval rift systems (Figs. 2.11 and 2.12). In the south-west Taranaki Basin, most of the mid-Cretaceous half-grabens display a strong erosional truncation where both syn-rift strata and footwall of half-grabens have been planated and overlain by Late Cretaceous post-rift reflectors (Fig. 2.12A - Strogen *et al.*, 2017).

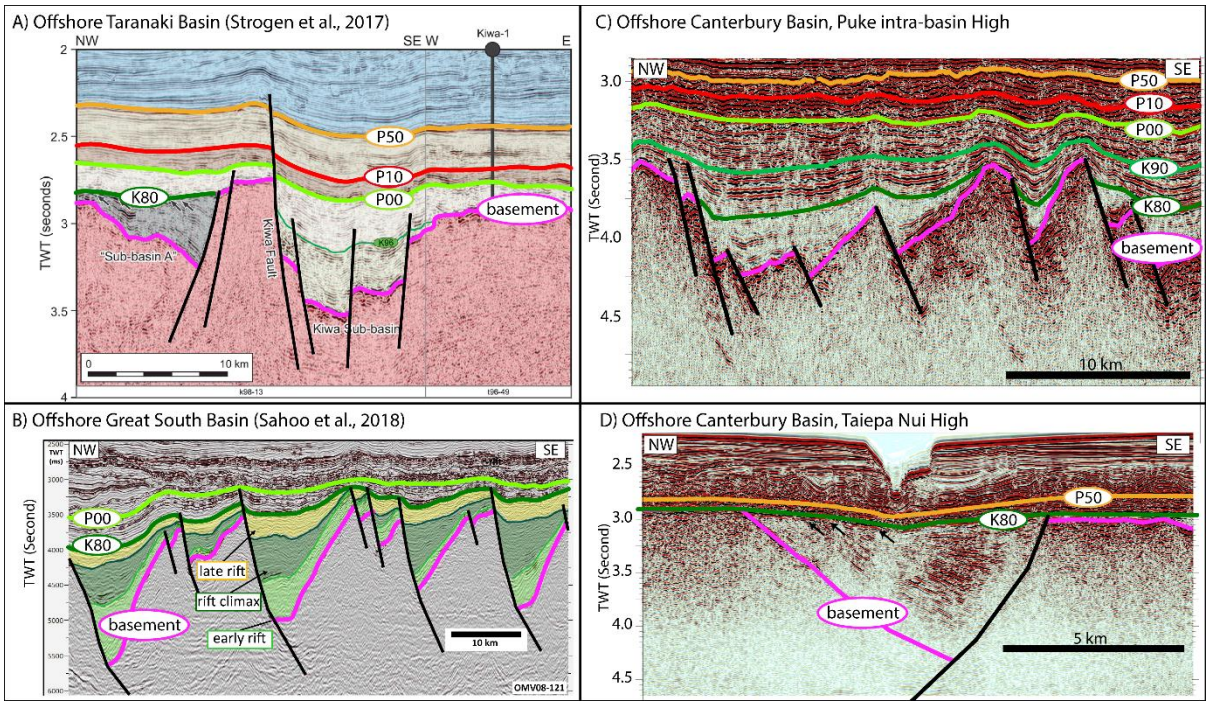

Figure 2.12 Series of seismic reflection profiles showing the differences in rift geometries and rift structures preservations across different Late Cretaceous rift basins of Zealandia. A) Composite seismic transect of the SW of the Taranaki Basin showing a mid-Cretaceous half-graben displaying erosional truncation and overlain by Late Cretaceous post-Eastern Gondwana breakup reflectors (adapted from Strogen et al., 2017). B) Seismic reflection profile across the offshore Great South Basin showing buried rift structures with little erosion (adapted from Sahoo et al., 2018). C) Seismic reflection profile offshore the Canterbury Basin located across the Puke intra-basin High showing buried rift structures with little erosion. D) Seismic reflection profile across a half-graben located over the Taiepa Nui High and displaying erosional truncation overlain by Eocene reflectors.

In contrast, for both the Canterbury and Great-South basins, most of the rift geometries were preserved by subsequent burial (Figs. 2.12B and 2.12C), at the exception of half-grabens located onshore and over some of the most pervasive structural highs in the offshore (Fig. 2.12D - e.g., the Taiepa Nui High, the Endeavour High, the Chatham Rise). For the onshore half-graben, their planated geometry is due to recent tectonic movements during the formation of the plate boundary and this cannot account for the case of the mid -Cretaceous half-grabens of the Taranaki Basin, as those were located in the south-eastern offshore Taranaki Basin, distant from any recent compression. In the second case, these half-grabens are overlain by Paleocene to Eocene reflectors, which were located over a basement structural high of both

pre- and syn-rift origins, that remained exposed to erosion for a protracted period of time (Fig. 2.12D).

Two scenarios could explain such difference in rift structures preservation and in the differences in the progression of the marine transgression: (1) The Taranaki Basin mid-Cretaceous rift could have occurred over highs of the basement equivalent to the Endeavour High and the Chatham Rise in the Canterbury Basin, which could explain subsequent erosion and poor preservation of its rift structures. (2) Erosion of rift structures in the Taranaki Basin resulted in a greater Late Cretaceous uplift in North Zealandia than in South Zealandia. The Taranaki Basin could have experienced a phase of uplift during or after breakup of Eastern Gondwana as suggested by Strogen *et al* (2017), while south Zealandia was stable and its rift basins were progressively buried over time.

However, we favor the second hypothesis as the planated half grabens of the Taranaki Basin are draped by Late Cretaceous reflectors which may not reflect an elevated position of the depocenter. Alternatively, the planated half-graben of the Taiepa Nui High (in the Canterbury Basin) is draped by Eocene reflectors, which indicates its structurally elevated position. In addition, the second hypothesis is consistent with the delay of the marine transgression in northern Zealandia, with respect to southern Zealandia rift basins in the Late Cretaceous (Figs. 2.12C and 2.12D). Indeed, northern Zealandia rift basins should have been transgressed more rapidly as space was generated by extension, while southern Zealandia was undergoing a quiescent phase. Instead, a greater uplift of the northern Zealandia basins could have delayed the marine transgression in northern Zealandia.

We think that the degree of preservation of rift structures in northern Zealandia, the development of the Taranaki Delta and related erosion (Strogen et al., 2017), and the delay of the marine transgression despite the formation of accommodation space during the Late Cretaceous, could suggest different large scale tectonic behaviors between North and South Zealandia. Such scenario could, for example, support the idea of a ceased subduction in South Zealandia versus a continuation of subduction in North Zealandia, or the presence of a proto-Alpine Fault between the north and south sections of Zealandia (Davy 2014; Lamb *et al.*, 2016; Mortimer, 2018; Crampton *et al*., 2019). Such features would account for difference in regional uplift between the north and south of Zealandia during the Late Cretaceous, tectonically separating both blocks of Zealandia.

2.7.4 Longevity of the Late Cretaceous-Eocene Paleogeography

Permian-Early Cretaceous subduction and mid-Cretaceous rift related structures seem to have persisted for a protracted period of time, as topographic highs inherited from the Late Cretaceous to, in some cases, the present day Canterbury Basin. For example, the present day paleogeography, such as the NE-SW orientation of the coastline and the shelf-break, together with bathymetric expression of the Chatham Rise are similar to the trends and locations of Cretaceous paleogeographic features (Figs 2.1, 2.5 and 2.13). Our seismic mapping indicates the trend of the post-rift Late Cretaceous to Eocene shelf-edge clinoforms have a similar NE-SW trend, with the Endeavour High (Figs. 2.5 and 2.13), and the present day coastline, present-day shelf-break. In the northern offshore Canterbury Basin, Paleocene and Eocene prograding clinoforms are parallel to E-W Cretaceous rift faults and to the trend of the Chatham Rise. In this region, the shelf-edge clinoforms appear to have stopped developing possibly when the

Chatham Rise became submerged at approximately the end of the Eocene. Similarly the development of Late Cretaceous to Eocene shelf-edge clinoforms suggest that Late Cretaceous topography was located west of the present-day Canterbury Basin and north until the submersion of the Chatham Rise. This present-day configuration with the Southern Alps that forms the main relief of the South Island of New Zealand providing the bulk of the sediment into the basin is very similar to the paleogeography of the Late Cretaceous where a western topographic high comprised the main Zealandia relief (Fig. 2.13). The "Zealandia Cordillera" corresponds one of these "old" reliefs that impacted sediment distribution during the basin history (Tulloch et al., 2009; Adams et al., 2017). However, the nature of the cordillera was magmatic and not tectonic, unlike the other basement highs, which would explain that no rejuvenation of the landscape occurred in this area.

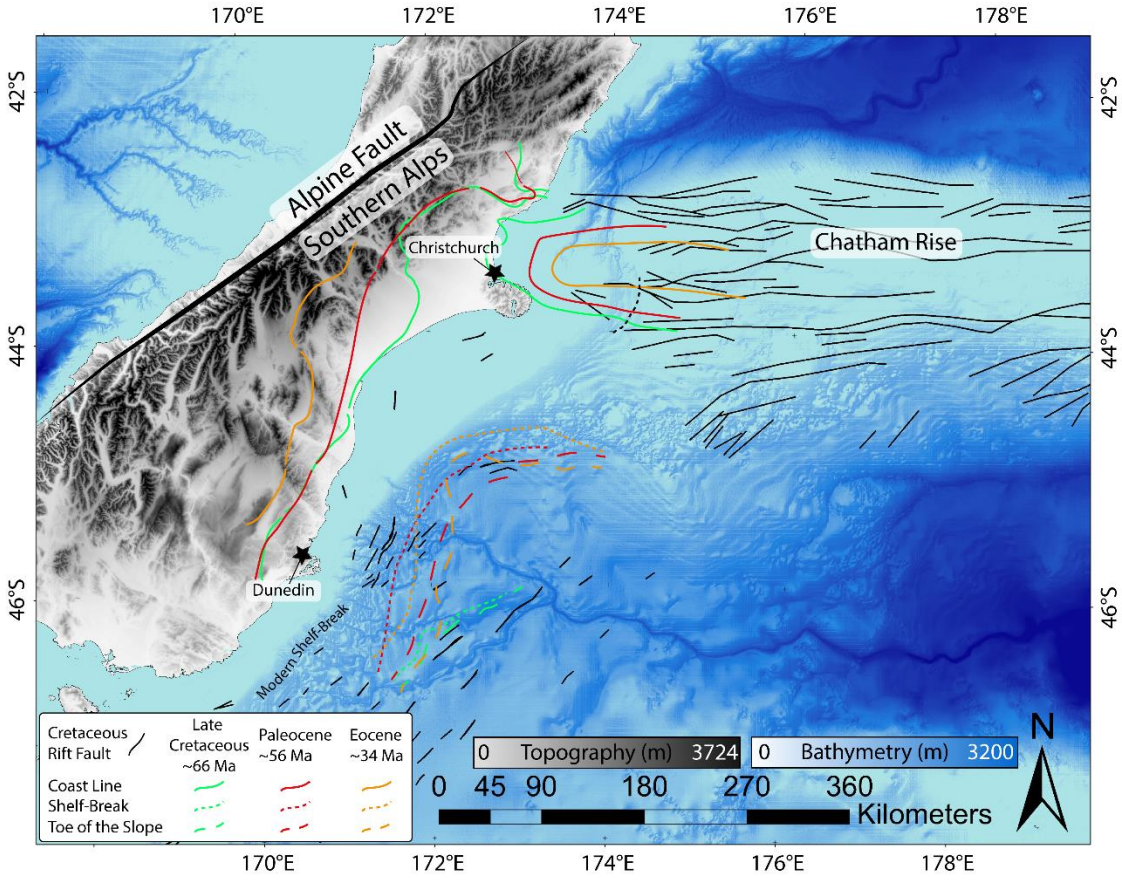

Figure 2.13 Present-day topographic and bathymetry maps of New Zealand South Island showing similarities in Late Cretaceous to recent paleogeographic trends and rift structures in the Canterbury Basin (Arnot & Bland, 2016; Sahoo & Bland, 2017). Position of the Late Cretaceous, Paleocene and Eocene coast line sourced form Field and Browne (1989). Topographic data sourced from LINZS: https://data.linz.govt.nz/. Bathymetric data licensed under NIWA Open Data Licence v1.0.v.

These elements raise the question of the long-lived influence of the Permian-Early Cretaceous subduction related structures and the mid-Cretaceous rift structures, on the development of the coastline and shelf-edge margin from the Late Cretaceous until Recent times. The topography providing sediments into the Canterbury Basin would have had a similar western position and could have been rejuvenated rather than being newly formed during the Neogene orogeny of the Southern Alps. Similarly, some of the faults which became active in the Christchurch earthquakes of 2010-2011 have been interpreted as Cretaceous faults that

became reactivated (Browne et al., 2012; Davy et al., 2012; Ghisetti and Sibson, 2012), a relationship that is found for other active faults throughout New Zealand (e.g., Barnes, 1994; Nicol and Van Dissen, 2002).

2.8. Conclusion

The Canterbury Basin contains mid Cretaceous (~110 Ma) to Recent strata up to 8 km thick. The basin initiated during eastern Gondwana breakup at ~110-85 Ma which resulted in the formation of depocenters that were under-filled by sediments at the end of rifting. The basin and range topography produced by normal faulting, persisted for a protracted period of time until its complete burial and draping during the Paleocene to Eocene. From the syn-rift to the post-rift phase, the interplay of rift structures and sedimentation impacted sedimentary records giving insights on the evolution of the Zealandia landmass. Several key conclusions are drawn from our study:

- Early syn-rift sedimentation (~110 Ma to 85 Ma) occurred in association with transverse and axial drainage systems, with alluvial fans developing along fault scarps into braided rivers flowing along rift valleys. Downstream, they were possibly connected either to lakes or to the sea, which progressively transgressed inland over time.
- After the Santonian (85 Ma; Late Cretaceous) following eastern Gondwana breakup, the rifting and crustal extension decreased significantly. Post-Gondwana breakup reflectors progressively draped the paleo-relief, as fan deltas formed along paleo-fault scarps and deltas were developed on top of horsts. When marine transgression covered the structural highs, horsts ceased to provide sediments to nearby areas and instead, pelagic sedimentation dominated when horsts were transgressed. Further offshore to the south-east, an accretionary shelf-edge clinoform developed along the eastern margin of the Taiepa Nui NE-SW rift depocenter.
- By the Paleocene and Eocene, shelf-edge clinoforms parallel to the present-day coast line and to the Chatham Rise, started to develop in the basin with deep-water fans accumulating at the toe of the shelf slope. These fans were depositing along the topographic depressions adjacent to the buried Taiepa Nui horst but not further east. Eocene shelf-edge clinoforms display an increase in thickness which could highlight basin subsidence or uplift in the western part of the basin.
- We suggest that whether the Canterbury Basin filled with sediment depended on potentially number of factors such as the availability of sediment, the duration of the rifting, the lack of surrounding paleo-topography, the type of drainage systems, the nature of the basement rocks providing source for detrital sedimentation, and paleo-climate. Of these, the more likely causes for the low sediment supply includes the postulated long transportation distance to bring sediment into the basin, the likelihood that the greywacke and schist source areas would produce little sand relative to other basins of Zealandia, and the overall small landmass feeding Zealandia rift basins for which Canterbury Basin was the furthest away from.
- The variable degree of preservation of rift structures and changes in the timing of the marine transgression between Northern and Southern Zealandia, during the Late Cretaceous, suggests differences in regional-scale tectonic behaviors between the north and south of Zealandia. Such differences could either be related to Late Cretaceous

uplift of Northern Zealandia associated with a continuation of subduction, or the presence of a structural boundary between the north and south of Zealandia since the Late Cretaceous.

- There are similarities in the pre-rift and rift structural orientations with Late Cretaceous-Eocene and Recent paleogeographic features, such as the western position of highlands and the orientation of both coastline and shelf-edge clinoforms. The persistent western position of the topography, as a sediment source for the Canterbury Basin, supports the hypothesis that the first-order topography of Zealandia could have existed since at least the Late Cretaceous.

2. Acknowledgments

We acknowledge the funding support provided by the Mason Trust from the Department of Geological Sciences, University of Canterbury. GHB acknowledges funding from the NZ government (MBIE) through Strategic Funding to GNS Science and the Sedimentary Basin Research programme. We thank a range of people for insightful discussions including Tusar Sahoo (GNS Science).

2. References

ADAMS, C.J. & RAINE, J.I. (1988) Age of Cretaceous Silicic Volcanism at Kyeburn, Central Otago, and Palmerston, Eastern Otago, South Island, New Zealand. New Zealand Journal of Geology and Geophysics, 31, 471-475 pp.

ADAMS, C.J., CAMPBELL, H.J., MORTIMER, N. & GRIFFIN, W.L. (2017) Perspectives on Cretaceous Gondwana Breakup from Detrital Zircon Provenance of Southern Zealandia Sandstones. Geological Magazine, 154, 661-682 pp.

ALLEN, P.A., P. HOMEWOOD, G. WILLIAMS (1986) Foreland Basins: An Introduction. IAS SP, 8, 3-12 pp.

ANDREW, P.B., FIELD, B.D., BROWNE, G.H., MCLENNAN, J.M., (1987) Lithostratigraphic Nomenclature for the Upper Cretaceous and Tertiary Sequence of Central Canterbury, New Zealand. New Zealand geological Survey record, 24, 40p.

ARNOT, M.J., BLAND, K.J., COMPILERS (2016) Atlas of Petroleum Prospectivity, Northwest Province: Arcgis Geodatabase and Technical Report. GNS Science Data Series, 23b, 34p +31p ArcGIS geodatabase +35p ArcGIS projects.

BALLY, A. (1987) Atlas of Seismic Stratigraphy. American Association of Petroleum Geologists Studies in Geology, 27, 125p.

BARNES, P.M. (1994) Inherited Structural Control from Repeated Cretaceous to Recent Extension in the North Mernoo Fault Zone, Western Chatham Rise, New Zealand. Tectonophysics, 237, 27-46 pp.

BEST, E. (1926) The Legend of Mahu and Taewha. Illustrating the Maori Belief in, and Practise of Magic, and the Ordeals to Which the Warlock Was Subjected. The Journal of the Polynesian Society, 35**,** 73-110 pp.

BISHOP, D.G., LAIRD, M.G. & MILDENHALL, D.C. (1976) Stratigraphy and Depositional Environment of the Kyeburn Formation (Cretaceous), a Wedge of Coarse Terrestrial Sediments in Central Otago. Journal of the Royal Society of New Zealand, 6, 55-71 pp.

BISHOP, D.G., TURNBULL, I.M., COMPILERS (1996) Geology of the Dunedin Area. Institute of Geological and Nuclear Sciences, 1:250 000 Geological map 21., 1-52 pp.

BROWNE, G. & REAY, M. (1993) The Warder Formation: Cyclic Fluvial Sedimentation During the Ngaterian (Late Albian-Cenomanian) of Marlborough, New Zealand. New Zealand Journal of Geology and Geophysics, 36, 27-35 pp.

BROWNE, G.H. (2003) Sedimentological Database for the Offshore Canterbury Basin, New Zealand. Unpublished data on CD. GNS Science, Lower Hutt.

BROWNE, G.H. & NAISH, T.R. (2003) Facies Development and Sequence Architecture of a Late Quaternary Fluvial-Marine Transition, Canterbury Plains and Shelf, New Zealand: Implications for Forced Regressive Deposits. Sedimentary Geology, 158, 57-86 pp.

BROWNE, G.H., KENNEDY, E.M., CONSTABLE, R.M., RAINE, J.I., CROUCH, E.M. & SYKES, R. (2008) An Outcrop-Based Study of the Economically Significant Late Cretaceous Rakopi Formation, Northwest Nelson, Taranaki Basin, New Zealand. New Zealand Journal of Geology and Geophysics, 51, 295-315 pp.

BROWNE, G.H., FIELD, B.D., BARRELL, D.J.A., JONGENS, R., BASSETT, K.N. & WOOD, R.A. (2012) The Geological Setting of the Darfield and Christchurch Earthquakes. New Zealand Journal of Geology and Geophysics, 55, 193-197 pp.

BROWNE, G.H., FIELD, B.D. (1985) The Lithostratigraphy of Late Cretaceous to Early Pleistocene Rocks of Northern Canterbury, New Zealand. New Zealand Geological Survey Record, 6, 63p.

CARTER, R.M. (1988) Post-Breakup Stratigraphy of the Kaikoura Synthem (Cretaceous-Cenozoic), Continental Margin, Southeastern New Zealand. New Zealand Journal of Geology and Geophysics, 31, 405-429 pp.

COLELLA, A. (1988) Fault-Controlled Marine Gilbert-Type Fan Deltas. Geology, 16, 1031-1034 pp.

COOK, R.A.S., R.; ZHU, H., COMPILERS (1999) Cretaceous - Cenozoic Geology and Petroleum Systems of the Great South Basin, New Zealand. 20, 190p.

COOPER, R., AGTERBERG, F.P., ALLOWAY, B., BEU, A., CAMPBELL, H., CRAMPTON, J.S., CROUCH, E., CRUNDWELL, M., GRAHAM, I.J., HOLLIS, C., JONES, C., KAMP, P., MILDENHALL, D.C., MORGANS, H., NAISH, T.R., RAINE, J.I., RONCAGLIA, L., SADLER, P.M., SCHIØLER, P. & WILSON, G. (2004) The New Zealand Geological Timescale. 22, 284p.

CRAMPTON, J.S., MORTIMER, N., BLAND, K.J., STROGEN, D.P., SAGAR, M., HINES, B.R., KING, P.R. & SEEBECK, H. (2019) Cretaceous Termination of Subduction at the Zealandia Margin of Gondwana: The View from the Paleo-Trench. Gondwana Research, 70, 222-242 pp.

CRAMPTON, J.S.H., C.J.; RAINE, J.I.; RONCAGLIA, L.; SCHIOLER, P.; STRONG, C.P.; WILSON, G.J. (2004) Cretaceous (Taitai, Clarence, Raukumara and Mata Series). In: The New Zealand Geological Timescale (Ed. Cooper, R.A.) Institute of Geological & Nuclear Sciences monograph, 22, 102-122 pp.

DANIEL, I., LOVIS, J. & REAY, M. (1988) A Brief Introductory Report on the Mid-Cretaceous Megaflora of the Clarence Valley, New Zealand. Proceedings of the 3rd International Organization of Palaeobotany Conference, Melbourne, 27-29 pp.

DAVISON, I. & UNDERHILL, J.R. (2012) Tectonics and Sedimentation in Extensional Rifts: Implications for Petroleum Systems. In: Tectonics and sedimentation: Implications for petroleum systems (Ed. Gao, D.), AAPG Memoir 100, 15-42 pp.

DAVY, B., HOERNLE, K. & WERNER, R. (2008) Hikurangi Plateau: Crustal Structure, Rifted Formation, and Gondwana Subduction History. Geochemistry, Geophysics, Geosystems, 9, 1-31 pp.

DAVY, B., STAGPOOLE, V., BARKER, D. & YU, J. (2012) Subsurface Structure of the Canterbury Region Interpreted from Gravity and Aeromagnetic Data. New Zealand Journal of Geology and Geophysics, 55, 185-191 pp.

DAVY, B. (2014) Rotation and Offset of the Gondwana Convergent Margin in the New Zealand Region Following Cretaceous Jamming of Hikurangi Plateau Large Igneous Province Subduction. Tectonics, 33, 1577-1595 pp.

ERIKSSON, K., SIMPSON, E. & JACKSON, M. (1994) Stratigraphical Evolution of a Proterozoic Syn-Rift to Post-Rift Basin: Constraints on the Nature of Lithospheric Extension in the Mount Isa Inlier, Australia. Tectonic controls and signatures in sedimentary successions, 203-221 pp.

EXXONMOBIL (2010) Great South Basin 3d/2d Seismic Interpretation Report, Pep 50117 Ministry of Economic Development New Zealand Unpublished Petroleum Report PR4233, 42p.

FEELEY, M.H., MOORE, T., LOUTIT, T.S. & BRYANT, W. (1990) Sequence Stratigraphy of Mississippi Fan Related to Oxygen Isotope Sea Level Index. AAPG Bulletin, 74, 407-424 pp.

FIELD, B.D. & BROWNE, G.H. (1989) Cretaceous and Cenozoic Sedimentary Basins and Geological Evolution of the Canterbury Region, South Island, New Zealand. Institute of Geological & Nuclear Sciences monograph, 2, 94p.

FIELD, B.D., BROWNE, G.H. (1986) Lithostratigraphy of Cretaceous and Tertiary Rocks, Southern Canterbury, New Zealand. New Zealand Geological Survey basin studies, 14, 55 pp.

FORDYCE, R.E. (2006) New Light on New Zealand Mesozoic Reptiles. Geological Society of New Zealand Newsletter, 140, 6-15 pp.

GAWTHORPE, R.L. & LEEDER, M.R. (2000) Tectono-Sedimentary Evolution of Active Extensional Basins. Basin Research, 12, 195-218 pp.

GREY, G. (1928) Nga Mahi a Nga Tupuna. T. Avery & Sons, limited.

GHISETTI, F. & SIBSON, R. (2012) Compressional Reactivation of E–W Inherited Normal Faults in the Area of the 2010–2011 Canterbury Earthquake Sequence. New Zealand Journal of Geology and Geophysics, 55, 177-184 pp.

HARDING, T.P. (1984) Graben Hydrocarbon Occurences and Structural Styles. AAPG Bulletin, 68, 333-362 pp.

HIGGS, K.E., BROWNE, G.H. & SAHOO, T.R. (2019) Reservoir Characterisation of Syn-Rift and Post-Rift Sandstones in Frontier Basins: An Example from the Cretaceous of Canterbury and Great South Basins, New Zealand. Marine and Petroleum Geology, 101, 1-29 pp.

HOLLIS, C.J., TAYLER, M.J.S., ANDREW, B., TAYLOR, K.W., LURCOCK, P., BIJL, P.K., KULHANEK, D.K., CROUCH, E.M., NELSON, C.S., PANCOST, R.D., HUBER, M., WILSON, G.S., VENTURA, G.T., CRAMPTON, J.S., SCHIØLER, P. & PHILLIPS, A. (2014) Organic-Rich Sedimentation in the South Paci Fi C Ocean Associated with Late Paleocene Climatic Cooling. Earth Science Reviews, 134, 81-97 pp.

HOLLIS, C.J., HINES, B.R., LITTLER, K., VILLASANTE-MARCOS, V., KULHANEK, D.K., STRONG, C.P., ZACHOS, J.C., EGGINS, S.M., NORTHCOTE, L. & PHILLIPS, A. (2015) The Paleocene–Eocene Thermal Maximum at Dsdp Site 277, Campbell Plateau, Southern Pacific Ocean. Clim. Past, 11, 1009-1025 pp.

KENNEDY, E.M. (2003) Late Cretaceous and Paleocene Terrestrial Climates of New Zealand: Leaf Fossil Evidence from South Island Assemblages. New Zealand Journal of Geology and Geophysics, 46, 295-306 pp.

KENNEDY, E.M., ARENS, N.C., REICHGELT, T., SPICER, R.A., SPICER, T.E.V., STRANKS, L. & YANG, J. (2014) Deriving Temperature Estimates from Southern Hemisphere Leaves. Palaeogeography, Palaeoclimatology, Palaeoecology, 412, 80-90 pp.

KING, P.R. & THRASHER, G.P. (1996) Cretaceous Cenozoic Geology and Petroleum Systems of the Taranaki Basin, New Zealand. 13, 243p.

KING, P.R., NAISH, T.R., BROWNE, G.H., FIELD, B.D. & EDBROOKE, S.W. (1999) Cretaceous to Recent Sedimentary Patterns in New Zealand. Institute of Geological and Nuclear Sciences Folio Series 1, 35p.

KING, P.R. (2000) Tectonic Reconstructions of New Zealand: 40 Ma to the Present. New Zealand Journal of Geology and Geophysics, 43, 611-638 pp.

KIRK, R. & CONSTABLE, R.M. (2010) Seismic Facies Mapping & Paleogeographic Interpretation from Seismic Sequence Straitigraphy. Ministry of Economic Development New Zealand Unpublished Petroleum Report, PR4347, 212p.

LAIRD, M.G. (1981) The Late Mesozoic Fragmentation of the New Zealand Segment of Gondwana. In: Gondwana Five (Eds. Cresswell, M.M. & Vella, P.), proceedings of the fifth International Gondwana Symposium. Balkema, Rotterdam, 1980, 311-318 pp.

LAIRD, M.G. (1992) Cretaceous Stratigraphy and Evolution of the Marlborough Segment of the East Coast Region. New Zealand Oil Exploration Conference. Christchurch, New Zealand, 37-49 pp.

LAIRD, M.G. (1993) Cretaceous Continental Rifts: New Zealand Region. In: Sedimentary basins of the world. South Pacific sedimentary basins (Ed. Ballance, P.E.), Elsevier Science Publisher 2, 37-49 pp.

LAIRD, M.G. (1995) Coarse-Grained Lacustrine Fan-Delta Deposits (Pororari Group) of the Northwestern South Island, New Zealand: Evidence for Mid-Cretaceous Rifting. Sedimentary Facies Analysis: A Tribute to the Research and Teaching of Harold G. Reading**,** 195-217.

LAIRD, M.G. & BRADSHAW, J.D. (2004) The Breakup of a Long-Term Relationship: The Cretaceous Separation of New Zealand from Gondwana. Gondwana Research, 7, 273-286 pp.

LAMB, S., MORTIMER, N., SMITH, E. & TURNER, G. (2016) Focusing of Relative Plate Motion at a Continental Transform Fault: Cenozoic Dextral Displacement> 700 Km on New Zealand's Alpine Fault, Reversing> 225 Km of Late Cretaceous Sinistral Motion. Geochemistry, Geophysics, Geosystems, 17, 1197-1213 pp.

LAMBIASE, J.J. & MORLEY, C.K. (1999) Hydrocarbons in Rift Basins: The Role of Stratigraphy. Philosophical Transactions of the Royal Society A: Mathematical, Physical and Engineering Sciences, 357, 877-900 pp.

LEVER, H. (2007) Review of Unconformities in the Late Eocene to Early Miocene Successions of the South Island, New Zealand: Ages, Correlations, and Causes. New Zealand Journal of Geology and Geophysics, 50, 245-261 pp.

LU, H., FULTHORPE, C.S. & MANN, P. (2003) Three-Dimensional Architecture of Shelf-Building Sediment Drifts in the Offshore Canterbury Basin, New Zealand. Marine Geology, 193, 19-47 pp.

LU, H. & FULTHORPE, C.S. (2004) Controls on Sequence Stratigraphy of a Middle Miocene–Holocene, Current-Swept, Passive Margin: Offshore Canterbury Basin, New Zealand. Geological Society of America Bulletin, 116, 1345-1366 pp.

LU, H., FULTHORPE, C.S., MANN, P. & KOMINZ, M.A. (2005) Miocene-Recent Tectonic and Climatic Controls on Sediment Supply and Sequence Stratigraphy: Canterbury Basin, New Zealand. Basin Research, 17, 311-328 pp.

LUYENDYK, B.P. (1995) Hypothesis for Cretaceous Rifting of East Gondwana Caused by Subducted Slab Capture. Geology, 23, 373-376 pp.

MAITRA, M., BASSETT, K. (2017) Detailed Facies Analysis and Sequence Stratigraphy of Potential Lacustrine Source Rocks, Greymouth Basin, New Zealand. Poster presentation at GeoConvention. Calgary, Canada, 15-19 May 2017.

MANN, P., GAHAGAN, L. & GORDON, M.B. (2003) Tectonic Setting of the World's Giant Oil and Gas Fields. AAPG Memoir, 78, 15-105 pp.

MARSAGLIA, K.M., BROWNE, G.H., GEORGE, S.C., KEMP, D.B., JAEGER, J.M., CARSON, D. & RICHAUD, M. (2017) The Transformation of Sediment into Rock: Insights from Iodp Site U1352, Canterbury Basin, New Zealand. Journal of Sedimentary Research, 87, 272-287 pp.

MITCHELL, M., CRAW, D., LANDIS, C.A. & FREW, R. (2009) Stratigraphy, Provenance, and Diagenesis of the Cretaceous Horse Range Formation, East Otago, New Zealand. New Zealand Journal of Geology and Geophysics, 52, 171-183 pp.

MITCHUM, R.M., SANGREE J.B., VAIL, P.R. AND WORNARDT W.W. (1985) Recognizing Sequences and Systems Tracts from Well Logs, Seismic Data, and Biostratigraphy: Examples from the Late Cenozoic of the Gulf of Mexico. In: Siliciclastic sequence stratigraphy: recent developments and applications (Eds. Weimer, P., Posamentier, H). AAPG Memoir 59, 163-197 pp.

MORTIMER, N., TULLOCH, A.J., SPARK, R.N., WALKER, N.W., LADLEY, E., ALLIBONE, A. & KIMBROUGH, D.L. (1999) Overview of the Median Batholith, New Zealand: A New Interpretation of the Geology of the Median Tectonic Zone and Adjacent Rocks. Journal of African Earth Sciences, 29, 257-268 pp.

MORTIMER, N. (2004) New Zealand's Geological Foundations. Gondwana Research, 7, 261-272 pp.

MORTIMER, N. & CAMPBELL, H. (2014) Zealandia: Our Continent Revealed, Auckland, New Zealand, Penguin, 272p.

MORTIMER, N., RATTENBURY, M.S., KING, P.R., BLAND, K.J., BARRELL, D.J.A., BACHE, F., BEGG, J.G., CAMPBELL, H.J., COX, S.C., CRAMPTON, J.S., EDBROOKE, S.W., FORSYTH, P.J., JOHNSTON, M.R., JONGENS, R., LEE, J.M., LEONARD, G.S., RAINE, J.I., SKINNER, D.N.B., TIMM, C., TOWNSEND, D.B., TULLOCH, A.J., TURNBULL, I.M. & TURNBULL, R.E. (2014) High-Level Stratigraphic Scheme for New Zealand Rocks. New Zealand Journal of Geology and Geophysics, 57, 402-419 pp.

MORTIMER, N., CAMPBELL, H.J., TULLOCH, A.J., KING, P.R., STAGPOOLE, V.M., WOOD, R.A., RATTENBURY, M.S., SUTHERLAND, R., ADAMS, C.J., COLLOT, J. & SETON, M. (2017) Zealandia: Earth's Hidden Continent. GSA Today, 27, 27-35 pp.

MORTIMER, N. (2018) Evidence for a Pre-Eocene Proto-Alpine Fault through Zealandia. New Zealand Journal of Geology and Geophysics, 61, 1-9 pp.

NATHAN, S., ANDERSON, H.J., COOK, R.A., HERZER, R.H., HOSKINS, R.H., RAINE, J.I., AND SMALE, D. (1986) Cretaceous and Cenozoic Sedimentary Basins of the West Coast Region, South Island, New Zealand. New Zealand Geological Survey basin studies, 1, 90p.

NICOL, A., MAZENGARB, C., CHANIER, F., RAIT, G., URUSKI, C. & WALLACE, L. (2007) Tectonic Evolution of the Active Hikurangi Subduction Margin, New Zealand, since the Oligocene. *Tectonics,* 26**,** 24 p.

NICOL, A. & VAN DISSEN, R. (2002) Up-Dip Partitioning of Displacement Components on the Oblique-Slip Clarence Fault, New Zealand. Journal of Structural Geology, 24, 1521-1535 pp.

ORANGE, C. (1998) Ngā Tāngata Taumata Rau. Auckland University Press & Te Tari Taiwhenua

PARRISH, J.T., DANIEL, I.L., KENNEDY, E.M. & SPICER, R.A. (1998) Paleoclimatic Significance of Mid-Cretaceous Floras from the Middle Clarence Valley, New Zealand. PALAIOS, 13, 149-159 pp.

PATRUNO, S. & HELLAND-HANSEN, W. (2018) Clinoform Systems: Review and Dynamic Classification Scheme for Shorelines, Subaqueous Deltas, Shelf Edges and Continental Margins. Earth-science reviews, 185, 202-223 pp.

PLAMPTON, W. (2018) Geometry and Distribution of Latest Cretaceous / Paleocene Turbidites and Their Prospectivity, Great South Basin, Offshore Se New Zealand. Poster presentation at PESGB SEAPEX Asia Pacific E&P Conference, Olympia Exhibition Centre, London, 27th – 28th June 2018.

POCKNALL, D.T. (1989) Late Eocene to Early Miocene Vegetation and Climate History of New Zealand. Journal of the Royal Society of New Zealand, 19, 1-18 pp.

POLE, M. (1995) Late Cretaceous Macrofloras of Eastern Otago, New Zealand: Gymnosperms. Australian systematic botany, 8, 1067-1106 pp.

POLE, M. & PHILIPPE, M. (2010) Cretaceous Plant Fossils of Pitt Island, the Chatham Group, New Zealand. Alcheringa, 34, 231-263 pp.

PŌTATAU, H. (1991) He Hokinga Mahara. Longman Paul.

RAINE, J.I., BEU, A.G., BOYES, A.F., CAMPBELL, H.J., COOPER, R.A., CRAMPTON, J.S., CRUNDWELL, M.P., HOLLIS, C.J., MORGANS, H.E.G. & MORTIMER, N. (2015) New Zealand Geological Timescale Nzgt 2015. New Zealand Journal of Geology and Geophysics, 58, 398-403 pp.

RAVNÅS, R. & STEEL, R.J. (1998) Architecture of Marine Rift-Basin Successions. AAPG Bulletin, 82, 110-146 pp.

REILLY, C., NICOL, A., WALSH, J.J. & SEEBECK, H. (2015) Evolution of Faulting and Plate Boundary Deformation in the Southern Taranaki Basin, New Zealand. Tectonophysics, 651-652, 1-18 pp.

SAHOO, T.R., KING, P.R., BLAND, K.J., STROGEN, D.P., SYKES, R. & BACHE, F. (2014) Tectono-Sedimentary Evolution and Source Rock Distribution of the Mid to Late Cretaceous Succession in Great South Basin, New Zealand. APPEA Journal, 54, 259-274 pp.

SAHOO, T.R., KROEGER, K.F., THRASHER, G., MUNDAY, S., MINGARD, H., COZENS, N. & HILL, M. (2015) Facies Distribution and Impact on Petroleum Migration in the Canterbury Basin , New Zealand. In: Eastern Australian Basins Symposium 2015: Publication of Proceedings. Petroleum Exploration Society of Australia, Perth, WA, 187-202 pp.

SAHOO, T.R., BLAND, K. J.,COMPILERS (2017) Atlas of Petroleum Prospectivity, Southeast Province: Arcgis Geodatabase and Technical Report. GNS Science Data Series, 23c, 50p + 51p ArcGIS geodatabase + 55p ArcGIS projects.

SAHOO, T.R., SEEBECK, H., NICOL. A. (2015) Polygonal Fault Systems in the Canterbury Basin, New Zealand. Poster presentation at Advantage New Zealand Petroleum Summit. Auckland, New Zealand, 29-31 March 2015.

SCHIØLER, P.R., J.I., COMPILERS (2011) Revised Biostratigraphy and Well Correlation, Canterbury Basin, New Zealand. GNS Science Consultancy Report 2011/12, PR4365, 142p.

SCHLISCHE, R.W., WITHJACK, M.O. & OLSEN, P.E. (2003) Relative Timing of Camp, Rifting, Continental Breakup, and Basin Inversion: Tectonic Significance. Geophysical Monograph-American Heophysical Union, 136, 33-60 pp.

SINCLAIR, H.D. (1997) Tectonostratigraphic Model for Underfilled Peripheral Foreland Basins: An Alpine Perspective. Bulletin of the Geological Society of America, 109, 324-346.

STAGPOOLE, V. & NICOL, A. (2008) Regional Structure and Kinematic History of a Large Subduction Back Thrust: Taranaki Fault, New Zealand. Journal of Geophysical Research: Solid Earth, 113, 1-19 pp.

STROGEN, D.P., SEEBECK, H., NICOL, A. & KING, P.R. (2017) Two-Phase Cretaceous – Paleocene Rifting in the Taranaki Basin Region, New Zealand; Implications for Gondwana Breakup. Journal of the Geological Society, 174, 929-946 pp.

STROGEN, D.P.K., P.R. (2014) A New Zealandia-Wide Seismic Horizon Naming Scheme. GNS Science Report, 2014/34, 20p.

THOMPSON, N.K., BASSETT, K.N. & REID, C.M. (2014) The Effect of Volcanism on Cool-Water Carbonate Facies During Maximum Inundation of Zealandia in the Waitaki–Oamaru Region. New Zealand Journal of Geology and Geophysics, 57, 149-169 pp.

TULLOCH A., B.M., KULA J., SPELL T., MORTIMER N. (2006) Cordillera Zealandia, the Sisters Shear Zone and Their Influence on the Early Development of the Great South Basin. New Zealand Petroleum Conference Proceedings, Wellington.

TULLOCH, A.J., RAMEZANI, J., MORTIMER, N., MORTENSEN, J., VAN DEN BOGAARD, P. & MAAS, R. (2009) Cretaceous Felsic Volcanism in New Zealand and Lord Howe Rise (Zealandia) as a Precursor to Final Gondwana Breakup. Geological Society, London, Special Publications, 321, 89-118 pp.

TURNBULL, I.M.U., C.I.; ANDERSON, H.J.; LINDQVIST, J.K.; SCOTT, G.H.; MORGANS, H.E.G.; HOSKINS, R.H.; RAINE, J.I.; MILDENHALL, D.C.; POCKNALL, D.T.; BEU, A.G.; MAXWELL, P.A.; SMALE, D.; WATTERS, W.A.; FIELD, B.D (1993) Cretaceous and Cenozoic Sedimentary Basins of Western Southland, South Island, New Zealand. New Zealand Geological Survey basin studies, 4, 86p.

VAJDA, V. & RAINE, J.I. (2003) Pollen and Spores in Marine Cretaceous/Tertiary Boundary Sediments at Mid-Waipara River, North Canterbury, New Zealand. New Zealand Journal of Geology and Geophysics, 46, 255-273 pp.

WELLMAN, H.W. (1979) An Uplift Map for the South Island of New Zealand and a Model for Uplift of the Southern Alps. In: The Origin of the Southern Alps (Eds. Walcott, R.I. & Cresswell, M.M.), . Royal Society of New Zealand Bulletin, 18, 13-20 pp.

WITHJACK, M.O., SCHLISCHE, R.W. & OLSEN, P.E. (2002) Rift-Basin Structure and Its Influence on Sedimentary Systems. Sedimentation in Continental Rifts, 57-81 pp.

WOOD, R.A. & HERZER, R.H. (1993) The Chatham Rise, New Zealand. In: South Pacific sedimentary basins (Ed. Ballance, P.F.). Elsevier Science Publishers. Sedimentary basins of the world 2. 329-349 pp.

WOOD, R.A. (1993) The Challenger Plateau. In: Sedimentary basins of the world. South Pacific sedimentary basins (Ed. Ballance, P.E.), Elsevier Science Publisher 2, 351-364 pp.

WOOD, R.A., ANDREW, P.B., HERZER, R.H., & COOK, R.A. (1989) Cretaceous and Cenozoic Geology of the Chatham Rise Region, South Island, New Zealand. New Zealand Geological Survey basin studies 3, 75p.

CHAPTER 3) COEVAL MULTI-DIRECTIONAL EXTENSION IN NEW ZEALAND'S CANTERBURY BASIN PRIOR TO CRETACEOUS BREAKUP OF EASTERN GONDWANA

A. Barrier[1], A. Nicol[1], G.H. Browne[2] and K. Bassett[1]

[1] *University of Canterbury, Department of Geological Science, Christchurch, New Zealand.*

[2]*GNS Science, PO Box 30368, Lower Hutt, New Zealand.*

3. Abstract:

The Canterbury Basin in eastern Gondwana was deformed by rift faults from ~110 to ~85 Ma with trends of NE-SW, E-W and NW-SE. Analysis of 2D and 3D seismic reflection lines tied to wells indicates that these three fault sets have primarily normal fault geometries and displacements. Displacements accrued synchronously on each fault set with N-S and NW-SE extension dominating along the Chatham Rise and in the southern Canterbury Basin, respectively. Each of the three fault sets are parallel to spreading centres that primarily define the present margins of Zealandia, with NE-SW trending faults in the southern basin being parallel to the mid-ocean ridge separating southern Zealandia and western Antarctica. The parallelism between spreading centres and rift faulting suggests that multi-directional extension in the Canterbury Basin records the early stages of Gondwana breakup. Faulting in the Canterbury Basin indicates that the plate tectonic forces responsible for Gondwana breakup commenced 10s of millions of years before breakup either soon after the cessation of subduction (e.g., < 5 Myr) or during the transition from subduction to rifting from ~110 to 105 Ma. With the onset of breakup, extension was focused along the spreading centres and multi-directional stretching of Zealandia ceased or continued at much diminished rates. Canterbury Basin multidirectional stretching differs from triple junction examples in that it was surrounded by multiple future spreading centres which vary in trend. In the Canterbury Basin case, the initial phase of Gondwana breakup appears to have been characterised by minor (<20%) extension while we speculate that it was significantly more than across the Canterbury Basin crust between spreading centres. With the onset of seafloor spreading, extension was focused along the spreading centres, and distributed stretching of Zealandia ceased or continued at much diminished rates.

3.1. Introduction:

Rift systems are the surface expression of crustal thinning and mantle convection which typically accommodate >20% stretching (β=1.12) over time periods of 5 to 20 Myr (Davison and Underhill, 2012). Extension can be confined to 10-100 km wide rift valleys or distributed across rift provinces >1000 km wide (Ravnås and Steel, 1998). Rifting may produce complex fault geometries controlled by orthogonal or oblique extension and by pre-rift zones of weakness within basement rocks (Morley et al., 2004; Philippon *et al.*, 2015; Morley, 2017). Displacements on rift faults vary from dip-slip to strike slip depending on the obliquity of the fault relative to the regional stretching direction (Fig. 3.1A - Ring et al., 1994; Morley et al., 2004; Philippon *et al.*, 2015). The trend of extension may change with time, resulting in changes to fault kinematics or to the creation of new sets of rift faults oriented oblique to the original rift faults (Fig. 3.1D Morley, 2017). Conversely, at rift triple junctions extension directions may also change spatially with near pure extension on synchronous rift systems that trend at a high angle (e.g., 30-90°) to each other (Fig. 3.1C - e.g., Jurassic North Sea rift system, Coward *et al.*, 2003; Zanella *et al.*, 2003; Late Cretaceous Southern Atlantic rift system, Heine *et al.*, 2013; African rift system, Morh, 1970; Koptev *et al.*, 2018). Outside of these triple junction rifts formed due to multiple directions of synchronous extension and the processes leading to their formation are rarely reported.

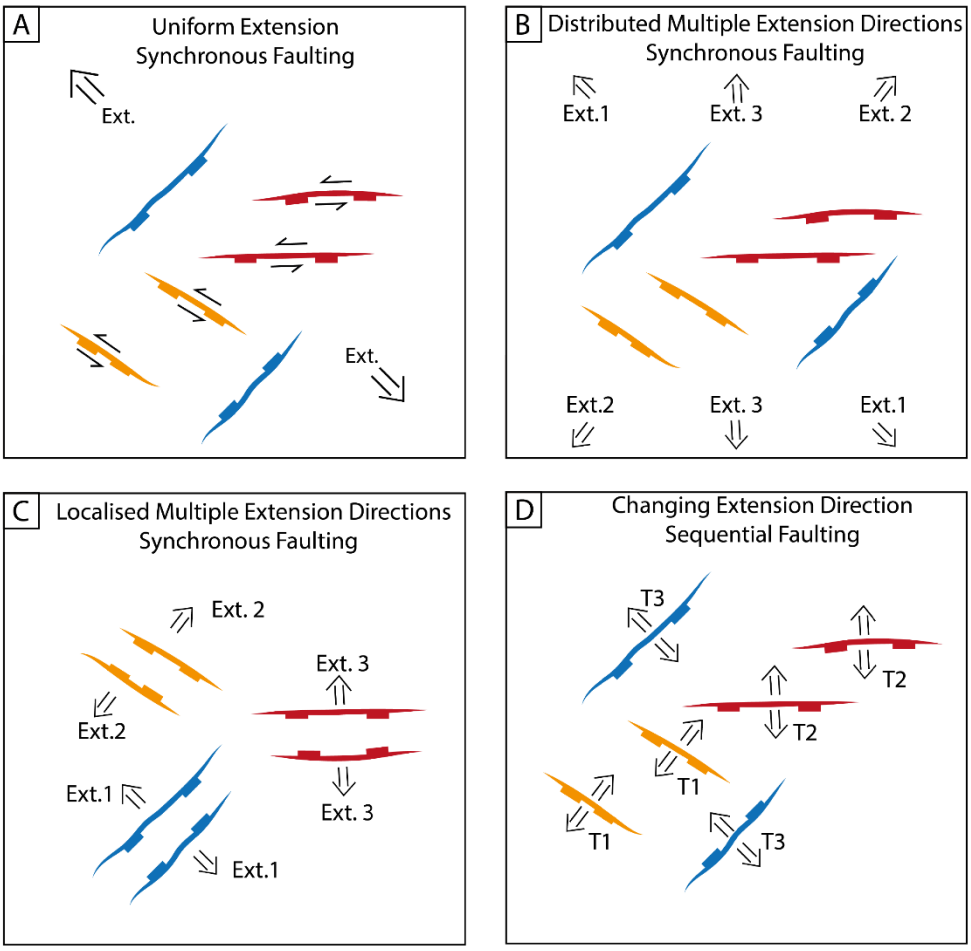

Figure 3.1 Sketch showing the three extension scenario accounting for the presence of the NE-SW, E-W and NW-SE rift faults in the Canterbury Basin: (A) Synchronous faulting with uniform extension (Ext. represent the regional direction of extension). (B) Synchronous faulting with multiple directions of extension (Ext.n represent different stretching directions). (C) Localised multiple extension directions with synchronous faulting (e.g., Triple Junctions) (Ext.n represent different stretching directions). (D) Sequential faulting with changing extension direction through time (Tn represent different rifting events).

In this paper we study a Late Cretaceous (~110-85 Ma) continental rift system comprising NE-SW, E-W and NW-SE striking fault sets in the Canterbury Basin, east of the South Island of New Zealand (Fig. 2 - Field and Browne, 1989; Browne *et al.*, 2012; Jongens *et al.*, 2012; Sahoo *et al.*, 2014). These normal faults are part of the large Late Cretaceous Rift Province (> 4 million km^2) that covered much of the Zealandia continent (Mortimer *et al.*, 2017) and produced several Mesozoic-Cenozoic rift basins (Fig. 3.2A - e.g., Laird and Bradshaw, 2004; Strogen *et al.*, 2017). Rifting mainly followed the cessation of Mesozoic subduction along eastern Gondwana (~105 Ma) (eg., Laird and Bradshaw, 2004; Davy, 2014) and immediately predated Gondwana breakup which in eastern Zealandia commenced between 86 Ma (Higgs *et al.*, 2019) and 85 Ma (Adams *et al.*, 2017; Strogen *et al.*, 2017).

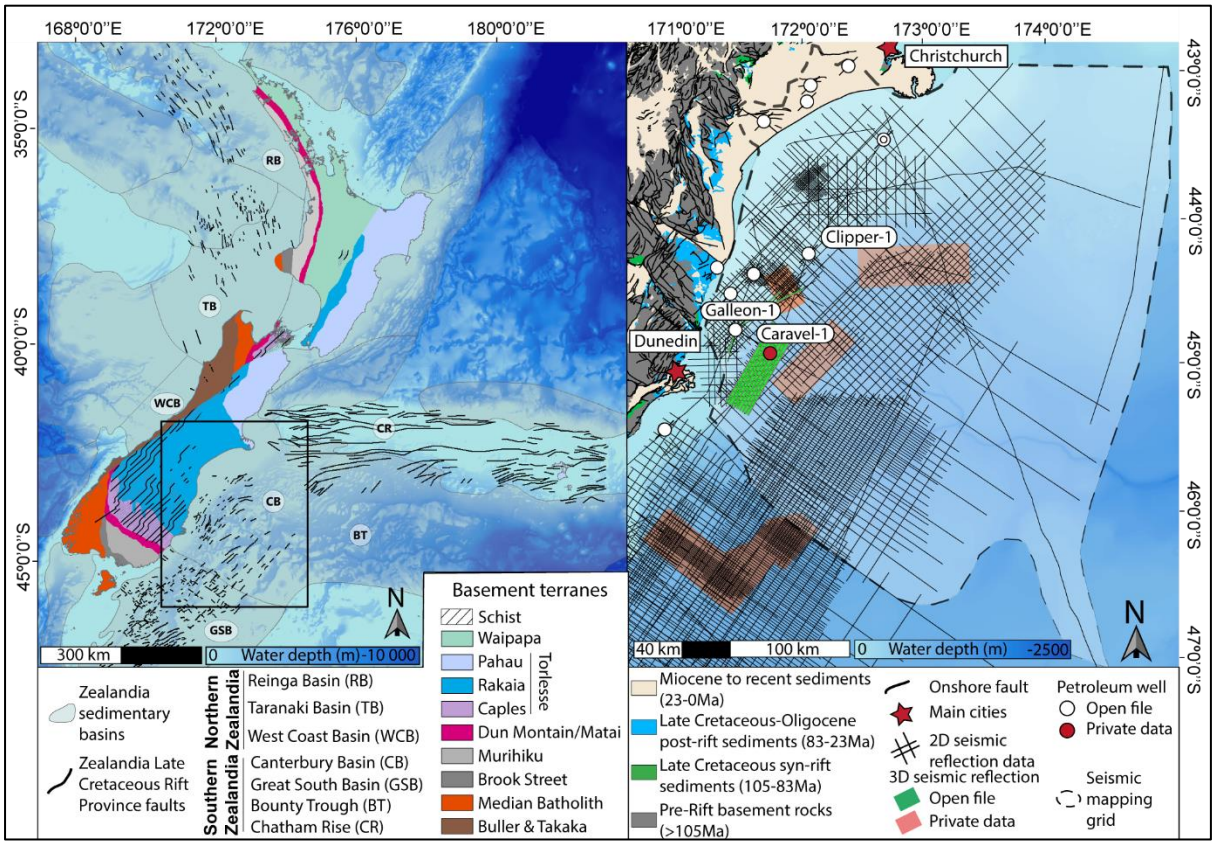

Figure 3.2(A) New Zealand basemap showing onshore basement terranes, offshore Late Cretaceous faults and associated sedimentary basins (adapted from Mortimer, 2004; Rift faults, Arnot & Bland, 2016; Sahoo & Bland, 2017). (B) Canterbury Basin dataset showing the locations of syn-rift outcrops, seismic reflection and well data. Bathymetric data licensed under NIWA Open Data Licence v1.0.v

Fault sets of variable orientations in the Canterbury Basin all accommodate a component of normal displacement and are often assumed to have formed at different times due to changing tectonic processes and extension directions (Fig. 3.1D - Tulloch *et al.*, 2019). The non-coeval hypothesis for the formation of different fault sets may be considered the most parsimonious explanation for the formation of these fault sets (Fig. 3.1B). For example, Tulloch *et al.*, (2019) propose multiple phases of rifting in Southern Zealandia with faults trending 130°, 90° and 70° forming at 98 to 95 Ma, 90 Ma and 89-82 Ma, respectively. Alternatively, all fault sets formed synchronously, perhaps associated with NW-SE extension with E-W and NW-SE trending fault sets carrying significant components of strike slip (Fig. 3.1A). Lastly, and considered least likely, each of the main fault sets were active synchronously and accrued mainly dip-slip movement to produce multi-directional extension of the basin (Fig. 3.1B).

Discriminating between these alternative hypotheses requires a combination of kinematic and age information for rifting. Despite extensive studies of rift evolution in the Canterbury Basin during the Cretaceous the timing and kinematics of the different sets is poorly constrained (Field and Browne, 1989; Browne *et al.*, 2012; Jongens *et al.*, 2012; Sahoo *et al.*, 2014).

Here we primarily use 2D seismic reflection lines from the offshore Canterbury Basin to determine the timing, geometries and kinematics of each of the three fault sets in the basin. With these data we examine whether the different fault sets were coeval and if they primarily accommodated normal displacement or a mix of dip slip and strike slip dependent on their orientations. The analysis has implications for continental extension prior to onset of breakup. Analysis of the available data suggests that the three main fault sets primarily accrued normal dip-slip coevally producing synchronous multi-directional extension. Prior to breakup, extension parallel to future spreading centers was distributed across much of Zealandia. Multi-directional extension may have widespread application throughout Zealandia and elsewhere.

3.2. Geological Setting and Data

The Canterbury Basin (Fig. 3.2) is part of Zealandia and comprises structures formed in the Mesozoic. The geological evolution of the Canterbury Basin can be divided into three main phases which are here referred to as; 1) East Gondwana Subduction, 2) Late Cretaceous rifting and, 3) post-rift drift (Fig. 3.3). The stratigraphy and structures formed during each of these phases are summarised in the following sections.

3.2.1. East Gondwana Subduction (>~105 Ma)

A prolonged period of Permian-Early Cretaceous (i.e., ~300-105 Ma) subduction and accretion between eastern Gondwana and the Paleo-Pacific plate produced the terranes which comprise the basement of Zealandia (Carter, 1988; Laird, 1993*;* Mortimer *et al.*, 1999; Laird and Bradshaw, 2004; Mortimer, 2004, Mortimer *et al.*, 2014*)*. The present-day E-W bathymetric high, the Chatham Rise, was the front of the subduction system and remained a structural high from the Late Mesozoic to Recent (Wood *et al.*, 1989; Browne *et al.*, 2012). In south Zealandia, subduction along the northern margin of the rise is inferred to have ended at around 105 Ma following its collision with the Hikurangi Plateau, a thickened section of oceanic crust (Laird and Bradshaw, 2004; Davy, 2014). In North Zealandia, the end of subduction is still debated and could post-date 105 Ma (Mazengarb and Harris, 1994; Sutherland *et al.*, 2009, Bland *et al.*, 2015; Strogen *et al.*, 2017; Crampton *et al.*, 2019). Possible evidence for post 105 Ma subduction may be provided by the Pounamu Terrane located in the Southern Alps, which is an enigmatic turbiditic metasedimentary unit deposited on an oceanic seafloor slightly older than 106 Ma (Cooper and Ireland, 2013, 2015; Cooper *et al.*, 2018). Metamorphism of the Pounamu terrane occurred between 90 and 64 Ma and has been interpreted to suggest the presence of an active subduction thrust along the central and northern Alpine fault during this time period (Cooper and Ireland, 2013, 2015; Cooper and Palin, 2018; Cooper *et al.*, 2018). Whatever the precise timing of the cessation of subduction, the subducted Hikurangi Plateau is inferred to be present below the South Island today where it strikes NE-SW (Reyners *et al.*, 2017). In addition, basement reflectivity in seismic lines is interpreted to have been deformed by thrusts and folds generated during Permian-Early Cretaceous subduction (Wood *et al.*, 1989; Tulloch *et al.*, 2019).

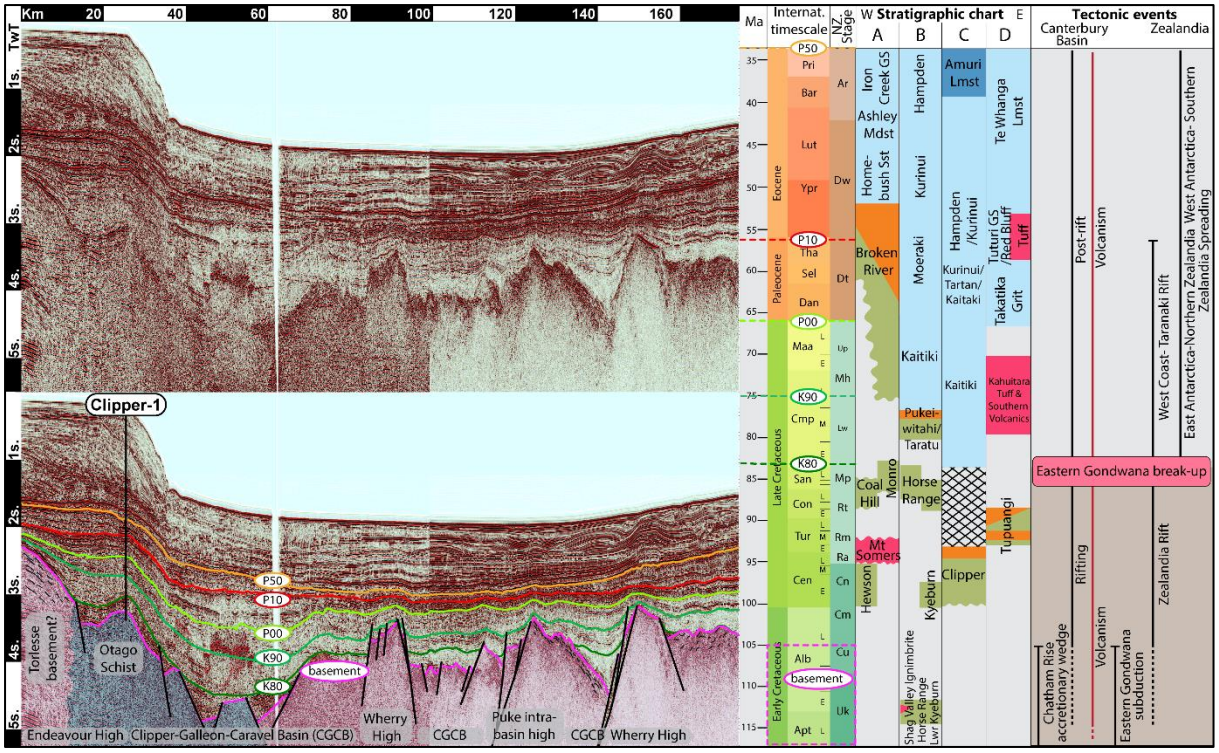

Figure 3.3Uninterpreted (top left) and interpreted (bottom left) composite seismic reflection profile tied to the Clipper-1 well showing rift geometries in the offshore Canterbury Basin; seismic horizon nomenclature is from Strogen and King (2004). Also displayed, stratigraphic chart of the Canterbury Basin (Strogen et al., 2017) and a summary of the major tectonic processes active in the Canterbury Basin and Zealandia from the Late Cretaceous to the Eocene (this study). A: Western Canterbury (Rakaia region); B: North Otago; C: Offshore Canterbury Basin (Clipper-1) and D: Chatham Island. See Figure 3.4 for location

The Canterbury Basin formed part of the Permian-Early Cretaceous accretionary prism of the subduction system (Laird and Bradshaw, 2004). These basement rocks comprise (from north to south) the Pahau, Rakaia and Caples terranes as well as the Otago schists, a portion of the exhumed Permian-Early Cretaceous accretionary prism (Mortimer *et al.*, 2014) (Fig. 3.2). Offshore, basement terrane boundaries trend east to east-north-east sub-parallel to the Chatham Rise (Tulloch *et al.*, 2019), with schist cropping out in the northern part of the Chatham Islands (Campbell *et al.*, 1993; Adams *et al.*, 2008). The terranes of the southern part of the South Island comprise from north to south the Matai or Dun Mountain Terrane, the Permian-Early Cretaceous Brook Street, the Murihiku and the Median Batholith. The northernmost terrane is the Early Permian ophiolite belt (Dun Mountain) unconformably overlain by a volcanoclastic and sedimentary sequence to the west (Maitai Group) (Fig. 3.2 – Mortimer *et al.*, 2014). These terranes are bounded to the south by the fourth basement terrane, the Median Batholith, a Devonian to Early Cretaceous mostly composed of igneous and meta-igneous rocks (Fig. 3.2 - Mortimer *et al.*, 1999). Basement terrane boundaries and associated Mesozoic faults form planes of weakness which in some cases have been reactivated during rifting and may play an important role in the formation and geometry of E-W and NW-SE striking Cretaceous rift faults.

3.2.2. Zealandia Late Cretaceous Rifting (~110-85 Ma)

A widespread phase of extension, referred to as the Zealandia rifting phase (Strogen *et al.*, 2017), produced extension of eastern Gondwana during the Late Cretaceous (~110-85 Ma). Stretching resulted in the formation of Zealandia Rift Province along >1000km of the eastern Gondwana margin. A succession of rift basins developed at this time with two distinct structural patterns (Fig. 3.2): (1) Basins with one set of rift faults parallel to both the post-breakup spreading centre and to the basement structural fabric (e.g., Reinga, Taranaki, West Coast basins, Bounty Trough and Chatham Rise). (2) Basins with several sets of rift fault, one parallel to the post-breakup spreading centre and other oblique to the post-breakup spreading centre and parallel to the basement structural fabric (e.g., Canterbury and Great South basins). The Canterbury Basin rift produced a series of horsts and half grabens (Fig. 3.3) in three main structural domains. The first domain is termed the Clipper domain (after Field and Browne, 1989) and comprises mainly NE-SW striking faults, parallel to the mid-ocean ridge between Southern Zealandia and western Antarctica. The second and third domains correspond to the North Otago domain with the NW-SE striking Waihemo Fault (Bishop, 1974; Bishop *et al.*, 1976) and to the Chatham Rise domain characterized by E-W trending faults (Wood *et al.*, 1989), respectively. Onshore, the geometries of rift faults are poorly constrained due to the tectonic overprint of Miocene-Recent deformation and to the poor or incomplete exposure of Late Cretaceous syn-rift rocks. Despite the relatively poor exposures, some outcrops and onshore seismic reflection profiles show evidence of both NE-SW and E-W rift faults during the Late Cretaceous (Browne *et al.* 2012; Jongens *et al.*, 2012).

3. 2.3. Zealandia Drift Phase (<~85 Ma)

The drift phase of Canterbury Basin sedimentation commenced with the onset of eastern Gondwana breakup at about 86-83 Ma (Adams *et al.*, 2017; Strogen *et al.*, 2017; Higgs *et al.*, 2019), and the formation of new oceanic crust between Zealandia, Antarctica and Australia (Wood *et al.*, 1989; Wood and Herzer, 1993*).* Following the onset of seafloor spreading the Canterbury region was tectonically quiet for >40 Ma (Fig. 3.2), during which time only minor normal faulting (<250 ms throws) occurred along rift faults (Field and Browne, 1989; Sahoo *et al.*, 2015). The Canterbury Basin was then a passive margin with little tectonic movement and the region drifted northward until the initiation of the present-day plate boundary during the Late Eocene to Miocene. In the last 20-30 Myr the onshore and coastal Canterbury Basin were affected by inversion, uplift and erosion post-Oligocene, while the eastern offshore remained unaffected by the plate boundary movements allowing the preservation of syn- and post-rift geometries (Field and Browne, 1989; Jongens et al., 2012; Barnes *et al.*, 2016).

3. 3. Methods

3.3.1. Seismic Mapping:

Faults have been mapped using ~26 000 line km of 2D seismic reflection profiles and one 3D seismic reflection survey acquired between 1966 and 2014 and provided by New Zealand Petroleum and Minerals (NZP&M) via their 2015-2018 data pack (Fig. 3.2). The seismic reflection lines interpreted for this study cover an area of ~ 160 000 km^2. The quality and coverage of the seismic data are variable, with the number and spacing of seismic lines decreasing eastwards. The average line spacing in the study area is around 5 to 50 km. The data acquired or reprocessed after 2006 have a good to very good quality and include the Waka 3D seismic survey in the southern offshore Canterbury Basin (Fig. 3.2). These high-quality data are the primary focus of this study.

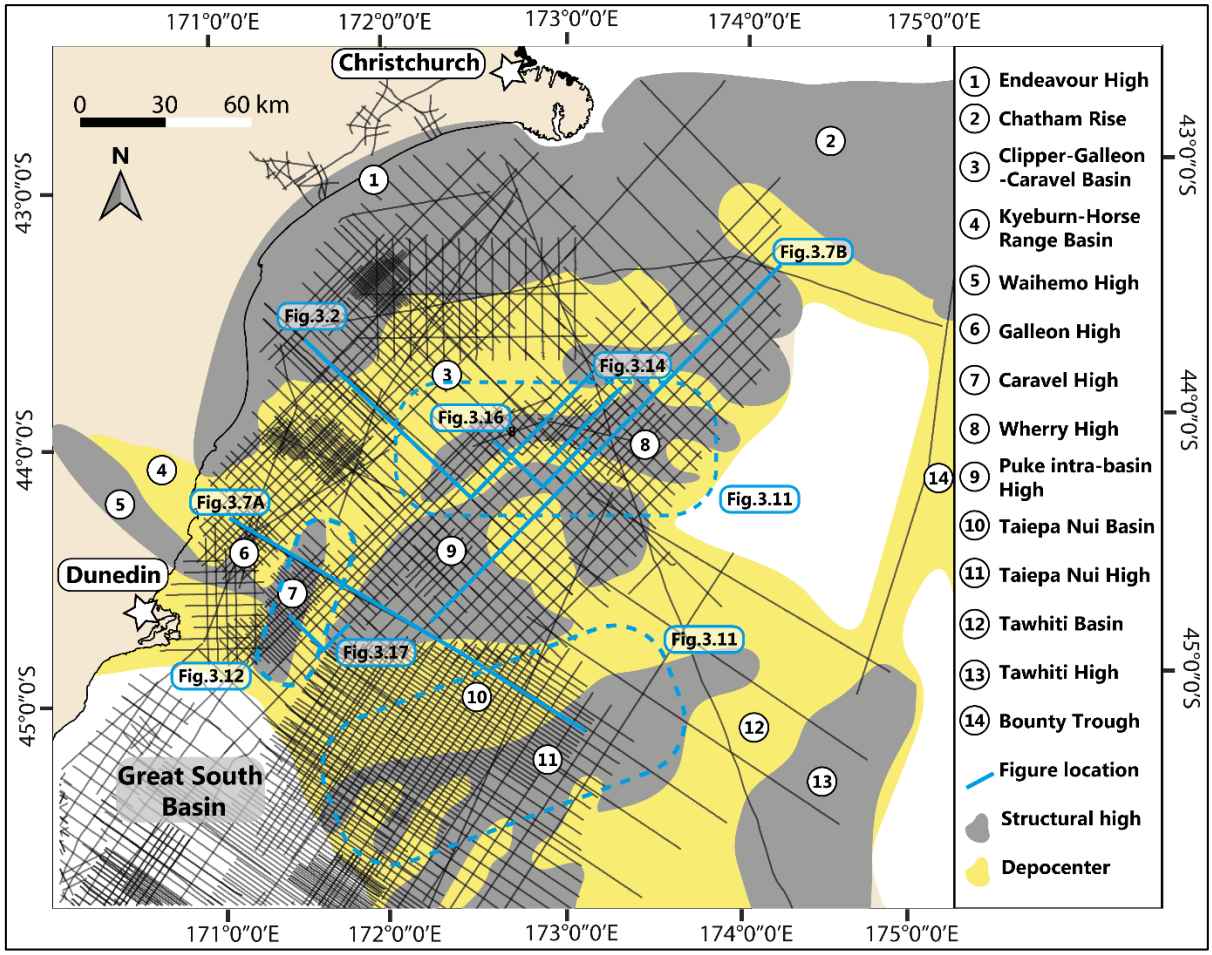

Figure 3.4 Simplified map of rift structural highs and sub-basins nomenclature with location of figures. Rift nomenclature is mostly derived from Field and Browne (1989) and Sahoo et al. (2015. For the new nomenclature, refer to section 2.3 of this thesis. The main rift faults across the Canterbury Basin are named accordingly to the horst and depocenters they separate.

Six horizons tied to the wells were interpreted (Table 3.1 and Fig. 3.3) and named using the GNS Science "K" and "P" seismic horizon naming convention (Strogen and King, 2014). Seismic data has been tied to the most recent biostratigraphic ages established from five

petroleum exploration wells in the offshore Canterbury Basin (Schiøler and Raine, 2011). Horizon ages are primarily assigned using the New Zealand and International Geological Time Scales (Cooper *et al.*, 2004; Raine *et al.*, 2015).

Table 3.1 Seismic horizon nomenclature used in this paper following GNS nomenclature (Strogen and King, 2014).

Color code	Horizon Name	GNS Science nomenclature (Strogen & King, 2014)	Age (Ma)	NZ Stage	International Stage	Mapped
	Top Eocene	P50	34	Runangan	Priabonian	yes
	Top Paleocene	P10	56	Teurian	Thanetian	yes
	Top Late Cretaceous post-rift	P00	66	upper Haumurian	Maastrichtian	yes
	Intra Late Cretaceous post-rift	K90	78	lower Haumurian	intra Campanian	yes
	Top Late Cretaceous syn-rift	K80	84.5±1.5	Piripuan	Santonian	yes
	Top Basement	basement	110±5	Urutawan to Korangan	Aptian-Albian	yes

Clipper-1 is the only exploration well in the offshore Canterbury Basin that penetrated Cretaceous syn-rift strata. The base of the syn-rift succession (110±5 Ma) is the unconformity between the top basement reflector and growth strata (see chapter 2 for further details). The top of syn-rift reflector (K80) was tied to the Clipper-1 well and constrained throughout the study area by mapping of growth strata geometries (as opposed to the draping geometries that are more typical of post-breakup reflector packages). The K80 reflector also defines the Gondwana breakup and onset of spreading along the oceanic ridges.

Structural contour and isochron grids were generated for the top basement (Fig. 3.5A), the top basement to K80 syn-rift interval (Fig. 3.6A - ~110 to 85 Ma; Aptian-Santonian), and the K80-P00 post-rift (Fig. 3.6B - ~85 to 66 Ma; Campanian to Maastrichtian). These maps have been used to show the locations and geometries of faults. In all maps the width at fault polygons is proportional to fault heave. In addition, the three isochron maps define a number of depocenters and structural highs with the names for these structures adopted from the literature (Field and Browne, 1989; Sahoo et al., 2015) and three introduced in this study (Fig. 3.4). The main rift faults across the Canterbury Basin are named accordingly to the horst and depocenters they separate.

3.3.2. Fault throw and length measurements

The basement and K80 (Urutawan to Piripuan, early Albian-Santonian; ~110 to 85 Ma) isochron structural maps show the geometry of faults with a component of normal displacement in the Canterbury Basin (Figs. 3.5 and 3.7). The largest faults in the system (here referred to as border faults) are segmented or form single traces which bound symmetrical grabens and asymmetric half-grabens (Figs. 3.5 and 3.7).

We have mapped 654 faults on seismic reflection profiles with vertical displacements of 67 to 2884 ms two way time (TwT) and lengths of 0.6 - 90 km for the top basement and syn-rift horizons. Maximum vertical displacements (i.e. throws) have been measured for K80, K90, P00, P10 and P50 horizons. Depth conversion and decompaction of syn-rift growth packages is generally not required (and has not been undertaken) to determine the first-order displacements of faults, as the changes in displacement due to depth conversion and

compaction is generally <20% (e.g., Taylor *et al.*, 2008). Where syn-rift (K80) reflectors were not present on the footwall of a fault, throw was measured between the top basement in the footwall and the top basement or syn-rift horizons in the hangingwall. These displacement measurements are minimums as basement and syn-rift strata in the fault footwall may have been eroded. For 6 faults, throws were measured on multiple seismic lines along the length of the trace and these are used to generate horizon separation diagrams. The displacement diagrams present the total throws that accumulated during rifting. In cases where small throws (< 250 ms TwT) post-date rifting these displacements have been subtracted from the top basement displacement to derive total values for syn-rift faulting.

Fault lengths were measured for all mapped faults in the seismic reflection dataset. In the majority of cases fault lengths measured are minimum values which are impacted to varying degrees by the seismic resolution and by the seismic line spacing. 3D seismic reflection datasets typically resolve shorter faults and have small absolute errors on the estimated lengths (e.g., Watterson *et al.*, 1996; Meyer *et al.*, 2002). Comparison of 3D and 2D seismic data demonstrates the impact of data quality on fault length measurements for this study and is presented in section 3.4.2. For the 2D datasets mainly used in this study, we expect underestimates of fault lengths of kilometres and under-sampling of the numbers of faults with lengths of up to ~20 km. To decrease the influence of seismic line spacing on measured fault lengths where possible we have projected fault traces beyond their last observed seismic line using observed decreases in throw towards the tip.

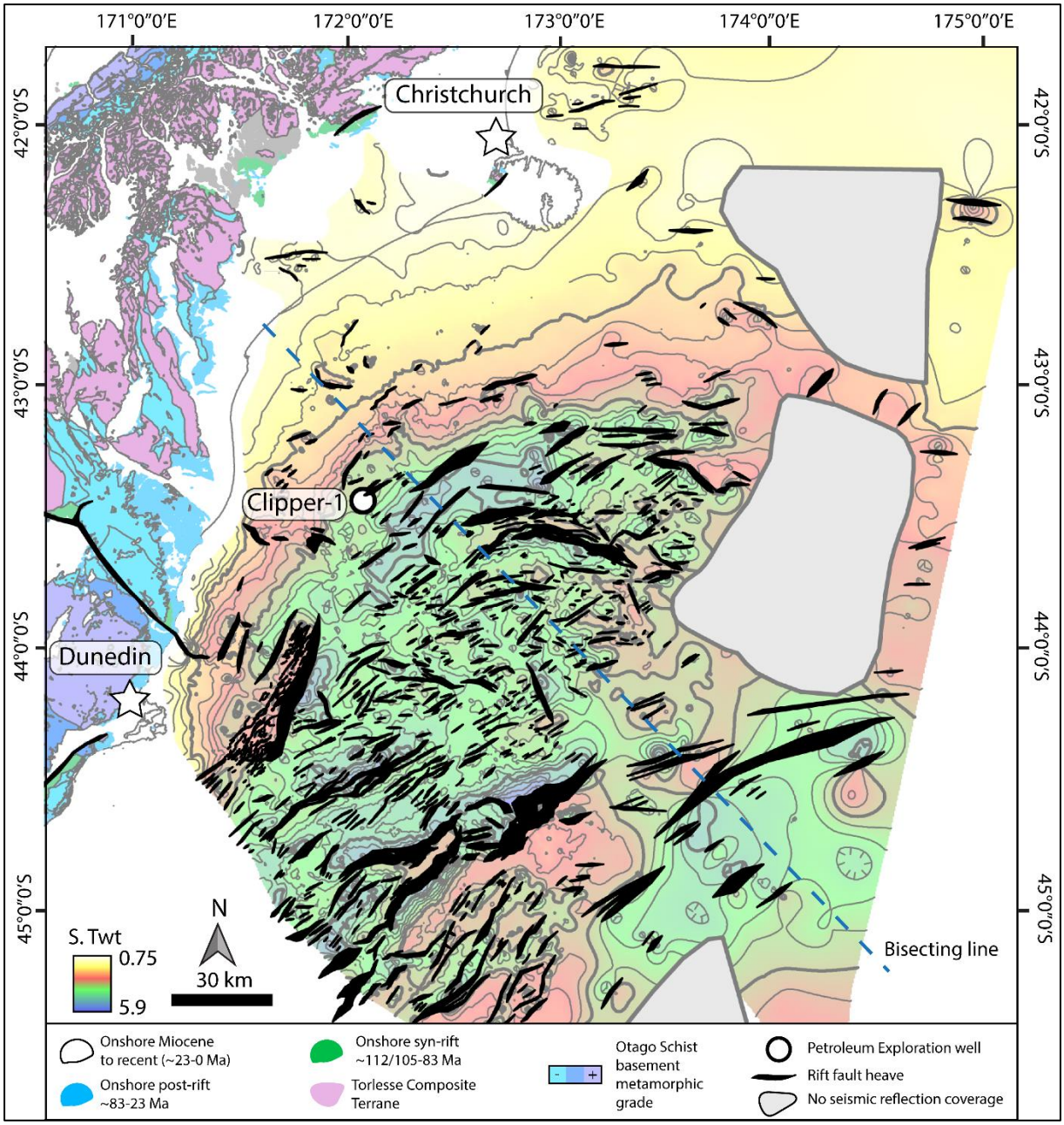

Figure 3.5 Top Basement structural contour map with fault polygons displaying rift fault heaves for the offshore Canterbury Basin. Blue dashed lie separates north and south areas (see text for further discussion of derivation of this line).

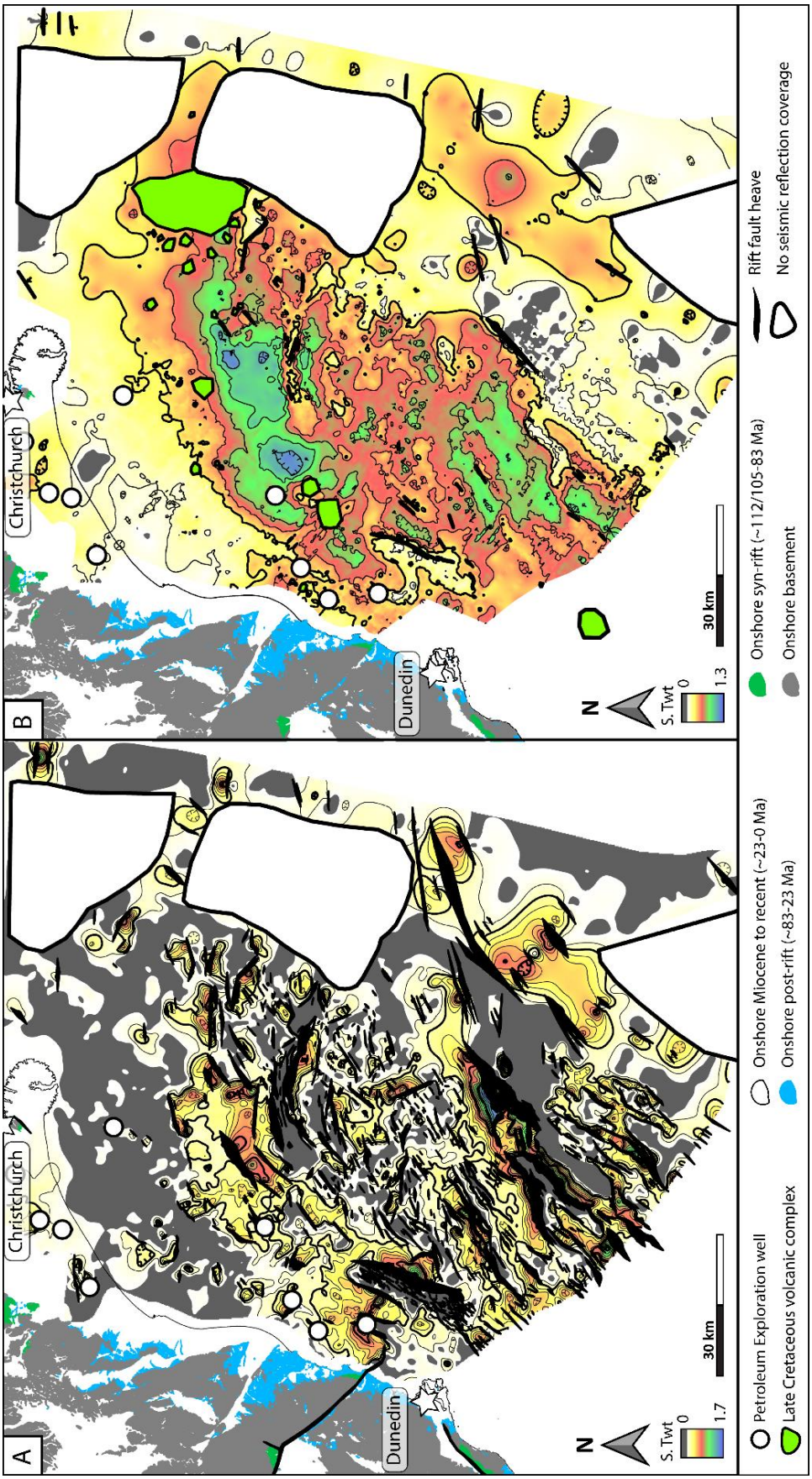

Figure 3.6(A) Syn-rift structural isochron map (~110-85 Ma) showing the location of depocenter and horst structures. (B) Post-rift Late Cretaceous isochron structural map (~85-66 Ma) showing the decrease of rift fault activity post-breakup of eastern Gondwana and the persistence of basin topography.

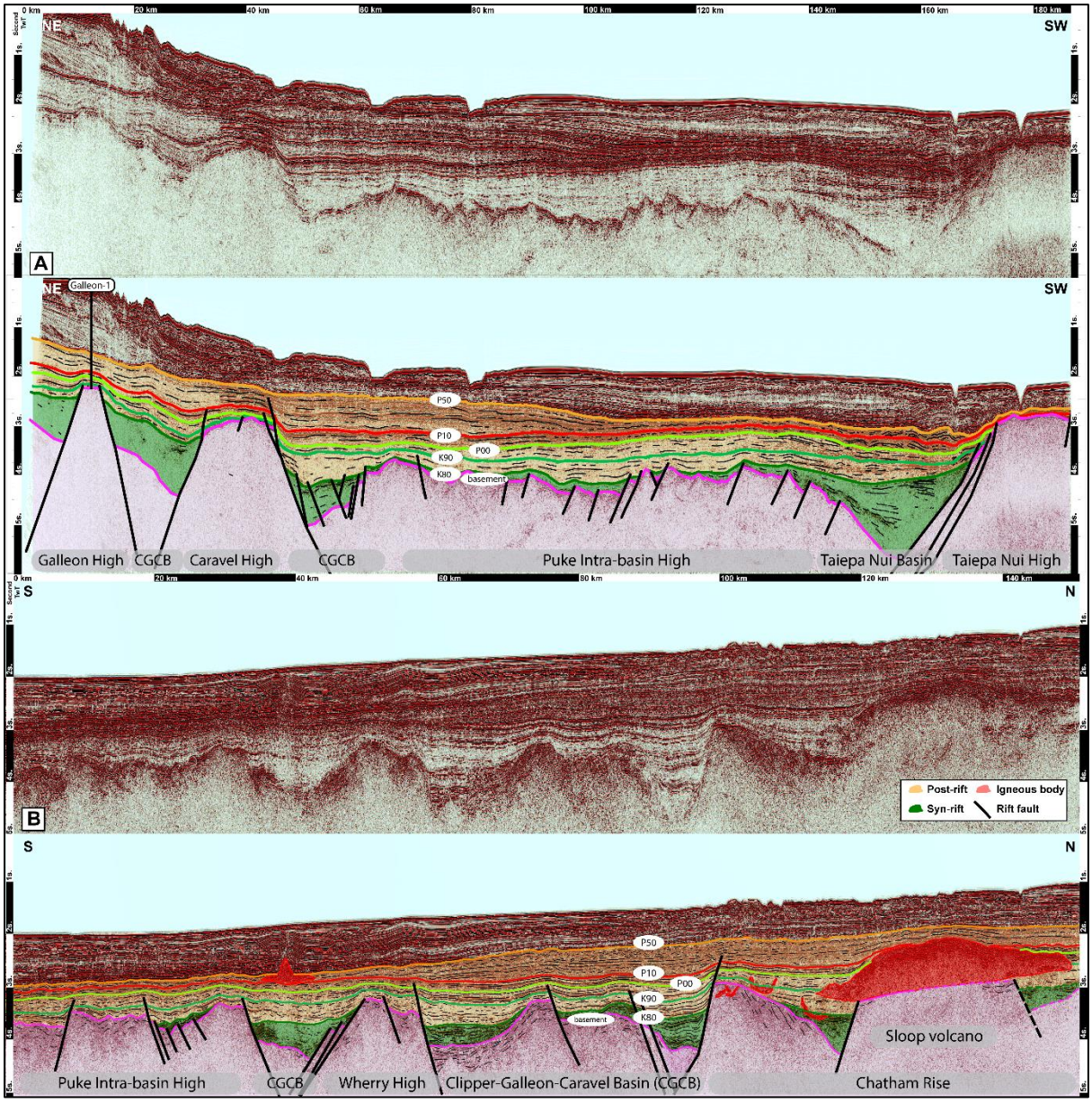

Figure 3.7(A) N-S and (B) E-W composite seismic profile sections showing rift depocenters and structural highs together with Late Cretaceous syn-rift and Late Cretaceous to Eocene post-rift sequences. Note that some of the main rift faults display minor (<250 ms TwT) post-rift displacement. See Figure 3.4 for location.

3.3.3. Rift Fault Trend, Timing and Kinematics

We use three parameters to analyse the kinematics and displacement histories of the different trends of rift faults. Firstly, fault trends are inferred to be parallel to line segments connecting the mapped tips of fault traces for 654 faults. The data trends of these line segments have been plotted in bi-directional rose diagrams. For curved faults that display segments varying in strike from NE to E, the strike of each individual segments was considered. The north and south sub-areas of the offshore Canterbury Basin discriminated in this study are separated by a line that forms the boundary between mainly NE-SW and E-W fault trends (Fig. 3.5, blue dashed line). Second, the timing of displacements for each of the three fault sets are determined using growth strata imaged on composite seismic lines that cross two of the three

fault sets (Fig. 3.8A). Ages for the growth strata are estimated by correlation of seismic reflectors to wells (see section 3.1). Third, we differentiate between dip-slip and strike-slip movement along the different sets of rift faults using fault geometries and displacements (Fig. 3.8B and C).

Strike-slip is difficult to identify on 2D seismic reflection lines where piercing points are often not clearly resolved. Here we infer the slip sense of seismically imaged faults using fault geometries and horizon separation diagram geometries (Fig. 3.8B and C). In the case of mainly dip-slip movement, faults display relay ramp and breached relay geometries (Walsh *et al.*, 1999), whereas for strike-slip faulting boundaries, segmentation will produce pull-apart basins, releasing bends and pop-up structures (e.g., Morley et al., 2004; Massironi *et al.*, 2014) (Fig. 3.8B). For separation diagrams footwall and hangingwall horizons define displacements that rise to a maximum (often near the fault centre) and in some cases produce symmetrical bell shape profiles (Fig 3.8C). For segmented normal faults, displacements decrease at relay ramps where they are accommodated by bed rotations in the ramp (e.g., Childs *et al.*, 2017). For strike slip faults apparent vertical displacements recorded by horizon separation diagrams can be highly variable with the greatest vertical displacements observed at segment boundaries. These faults may have both a reverse and normal sense of displacement along their length, with the slip sense being dependent on the sense of fault stepping. In cases where the sense of slip and fault stepping are the same normal displacements will be observed in pull-apart basins and in circumstances where they differ reverse faults and pop-ups would be expected. Therefore, vertical displacement profiles across segment boundaries offer the opportunity to identify strike-slip faulting. Horizon separation diagrams for oblique slip faults may display a combination of geometries depicted in Figure 3.8C, however, given the wide variation in fault set orientations we would expect at least one of these fault sets to have accommodated significant strike slip if the regional extension direction was uniform and faulting coeval.

We characterize the timing of rift faults (and their synchronicity) by comparing the relative ages of growth strata in adjacent depocenters controlled by two rift faults with different orientations (Fig. 3.8A). In the case where the bounding faults are deemed synchronous (Fig. 3.8A, left panel), growth strata would indicate contemporaneous fault displacement and in many cases display a laterally continuous reflector package of growth strata between the depocenters, which is draped by the same package of post-rift reflectors. Where the two rift faults of different trend are not coeval, growth strata would indicate the variable timing and are often not laterally continuous between the two sets of faults (Fig. 3.8A, right panel). In this case we would expect growth strata of the younger set of rift faults to overlie growth strata adjacent to the oldest rift fault with a potential angular unconformity and erosional truncation between the two sets of growth strata.

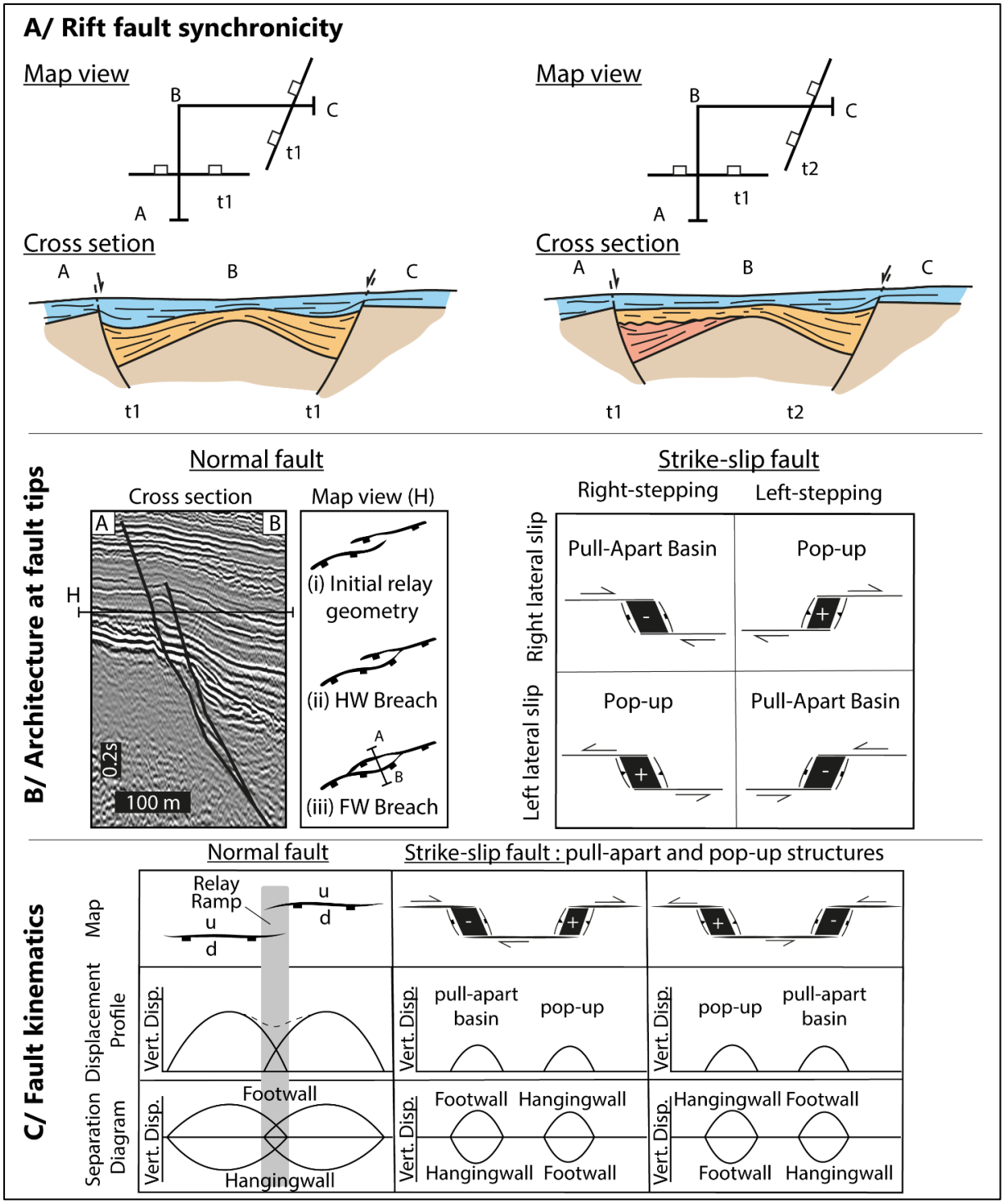

Figure 3.8 Summary of the parameters used to determine the timing of rift faults (A), while dip-slip or oblique slip movements have been discriminated using rift fault architecture (B) and displacement separation diagrams (C). In case of purely normal displacement, fault architecture displays relay and breach geometries. HW breach: Hangingwall breach; FW breach: Footwall breach (adapted from Walsh et al., 1999). In the case of strike-slip movement, faults display pop-up or pull-apart basin geometries (adapted from Massironi et al., 2014). (C) By examining the geometry of the separation diagram along the rift fault. The separation diagram will display a bell geometry with a symmetry in case of purely normal displacement. While in case of normal displacement with an oblique motion, the separation diagram will display a horizontal offset. To note that the footwall throw measured does not represent a maximal value due to erosion and smoothing of the relief generated by its uplift.

3.4. Rift Geometry

3.4.1. Fault Orientations

The Canterbury Basin comprises two main fault sets which strike NE-SW to E-W and are accompanied by a subsidiary fault set that strikes NW-SE. Three main trends of rift fault traces formed during mid-Late Cretaceous extension of the Canterbury Basin (Figs. 3.5 and 3.9):

(1) NE-SW faults range in trend from 10° to 70° with the majority of traces trending between 50° and 70°. This fault set is present throughout the Canterbury Basin, and dominates the fault system in the southeast part of the basin. These faults are approximately parallel to the southeastern margin of Zealandia and to the oceanic ridge (and associated spreading centre) that separates Zealandia and western Antarctica.

(2) E-W to WNW-ESE faults most often trend from 70° to 110°. They are more commonly located in the modern onshore area west and northwest of Bank Peninsula and in the north-eastern offshore Canterbury Basin. This fault set trends parallel to the Chatham Rise and to the former Mesozoic subduction margin north of the rise.

(3) NW-SE trending faults range in trend from 110° to 160° and are subordinate to NE-SW and E-W sets. They are most common in the southern Canterbury Basin and include the Waihemo Fault a major rift fault in the North Otago Region. The Waihemo fault, and NW-SE striking faults in general, are parallel to the axis of the Otago schist belt (Mortimer 1993; Mortimer 2000; Deckert *et al.*, 2002), and to other basement terrane boundaries in the southern South Island including the Rakaia Terrane and Otago Schist boundary (Fig. 3.2 and 3.4).

NW-SE and NE-SW faults occur in similar parts of the basin and form abutting relationships. By contrast, E-W trending faults are mainly present in the northern basin, with the faults changing in orientation progressively from NE-SW to E-W towards the north-east. The change in predominant fault trend from NE-SW to E-W occurs along a NW-SE trending line (Fig. 3.5, blue dashed line). Some individual faults cross this line and have different trends along their length. For example, the fault bounding the southern edge of the Wherry High comprises three right stepping segments. The trend of the three segments changes from west to east passing from NE-SW to E-W and to NW-SE along ~90km (Figs. 3.4, 3.5 and 3.7). In this case progressive rotation of the dominant trend of the fault is achieved by a series of small discrete changes in trend at segment boundaries.

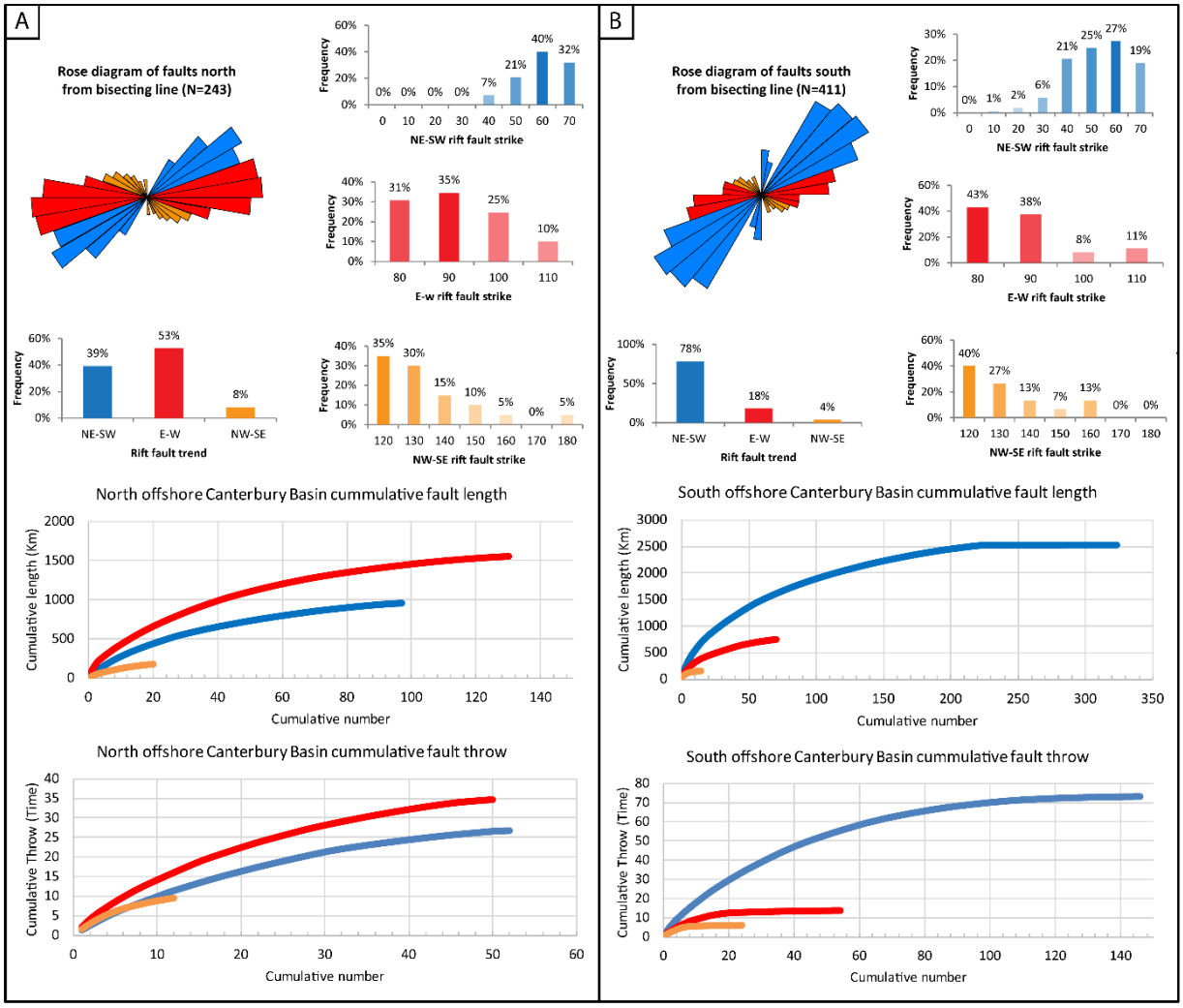

Figure 3.9 Analysis of the difference between rift fault trends, fault length and throw between (A) north offshore and (B) south offshore Canterbury Basin. Blue dashed line on Figure 3.4 separates north and south areas (see text for further discussion of derivation of this line).

3.4.2. Fault Lengths and Throws

Fault lengths and throws offshore range up to about 90 km and 2.9 second (~>4 km), respectively with the length population for each of the main fault sets being similar. Fault length is plotted against throw in Figure 3.10 which shows a broad accordance in the sizes of NE-SW and E-W faults sets. NW-SE trending faults are generally shorter for a given maximum displacement and have lower displacements (than the two other sets). Although the onshore Kyeburn fault is estimated to have a throw of >4 km, making it potentially the largest fault in the basin. In addition, NW-SE faults are also less common in the basin compared to the other fault sets, in some cases possibly because these faults are parallel to the primary seismic line orientation. Despite differences in the sampling and numbers of faults in each set, the fault length and displacement relationships are similar and cannot be used to infer that the origin or kinematics of the fault sets are different.

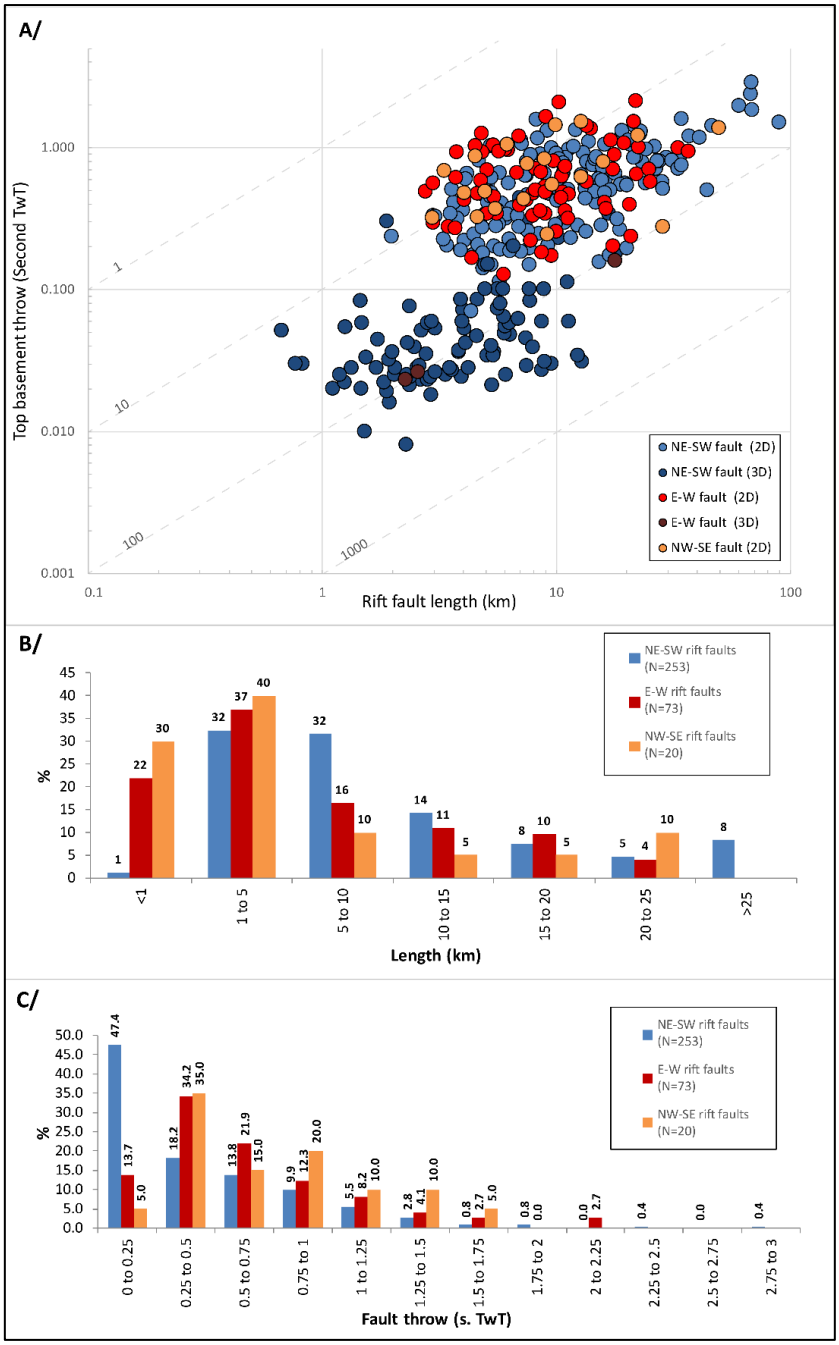

Figure 3.10 (A) Diagram showing the relationship between rift fault length and maximum vertical displacement. Graph shows weak linear trends for faults interpreted on 2D and 3D seismic datasets. (B) Histogram of rift fault length for NE-SW, E-W and NW-SE rift fault categories showing an approximate log-normal distribution centred on the 1-5km category. (C) Histogram of rift fault throw for NE-SW, E-W and NW-SE rift fault categories.

3.4.3 Fault Kinematics

Constraining fault kinematics is key for understanding the origins of Cretaceous faults in the Canterbury Basin. These faults universally display a component of normal dip slip and the available seismic reflection data provide little evidence of strike slip. We have analysed fault geometries and displacements at segment boundaries to test the hypothesis that one or more of the fault sets has a component of strike slip.

The Taiepa Nui fault trends NE-SW, dips NW and contains a large (~20 km wide) right-stepping overlap zone between the northern and southern segments of the fault (Fig. 3.11).

Within the overlap zone seismic horizons dip to the north (towards the fault hangingwall) and are displaced by faults that traverse the zone of overlap between segment tips and connect the primary segments. The north end of this overlap zone is displaced by the southern segment which connects with the northern segment at the base of the ramp. Displacements on the main fault segments decrease across the overlap zone, which appears to facilitate the transfer of displacement between segments (Fig. 3.11C). This geometry and displacement of the segmentation and overlap zone are characteristic of normal faults separated by a relay ramp and accruing predominantly dip-slip displacement (e.g., Childs *et al.*, 1995, 2017; Morley, 2017). If the relay ramp interpretation is correct, then the NE-SW striking Taiepa Nui fault primarily accommodated NW-SE extension orthogonal to the strike of the fault.

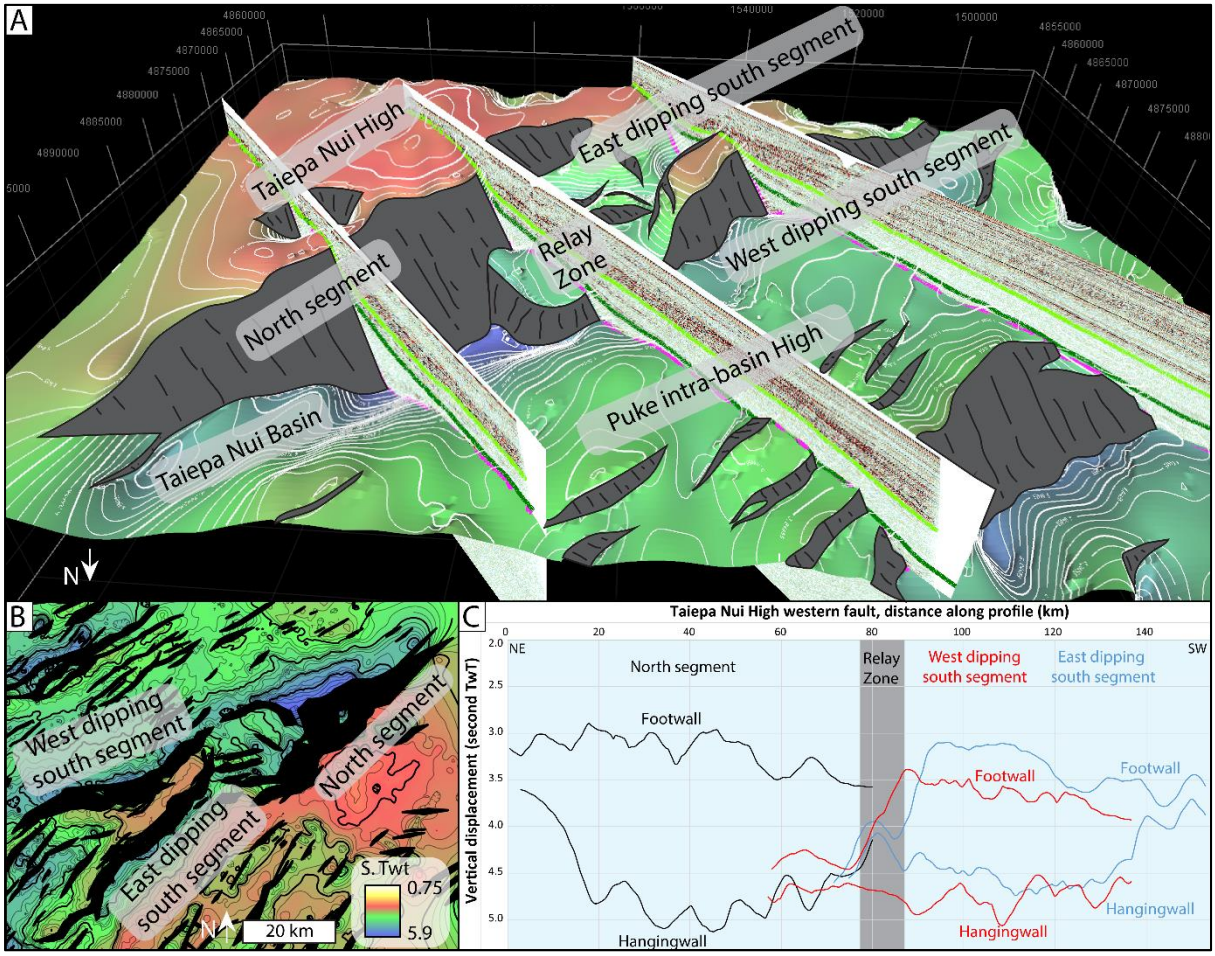

Figure 3.11(A) 3D view of the top basement grid with faults showing a ramp structure indicator of dip-slip movement along the NE-SW rift fault bounding the western edge of the Taiepa Nui High. (B) Top basement isochron map showing the geometry and nomenclature of the different segments of the Taiepa Nui High western fault. (C) Separation diagram along NE-SW Taiepa Nui Rift fault displaying complementary changes in displacement across the overlap zone, consistent with dip-slip faults. See Figure 3.4 for location.

Figure 3.12 shows a second example of an approximately NE-SW trending fault that bounds the eastern side of the Caravel Horst block and is imaged in the Waka 3D seismic volume. Similar to the previous example, the Caravel fault is segmented and forms a number of small-scale overlap zones (< 2km wide). The segmentation is consistent with the fault comprising a number of intact and breached relay-ramps (Fig. 3.12). The relay ramps suggest that this fault too is mainly normal dip slip.

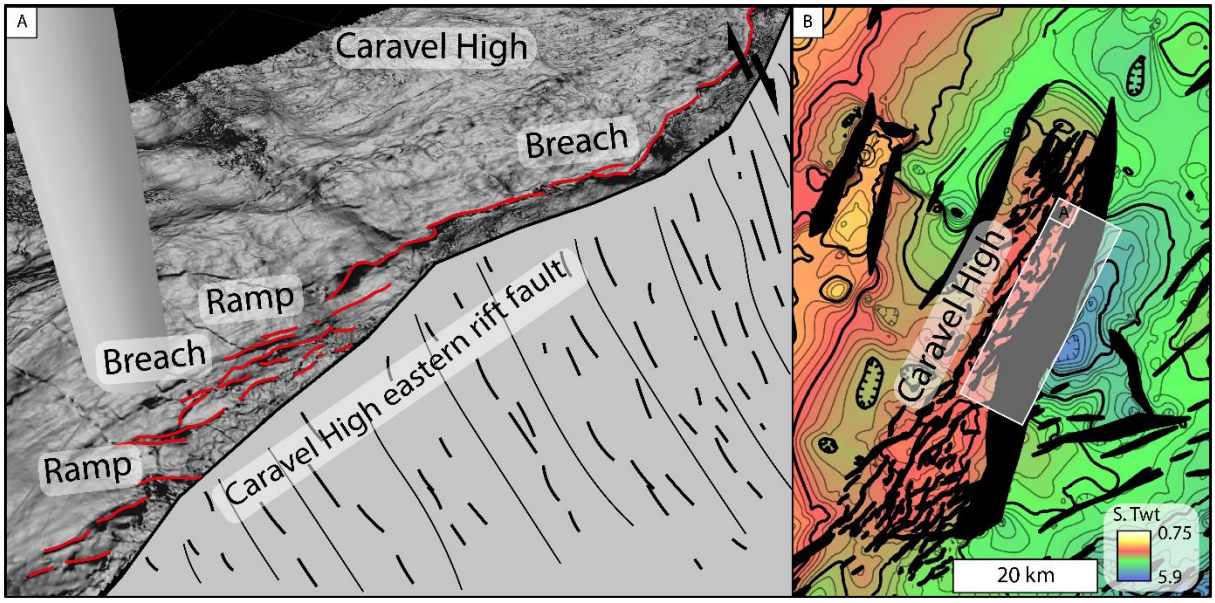

Figure 3.12 (A) 3D view of the top basement grid with dip of maximum similarity seismic attribute highlighting faults within the fault zone (red lines) and showing ramps and breached geometries indicative of dip-slip movement along the rift fault bounding the eastern edge of the Caravel High. (B) Top basement isochron map showing the geometry of the Caravel High eastern fault.

Segmentation analysis has also been conducted on the fault bounding the southern edge of the Wherry High, which comprises three segments that strike NE-SW, E-W and NW-SE (Fig. 3.13). Overlap zones between the three segments are <2km wide. If for example, the faults were accruing slip associated with a regional NW-SE extension direction, E-W faults would be expected to accommodate left-lateral strike-slip with right-stepping overlap zones forming pop-up structures. Instead, for all fault orientations the overlap zones have geometries consistent with breached relays (Fig. 3.13) and the entire fault is interpreted to have mainly accommodated normal dip slip. To test the dip-slip hypothesis we have generated a horizon separation diagram for the length of the fault. The horizon separation diagram along the fault (Fig. 3.13C) shows hangingwall and footwall top basement horizon geometries, with the greatest throw located towards the centre of the fault. These displacements do not indicate that the normal displacement decreases on E-W or NW-SE sections of the fault (as might be inferred if these parts of the fault accommodated significant strike slip). In addition, the separation diagram shows decreases in throw at the segment boundaries which is inconsistent with these overlap zones forming pop-up structures. Instead, displacement lows at overlap zone is consistent with these zones forming relay ramps on normal faults. Therefore, we conclude that the Wherry fault is mainly dip-slip along each of the three segments despite their variable strikes. If this interpretation is correct the E-W trending faults on the southern margin of the Chatham Rise were primarily formed in association with N-S extension.

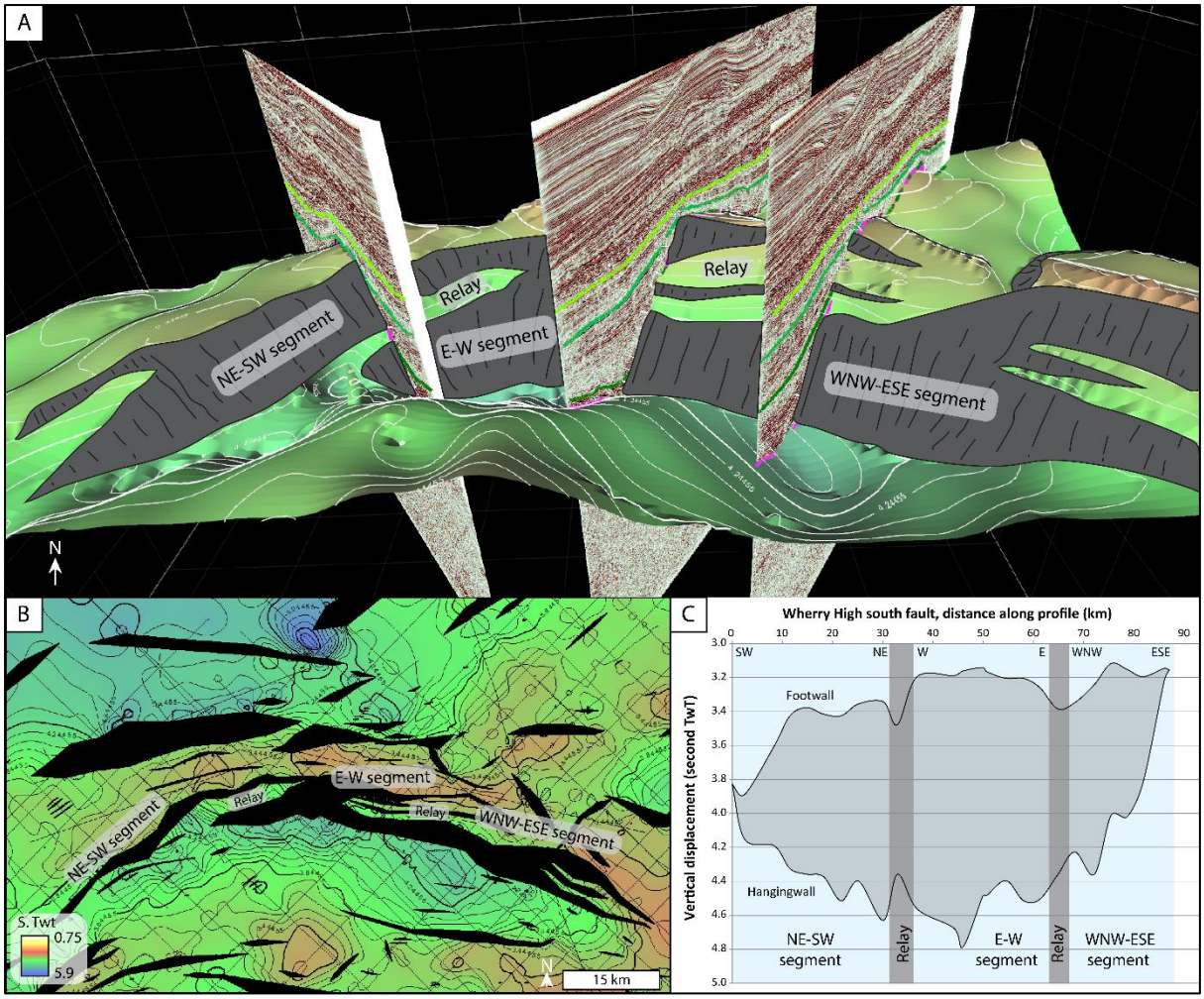

Figure 3.13(A) 3D view of the top basement surface along the Wherry fault with three segments of NE-SW, E-W and NW-SE orientations linked via overlap zones. (B) Top basement isochron map showing the geometry and nomenclature of the different segments of the Wherry fault. (C) Separation diagram along the Wherry fault displaying a bell geometry typical of dip-slip movement. The decrease in displacement around 32 km and 65 km reflect relay ramps between the NE-SW, E-W and NW-SE segments of the fault. See Figure 3.4 for location.

In summary, all of the mid-Cretaceous faults in the Canterbury Basin accommodated a component of normal dip-slip displacement. Geometric and displacement analysis of segmented NE-SW, E-W and NW-SE trending faults provide no indication of strike-slip and are interpreted to be mainly normal dip slip. We do not discount that some strike-slip along E-W and NW-SE trending fault sets, however, if present, strike-slip is not sufficiently large to be recorded at segment boundaries as pop-ups or pull-apart basins. Therefore, we conclude that the Canterbury Basin appears to have been extended in three directions, with N-S extension predominating on the southern Chatham Rise and NW-SE extension in the southeast of the basin.

The amount of extension across the basin is modest. Extension has been calculated by comparing fault heave surface area to the total mapped area of the surface and by calculating the ratio of the fault heave surface to total horizon length along line samples constructed from composite seismic sections. For the area calculation across the entire study area, the ratio between these two values gives a stretching of around 11% (β=1.111). Extension has also been

estimated from two composite sections, one oriented E-W in the southern offshore Canterbury Basin, intersecting mostly NE-SW faults and a second one oriented N-S, intersecting mostly E-W rift faults (Fig. 3.4 and 3.7). The E-W composite section returned an extension of 16.7% (β=1.167) and the N-S composite section 11.3% (β=1.113). These measurements suggest that NE-SW faults accommodate ~50% higher extension than E-W faults, with the values of extension being comparable to many other rift basins worldwide (stretching ~20%, β=1.120; Davison and Underhill, 2012).

3.4.4. Basement Structural Fabric

Prior to the onset of rifting, the basin was affected by Permian-Early Cretaceous compression, with contractional structures striking ~E-W (present-day orientation). High amplitude and relatively continuous reflectors are visible to up to 0.5 second TwT below the top basement reflector in the north-eastern offshore Canterbury Basin over 21 000 km^2. Low angle discontinuous reflectors within basement rocks are interpreted as thrusts with associated fault-related folds (Fig. 3.14). Antiforms and synforms have generally a long-shallow dipping limb and a short-steep limb with more discontinuous reflectivity at the antiform hinges. In most cases fold vergence is towards the north, except in the area south of the E-W Wherry structural high where folds verge southward. The dip-direction of the reflectors changes within the basement and shows EW, WNW-ESE to NW-SE fold axis within kilometre-scale wave lengths (Figs. 3.14 and 3.15). An erosive surface is often present at the hinge of antiforms that can either be overlain by syn-rift or post-rift Late Cretaceous reflectors. In the hinge of synforms, overlying reflectors tend to be conformable while on the fold limbs they onlap the basement reflectors.

The nature of these reflectors is unknown but thereof could correspond to onshore basement terrane boundaries or to the structural fabric (i.e., bedding, schistosity, jointing) within the basement rocks (Tulloch *et al*., 2019). Basement rocks of the Canterbury Basin include zeolite and prehnite-pumpellyite grade metasedimentary rocks of the Torlesse Composite Terrane, in addition to, chlorite-grade schists belonging to the Otago Schists in the south (Fig. 3.15 – e.g., MacKinnon, 1980; Mortimer, 2004; Tulloch *et al.*, 2019). The possibility of these reflectors being some unknown facies not cropping out onshore is also plausible. Bache *et al.* (2014) interpreted the extent of the Murihiku terrane offshore by comparing onshore structural trend to the one of offshore basement reflectors (Fig. 3.15). Applying the same methodology, the E-W to WNW-ESE trends of basement reflectors could match with the Otago schist intersected at Clipper-1 or the Torlesse Composite Terrane (Fig. 3.15).

In the offshore Canterbury Basin, basement reflectors are most obvious where rift faults predominantly strike E-W (Figs. 3.5 and 3.15). Even though no seismic reflection profiles display Late Cretaceous fault reactivation of thrust faults, the basement structural fabric may have influenced fault orientation in this part of the Canterbury Basin due to the presence of pre-existing weakness zones or lineaments in the basement. Basement control of the location and trend of NW-SE is supported by seismic reflection lines from the Great South Basin where NW-SE trend of faults are restricted to area where the Murihiku Terrane extends offshore (Sahoo *et al.*, 2018).

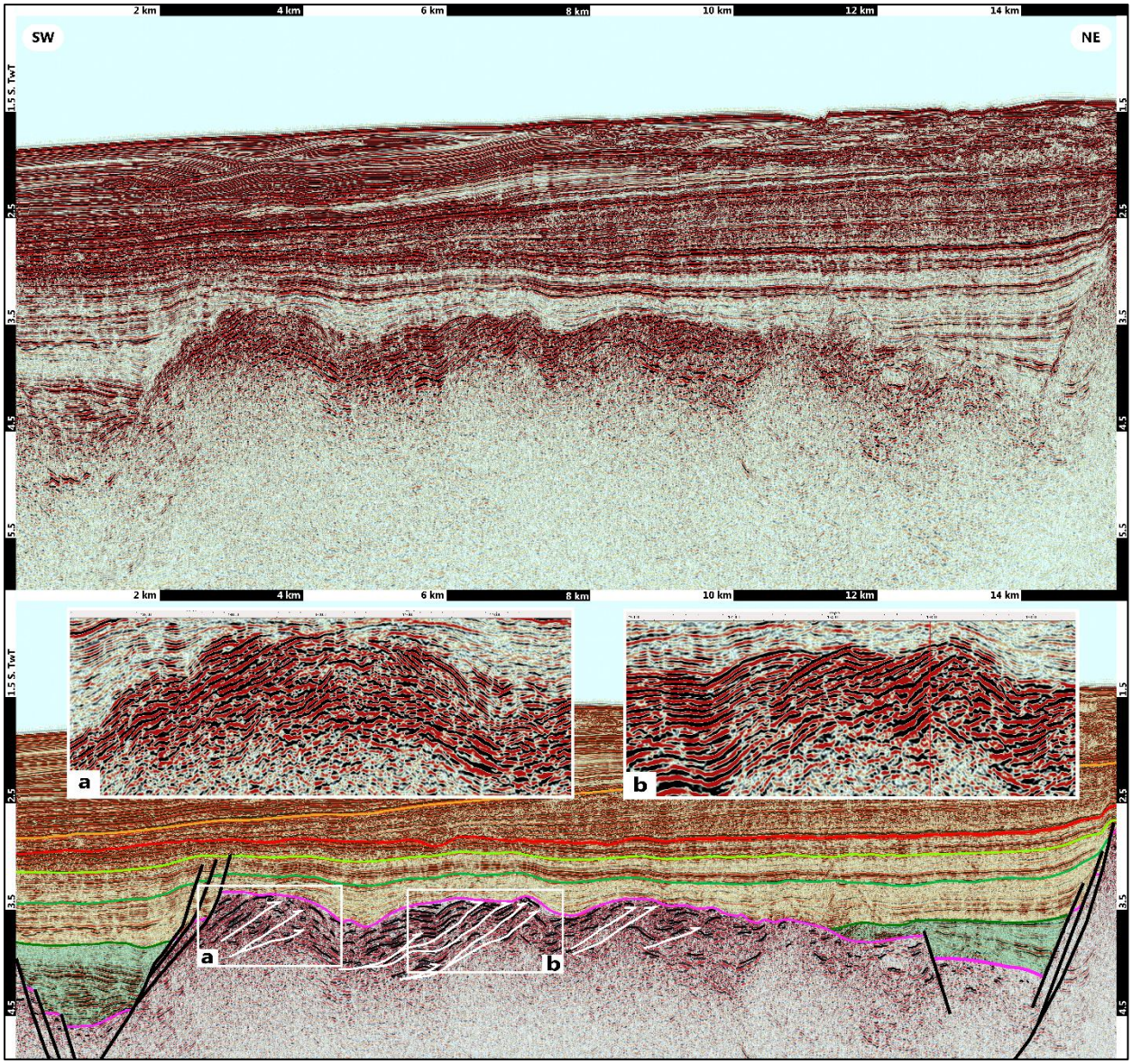

Figure 3.14 Seismic reflection profile in the north offshore Canterbury Basin showing basement reflectivity that can be interpreted as a succession of folds and imbricated thrusts over a rift structural high covered by early Late Cretaceous post-rift sediments. See Figure 3.4 for location.

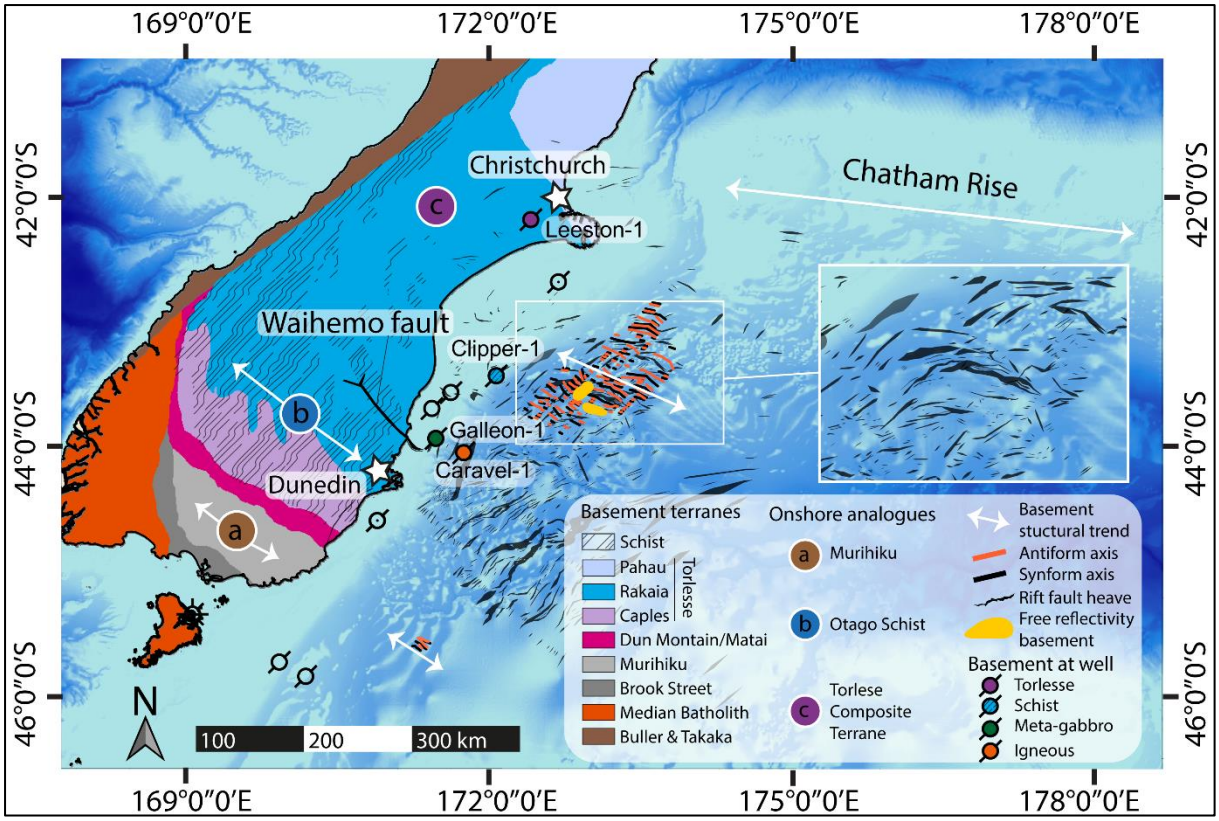

Figure 3.15 Map of the offshore Canterbury Basin showing the orientation of basement reflectors fold axis in the offshore East Coast of the South Island with onshore basement terranes (Adapted from Mortimer (2004) and basement lithology drilled in the Canterbury Basin. Data from Caravel-1 well, confidential data, comes from Blanke (2015). The extent of the Murihiku terranes from Bache et al. (2014). Bathymetry data licensed under NIWA Open Data Licence v1.0.v.

3.5. Fault Displacement Timing

The geometries of growth strata along extensional faults can be used to examine if faults of different trends were accruing displacement simultaneously and formed synchronously. On a basin-wide scale the top basement to K80 isochron thickens in the hangingwall of each of the main fault sets, suggesting an element of synchroneity in their displacement histories. To test this idea further we have generated composite seismic lines that cross two of the three fault sets. These composite lines universally indicate that all fault sets were active synchronously and here we present two examples. On the Wherry High (Fig. 3.4) a composite seismic reflection intersects both NE-SW and E-W faults. Because the depocenters associated with each fault set are under-filled, growth strata are not laterally continuous across the section (Fig. 3.16), however, the same lower Haumurian (K90, intra Campanian, ~83 to 78 Ma) post-rift reflector package overlies both growth strata packages. Therefore, the different orientation faults are interpreted to have been active synchronously and ceased accruing displacement at about the same time. Due to the poor age resolution at the base of the sequence it remains possible that the onset of displacement on the two fault sets was not precisely coeval, although the similar depocenter geometries support the interpretation for both fault sets that most of the faulting was synchronous.

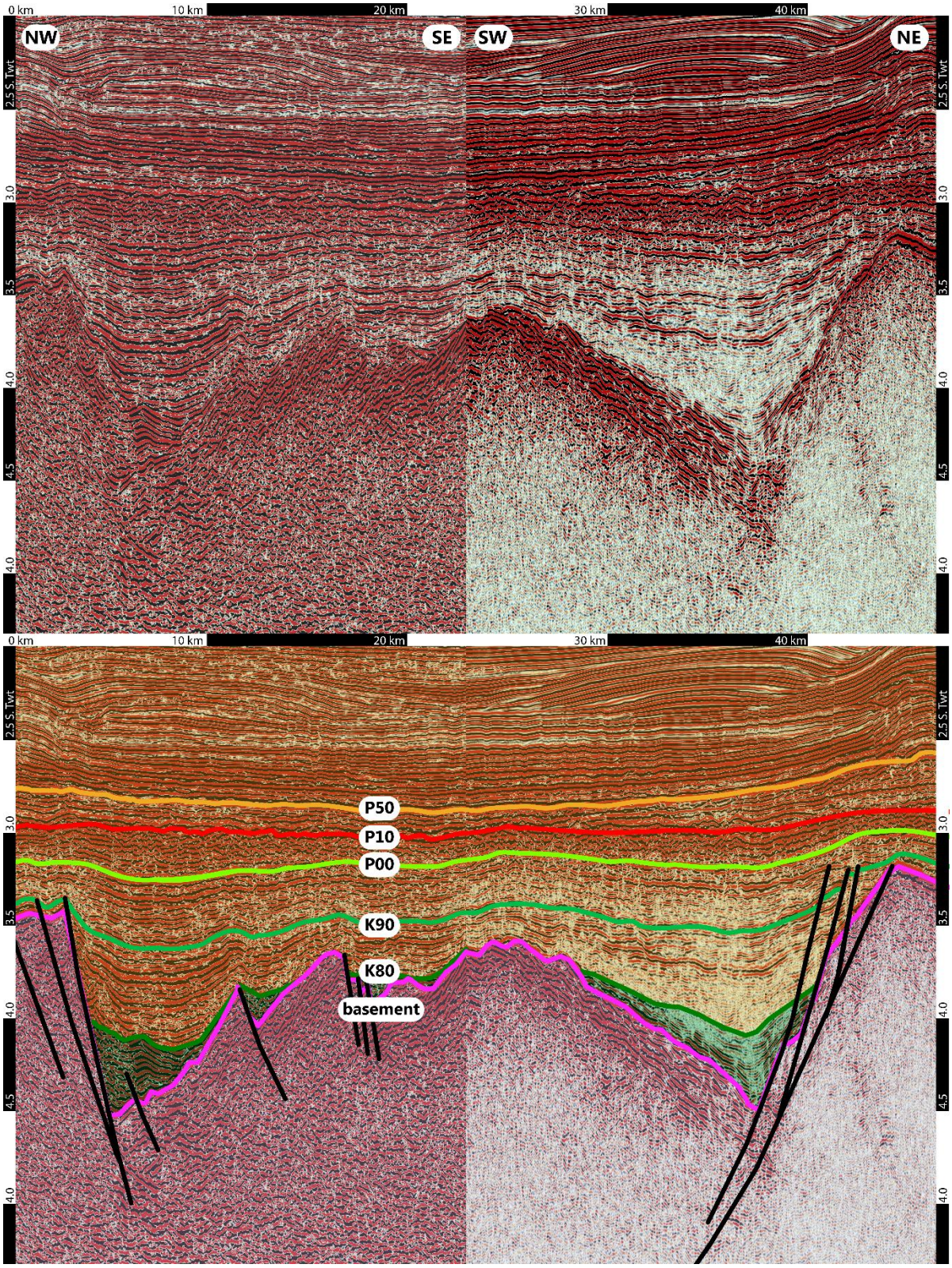

Figure 3.16 Composite seismic reflection profile in the Wherry High region crossing a NE-SW and E-W rift fault showing their approximate synchronicity. See Figure 3.4 for location.

A second reflection profile was constructed across the eastern Caravel High and intersects both NE-SW and NW-SE faults (Fig. 3.17). The section displays a lateral continuity between the two sets of growth strata which is overlain by the same lower Haumurian (K90, intra Campanian, ~85 to 78 Ma) post-rift reflector package. Therefore, these two faults ceased

accruing displacement during rifting around the same time. The timing of the onset of faulting is again difficult to assess but the geometries of both sets of growth strata are similar and indicate that each fault set commenced movement around the same time. Therefore, we consider the NE-SW and NW-SE rift faults were accruing displacement simultaneously.

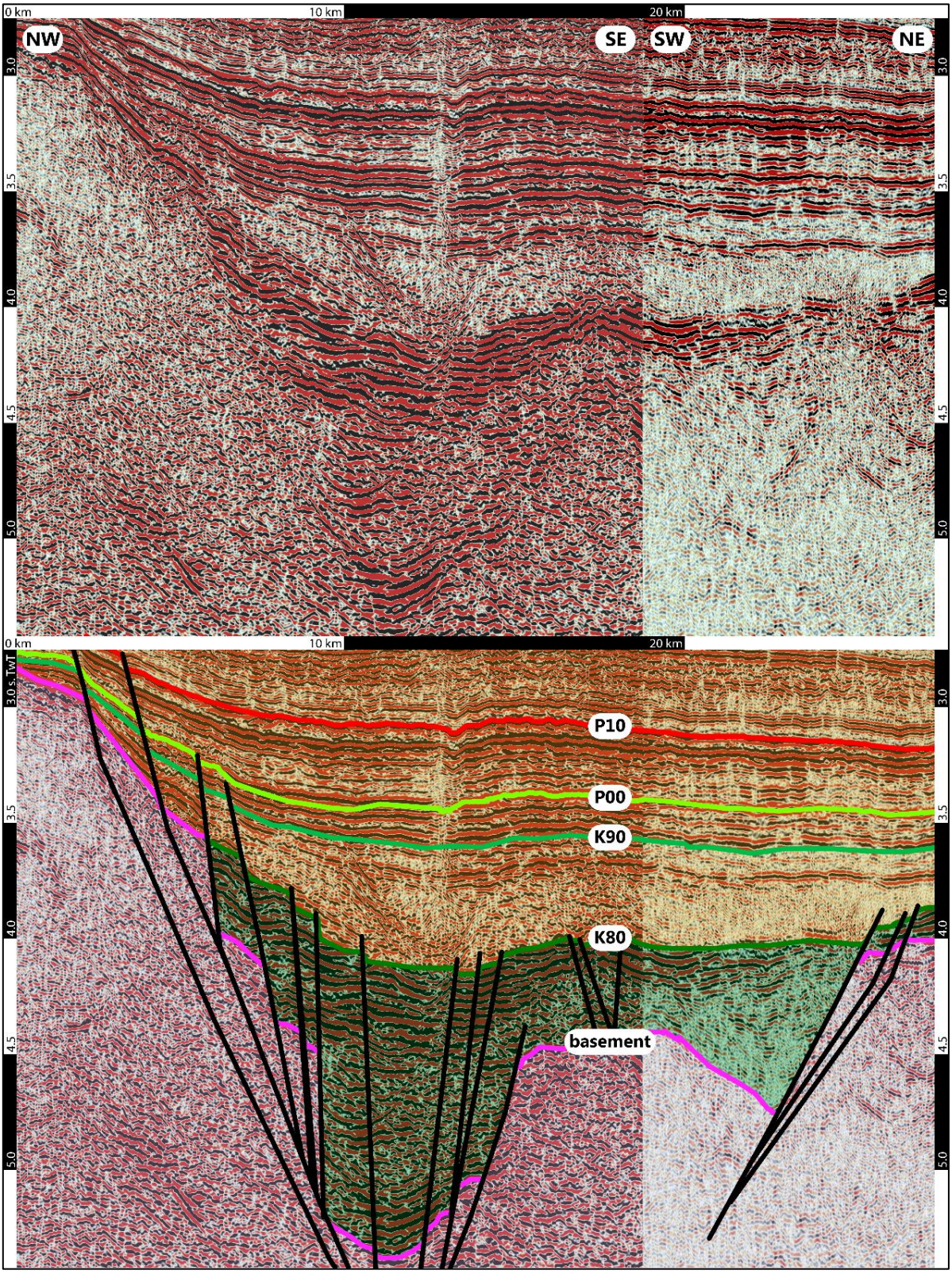

Figure 3.17 Composite seismic reflection profile adjacent to the Caravel High crossing a NE-SW and NW-SE rift fault showing their synchronicity. See Figure 3.4 for location.

The three sets of faults are all overlain by the lower Haumurian (K90, intra Campanian, ~85 to 78 Ma) post-rift reflector package. Although the geometries of both the growth strata and the post-rift package are approximate only, they are sufficiently good to suggest that to a first-order all fault sets were active coevally during the main rifting phase. Some minor displacements occurred after the cessation of rifting at ~85 Ma, with throws of 0.10-0.25 second TwT, 0.11-0.23 second TwT and 0.07-0.10 second TwT on NE-SW, E-W and NW-SE rift faults, respectively (Figs. 3.6 and 3.7). These late stage displacements are an order of magnitude less than the main phase of rifting and are not discussed further here.

3.5. Discussion

To explore the tectonic drivers for this multi-directional extension we consider the Gondwana setting of the basin and local factors within the basin that could influence the orientations and kinematics of faulting. We present a series of cartoons using observations from this manuscript together with data from the literature, to show the evolution of the breakup of eastern Gondwana from ~105 Ma to ~85 Ma (Fig. 3.18). In the schematic diagrams cessation of Mesozoic subduction occurred due to collision of Hikurangi Plateau with the eastern Gondwana margin. Collision of the Hikurangi Plateau indenter produced an embayment in the subduction system (Fig. 3.18A) which may be reflected in a thinning of the Permian-Early Cretaceous Murihiku and Brook-Street terranes approaching the present day Alpine Fault (Figs. 3.2 and 10B – Mortimer, 2014; Lamb *et al.*, 2016 and Mortimer, 2018). Such an embayment configuration could partially explain the subduction interface west of the Canterbury Basin inferred from the Pounamu ultramafics in the Southern Alps (Cooper and Ireland, 2013, 2015; Cooper and Palin, 2018; Cooper *et al.*, 2018), and the presence of the Hikurangi Plateau beneath the South Island (Reyners *et al.*, 2017). The cessation of embayment formation and subduction here inferred to have occurred at about 105 Ma, although this timing is poorly constrained (e.g., ±5 Myr).

While subduction primarily predates rifting, it is not possible to completely discount some overlap in the timing of the two processes. Such overlap would require that extensional faults were initially formed or influenced by subduction processes and formed sub-parallel to the active subduction front between ~110 and 105 Ma. Subsequently to the cessation of subduction, normal faults accrued slip as part of the continental breakup process. The simplest explanation, however, is that normal faulting formed entirely due to continental breakup processes. In support of the simplest explanation, normal faults appear to transect the basement fabric (Mortimer et al., 2014) and do not appear to bend in sympathy with the proposed embayment geometry as would be expected if faulting initiated during subduction.

The available fault data from the Canterbury Basin supports the view that faults with NE-SW, E-W and NW-SE trends accommodated extension coevally, which places constraints on the regional tectonics of Zealandia during the initial stages of Gondwana breakup in the Late Cretaceous. The breakup model for normal faulting in the Canterbury Basin is supported by the comparable geometries of these faults and the spreading centres that define the margins of Zealandia. The orientation of faulting in the Canterbury Basin in the initial stages of Gondwana breakup is at least partly parallel to the orientations of future ocean-floor spreading ridges (Fig. 3.18). Sea-floor spreading and the associated mid-ocean ridges vary in orientation along the margins of Zealandia and these variations may partly account for the multiple

directions of extension in the Canterbury Basin. The NE-SW trends of rift faults which dominate the southern Canterbury and Great South basins are approximately parallel to southern Zealandia and western Antarctica margins (and the associated mid-ocean spreading ridge) (blue line on Fig. 3.18C). In addition, this trend is also sub-parallel to the spreading ridge or transform fault between the Hikurangi Plateau and the Ontong Java Plateau since subducted beneath northern Zealandia (blue line on Fig. 3.18C - Davy, 2014; Mortimer *et al.*, 2019). The trend of rift faults observed along the Chatham Rise and the Bounty Trough are parallel to the spreading centre that formed between the eastern end of the Bounty Trough and western Antarctica (red line on Fig. 3.18C). East-west rift faults on the southern Chatham Rise are also approximately parallel to the spreading centre between the Hikurangi and Manihiki plateaus (red line on Fig. 3.18C), which was likely at least 1000 km north of the Canterbury Basin in the Mid-Cretaceous (~110-85 Ma). Lastly, NW-SE fault trends are approximately parallel to the spreading centre between north Zealandia and Australia, again despite being located more than 1000 km from the study area. NW-SE trending faults was also sub-parallel to the spreading ridge between the Ontong-Java and Manihiki plateaus.

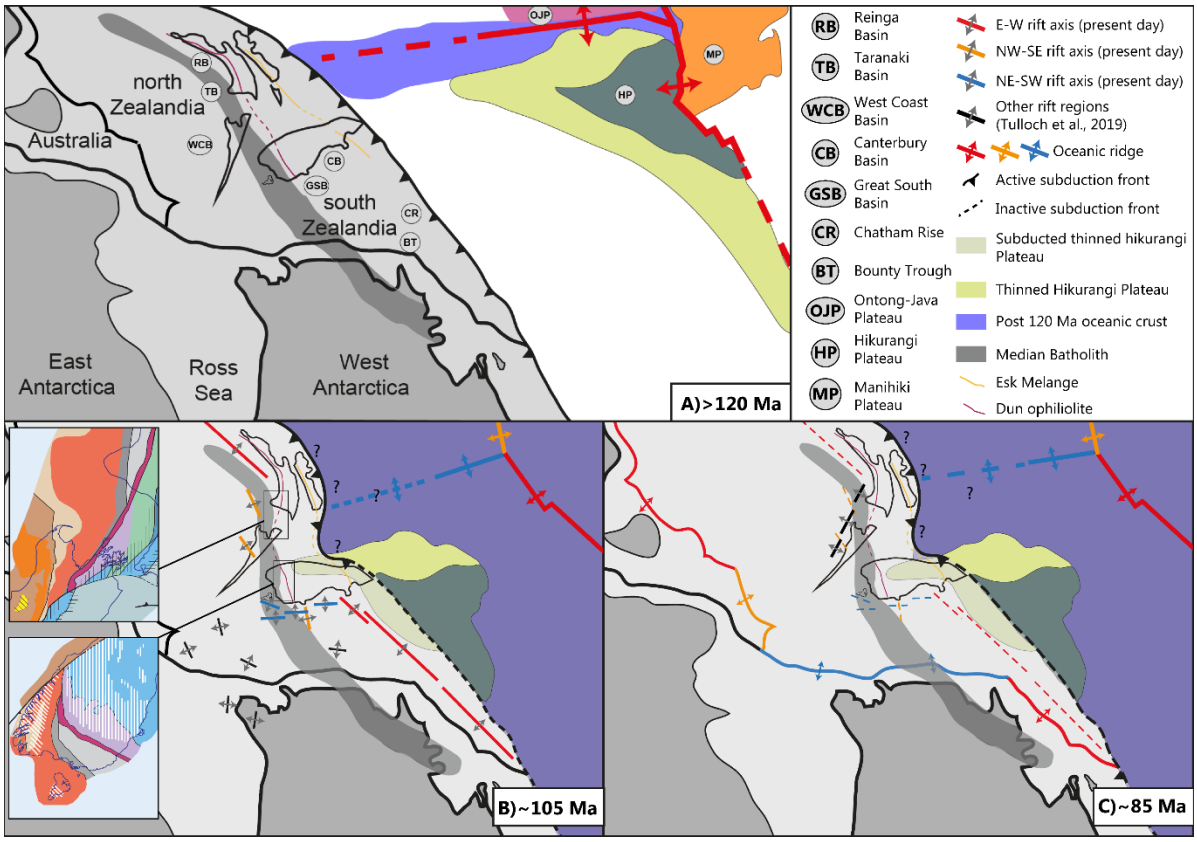

Figure 3.18 Zealandia Cretaceous geodynamic reconstruction during eastern Gondwana breakup showing the relation between subduction and the formation of Zealandia Late Cretaceous Rift Province. Geodynamic reconstruction modified from MacFadden et al. (2015); Lamb et al. (2016); Strogen et al. (2017) and Mortimer (2018).

Therefore, we hypothesise that the multiple directions of extension observed in the Canterbury Basin are primarily due to far-field stretching imposed on Zealandia as part of the Gondwana breakup process. In this model changes in predominant fault set across the Canterbury Basin reflect the changing proximity and influence of future spreading centres on basin faulting (Fig. 3.19). For example, NE-SW faults predominate in the southern Canterbury

and Great South basins which are closest to the west Antarctica southern Zealandia boundary where it trends NE-SW. If this model is correct then we would expect that Cretaceous normal faults elsewhere in Zealandia are also mainly parallel to future breakup mid-ocean ridge systems. To a first-order this appears to be the case with, for example, ~110-85 Ma aged rift faults in northern (Reinga and North Taranaki) and western Zealandia (South Taranaki and in the West Coast) trending sub-parallel to Australia-north Zealandia and eastern Antarctica-northern Zealandia spreading centres, respectively (Figs. 3.18C and 3.19). In the Canterbury Basin E-W and NW-SE trending faults are parallel to pre-existing faults and basement fabric, which could represent zones of crustal weakness that were exploited when favourably oriented to accommodate extension imposed by the far-field plate tectonics (Fig. 3.18B). These favourably orientated zones of weakness may locally promote extension distal from the related (i.e., parallel) spreading centre and multiple directions of coeval extension.

Multi-directional stretching is widely observed at triple junctions, although the dimensions of these junction zones (where multi-directional extension may be occurring) are typically smaller than the 100s thousands square kilometres of distributed extension in the Canterbury Basin. For example, the North Sea Mesozoic triple junction formed a three-arm rift system where at the intersection the rift arms, multiple sets of synchronous rift faults are present (Coward et al., 2003). Distal to the North Sea junction zone, only one set of approximately parallel faults are observed (e.g., Coward et al., 2003). Canterbury Basin stretching differs from triple junction examples in that it was surrounded by multiple future spreading centres which vary in trend (Fig. 3.18). In the Canterbury Basin case, the initial phase of Gondwana breakup appears to have been characterised by minor (<20%) extension across much of the Zealandia continental crust. During the initial breakup phase, between ~105 and 85 Ma, it is not clear how much extension occurred along the future spreading centres, although we speculate that it was significantly more than across the Canterbury Basin crust between spreading centres (Fig. 3.18).

With the onset of seafloor spreading (~85 Ma), extension was focused along the newly created mid-ocean ridge systems and displacement rates on normal faults in the Canterbury Basin ceased or decreased by an order of magnitude or more (Fig. 3.18). This focusing of extension along spreading centres may be comparable to the localisation of strain onto the largest faults in extensional fault systems (Walsh et al., 2001; Meyer et al., 2002). Unlike in the West Coast-Taranaki-Reinga basins, the Canterbury Basin was not subject to a second phase of rifting which may correspond to either the far-field expression of a transform fault associated to the Zealandia-Western Antarctica oceanic ridge or to a failed rift linked to a triple junction south of New Zealand (Strogen *et al*., 2017).

Cretaceous rift faults across much of Zealandia formed prior to the onset of Gondwana breakup at 86-83 Ma. Given the parallelism of the rift faults with the subsequent spreading centres we suggest that the rift structures formed as part of the breakup process which are interpreted to have commenced ~5 Myr before or following the cessation of subduction (~110 Ma). This pre- breakup phase of extension was characterised by ~25 Myr of mild (~10-20%) extension distributed across Zealandia which was being stretched in multiple directions coevally to produce a rift province >4000 km long and >1000 km wide (Figs. 3.18B). The duration of the pre- breakup extension may reflect the time taken to thin the continental crust sufficiently for the generation of new oceanic crust. If this model is correct, then Gondwana breakup probably occurred where the rates of pre- breakup extension were highest (Fig. 3.18).

An important implication of the rift systems in this study is that, the orientations of mid-ocean breakup structures and the associated extension direction may have been established 10s of millions of years before the onset of seafloor spreading. The multi-direction stretching and eventual Gondwana breakup was likely driven by plate-scale tectonic processes (e.g., Merle, 2011; Murphy and Nance, 2013), with mantle convection or mantle plume processes (e.g., Weaver *et al.*, 1994; Storey *et al*., 1999; Laird and Bradshaw, 2004).

3.6. Conclusion

The Canterbury Basin in eastern Gondwana was deformed by extensional faults from ~110 to ~85 Ma with general trends of NE-SW, E-W and NW-SE. These fault sets occur throughout the basin, although E-W and NE-SW trending structures dominate along the Chatham Rise and in the southern Canterbury Basin, respectively. Each of these fault sets is characterised by segmentation and relay ramps consistent with normal faulting. The normal-faulting hypothesis is further supported by horizontal separation diagrams and displacement analysis which indicate that all fault sets primarily accrued normal dip-slip, with displacement lows at segment boundaries; there is presently no evidence that segment boundaries have the pop-up or pull-apart basin geometries expected for strike-slip faults. Analysis of growth strata indicates that the three fault sets accrued displacements synchronously. The available data support the view that the Canterbury Basin accommodated multiple directions of extension coevally during the Cretaceous. The three fault sets are each parallel to spreading centres that define the present margins of Zealandia, with NE-SW trending faults in the southern basin being parallel to the mid-ocean ridge separating southern Zealandia and western Antarctica. The parallelism between spreading centres and normal faults suggests that the multi-directional extension in the Canterbury Basin records the early stages of Gondwana breakup. The plate tectonic forces responsible for Gondwana breakup produced distributed extension across much of Zealandia and influenced its continental crust for about 25 Myr prior to breakup. Canterbury Basin multidirectional stretching differs from triple junction examples in that it was surrounded by multiple future spreading centres which vary in trend. In the Canterbury Basin case, the initial phase of Gondwana breakup appears to have been characterised by minor (<20%) extension while we speculate that it was significantly more in the area of future spreading centres. With the onset of seafloor spreading, extension was focused along the spreading centres, and distributed stretching of Zealandia ceased or continued at much diminished rates.

3. Acknowledgement

We would like to thank A. Auzemery, S. Blanke, J. Bradshaw, N. Mortimer and T. Sahoo for the discussions that helped several aspects of this paper, which promoted new ideas about Cretaceous faulting in the Canterbury Basin. GHB acknowledges funding from the NZ government (MBIE) through Strategic Funding to GNS Science and the Sedimentary Basin Research programme.

3. References

ADAMS, C., CAMPBELL, H. & GRIFFIN, W. (2008) Age and Provenance of Basement Rocks of the Chatham Islands: An Outpost of Zealandia. New Zealand Journal of Geology and Geophysics, 51, 245-259 pp.

ADAMS, C.J., CAMPBELL, H.J., MORTIMER, N. & GRIFFIN, W.L. (2017) Perspectives on Cretaceous Gondwana Break-up from Detrital Zircon Provenance of Southern Zealandia Sandstones. Geological Magazine, 154, 661-682 pp.

ARNOT, M., BLAND, K., BOYES, A., BULL, S., FUNNELL, R., GRIFFIN, A., HILL, M., KROEGER, K., LUKOVIC, B. & SCADDEN, P. (2016) Atlas of Petroleum Prospectivity, Northwest Province: Arcgis Geodatabase and Technical Report. GNS Science Data Series 23b, 1.

BACHE, F., MORTIMER, N., SUTHERLAND, R., COLLOT, J., ROUILLARD, P., STAGPOOLE, V. & NICOL, A. (2014) Seismic Stratigraphic Record of Transition from Mesozoic Subduction to Continental Breakup in the Zealandia Sector of Eastern Gondwana. Gondwana Research, 26, 1060-1078 pp.

BARNES, P.M., GHISETTI, F.C. & GORMAN, A.R. (2016) New Insights into the Tectonic Inversion of North Canterbury and the Regional Structural Context of the 2010–2011 Canterbury Earthquake Sequence, New Zealand. Geochemistry, Geophysics, Geosystems, 17, 324-345 pp.

BISHOP, D.G. (1974) Stratigraphic, Structural, and Metamorphic Relationships in the Dansey Pass Area, Otago, New Zealand. New Zealand Journal of Geology and Geophysics, 17, 301-335 pp.

BISHOP, D.G., LAIRD, M.G. & MILDENHALL, D.C. (1976) Stratigraphy and Depositional Environment of the Kyeburn Formation (Cretaceous), a Wedge of Coarse Terrestrial Sediments in Central Otago. Journal of the Royal Society of New Zealand, 6, 55-71 pp.

BLAND, K.J., URUSKI, C.I. & ISAAC, M.J. (2015) Pegasus Basin, Eastern New Zealand: A Stratigraphic Record of Subsidence and Subduction, Ancient and Modern. New Zealand Journal of Geology and Geophysics, 58, 319-343 pp.

BLANKE, S.J. (2015) Caravel-1: Lessons Learned in the Deepwater Canterbury Basin. International Conference and Exhibition, Melbourne, Australia 13-16 September 2015.

BROWNE, G.H., FIELD, B.D., BARRELL, D.J.A., JONGENS, R., BASSETT, K.N. & WOOD, R.A. (2012) The Geological Setting of the Darfield and Christchurch Earthquakes. New Zealand Journal of Geology and Geophysics, 55, 193-197 pp.

CAMPBELL, H.J.A., P.B.; BEU, A.G.; MAXWELL, P.A.; EDWARDS, A.R.; LAIRD, M.G.; HORNIBROOK, N. DE B.; MILDENHALL, D.C.; WATTERS, W.A.; BUCKERIDGE, J.S.; LEE, D.E.; STRONG, C.P.; WILSON, G.J.; HAYWARD, B.W. (1993) Cretaceous-Cenozoic Geology and Biostratigraphy of the Chatham Islands, New Zealand. 2, 269 p.

CARTER, R.M. (1988) Post-Breakup Stratigraphy of the Kaikoura Synthem (Cretaceous-Cenozoic), Continental Margin, Southeastern New Zealand. New Zealand Journal of Geology and Geophysics, 31, 405-429 pp.

CHILDS, C., WATTERSON, J. & WALSH, J. (1995) Fault Overlap Zones within Developing Normal Fault Systems. Journal of the Geological Society, 152, 535-549 pp.

CHILDS, C., HOLDSWORTH, R.E., JACKSON, C.A.-L., MANZOCCHI, T., WALSH, J.J. & YIELDING, G. (2017) Introduction to the Geometry and Growth of Normal Faults. Geological Society, London, Special Publications, 439, 10 p.

COOPER, A. & IRELAND, T. (2013) Cretaceous Sedimentation and Metamorphism of the Western Alpine Schist Protoliths Associated with the Pounamu Ultramafic Belt, Westland, New Zealand. New Zealand Journal of Geology and Geophysics, 56, 188-199 pp.

COOPER, A., PRICE, R. & REAY, A. (2018) Geochemistry and Origin of a Mesozoic Ophiolite: The Pounamu Ultramafics, Westland, New Zealand. New Zealand Journal of Geology and Geophysics, 61, 1-17 pp.

COOPER, A.F. & IRELAND, T.R. (2015) The Pounamu Terrane, a New Cretaceous Exotic Terrane within the Alpine Schist, New Zealand; Tectonically Emplaced, Deformed and Metamorphosed During Collision of the Lip Hikurangi Plateau with Zealandia. Gondwana Research, 27, 1255-1269 pp.

COOPER, A.F. & PALIN, J.M. (2018) Two-Sided Accretion and Polyphase Metamorphism in the Haast Schist Belt, New Zealand: Constraints from Detrital Zircon Geochronology. GSA Bulletin, 130, 1501-1518 pp.

COOPER, R.A.E. (2004) The New Zealand Geological Timescale. 22, 284 p.

COWARD, M., DEWEY, J., HEMPTON, M. & HOLROYD, J. (2003) Tectonic Evolution. The Millennium Atlas: Petroleum Geology of the Central and Northern North Sea. Geological Society, London, 17, 33 p.

CRAMPTON, J.S., MORTIMER, N., BLAND, K.J., STROGEN, D.P., SAGAR, M., HINES, B.R., KING, P.R. & SEEBECK, H. (2019) Cretaceous Termination of Subduction at the Zealandia Margin of Gondwana: The View from the Paleo-Trench. Gondwana Research, 70, 222-242 pp.

DAVISON, I. & UNDERHILL, J.R. (2012) Tectonics and Sedimentation in Extensional Rifts: Implications for Petroleum Systems. In: Tectonics and Sedimentation: Implications for Petroleum Systems (Ed. by D. Gao), AAPG Memoir 100, 15-42 pp. American Association of Petroleum Geologists.

DAVY, B. (2014) Rotation and Offset of the Gondwana Convergent Margin in the New Zealand Region Following Cretaceous Jamming of Hikurangi Plateau Large Igneous Province Subduction. Tectonics, 33, 1577-1595 pp.

DECKERT, H., RING, U. & MORTIMER, N. (2002) Tectonic Significance of Cretaceous Bivergent Extensional Shear Zones in the Torlesse Accretionary Wedge, Central Otago Schist, New Zealand. New Zealand Journal of Geology and Geophysics, 45, 537-547 pp.

FIELD, B.D. & BROWNE, G.H. (1989) Cretaceous and Cenozoic Sedimentary Basins and Geological Evolution of the Canterbury Region, South Island, New Zealand. Institute of Geological & Nuclear Sciences Monograph, 2, 94 p.

HEINE, C., ZOETHOUT, J. & MÜLLER, R.D. (2013) Kinematics of the South Atlantic Rift. Solid Earth, 4, 215-253 pp.

HIGGS, K.E., BROWNE, G.H. & SAHOO, T.R. (2019) Reservoir Characterisation of Syn-Rift and Post-Rift Sandstones in Frontier Basins: An Example from the Cretaceous of Canterbury and Great South Basins, New Zealand. Marine and Petroleum Geology, 101, 1-29 pp.

JONGENS, R., BARRELL, D.J.A., CAMPBELL, J.K. & PETTINGA, J.R. (2012) Faulting and Folding beneath the Canterbury Plains Identified Prior to the 2010 Emergence of the Greendale Fault. New Zealand Journal of Geology and Geophysics, 55, 169-176.

KOPTEV, A., GERYA, T., CALAIS, E., LEROY, S. & BUROV, E. (2018) Afar Triple Junction Triggered by Plume-Assisted Bi-Directional Continental Break-Up. Scientific reports, 8, 7 p.

LAIRD, M.G. (1993) Cretaceous Continental Rifts: New Zealand Region. In: Sedimentary Basins of the World. (Ed. by P. E. Ballance), South Pacific sedimentary basins 2, 37-49 pp. Elsevier Science Publisher.

LAIRD, M.G. & BRADSHAW, J.D. (2004) The Break-up of a Long-Term Relationship: The Cretaceous Separation of New Zealand from Gondwana. Gondwana Research, 7, 273-286 pp.

LAMB, S., MORTIMER, N., SMITH, E. & TURNER, G. (2016) Focusing of Relative Plate Motion at a Continental Transform Fault: Cenozoic Dextral Displacement> 700 Km on New Zealand's Alpine Fault, Reversing> 225 Km of Late Cretaceous Sinistral Motion. Geochemistry, Geophysics, Geosystems, 17, 1197-1213 pp.

MCFADDEN, R., TEYSSIER, C., SIDDOWAY, C.S., COSCA, M.A. & FANNING, C.M. (2015) Mid-Cretaceous Oblique Rifting of West Antarctica: Emplacement and Rapid Cooling of the Fosdick Mountains Migmatite-Cored Gneiss Dome. Lithos, 232, 306-318 pp.

MACKINNON, T.C. (1984) Origin of the Torlesse Terrane and Coeval Rocks, South Island, New Zealand: Discussion and Reply: Reply. GSA Bulletin, 95, 967-985 pp.

MASSIRONI, M., DI ACHILLE, G., ROTHERY, D.A., GALLUZZI, V., GIACOMINI, L., FERRARI, S., ZUSI, M., CREMONESE, G. & PALUMBO, P. (2015) Lateral Ramps and Strike-Slip Kinematics on Mercury. Geological Society, London, Special Publications, 401, 269-290 pp.

MAZENGARB, C. & HARRIS, D. (1994) Cretaceous Stratigraphic and Structural Relations of Raukumara Peninsula, New Zealand: Stratigraphic Patterns Associated with the Migration of a Thrust System. Annales Tectonicae, 8, 100-118 pp.

MERLE, O. (2011) A Simple Continental Rift Classification. Tectonophysics, 513, 88-95 pp.

MEYER, V., NICOL, A., CHILDS, C., WALSH, J. & WATTERSON, J. (2002) Progressive Localisation of Strain During the Evolution of a Normal Fault Population. Journal of Structural Geology, 24, 1215-1231 pp.

MOHR, P. (1970) The Afar Triple Junction and Sea-Floor Spreading. Journal of Geophysical Research, 75, 7340-7352 pp.

MORLEY, C., HARANYA, C., PHOOSONGSEE, W., PONGWAPEE, S., KORNSAWAN, A. & WONGANAN, N. (2004) Activation of Rift Oblique and Rift Parallel Pre-Existing Fabrics During Extension and Their Effect on Deformation Style: Examples from the Rifts of Thailand. Journal of Structural Geology, 26, 1803-1829 pp.

MORLEY, C.K. (2017) The Impact of Multiple Extension Events, Stress Rotation and Inherited Fabrics on Normal Fault Geometries and Evolution in the Cenozoic Rift Basins of Thailand. Geological Society, London, Special Publications, 439, 413-445 pp.

MORTIMER, N. (1993) Geology of the Otago Schist and Adjacent Rocks. Scale 1:500 000. Lower Hutt: Institute of Geological & Nuclear Sciences., Institute of Geological & Nuclear Sciences geological map 7.

MORTIMER, N., TULLOCH, A.J., SPARK, R.N., WALKER, N.W., LADLEY, E., ALLIBONE, A. & KIMBROUGH, D.L. (1999) Overview of the Median Batholith, New Zealand: A New Interpretation of the Geology of the Median Tectonic Zone and Adjacent Rocks. Journal of African Earth Sciences, 29, 257-268 pp.

MORTIMER, N. (2000) Metamorphic Discontinuities in Orogenic Belts: Example of the Garnet–Biotite–Albite Zone in the Otago Schist, New Zealand. International Journal of Earth Sciences, 89, 295-306 pp.

MORTIMER, N. (2004) New Zealand's Geological Foundations. Gondwana Research, 7, 261-272 pp.

MORTIMER, N. (2014) The Oroclinal Bend in the South Island, New Zealand. Journal of Structural Geology, 64, 32-38 pp.

MORTIMER, N., RATTENBURY, M.S., KING, P.R., BLAND, K.J., BARRELL, D.J.A., BACHE, F., BEGG, J.G., CAMPBELL, H.J., COX, S.C., CRAMPTON, J.S., EDBROOKE, S.W., FORSYTH, P.J., JOHNSTON, M.R., JONGENS, R., LEE, J.M., LEONARD, G.S., RAINE, J.I., SKINNER, D.N.B., TIMM, C., TOWNSEND, D.B., TULLOCH, A.J., TURNBULL, I.M. & TURNBULL, R.E. (2014) High-Level Stratigraphic Scheme for New Zealand Rocks. New Zealand Journal of Geology and Geophysics, 57, 402-419 pp.

MORTIMER, N., CAMPBELL, H.J., TULLOCH, A.J., KING, P.R., STAGPOOLE, V.M., WOOD, R.A., RATTENBURY, M.S., SUTHERLAND, R., ADAMS, C.J., COLLOT, J. & SETON, M. (2017) Zealandia: Earth's Hidden Continent. GSA Today, 27, 27-35 pp.

MORTIMER, N. (2018) Evidence for a Pre-Eocene Proto-Alpine Fault through Zealandia. New Zealand Journal of Geology and Geophysics, 61, 1-9 pp.

MORTIMER, N., VAN DEN BOGAARD, P., HOERNLE, K., TIMM, C., GANS, P., WERNER, R. & RIEFSTAHL, F. (2019) Late Cretaceous Oceanic Plate Reorganization and the Breakup of Zealandia and Gondwana. Gondwana Research, 65, 31-42 pp.

MURPHY, J.B. & NANCE, R.D. (2013) Speculations on the Mechanisms for the Formation and Breakup of Supercontinents. Geoscience Frontiers, 4, 185-194 pp.

PHILIPPON, M., WILLINGSHOFER, E., SOKOUTIS, D., CORTI, G., SANI, F., BONINI, M. & CLOETINGH, S. (2015) Slip Re-Orientation in Oblique Rifts. Geology, 43, 147-150 pp.

RAINE, J.I., BEU, A.G., BOYES, A.F., CAMPBELL, H.J., COOPER, R.A., CRAMPTON, J.S., CRUNDWELL, M.P., HOLLIS, C.J., MORGANS, H.E.G. & MORTIMER, N. (2015) New Zealand Geological Timescale Nzgt 2015. New Zealand Journal of Geology and Geophysics, 58, 398-403 pp.

RAVNÅS, R. & STEEL, R.J. (1998) Architecture of Marine Rift-Basin Successions. AAPG Bulletin, 82, 110-146 pp.

REYNERS, M., EBERHART-PHILLIPS, D., UPTON, P. & GUBBINS, D. (2017) Three-Dimensional Imaging of Impact of a Large Igneous Province with a Subduction Zone. Earth and Planetary Science Letters, 460, 143-151 pp.

RING, U., BETZLER, C. & DELVAUX, D. (1992) Normal Vs. Strike-Slip Faulting During Rift Development in East Africa: The Malawi Rift. Geology, 20, 1015-1018 pp.

SAHOO, T., BLAND, K., ARNOT, M., BOYES, A., FUNNELL, R., GRIFFIN, A., KROEGER, K., LAWRENCE, M., O'BRIEN, G. & SCADDEN, P. (2017) Atlas of Petroleum Prospectivity, Southeast Province: Arcgis Geodatabase and Technical Report. GNS Science Data Series 23c, 1.

SAHOO, T.R., KING, P.R., BLAND, K.J., STROGEN, D.P., SYKES, R. & BACHE, F. (2014) Tectono-Sedimentary Evolution and Source Rock Distribution of the Mid to Late Cretaceous Succession in Great South Basin, New Zealand. APPEA Journal, 54, 259-274 pp.

SAHOO, T.R., KROEGER, K.F., THRASHER, G., MUNDAY, S., MINGARD, H., COZENS, N. & HILL, M. (2015) Facies Distribution and Impact on Petroleum Migration in the Canterbury Basin , New Zealand. In: Eastern Australian Basins Symposium 2015: Publication of Proceedings. Petroleum Exploration Society of Australia, Perth, WA, 187-202 pp.

SAHOO, T.R.B., G.H., NICOL, A., O'BRIEN, G. (2018) Evolution of Cretaceous Rifting in the Great South Basin: Key Observations on Fault Geometries and Sedimentary Response. Oral presentation at NZ Petroleum Geoscience workshop, 27-28 September 2018, Lower Hutt, New Zealand.

SCHIØLER, P. & RAINE, J.I., COMPILERS (2011) Revised Biostratigraphy and Well Correlation, Canterbury Basin, New Zealand. Ministry of Economic Development New Zealand Unpublished Petroleum Report PR4365, 142 p.

STOREY, B.C., LEAT, P.T., WEAVER, S.D., PANKHURST, R.J., BRADSHAW, J.D. & KELLEY, S. (1999) Mantle Plumes and Antarctica-New Zealand Rifting: Evidence from Mid-Cretaceous Mafic Dykes. Journal of the Geological Society, 156, 659-671 pp.

STROGEN, D., P, & KING, P.R. (2014) A New Zealandia-Wide Seismic Horizon Naming Scheme. GNS Science Report, 2014/34, 20 p.

STROGEN, D.P., SEEBECK, H., NICOL, A. & KING, P.R. (2017) Two-Phase Cretaceous – Paleocene Rifting in the Taranaki Basin Region, New Zealand; Implications for Gondwana Break-Up. Journal of the Geological Society, 174, 929-946 pp.

SUTHERLAND, R., STAGPOOLE, V., URUSKI, C., KENNEDY, C., BASSETT, D., HENRYS, S., SCHERWATH, M., KOPP, H., FIELD, B. & TOULMIN, S. (2009) Reactivation of Tectonics, Crustal Underplating, and Uplift after 60 Myr of Passive Subsidence, Raukumara Basin, Hikurangi-Kermadec Fore Arc, New Zealand: Implications for Global Growth and Recycling of Continents. Tectonics, 28 p.

TAYLOR, S.K., NICOL, A. & WALSH, J.J. (2008) Displacement Loss on Growth Faults Due to Sediment Compaction. Journal of Structural Geology, 30, 394-405 pp.

TULLOCH, A., MORTIMER, N., IRELAND, T., WAIGHT, T., MAAS, R., PALIN, M., SAHOO, T., SEEBECK, H., SAGAR, M., BARRIER, A. & TURNBULL, R. (2019) Reconnaissance Basement Geology and Tectonics of South Zealandia. Tectonics, 38, 516-551 pp.

WALSH, J., CHILDS, C., MEYER, V., MANZOCCHI, T., IMBER, J., NICOL, A., TUCKWELL, G., BAILEY, W., BONSON, C. & WATTERSON, J. (2001) Geometric Controls on the Evolution of Normal Fault Systems. Geological Society, London, Special Publications, 186, 157-170 pp.

WALSH, J.J., WATTERSON, J., BAILEY, W.R. & CHILDS, C. (1999) Fault Relays, Bends and Branch-Lines. Journal of Structural Geology, 21, 1019-1026 pp.

WATTERSON, J., WALSH, J., GILLESPIE, P. & EASTON, S. (1996) Scaling Systematics of Fault Sizes on a Large-Scale Range Fault Map. Journal of Structural Geology, 18, 199-214 pp.

WEAVER, S., STOREY, B., PANKHURST, R., MUKASA, S., DIVENERE, V. & BRADSHAW, J. (1994) Antarctica-New Zealand Rifting and Marie Byrd Land Lithospheric Magmatism Linked to Ridge Subduction and Mantle Plume Activity. Geology, 22, 811-814 pp.

WOOD, R.A. & HERZER, R.H. (1993) The Chatham Rise, New Zealand. In: South Pacific Sedimentary Basins (Ed. by P. F. Ballance), Sedimentary Basins of the World 2, 329-349 pp. Elsevier Science Publishers, Amsterdam.

WOOD, R.A., ANDREWS, P. B., HERZER, R. H., & COOK, R. A. (1989) Cretaceous and Cenozoic Geology of the Chatham Rise Region, South Island, New Zealand. New Zealand Geological Survey Basin Studies 3, 75 p.

ZANELLA, E., COWARD, M., EVANS, D., GRAHAM, C., ARMOUR, A. & BATHURST, P. (2003) Structural Framework. The Millennium Atlas: Petroleum Geology of the Central and Northern North Sea. Geological Society, London, 45, 59 p.

CHAPTER 4) RELATION BETWEEN SYN-RIFT SEDIMENT FILL AND NORMAL-FAULT THROW AT THE CESSATION OF RIFTING

A. Barrier[1], A. Nicol[1], G. Browne[2], K. Bassett[1,] and V. Paumard[3]

[1] *University of Canterbury, Department of Geological Science, Christchurch, New Zealand.*

[2]*GNS Science, PO Box 30368, Lower Hutt, New Zealand.*

[3] *Centre for Energy Geoscience, School of Earth Sciences, The University of Western Australia, 35 Stirling Highway, Crawley, WA 6009, Australia.*

4. Abstract

Rift basins promote sediment accumulation and local thickening of strata. We quantify the geometries of rift fill in seismic reflection lines using the ratio of syn-rift strata thickness to syn-rift fault throw (here referred to as the Sediment Fill Ratio - SFR). Measurements are from seven sedimentary basins globally, with the largest and most comprehensive dataset from the Canterbury Basin in New Zealand. The Sediment Fill Ratio ($\mathrm{SFR} = \frac{\text{syn-rift thickness}}{\text{syn-rift fault throw}}$) permits recognition of four types of rift basins: (1) starved (SFR≤0.2), (2) under-filled (0.2<SFR≤0.9), (3) balanced-filled (0.9<SFR≤1.1), and (4) over-filled (SFR>1.1). The degree of syn-rift basin fill, at the cessation of rifting, varies with fault size across the same basin and between different rift basins. A negative non-linear relationship between fault displacement and SFR is observed in rift basins sampled. Small faults are more often characterized by balanced or over-filled geometries because they have low displacement rates and are located in the hangingwall of larger faults (e.g., >1 seconds TwT throw) where sedimentation rates are locally high. Rift systems dominated by large faults, such as the Canterbury Basin, tend to be under-filled, and require sediment supply from outside the rift system to become over-filled.

4.1. Introduction

Sediment fill of syn-rift basins is mainly controlled by subsidence along local basin-bounding faults and by sediment supply (Roberts and Yielding, 1994; Lambiase and Bosworth, 1995; Ravnås and Steel, 1998; Gawthorpe and Leeder, 2000; Morley, 2002; Whitjack *et al.*, 2002; Davison and Underhill, 2012). The degree of rift filling is ultimately dependent on the relations between the rates of fault displacement and sedimentation, which reflect a wide range of factors including tectonics, topography and climate (Lambiase and Bosworth 1995; Ravnås and Steel, 1998; Gawthorpe and Leeder 2000). In this paper we examine how fault displacement, displacement rates and size distributions can impact the degree of rift infilling.

Starved, under-filled, balanced-filled and over-filled types of rift basin infill have been identified in outcrop and exploration wells for siliciclastic facies successions (Ravnås and

Steel, 1998). Over the last 30 years rift basins have been increasingly imaged in seismic reflection lines, where the degree of syn-rift basin infill at the cessation of rifting can be directly observed in cross sections (Fig. 4.1). Here we use the ratio of hangingwall maximum syn-rift sediment thickness and syn-rift fault displacement for individual faults (Sediment Fill Ratio - SFR_f) and for entire basins (Sediment Fill Ratio – SFR_b) to quantify the interplay between fault displacement and syn-rift basin sedimentation at the end of rifting for cross sections.

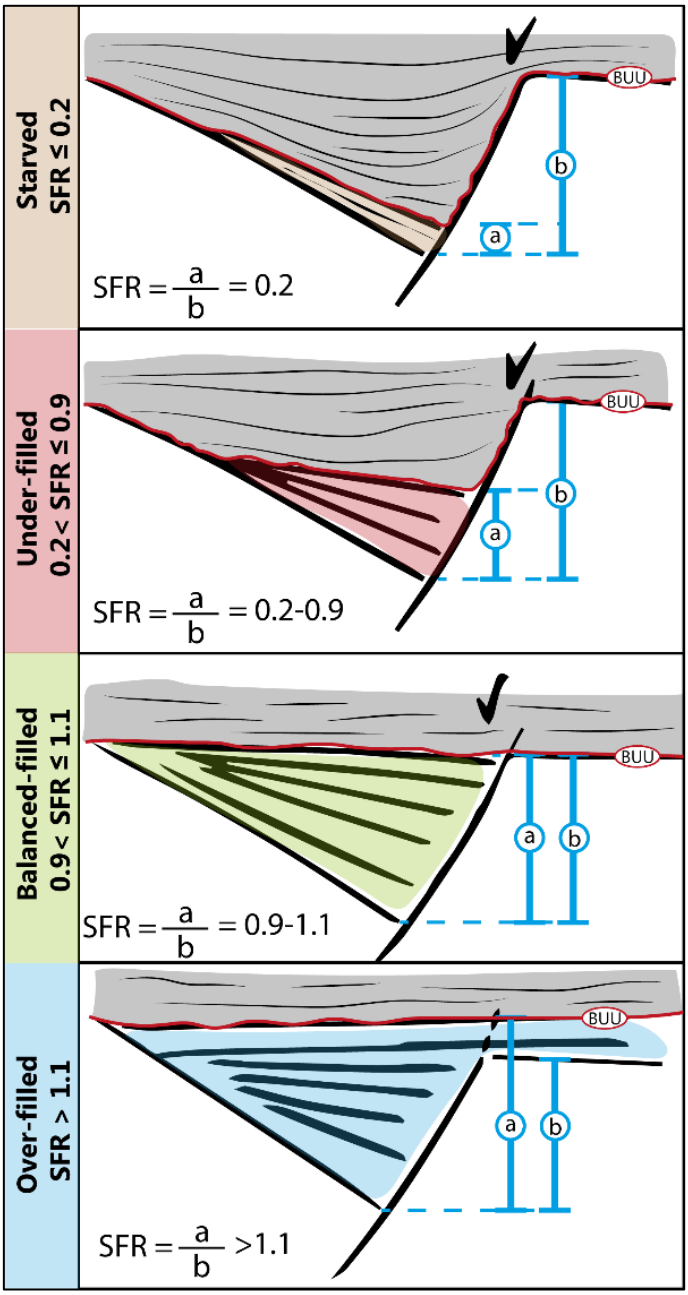

Figure 4.1 Half-graben fill classification comparing (a) thickness of syn-rift sequence and (b) syn-rift fault throw. Syn-rift succession corresponds to brown (starved), red (under-filled), green (balanced-filled) and blue (over-filled) fills and are separated from the post-rift succession (grey) by the breakup unconformity (BUU). When a rift fault shows evidence of reactivation during the post-rift phase, the post-rift displacement is subtracted to the top basement vertical displacement to restore the syn-rift fault displacement. However, the vertical displacement of the top basement corresponds to a minimal value as basement on the hanging wall of the fault can be eroded as shown by the truncations along fault scarps and flattened surfaces and therefor is not necessarily recording maximum vertical displacement.

Different types of rift-fill are examined in this paper using seismic reflection lines from the (1) Canterbury Basin (CB), offshore of the eastern South Island of New Zealand (Figs. 4.1 and 4.2), and from the (2) Northern Carnarvon Basin (Australia), (3) Northern Taupo Rift (New Zealand), (4) Punta del Este and Pelotas basins (offshore Uruguay), (5) Mergui Basin (Andaman Sea, offshore Thailand), (6) Pannonian Basin (Central Europe) and (7) Corinth Gulf Rift (Greece) (Fig. 4.2). Collectively, these datasets contain 887 measurements on normal faults from a range of tectonic and sedimentalogical setting (Table 4.1). They provide generic conclusions on rift sedimentation, indicating that the degree of rift sediment fill varies between basins and that fault size is a critical determinant for rift filling, with smaller displacement faults and basins comprising mainly smaller faults more likely to be over-filled because they had lower displacement rates and generate less accommodation.

Table 4.1 Details of rift basins analysed in this study.

Sedimentary Basin	Location	Number of measurements	Min/Max fault throw (s. TwT)	Min/Max SFR	Reference
Canterbury	New Zealand	582	<0.1/2.9	0/3.6	This study
Gulf of Corinth Rift	Greece	23	0.1/2.7	0/6	Taylor et al., 2011
Pannonian	Central Europe	55	0.2/2.2	0.5/8	Borgh et al., 2015; Balázs et al., 2016
Punta del Este and Pelotas	Offshore Uruguay	10	0.6/2.7	1/1.3	Morales et al., 2017
Mergui	Andaman Sea	11	0.1/2.6	0.7/6	Morley et al., 2011
Northern Taupo Rift	New Zealand	11	0.1/2.6	1.3/>10	Mousopoulou et al., 2008
Northern Carnarvon	Offshore eastern Australia	195	<0.1/3.5	0.9/>10	Marshall & Lang, 2013; Paumard et al., 2018

4.2. Rift-fill Measurements and Data

The relations between fault displacement and sediment fill have been quantified using fault vertical displacement (i.e. throw) and maximum sediment thickness in the fault hangingwall. SFR_f records the ratio of accommodation filled by sediments along an individual rift fault where $SFR_f = \frac{\text{syn-rift thickness}}{\text{syn-rift fault throw}}$. SFR_f values are displayed against fault throw to highlight the relationship between the four types of basin fill and fault size within a rift basin (Fig. 4.3A). SFR_b was used to facilitate the comparison of syn-rift strata thickness and vertical displacements between rift basins, where $SFR_b = \frac{\sum \text{syn-rift thickness}}{\sum \text{syn-rift fault throw}}$ for fault throw intervals of 0.25 second TwT (Fig. 4.3B). SFR_b values are displayed as curves in Fig. 4.3B permitting a

quick comparison of the relative vertical position of each rift basin studied, which provides insights into differences of infill architecture between rift basins.

Using the nomenclature of Ravnås and Steel (1998) and SFR values derived here we are able to identify (1) starved (SFR≤0.2), (2) under-filled (0.2<SFR≤0.9); (3) balanced-filled (0.9<SFR≤1.1); and (4) over-filled (SFR>1.1) rift basins (Fig. 4.1). In starved and under-filled rift basins, the rate of fault displacement exceeds sedimentation rates with preservation of topography during rifting and potential for complete basin filling only achieved by sedimentation after the cessation of rifting. Conversely, in balanced and over-filled basins topography generated by faulting is entirely buried at the end of the rifting and growth strata typically record the evolution of fault growth (Childs *et al.*, 1993, 2003). In such cases measures of Expansion Index (EI= HW/FW thicknesses) or Growth Index (GI = (HW-FW)/FW thicknesses) exceeding one are interpreted to indicate fault growth and have proved invaluable for charting fault evolution (e.g., Thorsen, 1963; Cartwright et al., 1998; Childs et al., 2003, 2017; Jackson *et al.*, 2017; Liu *et al.*, 2017). However, EI and GI are of limited value in under-filled rifts where growth strata are not preserved on fault footwalls and, as a consequence, these indices return undefined values. In such cases SFR returns positive and arithmetically defined values for each of the four types of sediment fill identified by Ravnås and Steel (1998) and has wide application.

Rift-fill thicknesses and fault displacements have been collected from seismic reflection lines in seven rift basins (Fig. 4.2). In each case fault vertical displacements were measured between horizon cutoffs while the maximum thickness of syn-rift strata was measured in the immediate hangingwall of the fault at the deepest point of the syn-rift sequence (Fig. 4.1). All measurements are cross-sectional 2D samples and do not necessarily sample the center of these basins or fault maximum displacements. Measurements are in Two-way travel time (TwT) and neither fault displacements nor sediment thicknesses include decompaction. Our preliminary calculations indicate that depth conversion and decompaction do not significantly alter the first-order results. For example, depth conversion increases SFR_f by <10% in over-filled, decreases SFR_f by <15% in under-filled rifts and makes little difference (±2%) to balance filled rifts (See supplementary material 1 for more details). Despite these uncertainties our analysis demonstrates that the technique has general applicability for discriminating different types of rift basin fill.

The number of faults sampled in each basin, range of fault sizes and maximum sediment thickness vary between basins (Table 4.1). The primary dataset analysed is from the Canterbury Basin, in offshore New Zealand, where 346 Cretaceous (~110 to ~84 Ma) rift faults with vertical displacements of <0.1 to 2.9 seconds two-way-time (TwT) were sampled from ~26 000 line kilometers of seismic reflection lines (Field and Browne, 1989; Strogen *et al.*, 2017; this study).

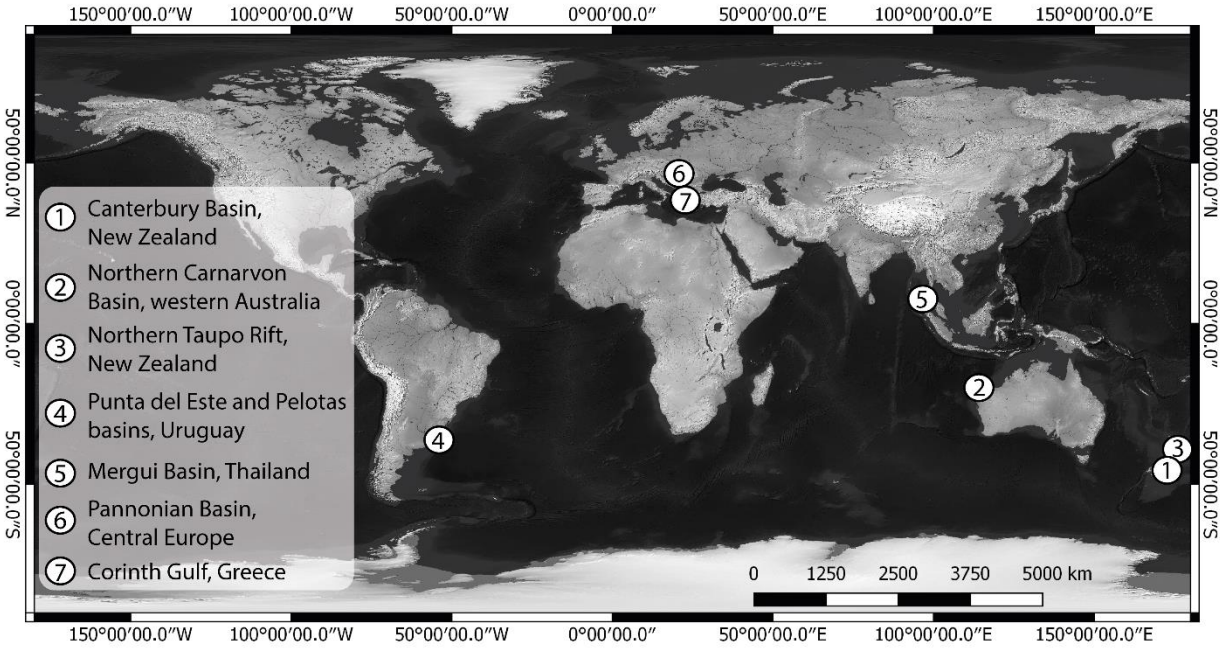

Figure 4.2 Location map of rift basins used in this study

4.3. Rift-fill Geometries

The available data highlight differences in the SFR_b and the relationships between SFR_f and fault size for the basins sampled (Figs. 4.3 and 4.4). The Canterbury Basin is under-filled with an average SFR_b for all fault-throw categories of 0.76. The low value of SFR_b for the Canterbury Basin indicates that sediment supply and deposition was significantly lower than normal-fault displacements. Consequently, the basin contained many uplifted footwall blocks that remained topographic highs during the entire rifting period and for >30 Myr after rift cessation (Fig. 4.4). In general, SFR_b is higher for the other basins sampled and the resulting curves are located above the Canterbury Basin on the graph in Fig. 4.3B. For example, the Northern Carnarvon (Australia) and Northern Taupo Rift (active rift, New Zealand) basins have no under-filled SFR_f values for large faults (throw >1 second TwT), the Punta del Este and Pelotas basins (Uruguay) have SFR_f values close to a balanced-filled rift basin, while the Mergui Basin (Andaman Sea, offshore Thailand), the Pannonian (Central Europe) and the Gulf of Corinth Rift (Greece), display under-filled SFR values mostly for faults with throws of > 1.5 second TwT. At first glance the basins plotted in Fig. 4.3B suggest a predominance of balanced and over-filled geometries, however, these basins are strongly biased towards offshore basins and likely under represent terrestrial onshore rifts that are under-filled or sediment starved (e.g., Basin and Range, USA; East African Rift).

For all rift basins sampled the SFR is partly dependent on fault size, with a negative non-linear relation between fault displacement and SFR being common (Fig. 4.3). The data in Figure 4.3 define upwardly concave curves with SFR_f and SFR_b values typically highest for the smaller resolved faults in the systems and often rising rapidly for throws of <1 seconds TwT. In the Canterbury Basin, for example, ~90%, ~60% and ~40% of rift depocenters associated with large faults (≥1 second TwT throw, N=123), intermediate faults (0.5-1 second

TwT throw, N=206) and small faults (<0.5 seconds TwT throw, N=253) were under-filled at the end of rifting, respectively. While the proportions of under-filled rift depocenters for different rift systems may vary, the data on Fig. 4.3 suggest that balanced or over-filled basins are mostly observed for depocenters associated with normal faults of <0.5 seconds TwT throw, with under-filled depocenters more often formed by larger faults with >1 second TwT. Therefore, in cases where regional strain rates and sediment rates are similar, rift systems dominated by large faults (e.g., > 1 second) are more likely to be under-filled than systems comprising many small faults (e.g., <0.5 seconds). The preponderance of over-filled smaller faults may partly reflect the tendency for such faults to have lower displacements rates and their depocenters are therefore more likely to be overwhelmed by sedimentation. Over-filling of depocenters associated with smaller faults may also arise because an order of magnitude increase in fault displacement produces a two to three orders of magnitude increase in the volume of depocenter available to receive sediments. Therefore, many more small faults than large faults are required to produce the same depocenter volume (see supplementary material 2).

The number and size distribution of faults (including the maximum fault displacement and the scaling properties of the faults) in rift systems can be dependent on the structural maturity of faulting (Scholz and Cowie, 1990; Walsh et al., 1991). In some normal fault systems extension initially produces many small faults distributed across the basin, with strain subsequently localized onto larger faults as finite extension increases (e.g., Morley, 1999; Meyer *et al.*, 2002; Childs *et al.*, 2003, 2017). Therefore, in cases where sediment supply is maintained strain localization would be expected to be accompanied by a decrease in SFR. Localization of extension could also be accompanied by death of smaller faults (e.g., Meyer *et al.*, 2002) and these faults will be subsequently buried by syn-rift strata associated with larger faults. The present analysis assumes that all faults were active for the same time interval and does not permit a fault that died early (and was subsequently buried) to be discriminated from depocenters that were over-filled during faulting. In the Canterbury Basin, for example, ~20% of faults cease activity after <50% of the duration of rifting and typically display small throws (<1 second TwT). As a consequence of their early death, the vertical displacement of these smaller faults is often less than the thickness of the entire syn-rift succession, resulting in SFR_f >1.1. Although the duration of faulting is clearly a factor that influences basin infilling, this cannot account for all of the changes in SFR with fault size depicted for the Canterbury Basin in Figure 4.3A.

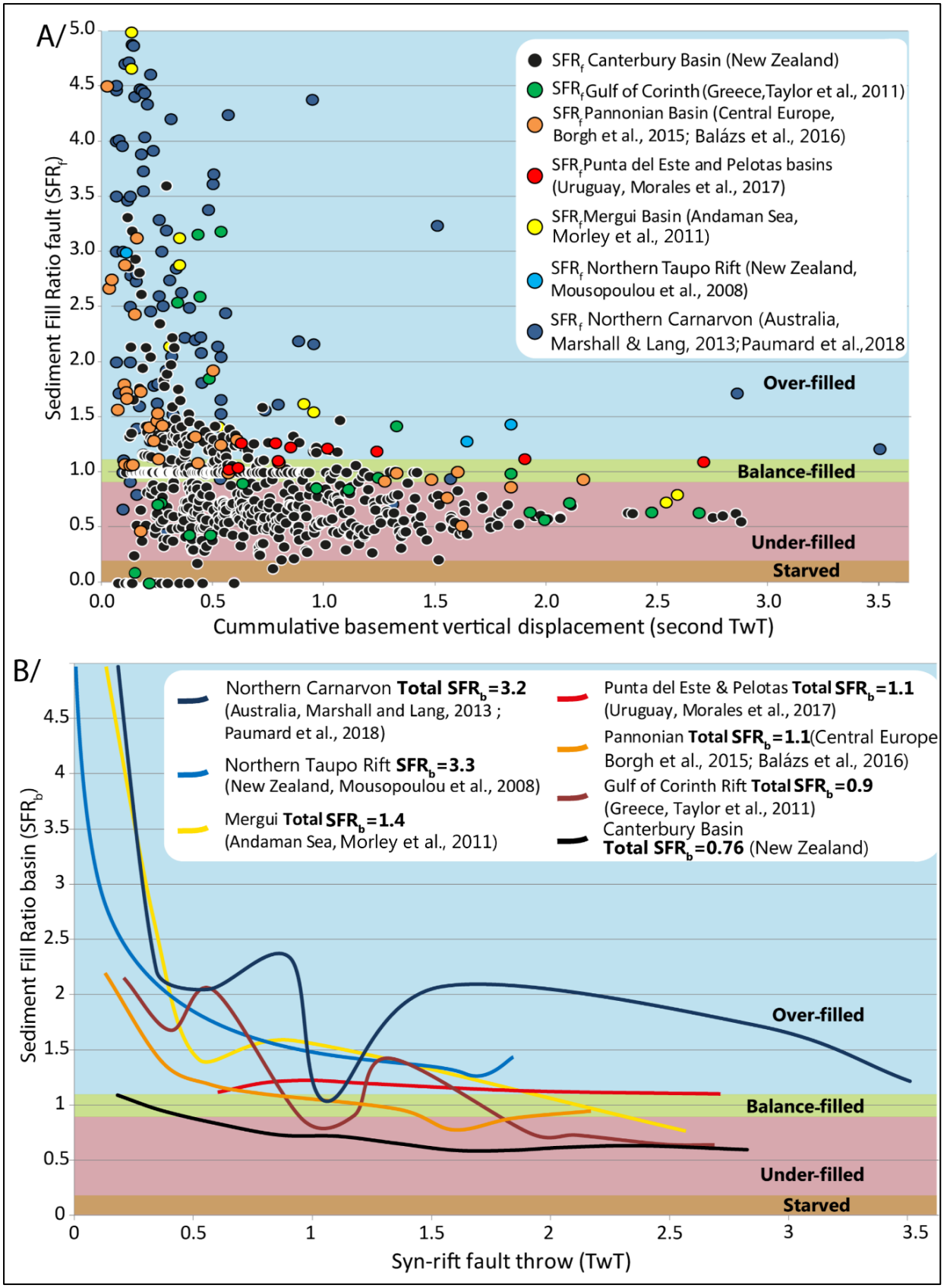

Figure 4.3 Summary of the use of the Sediment Fill Ratio (SFR_f): Comparison of the (A) SFR_f and (A) SFR_b of different rift basins.

The data presented also suggest that smaller faults display an increase in the spread of SFR_f and the value of this spread is negatively related to fault size with the Canterbury Basin, Corinth Rift and Pannonian Basin, all of which comprise under-filled, balanced-filled and over-filled depocenters for smaller faults <0.5 seconds TwT (Fig. 4.4A). These basins were all characterized by under-filling of depocenters adjacent to the largest faults with emergent footwall highs and sedimentation primarily in adjacent grabens or half-grabens. In the Canterbury Basin the spread of SFR values for low displacement faults (< 0.5 seconds TwT) is influenced by their spatial distribution (Fig. 4.4). Small faults located in the hangingwall of higher displacement faults (e.g., >1 second TwT) typically produce second-order half-grabens that are over filled. In such cases over-filling arises because accommodation and sedimentation rates adjacent to these small faults are influenced by displacements on the larger faults that control the first-order half-graben locations and sedimentation patterns (Fig. 4.4). Conversely, smaller faults also formed in the uplifted footwall blocks of larger faults where sedimentation rates are often relatively low and small rift basins are starved or under-filled (SFR≤0.9). In such footwall areas erosion or non-deposition would produce SFR values approaching zero. However, the absence of displacement marker horizons and the possibility that faults have been eroded will likely result in under sampling of these starved and under-filled basins (Fig. 4.4).

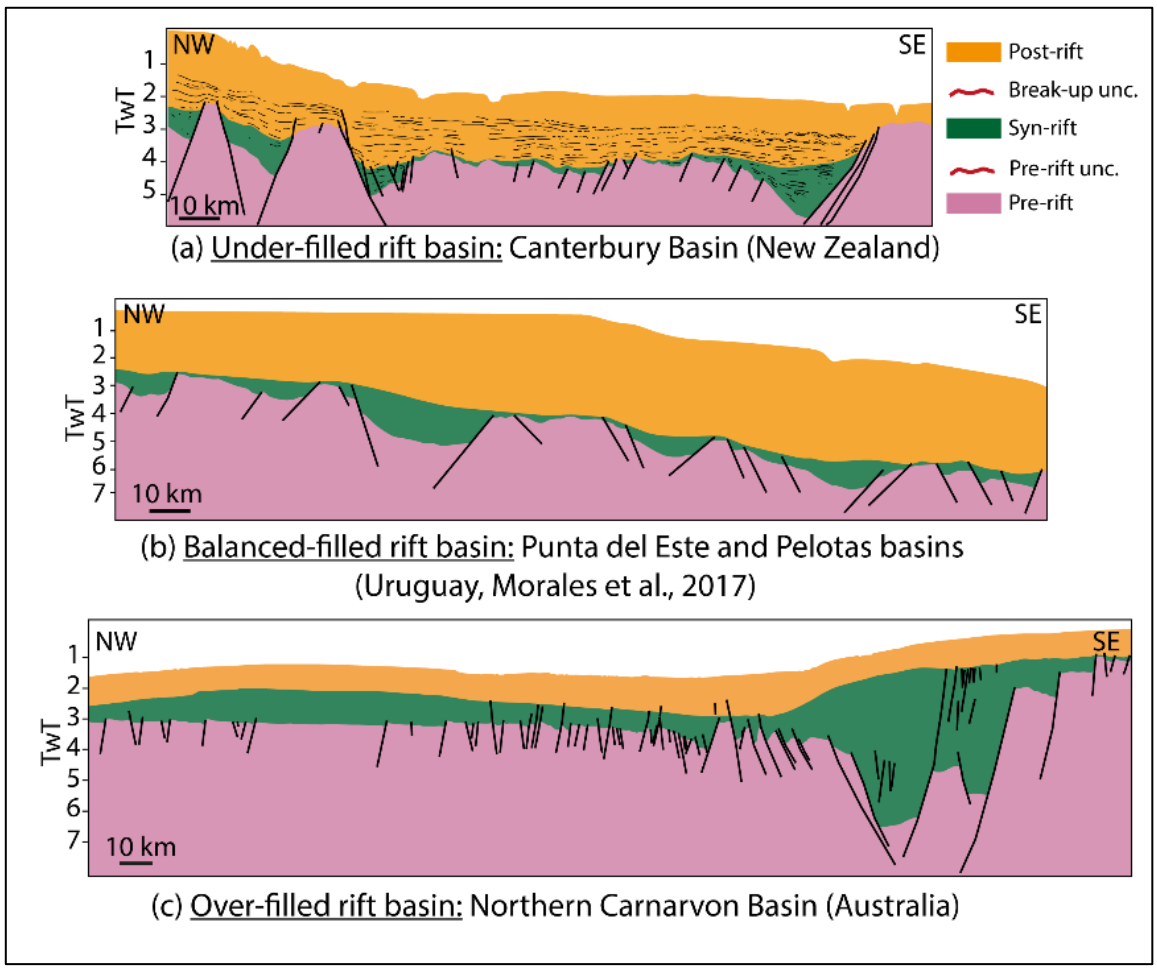

Figure 4.4 Schematic cross section of (a) an under-filled syn-rift basin (Canterbury Basin, New Zealand), (b) balanced-filled syn- basin (Punta del Este and Pelotas basins, Uruguay) and over-filled syn-rift basin (Northern Carnarvon Basin, Australia). In the case of the Northern Carnarvon Basin, the top basement interpretation is hampered by basement internal reflectivity and its depth (for more information see Marshall and Lang, 2013; Paumard et al., 2018). Therefore, for the Northern Carnarvon Basin, top basement was interpreted at minimal depth involving that SFR and SFI values could be higher.

4.4. Discussion

Rift infill architecture is strongly influenced by sediment supply which is controlled by sediment yield of topography higher in altitude than the basin floor and can be shaped by; the geologic composition, size and topography of the catchment areas, the lengths and patterns of the drainage networks, vegetation type and coverage, climate, transport mechanism (fluvial, eolian, lacustrine, marine) and the geodynamic setting of the rift basin (e.g. Roberts and Yielding 1994; Lambiase and Bosworth 1995; Ravnås and Steel, 1998; Gawthorpe and Leeder 2000). The resulting sediment may be sourced from uplifted fault-bound blocks within the rift systems and from outside the rift.

In cases where the distribution of fault sizes is similar, the primary control on SFR_b appears to be the sediment supply, hence the vertical position of the SFR_b curves in Figure 4.3B increases as sediment supply keeps-pace with formation of space. For example, the Canterbury, Punta del Este and Pelotas and Northern Carnarvon basins, which have maximum fault throws > 2 seconds TwT are under-filled, balanced-filled and over-filled, respectively. Thus, the rate of sediment supply (S) was high enough to keep-pace with the rate of accommodation creation (A) in the Punta del Este basin (A/S=1). In contrast, the rate of accommodation creation outpaces the rate of sediments supply in the Canterbury Basin (A/S<1) whereas the opposite occurs in the Northern Carnarvon Basin (A/S>1). In the Canterbury Basin rift under-filling reflects the low sediment supply with sedimentation rates about half the fault displacement rates for fault throws >1 second TwT. For the Canterbury Basin, sediment deposited in rift depocenters is derived from a combination of local erosion of fault footwalls and regional erosion of a low-topograpghy proto-New Zealand landmass located at least 100 km west of the Canterbury Basin (see chapter 2 of this thesis for further details). In the case of the Canterbury Basin, balanced and over-filled rift depocenters cannot be achieved by erosion of uplifted fault footwall areas alone and would require at least a 50% increase in sediment supply from outside the basin. Almost complete over-filling of depocenters in the Punta del Este and Pelotas basins, Mergui Basin, Northern Taupo Rift and Northern Carnarvon Basin may largely reflect the high sediment supply into these basins sourced from outside these rift systems.

4.5. Conclusion

Rift systems are generally sites of sediment deposition which occurs in depocenters produced by faulting. The degree of rift basin infill after rift cessation is here defined using the Sediment Fill Ratio (SFR), which the ratio of syn-rift maximum sedimentation to syn-rift fault throw. The parameters are measured in the immediate hangingwall of each fault using seismic reflection lines. Rift basins are defined as being starved (SFR $\leq$0.2), under-filled (0.2<SFR$\leq$0.9, balanced-filled (0.9<SFR$\leq$1.1) and over-filled (SFR>1.1). The fill geometry of the seven rift systems studied here range from being under-filled to over-filled. Within each basin the degree of filling of depocenters in the immediate hangingwall of each fault is dependent on fault size. Curves of SFR vs fault throw typically show a non-linear negative relationship with smaller faults (e.g., throws <0.5 seconds TwT) most likely to be over-filled.

This over-filling may reflect the lower displacement rates on smaller faults. Under-filling is most common proximal to large faults (e.g., throws >1 seconds TwT) and in rift systems dominated by large faults. Rift systems comprising entirely over-filled depocenters may have received a significant supply of sediment from outside the rift system.

4. Acknowledgements

We would like to acknowledge J.M. Gaulier whose discussions about the Canterbury Basin triggered the idea of analyzing the filling of rift basins. We are grateful to The Western Australian Department of Mines, Industry Regulation and Safety and Geoscience Australia for providing the open-file well and 2D seismic data used in this study for the Northern Carnarvon Basin.

4. References

BALÁZS, A., MATENCO, L., MAGYAR, I., HORVÁTH, F. & CLOETINGH, S. (2016) The Link between Tectonics and Sedimentation in Back-Arc Basins: New Genetic Constraints from the Analysis of the Pannonian Basin. Tectonics, 35, 1526-1559 pp.

BORGH, M., RADIVOJEVIĆ, D. & MATENCO, L. (2015) Constraining Forcing Factors and Relative Sea-Level Fluctuations in Semi-Enclosed Basins: The Late Neogene Demise of Lake Pannon. Basin Research, 27, 681-695 pp.

CARTWRIGHT, J., BOUROULLEC, R., JAMES, D. & JOHNSON, H. (1998) Polycyclic Motion History of Some Gulf Coast Growth Faults from High-Resolution Displacement Analysis. Geology, 26, 819-822 pp.

CHILDS, C., EASTON, S., VENDEVILLE, B., JACKSON, M., LIN, S., WALSH, J. & WATTERSON, J. (1993) Kinematic Analysis of Faults in a Physical Model of Growth Faulting above a Viscous Salt Analogue. Tectonophysics, 228, 313-329 pp.

CHILDS, C., NICOL, A., WALSH, J.J. & WATTERSON, J. (2003) The Growth and Propagation of Synsedimentary Faults. Journal of Structural geology, 25, 633-648 pp.

CHILDS, C., HOLDSWORTH, R.E., JACKSON, C.A.-L., MANZOCCHI, T., WALSH, J.J. & YIELDING, G. (2017) Introduction to the Geometry and Growth of Normal Faults. Geological Society, London, Special Publications, 439, 10p.

DAVISON, I. & UNDERHILL, J.R. (2012) Tectonics and Sedimentation in Extensional Rifts: Implications for Petroleum Systems. In: Tectonics and sedimentation: Implications for petroleum systems (Ed. Gao D.), AAPG Memoir 100, 15-42 pp.

FIELD, B.D. & BROWNE, G.H. (1989) Cretaceous and Cenozoic Sedimentary Basins and Geological Evolution of the Canterbury Region, South Island, New Zealand. Institute of Geological & Nuclear Sciences monograph, 2, 94p.

GAWTHORPE, R.L. & LEEDER, M.R. (2000) Tectono-Sedimentary Evolution of Active Extensional Basins. Basin Research, 12, 195-218 pp.

JACKSON, C.A.-L., BELL, R.E., ROTEVATN, A. & TVEDT, A.B. (2017) Techniques to Determine the Kinematics of Synsedimentary Normal Faults and Implications for Fault Growth Models. Geological Society, London, Special Publications, 439, 187-217 pp.

LAMBIASE, J.J. & BOSWORTH, W. (1995) Structural Controls on Sedimentation in Continental Rifts. Geological Society, London, Special Publications, 80, 117-144 pp.

LIU, Y., CHEN, Q., WANG, X., HU, K., CAO, S., WU, L. & GAO, F. (2017) Influence of Normal Fault Growth and Linkage on the Evolution of a Rift Basin: A Case from the Gaoyou Depression of the Subei Basin, Eastern China. AAPG Bulletin, 101, 265-288 pp.

MARSHALL, N. & LANG, S. (2013) A New Sequence Stratigraphic Framework for the North West Shelf, Australia. The Sedimentary Basins of Western Australia 4: Proceedings PESA Symposium. Perth, 1-32 pp.

MEYER, V., NICOL, A., CHILDS, C., WALSH, J. & WATTERSON, J. (2002) Progressive Localisation of Strain During the Evolution of a Normal Fault Population. Journal of Structural Geology, 24, 1215-1231 pp.

MORALES, E., CHANG, H.K., SOTO, M., CORRÊA, F.S., VEROSLAVSKY, G., DE SANTA ANA, H., CONTI, B. & DANERS, G. (2017) Tectonic and Stratigraphic Evolution of the Punta Del Este and Pelotas Basins (Offshore Uruguay). Petroleum Geoscience, 23, 415-426 pp.

MORLEY, C.K. (1999) Patterns of Displacement Along Large Normal Faults: Implications for Basin Evolution and Fault Propagation, Based on Examples from East Africa. AAPG bulletin, 83, 613-634 pp.

MORLEY, C.K. (2002) Tectonic Settings of Continental Extensional Provinces and Their Impact on Sedimentation and Hydrocarbon Prospectivity. In: Sedimentation in Continental Rifts (Eds. Renaut, R. W. & Ashley, G.M.), SEPM Special Publication, 73, 25-55 pp.

MORLEY, C.K., RACEY, A., RIDD, M., BARBER, A. & CROW, M. (2011) Tertiary Stratigraphy. In: The Geology of Thailand (Eds. Ridd, M.F., Barber, A.J., Crow, M.J.). The Geological Society (London), 223-272 pp.

MOUSLOPOULOU, V., NICOL, A., WALSH, J.J., BEETHAM, D. & STAGPOOLE, V. (2008) Quaternary Temporal Stability of a Regional Strike-Slip and Rift Fault Intersection. Journal of Structural Geology, 30, 451-463 pp.

PAUMARD, V., BOURGET, J., PAYENBERG, T., AINSWORTH, R.B., GEORGE, A.D., LANG, S., POSAMENTIER, H.W. & PEYROT, D. (2018) Controls on Shelf-Margin Architecture and Sediment Partitioning During a Syn-Rift to Post-Rift Transition: Insights from the Barrow Group (Northern Carnarvon Basin, North West Shelf, Australia). Earth-Science Reviews, 177, 643-677 pp.

RAVNÅS, R. & STEEL, R.J. (1998) Architecture of Marine Rift-Basin Successions. AAPG Bulletin, 82, 110-146 pp.

ROBERTS, A., & YIELDING, G. (1994) Continental Extensional Tectonics. In: Continental deformation (Ed. Hancock, P. L.), Pergamon Press, 223-250 pp.

SCHLISCHE, R.W., YOUNG, S.S., ACKERMANN, R.V. & GUPTA, A. (1996) Geometry and Scaling Relations of a Population of Very Small Rift-Related Normal Faults. Geology, 24, 683-686 pp.

SCHOLZ, C. & COWIE, P.A. (1990) Determination of Total Strain from Faulting Using Slip Measurements. Nature, 346, 837-839 pp.

STROGEN, D.P., SEEBECK, H., NICOL, A. & KING, P.R. (2017) Two-Phase Cretaceous – Paleocene Rifting in the Taranaki Basin Region, New Zealand; Implications for Gondwana Breakup. Journal of the Geological Society, 174, 929-946 pp.

TAYLOR, B., WEISS, J.R., GOODLIFFE, A.M., SACHPAZI, M., LAIGLE, M. & HIRN, A. (2011) The Structures, Stratigraphy and Evolution of the Gulf of Corinth Rift, Greece. Geophysical Journal International, 185, 1189-1219 pp.

THORSEN, C.E. (1963) Age of Growth Faulting in Southeast Louisiana.

WALSH, J., WATTERSON, J. & YIELDING, G. (1991) The Importance of Small-Scale Faulting in Regional Extension. Nature, 351, 391-393 pp.

WITHJACK, M.O., SCHLISCHE, R.W. & OLSEN, P.E. (2002) Rift-Basin Structure and Its Influence on Sedimentary Systems. Sedimentation in Continental Rifts, 57-81 pp.

CHAPTER 5) EARLY OLIGOCENE MARINE CANYON-CHANNEL SYSTEMS: IMPLICATIONS FOR PALEOGEOGRAPHY AND TECTONICS IN THE CANTERBURY BASIN, NEW ZEALAND

A. Barrier[1], A. Nicol[1], G.H. Browne[2] and K. Bassett[1]

[1] *University of Canterbury, Department of Geological Science, Christchurch, New Zealand.*

[2]*GNS Science, PO Box 30368, Lower Hutt, New Zealand.*

5. Abstract

The Oligocene is a time of maximum submersion of the Zealandia landmass; it coincides with changes in oceanographic currents as well as with the inception of the Cenozoic plate boundary through New Zealand. Offshore wells and seismic reflection lines in the Canterbury Basin reveal condensed Oligocene strata (<150 m thick), which were eroded by mid-Oligocene (~32-29 Ma) channels 1-10 km wide, 15-90 km long and up to ~200 milliseconds two-way-time deep. Onshore, corridors of complete erosion of the Early Oligocene Amuri Limestone, overlain by younger Oligocene and Miocene strata have been mapped using measured sections from the published literature and offshore seismic reflection data. The synchronicity, similar trends, and comparable morphology of onshore and offshore channels suggest that they may have formed part of the same erosive system. We propose that a sea-level fall at ~32 Ma initiated the development of this drainage system with erosive channels converging towards canyons in the deeper water offshore. The drainage was active for up to 17 Ma, flowing both towards the south-east into the present-day Bounty Trough and the north-east into the Pegasus Basin. The temporal (millions of years) and the spatial (hundreds of metres) scales of the sea-level fall are larger than would be expected for eustatic processes and we suggest that regional tectonic uplift may have played an important role in channel formation. The channel orientations and their eastward gradients together with the Oligocene sedimentary facies observed in outcrop, suggest that the axis of uplift (and maximum topography) was primarily west of the Canterbury Basin. Tectonic shortening that collectively affected the western North Island – Marlborough Sounds – western Otago high may have produced uplift and eastward flowing Early Oligocene channels in the Canterbury Basin. The orientations, geometries, and locations of Early Oligocene drainage is similar to present day systems, suggesting they have persisted as physiographic entities for at least 30 Myr, throughout Late Cenozoic plate tectonic deformation.

5.1. Introduction

Lateral discontinuity of stratigraphic units are common place in geology and can be controlled by tectonic, magmatic, eustatic or sedimentary processes which typically complicate stratigraphic correlation across a sedimentary basin (e.g., Miall, 2000). Among these processes, erosion is universal to all sedimentary basins (e.g., Shanmugan, 1988). Erosional surfaces can be of regional extent and produce mappable erosion surfaces across basins (e.g., Swift, 1968; Nummedal and Swift, 1987; Catuneanu et al., 2011, 2017), while other erosional surfaces are localised and produce differential erosion (e.g., Shanmugan, 1988; Montgomery, 2002; Catuneanu et al., 2011, 2017). Understanding erosional surfaces is key to determining allocyclic and autocyclic processes occurring in a sedimentary basin (e.g., Shanmugan, 1988; Miall, 2000).

Erosional processes have undoubtedly influenced the preservation of Oligocene rocks in New Zealand (Fig. 5.1- e.g., King et al., 1999), which represent a key period in local Cenozoic geological history (e.g., Lever, 2007; Strogen et al., 2014; Strogen et al., 2019). The Oligocene corresponds to a time of maximum submersion of the Zealandia landmass, to a period of fundamental change in paleo-oceanography created by the initiation of circum-polar ocean currents, and to the inception of the Cenozoic plate boundary through New Zealand (Fig. 5.1 - e.g., King et al., 1999; Stagpoole and Nicol, 2008; Mildenhall et al., 2014; Strogen et al. 2014; Higgs and King, 2018; Strogen et al., 2019). Carbonate and fine-grained sediments predominated during the Late Eocene and Oligocene, and largely reflect shelf and deep-water settings across Zealandia (Nelson, 1978; King et al., 1999; Mortimer and Strong, 2014; Strogen et al., 2014, 2019).

Oligocene mixed siliciclastic and carbonate strata of the Canterbury Basin in the eastern South Island of New Zealand contain important discontinuities which have been referred to as the Marshall Unconformity (or Paraconformity; Carter and Landis 1972, Findlay 1980; Carter et al., 1982; Lewis, 1992; Lever 2007). During the Early Oligocene, sediments are interpreted to have been deposited on a carbonate passive margin in a shelf setting at the maximum inundation of a second order marine transgression (Lewis and Belliss 1984; Field and Browne, 1989; King et al., 1999; Thompson, 2013; Thompson et al., 2014). The carbonate depositional environment is thought to have promoted laterally continuous sedimentation, however, studies in the Canterbury Basin and elsewhere in New Zealand, using sparse and discontinuous outcrops, highlight multiple diachronous unconformities that are often difficult to correlate between sections. Many studies have been undertaken on these surfaces, however, considerable uncertainty and debate remains as to the character, distribution, and causes (e.g., Carter and Landis, 1972; Findlay, 1980; Carter et al., 1982; Field, 1985; Lewis, 1992; Fulthorpe et al., 1996; Lever, 2007). In large part, this ambiguity has arisen because the vast majority of studies have concentrated on outcrop sections, with little focus on seismic reflection data that mainly exists in offshore regions. The interpretation of regional seismic reflection profiles in the offshore Canterbury Basin provides a new perspective on the geometry and origin of these Oligocene unconformities, both locally and throughout New Zealand.

Here we present the first systematic review of Oligocene strata from seismic data in the Canterbury Basin. These data permit correlation between offshore and onshore regions in the basin, and provide an improved understanding of how and why erosive processes, of either tectonic or eustatic origin, have caused discontinuities and differential erosion in the Early Oligocene strata of the Canterbury Basin. These unconformities are approximately synonymous with the Marshall Unconformity of other workers. However, we refrain from using this nomenclature here, as debate and uncertainty exists around its definition, aspects of which have been the subject for previous papers (e.g., Carter and Landis, 1972; Findlay, 1980;

Carter et al., 1982; Field, 1985; Lewis, 1992; Fulthorpe et al., 1996; Lever, 2007). We use seismic reflection and outcrop data to characterise the geometry, spatial distribution, and timing of Early Oligocene erosion in the onshore and offshore Canterbury Basin. We present evidence for differential erosion of up to ~200 milliseconds two-way time (TwT) deep that can cut into Eocene strata and form kilometre-wide channels. These mapped channels grade towards the east and southeast of the basin, providing constraints on the eustatic and regional tectonic processes operating in the eastern South Island in the Early Oligocene. The results have implications for mid-Cenozoic paleogeography, the onset of plate tectonic activity in Zealandia and highlight the longevity of drainage systems within, and immediately adjacent to, an active plate boundary zone. The latter is surprising given the subsequent active tectonic deformation in this area during the Neogene.

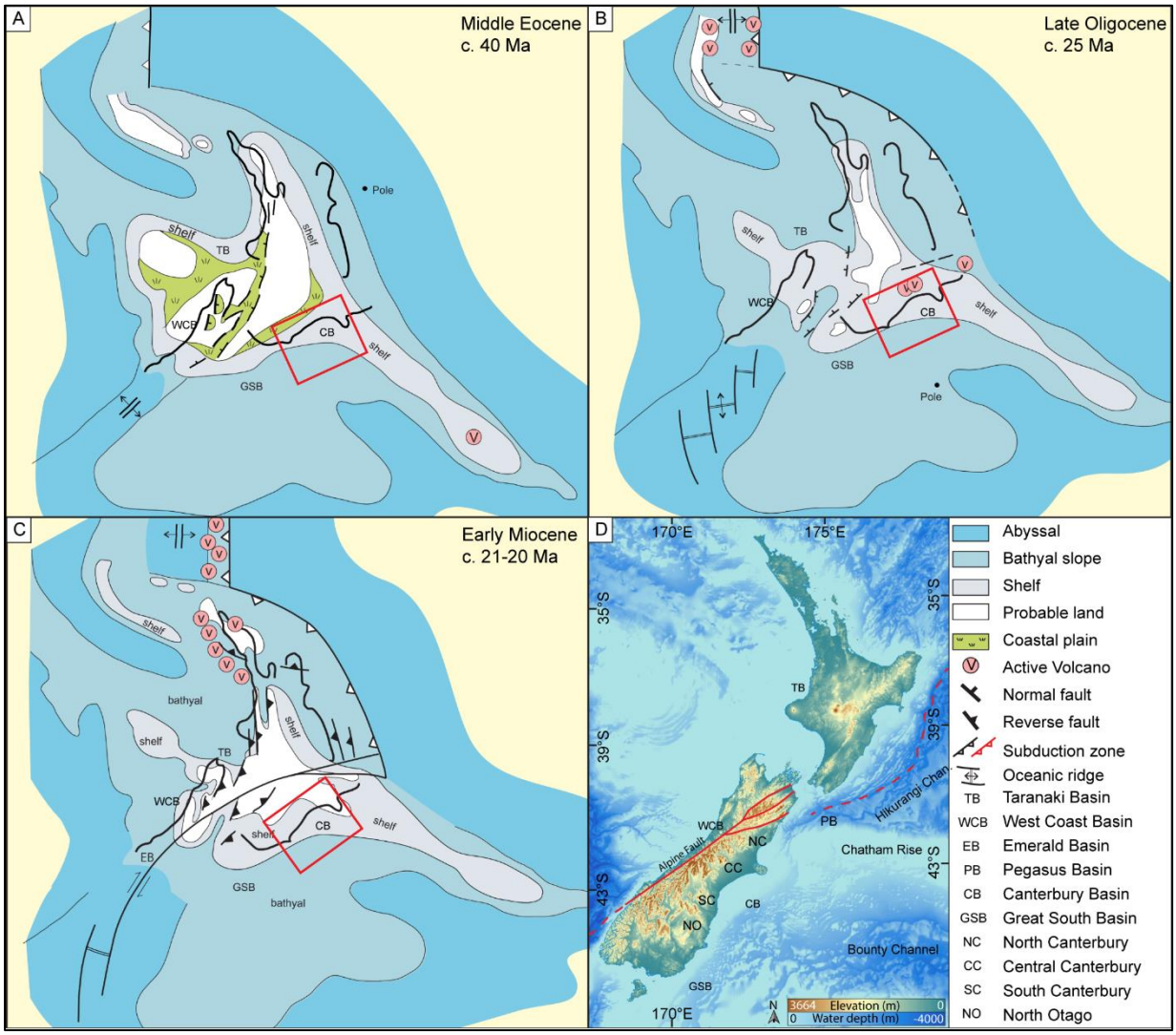

Figure 5.1 Paleogeographic evolution of Zealandia from King et al. (1999): (A) Middle Eocene ~40 Ma), (B) Late Oligocene (~25 Ma), (C) Early Miocene (~21-20 Ma), (D) Present day map of New Zealand with the main sedimentary basins labelled, structural highs and sedimentological features addressed in this paper. Topographic data sourced from LINZ Data Service and bathymetric data licensed under NIWA Open Data Licence v1.0.v.

5.2. Geological Regional Setting and Data

New Zealand comprises nineteen sedimentary basins that contain strata up to 10 km thick with a maximum age of mid-Cretaceous (~110±5 Ma) (Fig. 5.1, King et al., 1999). The present study is focused on the Canterbury Basin which covers an area of ~ 160 000 km^2 in the central to eastern region of the South Island. The majority of the basin occurs in the offshore region, with an eroded succession exposed onshore (Fig. 5.1). The Canterbury Basin initiated as an intra-continental rift formed due to widespread extension of Zealandia during the mid-Cretaceous (late Albian, ~110±5 Ma) (Field and Browne, 1989; Sahoo et al., 2014, 2015). Zealandia, as defined by Mortimer et al. (2017), drifted away from western Antarctica and Australia during the Late Cretaceous to Early Eocene post-rift (~84 to ~40 Ma) (King, 2000). Initial rift and early post-rift sedimentation was dominated by sandstone and conglomerate, but subsequent Paleogene sedimentation became progressively finer-grained and more calcareous. These changes occurred synchronously with increasing water depths until the Early Oligocene when the basin reached maximum drowning and transgression (Figs. 5.1, 5.2, and 5.3 - Field and Browne, 1989; King et al., 1999; Mildenhall, 2014; Mortimer et al., 2017; Higgs and King, 2018). There has been considerable debate as to whether Zealandia was either completely or only partially submerged in the Oligocene (Wellman, 1953; Fleming, 1962; Suggate et al., 1978; Cooper and Cooper, 1995; King et al. 1999; Mildenhall et al., 2014), although there is a general consensus that some land or island archipelagos existed (e.g., Landis et al., 2008; Mildenhall, 2014; Strogen et al., 2014; Strogen et al., 2019).

The Late Eocene to Early Oligocene represents a period of major changes in oceanic current circulation in the southern Pacific Ocean, which impacted the marine sediment distribution (Nelson and Cook, 2001; Carter et al., 2004; Exon et al., 2004; Stickley et al., 2004; Livermore et al., 2007; Katz et al., 2011). The opening of the Tasmanian Gateway and the Drake Passage during the Late Eocene induced the inception of oceanic bottom currents, such as the Antarctic Circumpolar Current (ACC) along the eastern South Island of New Zealand (Carter et al., 2004). During the Late Oligocene-Early Miocene, oceanic bottom currents formed drift accumulations while detrital sediment input into the basin was restricted due to the widespread submergence of Zealandia (Carter et al., 2004).

The timing of the onset of plate boundary deformation is a point of debate and may have varied spatially throughout New Zealand. Eocene-Oligocene strata may record the earliest onset of Cenozoic plate boundary deformation, including the opening of the Emerald Basin and simultaneous inversion of the Taranaki and West Coast basins (Fig. 5.1 - e.g., King, 2000; Hansen and Kamp, 2004; Stagpoole and Nicol, 2008; Strogen et al., 2014; Reilly et al., 2015; Strogen et al., 2019). From the end of the Oligocene to the present day, only the western margin of the Canterbury Basin, within ~150 km of the Alpine Fault, has experienced tectonic deformation, uplift, and erosion (Wellman, 1979; Adams, 1980). Offshore, the Canterbury Basin has remained relatively undeformed during the Cenozoic and contains a near-complete sedimentary record from the mid-Cretaceous to Recent (Fig. 5.1 – Field and Browne, 1989; Browne and Naish, 2003; Lu et al., 2003, 2005; Lu and Fulthorpe, 2004; Sahoo et al., 2014; 2015; Barnes et al., 2016; Marsaglia et al., 2017). Despite this lack of deformation, Oligocene-Recent erosion and deposition in the basin record the far-field effects of plate boundary deformation.

The Late Eocene to Oligocene succession in the Canterbury Basin is the main focus of this study. These strata were mainly deposited in marine environments and comprise the Late Eocene to Early Oligocene Amuri Limestone overlain by Late Oligocene glauconitic sandstone and bioclastic limestones (Figs. 5.2, 5.3 and 5.4 – e.g., Browne and Field, 1985; Field and Browne, 1986; Andrew et al., 1987; Field and Browne, 1989; Lever, 2007). These two successions are separated by multiple unconformities of different ages, which are difficult to correlate (Figs. 5.2 and 5.3).

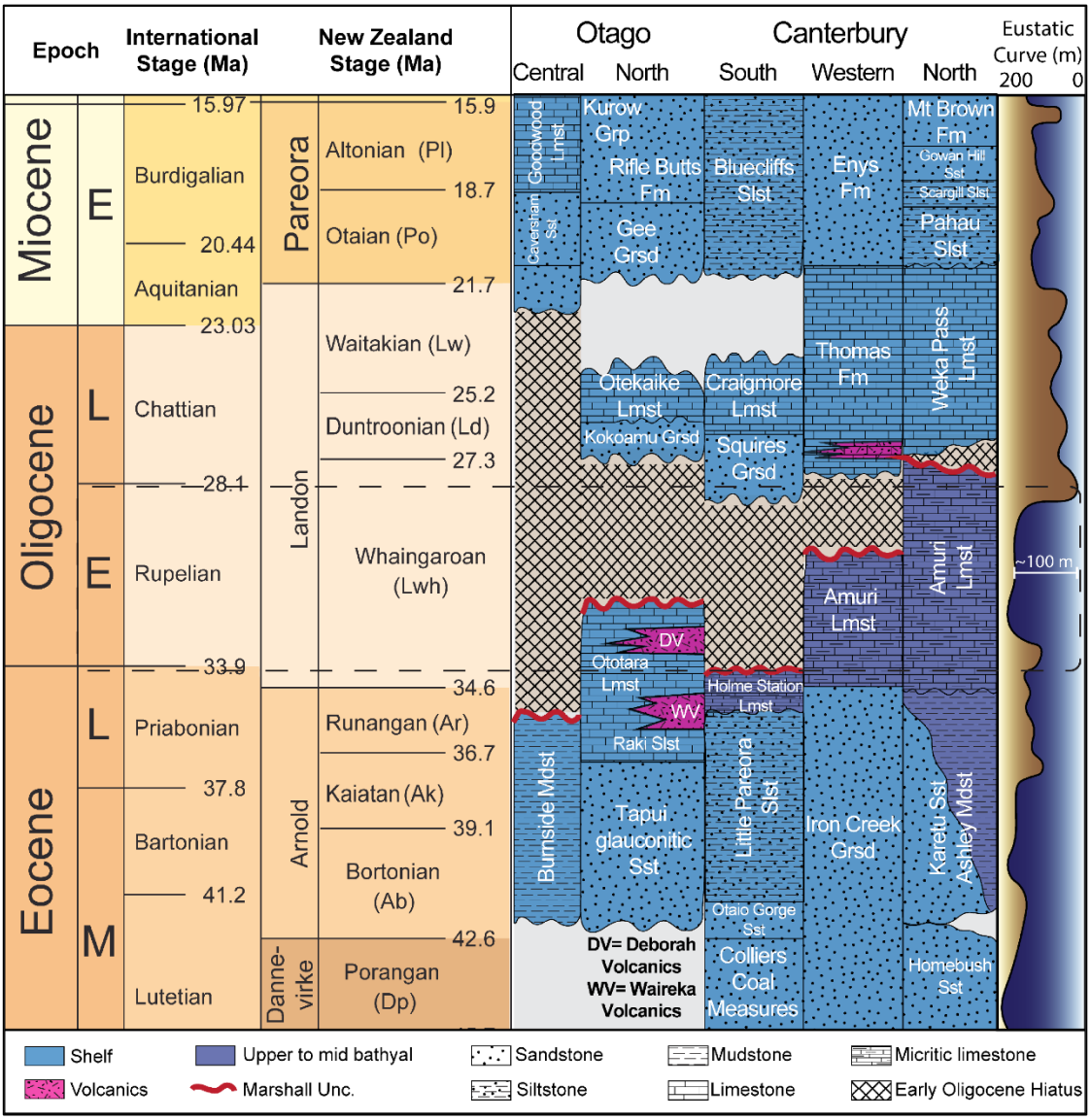

Figure 5.2 Eocene to Early Miocene south to north stratigraphic chart of the onshore Canterbury Basin adapted from Lever (2007). Eustatic curve from Haq et al. (1987). See Figure 5.5 for location. Fm: Formation; Lmst: Limestone; Sst: Sandstone; Slst: Siltstone; Grsd: Green sand; Mdst: Mudstone.

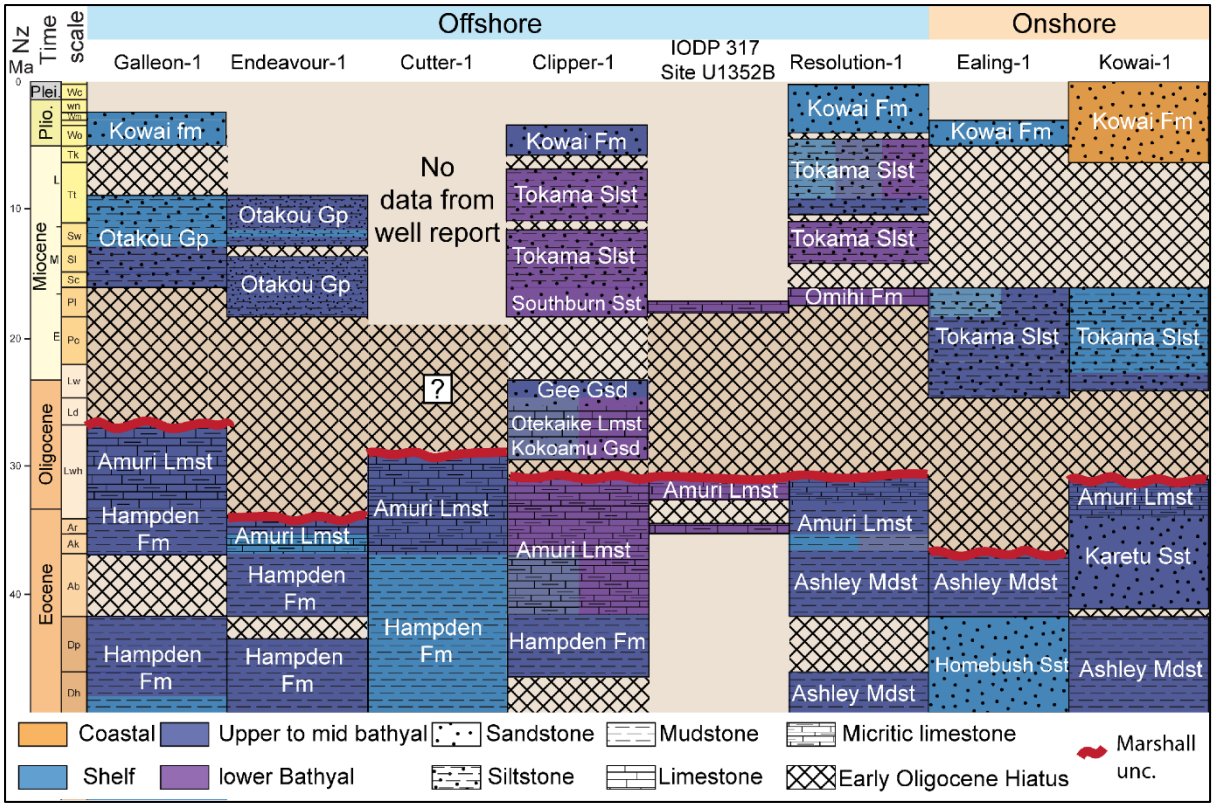

Figure 5.3 Stratigraphic correlation across onshore and offshore wells in the Canterbury Basin for the Eocene-Pliocene time interval. Various unconformity and hiatus intervals are indicated (dating from Schiøler and Raine, 2011). See Figure 5.5 for location. Fm: Formation; Gp; Group; Lmst: Limestone; Sst: Sandstone; Slst: Siltstone; Grsd: Green sand; Mdst: Mudstone.

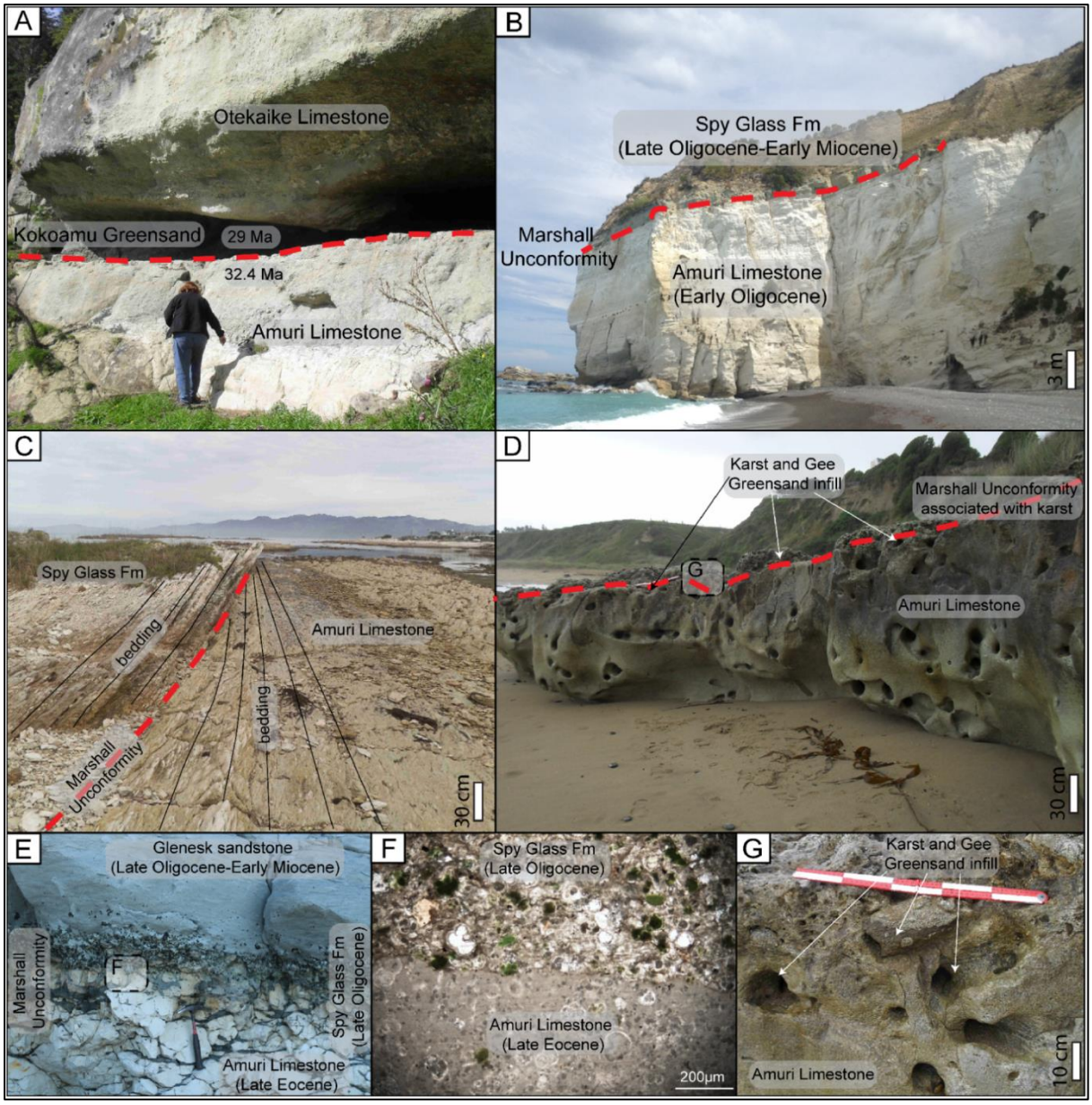

Figure 5.4 Outcrop photos and a thin section photomicrograph of the Marshall unconformity (or assumed equivalents) in Canterbury Basin. (A) At its type section (Squires Farm in South Canterbury, person for scale). (B) At Nape Nape Beach in North Canterbury. (C) At South Bay, Kaikoura (Marlborough) showing an angular unconformity between the Amuri Limestone (right) with the overlying Spy Glass Formation (left). (D) At Kakanui (North Otago) showing karst affecting the top of the Amuri Limestone (E) At Gore Bay (North Canterbury, rock hammer for scale) showing the irregular surface with bioturbation and phosphatised and glauconitic pebbles. (F) Photomicrograph from Gore Bay (North Canterbury) showing the wackstone Amuri Limestone in contact with a glauconitic packstone of the Spy Glass Formation. (G) Detailed photo of D (Kakanui) showing glauconitic infill of karst features at the top of the Amuri Limestone (scale is 50 cm with 10 cm divisions). See Figure 5.5 for location.

5.3. Data and Methods

We primarily use data from onshore outcrops together with offshore 2D seismic reflection lines and wells to study the Early Oligocene drainage system in the Canterbury Basin. Offshore, we have interpreted ~26 000 line kilometres of 2D seismic reflection profiles, tied to data from five petroleum exploration wells provided by New Zealand Petroleum and Minerals (NZP&M, for details see https://data.nzpam.govt.nz) and to IODP Expedition 317 wells located on the shelf and upper slope (Sites U1351 to U1354, Figs. 5.3 and 5.5 - Fulthorpe et al., 2011). Although acquisition of regional 2D seismic data commenced in the 1970s and 1980s, the present study was only possible after collection of high quality 2D data post-2000 and 3D surveys dating from 2007. The seismic lines are mainly oriented SE and NE with spacing of <1 km to 50 km within 10 to 30 km of the coast. In addition to the 2D data, the Waka 3D seismic survey permits continuous imaging of Early Oligocene channels over an area of 3 000 km^2. The seismic profile spacing for 2D data is sufficiently close to enable correlation of the largest channels and canyons (> 2 km wide and > 50 ms TwT deep) that incise the top Eocene-base Oligocene reflector. For seismic data, canyon and channel sinuosity (CS) has been quantified using the ratio of canyon-channel complex length over the length of the shortest straight line between both ends of the canyon-channel complexes (Brice, 1964). Canyon-channel complex sinuosity is defined as straight for CS <1.05, sinuous for 1.05<CS<1.3, and meandering for CS>1.3 (Brice, 1964).

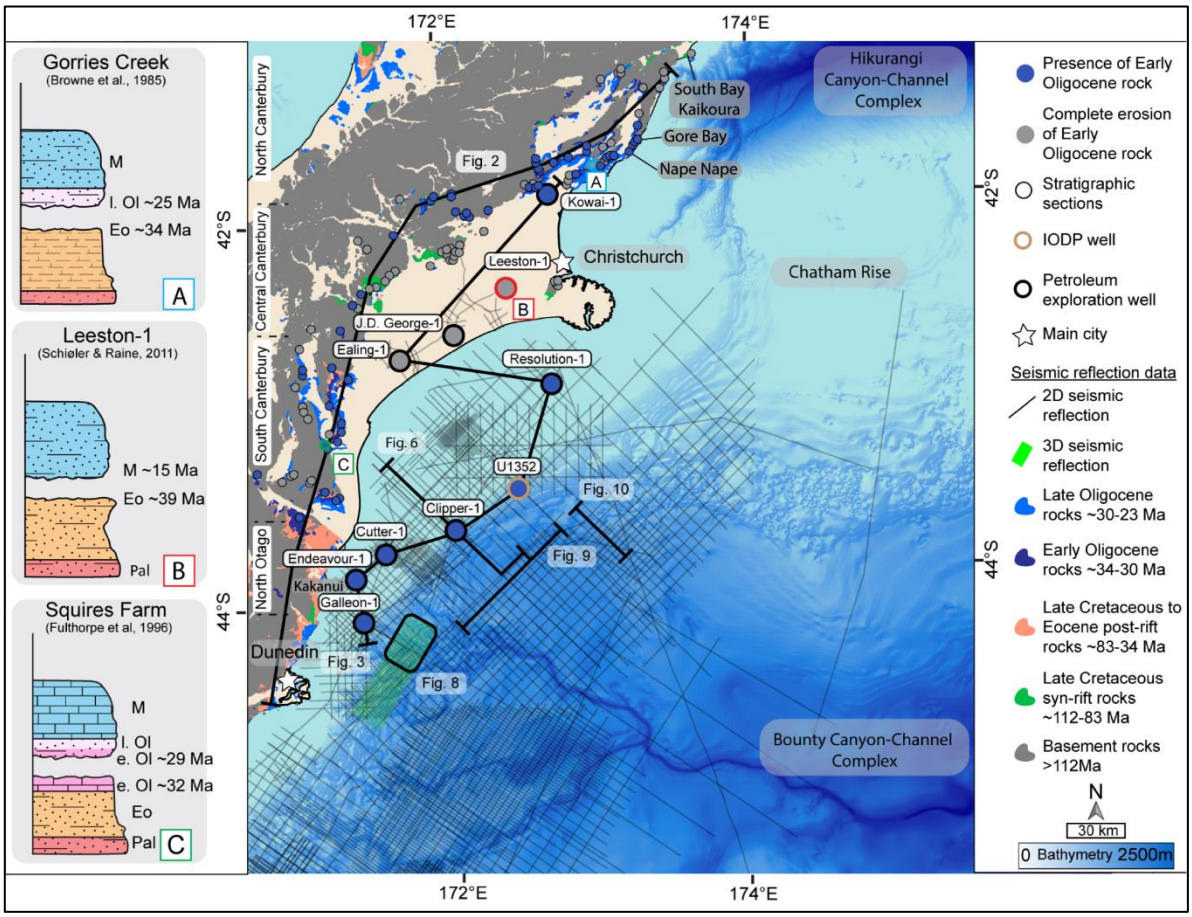

Figure 5.5 Basemap of the Canterbury Basin showing seismic reflection data used in this paper, together with the position of onshore measured sections and wells. Left of the basemap shows three schematic stratigraphic section of the Paleocene to Miocene succession from North, Central and South Canterbury. M: Miocene; l.Ol: Late Oligocene; e.Ol: Early Oligocene; Eo: Eocene; Pal: Paleocene.

The dataset contains six exploration wells where Late Eocene-Oligocene strata have been recognised, both onshore and offshore. In the five offshore wells available, Oligocene strata thicknesses range from 0-161 m. The thickness of Early Oligocene Amuri Limestone in wells ranges from 0-61 m.

The Eocene and Oligocene seismic packages are the focus of this study and have been tied to five offshore wells (Figs. 5.3, 5.5 and 5.6) using well biostratigraphic data from Schiøler and Raine (2011) and Fulthorpe et al. (2011). Oligocene strata are condensed being 0-161m thick in the offshore exploration wells. The top Oligocene horizon is typically indistinguishable from the top Eocene horizon in seismic reflection lines. The primary exception to this condensed section is within Oligocene erosive channels where erosional truncation is visible and part of the infill is inferred to be Oligocene in age (Fig. 5.6). Due to the condensed nature of the Oligocene section in the offshore, we have not attempted to systematically map the thickness of the Oligocene strata across the basin. Instead, the top Eocene reflector, which appears to record regionally extensive erosion, was gridded and the resulting map used to locate channels formed by Oligocene erosion.

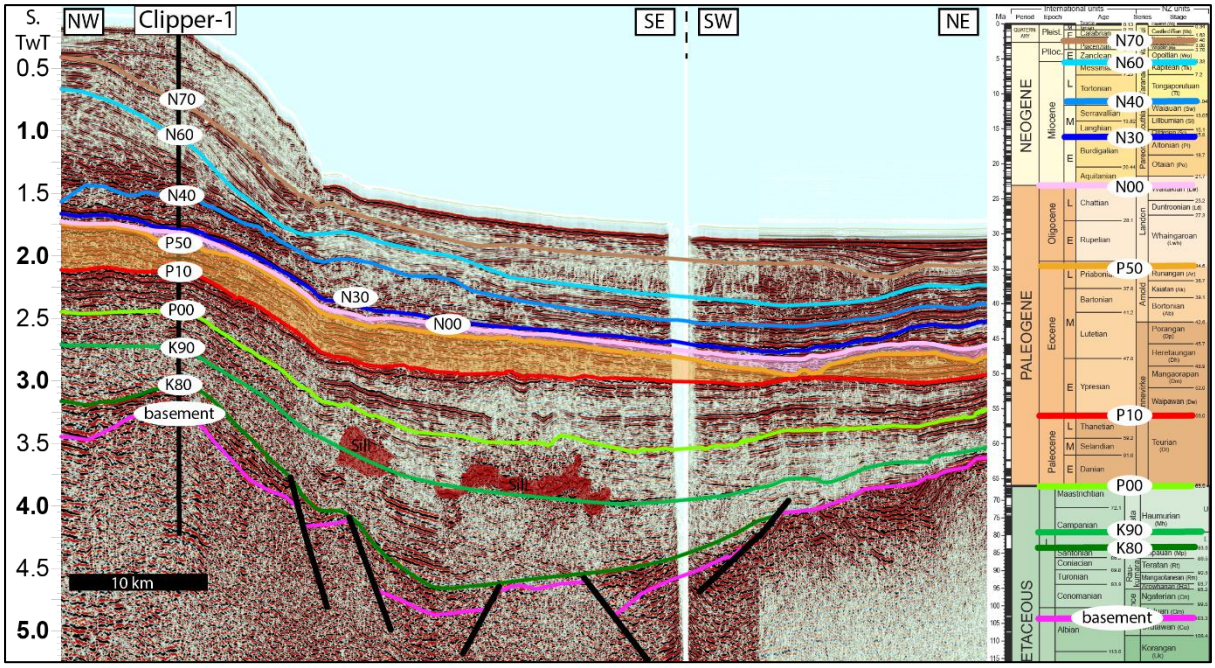

Figure 5.6 Composite seismic profile oriented NW-SE to SW-NE showing seismic horizon nomenclature (after Strogen and King, 2014) tied to Clipper-1 well. P50, the top Eocene horizon is affected by erosion, visible on the south-eastern end of the seismic profile. See Figure 5.5 for location.

To study channelization onshore we have primarily used over 110 stratigraphic sections measured by the New Zealand Geological Survey in the 1980s (Fig. 5.5, Browne and Field, 1985; Field and Browne, 1986; Andrew et al., 1987; Field and Browne, 1989), together with sections reviewed by Fulthorpe et al. (1996), Lever (2007), Fordyce (2009) and Fordyce and Richards (2016). Fifty-two stratigraphic sections show areas with complete erosion of Early Oligocene Amuri Limestone. The remaining outcrop sections are discontinuous and some display one or more erosion surfaces for the Late Eocene and Oligocene that are difficult to correlate between outcrops. The stratigraphic sections are plotted in map view and used to

determine the orientations, geometries and spatial distribution of stratigraphic sections that include no Oligocene strata.

5.4. Late Eocene to Oligocene Stratigraphy and Unconformities

5.4.1 Amuri Limestone

At many locations in the Canterbury Basin, latest Eocene and Early Oligocene sedimentation comprised the Amuri Limestone, which varies in thickness from 0 to 100m (Figs. 5.2, 5.3 and 5.4 - Browne and Field, 1985; Field and Browne, 1989). The Amuri Limestone is a coccolith and foraminifera-rich marl, or micrite to wackestone, containing outer neritic to bathyal microfauna which is characteristic of an outer shelf to slope depositional environment on an extensive carbonate platform (Fig. 5.4 - Lewis, 1992). The Amuri Limestone can be siliceous or contain siliceous nodules, such as in the North Canterbury and Marlborough regions where the age of the limestone spans from Late Cretaceous to Early Oligocene (Suggate et al., 1978). By the Early Oligocene, the micritic limestone reached the south-west and western edge of the Canterbury Basin (maximum transgressive phase). Towards the south-east, carbonate sedimentation was influenced by contemporaneous volcanic activity at Oamaru, where deposition occurred in a shallow water bryozoan platform (Fig. 5.2, Thompson, 2013; Thompson et al., 2014). Offshore wells record the presence of calcareous mudstone and micritic limestone of Eocene to Early Oligocene age (Fig. 5.3). Clipper-1 well, the easternmost offshore exploration well, drilled marls of Eocene to Oligocene age that indicate a deep mid bathyal (~800 m) to deep lower bathyal (~1500 m) paleo-water depths (Schiøler and Raine, 2011). The nearby IODP Site U1352 drill hole intersected Late Eocene Amuri Limestone at the base of the well (Fulthorpe et al., 2011; Marsaglia et al., 2017). Of the rocks studied here, only the latest Eocene Tengawai Coal Measures in the south-western onshore Canterbury Basin could be interpreted to indicate that the contemporaneous coast line was nearby during the Early Oligocene (Field and Browne, 1986, 1989).

Regionally these sedimentary thicknesses may increase towards the east (Lewis, 1992), however, over distances of 10s of kilometres the thicknesses can change by 50% or more. These local thickness variations partly reflect differential erosion of the Amuri Limestone during the Early Oligocene across the Canterbury Basin, which in places resulted in the complete removal of the Amuri Limestone (Figs. 5.2, 5.3, and 5.5).

5.4.2 Oligocene Erosions

Oligocene unconformities are common throughout the Canterbury Basin, where they can be concordant with enclosing beds or separate beds with a small angular discordance (<10 °) (Fig. 5.4C – Lewis, 1992; Lewis and Belliss, 1984). Numerous studies have attempted to reconcile multiple unconformities at a given location, although determining their age is generally difficult in the condensed Oligocene succession (Figs. 5.2, 5.3 and 5; Carter and

Landis, 1972; Findlay, 1980; Carter et al., 1982; Field 1985; Lewis, 1992; Fulthorpe et al., 1996; Lever 2007). These unconformities display a range of characteristics at different locations which include low-angle joints and karst features filled with overlying sediments, hardgrounds formed by *Thalassinoides* burrows and borings, and glauconitic, phosphatic, and limestone rounded clasts (Fig. 5.4 - Van der Lingen et al., 1978; Lewis, 1992; Lewis and Belliss, 1984).

Dating the age of these erosions is problematic. Typically, deep-water faunas (foraminifera) are used in New Zealand biostratigraphy, however, since the outcrop successions are shallow water environments, the planktic foraminiferas are not abundant. The more readily available benthic forams and macrofaunas are not particularly age diagnostic (for discussion see Morgans in Cooper et al, 2004). Some authors have attempted absolute dating using techniques such as strontium isotope geochronology (e.g., Fulthorpe et al., 1996), with the Amuri Limestone beneath dated at 32.4 Ma and the overlying Kokoamu Greensand dated at 29.0 Ma, at one locality (Squires Farm). These authors indicate a stratigraphic time gap of ~3.5 Myr at Squires Farm (Figs. 5.3 and 5.5A - Fulthorpe et al., 1996) and longer durations of erosion at other locations.

The origins and lateral extent of the erosion is also a point of debate (Vella, 1967; Loutit and Kennett, 1981; Lever, 2007), and possible explanations for erosion include sea-level fall, sediment starvation during a sea-level highstand, volcanism, tectonic uplift, and sea bottom currents (Gage, 1957; Sevon, 1969; Gage, 1970; Lewis and Belliss, 1984; McLennan and Bradshaw, 1984; Carter, 1985; Lewis, 1992; Carter et al., 2004; Lever, 2007; Thompson et al., 2014).

5.4.3 Late Oligocene Stratigraphy

Late Oligocene strata overlying the Amuri Limestone are dominated by bioturbated glauconitic sandstone overlain by, or interfingering with, inner to mid shelf bioclastic limestones (Figs. 5.2 and 5.4, Field and Browne, 1989). Locally, Late Oligocene to Early Miocene carbonaceous terrestrial sediments occur in the western Canterbury Basin and rest on basement rocks (Pocknall and Mildenhall, 1984; Field and Browne, 1986). However, the majority of sediments of this age exposed onshore were deposited at shelf depths (<200 m) and further east, offshore, at deeper water depth (200-2000 m) (Field and Browne, 1989; Schiøler and Raine, 2011). For example, in the onshore Canterbury Basin, calcareous sand was deposited in high-energy, cross bedded, shallow marine areas atop local highs. These high energy sands indicate eastward transport of sediment into the shallow water basin, with sporadic northward-directed storm-induced longshore drift currents breaching the Endeavour High (Ward and Lewis, 1975). In the offshore, the Clipper-1 and IODP U1352 drillholes intersected Late Oligocene bathyal greensand, marl, and limestone (Fig. 5.3 - Schiøler and Raine, 2011; Fulthorpe et al., 2011; Marsaglia et al., 2017).

5.5. Oligocene Drainage System

5.5.1 Canyons and Channels Offshore

The top Eocene reflector in offshore 2D and 3D seismic lines is locally affected by erosional truncations that display broad channel geometries, overlain by Late Oligocene or Early Miocene reflectors (Figs. 5.6, 5.7, 5.8, 5.9 and 10). Mapping individual channels shows a drainage pattern converging towards the south-east with erosional corridors (channel thalwegs) that on average trend E-W to NE-SW. Channels vary in width from 1 to 12 km, along-channel lengths of 15 to 90 km, and channel depths of 100 to 200 ms TwT (Fig. 5.7). All of the channels are observed on the top Eocene paleo-slope (See chapter 2 for further discussions). Towards the basin floor in the SE, erosion and channels cannot be mapped as they either do not exist or cannot be resolved, either because the seismic coverage or seismic resolution is not sufficiently high. We interpret these erosive geometries as canyon-channel complexes restricted to the shelf edge and slope (e.g., Talling, 1998).

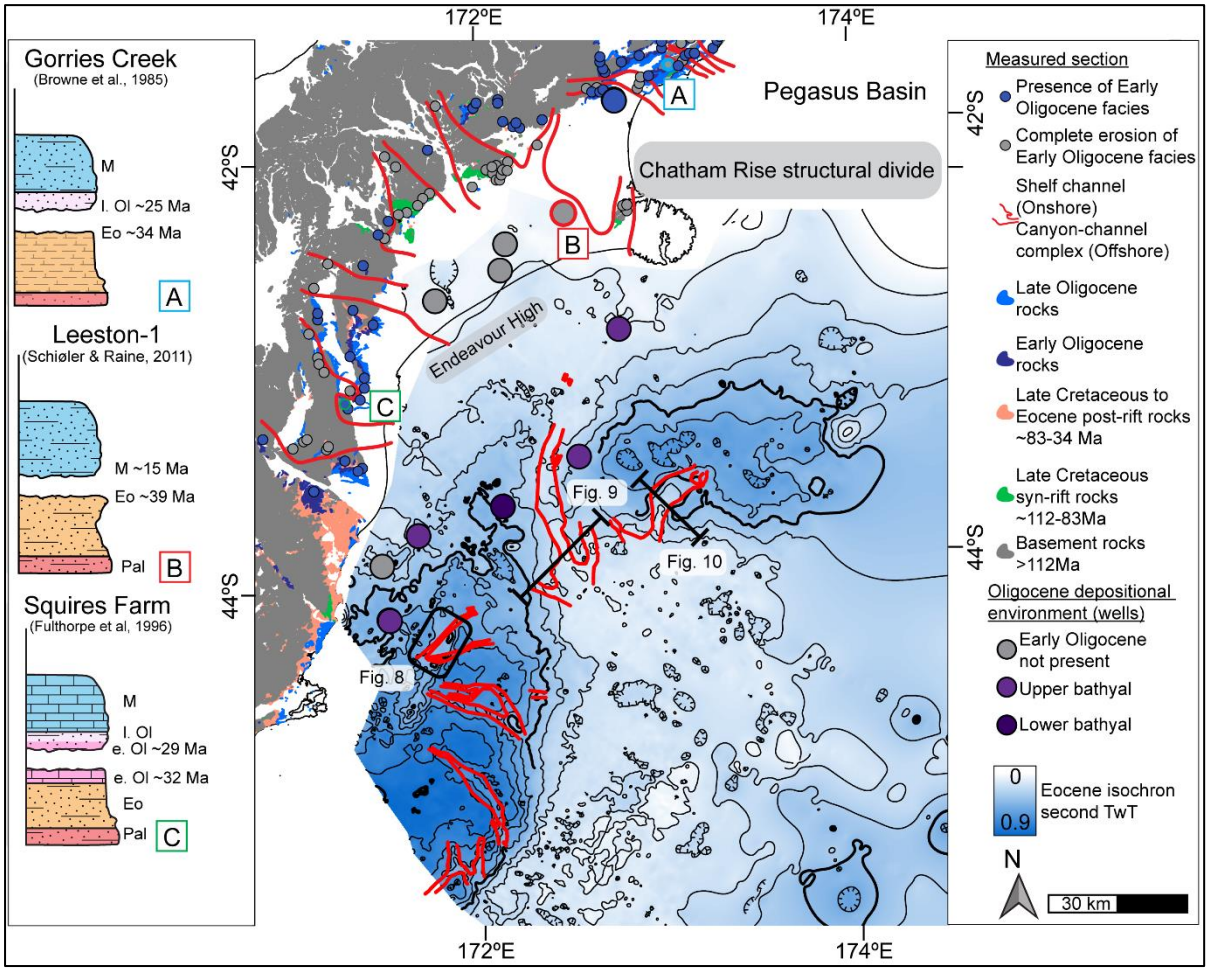

Figure 5.7 Onshore and offshore erosive channels (channel-canyon complexes) mapped using measured sections (onshore) and seismic reflection profiles (offshore). We show representative schematic measured sections and their location in relation to the channel features. M: Miocene; l.Ol: Late Oligocene; e.Ol: Early Oligocene; Eo: Eocene; Pal: Paleocene.

The largest canyon-channel complex is located at the intersection of the Endeavour High (Field and Browne, 1989) and the Chatham Rise, a long lived structural high inherited from the Permian to Early Cretaceous subduction phase (Wood et al., 1989; Laird and Bradshaw, 2004; Davy, 2014). This canyon-channel complex is oriented NW-SE and is >10 km wide, 90 km long, and 200 ms TwT deep (Fig. 5.7). Mapping of these canyon-channel complexes from 2D and 3D seismic data suggests straight to sinuous thalweg geometries (CS<1.3) (Fig. 5.8).

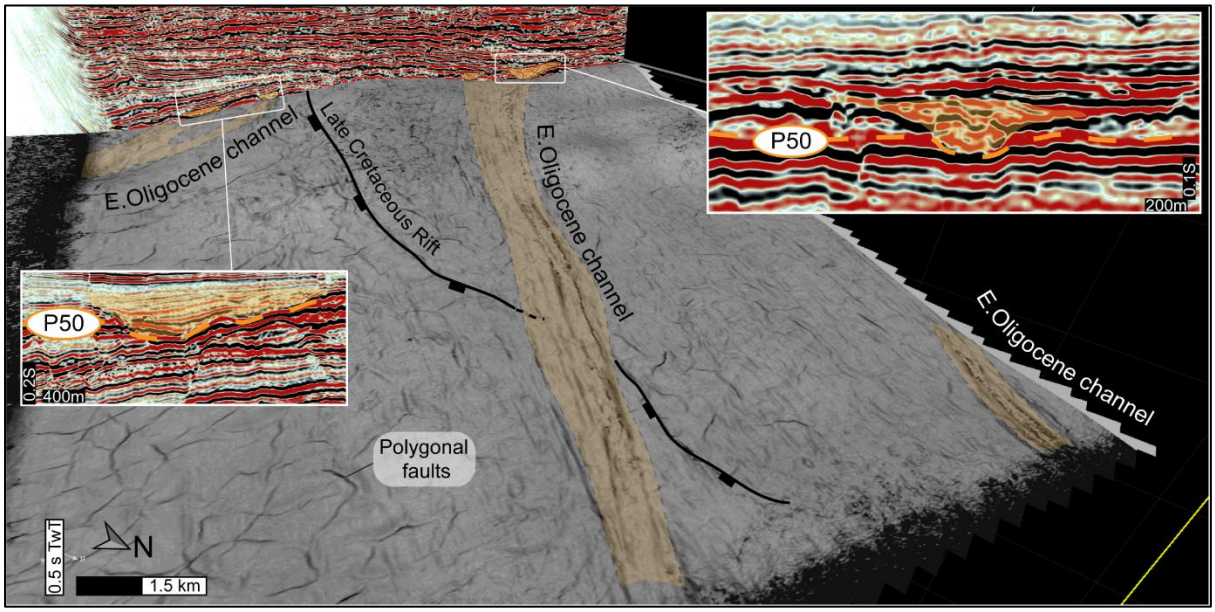

Figure 5.83D view of Early Oligocene erosive channels affecting the top Eocene horizon in the Waka 3D seismic survey. Top Eocene grid displays dip of maximum similarity seismic attribute. Note polygonal faults on the top Eocene horizon. See Figures 5.5 and 5.7 for location.

The geometry of the contact between reflectors overlying and underlying the erosional surface varies laterally from the centre to the margins of each canyon-channel complex (Figs. 5.9 and 5.10). Towards the centre of the canyon-channel complexes, where the erosion is at a maximum, reflectors overlying and underlying the erosion surface tend to be sub-parallel despite the presence of a hiatus in sedimentation. In the canyon-channel complex centres, erosion can produce complete removal of Eocene strata and incise into the top of the underlying Paleocene reflector package (Fig. 5.9). On the margins of erosive canyon-channel complexes, the contact is marked by erosional truncation of underlying reflectors and by onlap or draping of the overlying reflectors onto the channel margins (Figs. 5.9 and 5.10). The relationships on the margins of the channels produce small (<5°) angular discordances of reflectors across the erosional surface, which cuts into the upper part of Eocene reflectors. The last configuration is the case outside of the canyon-channel complexes, as at the Clipper-1 well, where reflectors above and below the top Eocene are parallel despite the presence of a hiatus in sedimentation (Fig. 5.3). In such scenario, the hiatus in sedimentation could reflect the formation of hardgrounds associated to low sedimentation rates and possible by-pass of sediments.

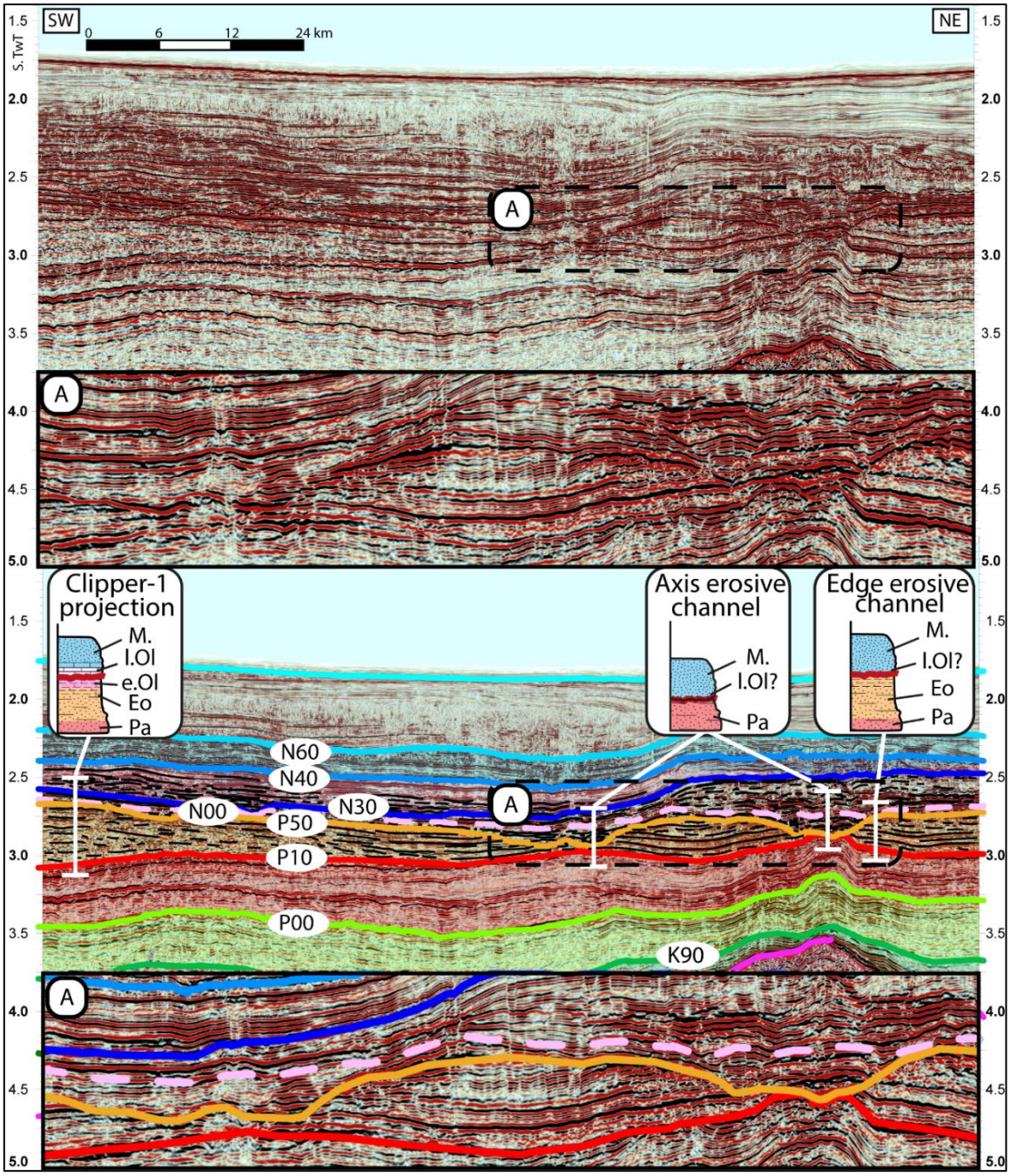

Figure 5.9 NE-SW seismic reflection profile showing erosional truncation of the top Eocene (P50) horizon. Schematic measured sections from the onshore are used as analogues of the potential stratigraphic succession in the axis, on the edge and away from the erosive channel. These erosive channels flowed from the Endeavour High. M: Miocene; l.Ol: Late Oligocene; e.Ol: Early Oligocene; Eo: Eocene; Pal: Paleocene. See Figures 5.5 and 5.7 for location.

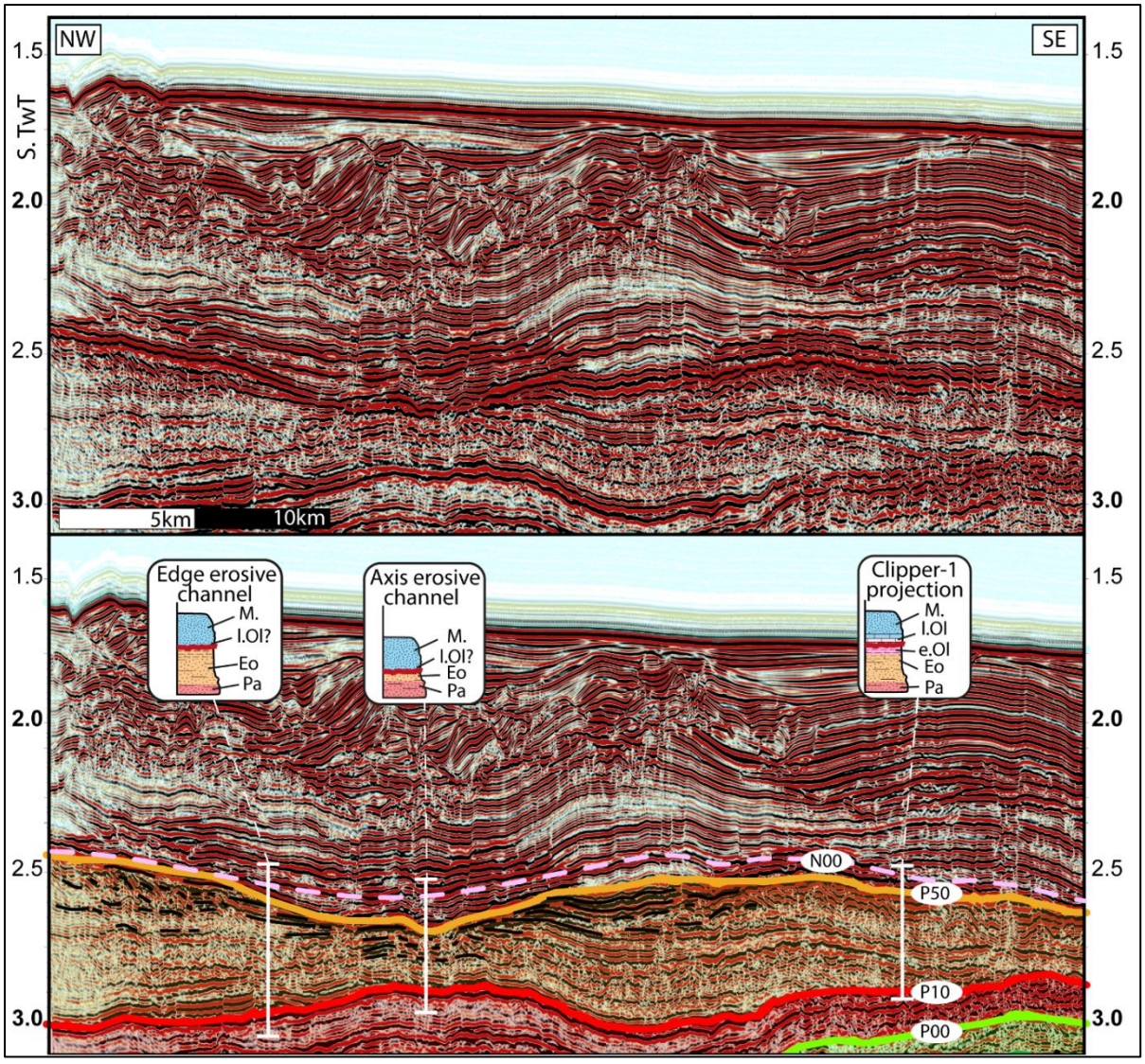

Figure 5.10 NE-SW seismic reflection profile showing erosional truncation of the top Eocene (P50) horizon. Representative schematic measured sections from the onshore are used as analogues of the potential stratigraphic succession in the axis, on the edge and away from the erosive channels. In this example, the erosive channels flowed from the Chatham Rise. M: Miocene; l.Ol: Late Oligocene; e.Ol: Early Oligocene; Eo: Eocene; Pal: Paleocene. See Figures 5.5 and 5.7 for location.

Canyon-channel complexes mapped in the offshore Canterbury Basin display a dendritic planform bifurcating towards the NW (Fig. 5.7). These canyon-channel complexes are primarily developed on the paleo-slope of the sedimentary basin and can be interpreted to have been fed by a sediment source from topographic highs situated west and north of the mapped area. The mapped canyon-channel complexes flowed south from the southern margin of the Chatham Rise, which suggests that the Chatham Rise was a bathymetric high in the Oligocene along with a western hinterland (Fig. 5.7). The Chatham Rise topographic high was long-lived and originated during Mesozoic subduction that ceased at about 105 Ma (e.g., Davy, 2014); it remains a positive sea floor high today. By contrast, in deep water regions to the SE, canyon-channel complexes are not observed and are interpreted to either not be present or to be subdued features on the basin floor with reduced incision based on the available seismic data.

5.5.2 Channels Onshore

In 52 of 110 measured outcrop sections, the Early Oligocene Amuri Limestone is absent with the Late Oligocene or younger strata resting either unconformably or disconformably on Eocene sediments (Figs. 5.5 and 5.7). In such cases (e.g., Gorries Creek and Leeston-1 well), the hiatus ranges from 9 to 23 Myr (Figs. 5.5 and 5.7) with Eocene strata overlain directly by strata as young as Middle Miocene. In the remaining 58 sections, the thickness of the Amuri Limestone varies between 5 to 140 m.

While it is possible that the sedimentary hiatus observed onshore could represent a period of non-deposition, the comparable age of canyon-channel complexes offshore is consistent with the notion that the unconformity at the top of the Amuri Limestone onshore formed due to differential erosion. To test this hypothesis, we have mapped the geographic distribution of stratigraphic sections where the Amuri Limestone has been completely removed (Fig. 5.7). Although these outcrop data are sparse and discontinuous, they appear to define a number of erosional corridors about 5 to 40 km wide which trend to the SE toward the offshore Canterbury Basin. The heterogeneous erosion and inferred erosive corridors could suggest the development of channels cut on the shelf, similar to shelf channels described by Lewis (1982) from outcrops in North Canterbury. The detailed geometries and dimensions of these shelf channels cannot be determined from the available outcrop data as the stratigraphic sections provide one-dimensional sample lines through the strata. Typically, when stratigraphic sections have spacing of >10s of km (i.e., Canterbury Basin), they are unable to directly constrain the lateral geometries of the erosional event. The age of strata infilling the channels suggests that, in some cases, erosion commenced in the Early Oligocene and continued until the Early Miocene (Fig. 5.7). The synchronicity and similar trends of the proposed shelf channels onshore and canyon-channel complexes mapped in the offshore suggest that they may form part of the same connected erosive system. In such a system, the onshore Canterbury Basin represents the more proximal part of the drainage system and the offshore region the more distal settings towards the slope and basin floor.

5.6. Early Oligocene Paleogeography

During the Oligocene, at the time of maximum inundation of Zealandia, there is debate concerning the presence or absence of emergent area forming an island archipelago (Landis et al., 2008). We argue that land in the vicinity of the present-day central South Island may have been the source of sediment feeding the Oligocene drainage system in the Canterbury Basin. Onshore, the stratigraphy during the Early Oligocene was dominated by the Amuri Limestone which was deposited in mid-shelf to upper-slope depths (50-600 m) (Fig. 5.2 - Field and Browne, 1989). Partial sub-aerial exposure of the Amuri Limestone is indicated by spatially sporadic karst structures, although most of the onshore basin appears to have remained below sea level and in shallow water for much of the Oligocene (Van der Lingen et al., 1978; Lewis, 1992; Lewis and Belliss, 1984). Isolated outcrops of Early Oligocene non-marine, shallow marine glauconitic and quartzose sandstone (e.g., the Tengawai Coal Measures, Nessing Greensand, Karetu and Coleridge formations) occur in the central Canterbury region indicating

land towards the west (Browne and Field, 1985; Field and Browne, 1986; Andrews et al., 1987; Congdon 2003). The offshore Canterbury Basin comprised a slope and basin floor defined by shelf-edge clinoforms that formed during the Eocene and persisted into the Oligocene (Fig. 5.11A – See chapter 2 for further discussions). The Clipper-1 well, for example, indicates sedimentation in an upper to lower bathyal setting (water depths 800-1500 m) associated with a condensed Oligocene succession (Schiøler and Raine, 2011).

The Canterbury Basin formed an amphitheatre shape during the Early Oligocene, being bounded by the Chatham Rise to the north, and by potential land to the west and in the Otago region to the southwest (Fig. 5.11B). The Chatham Rise initially formed in response to Permian-Early Cretaceous subduction and persists today (Field and Browne, 1989; Wood and Herzer, 1993; Laird and Bradshaw, 2004). The Early Oligocene paleo-slope dipped southwards in the vicinity of the Chatham Rise and towards the southeast in the western Canterbury Basin, controlling the flow directions of shelf channels and canyon-channel systems. The influence of the Chatham Rise in the Early Oligocene may have extended onshore where a structural divide separated south-east and north-east flowing corridors of erosion, in central and northern Canterbury Basin (Fig. 5.11B). The main offshore canyon-channel complex formed along the line of intersection between the NE-SW trending Endeavour High and the E-W Chatham Rise, forming a conduit for sediment to flow into offshore parts of the basin (Fig. 5.11B).

We propose a model in which shelf channels transported sediment towards the east and south of the Canterbury Basin, merging into bathyal canyons-channel complexes that were incising into the slope further offshore and ultimately onto basin floor settings in the extreme southeast. These channels/canyons permitted sedimentation to by-pass the shelf where it resulted in a condensed Oligocene interval, with development of hard grounds and multiple unconformities. The shelf channels in the onshore Canterbury Basin change in trend from N-S to NW-SE and EW respectively in north, central and south Canterbury Basin (Fig. 5.11B). This change in orientation is interpreted to reflect the presence of the Chatham Rise and potential landmass west of the Canterbury Basin and in the Otago region up dip from the channels. Deepening of the Canterbury Basin to the east and south is consistent with the flow of shelf channels and canyons-channel complexes towards the basin. The canyon-channel complexes cannot be traced from the slope onto the contemporaneous basin floor and there is presently no clear evidence for the formation of basin floor fans in the distal portions at canyon terminations. This may be a result of sediment transported further east beyond the study area (and our available seismic coverage), or if fans were deposited, they were subsequently eroded or reworked by oceanic bottom currents similar to those described by Nelson and Cook (2001) and Carter et al. (2004) (Fig. 5.11B). An alternative is that the canyon-channel complexes were less incised in deep water settings and are therefore not resolved in the seismic data.

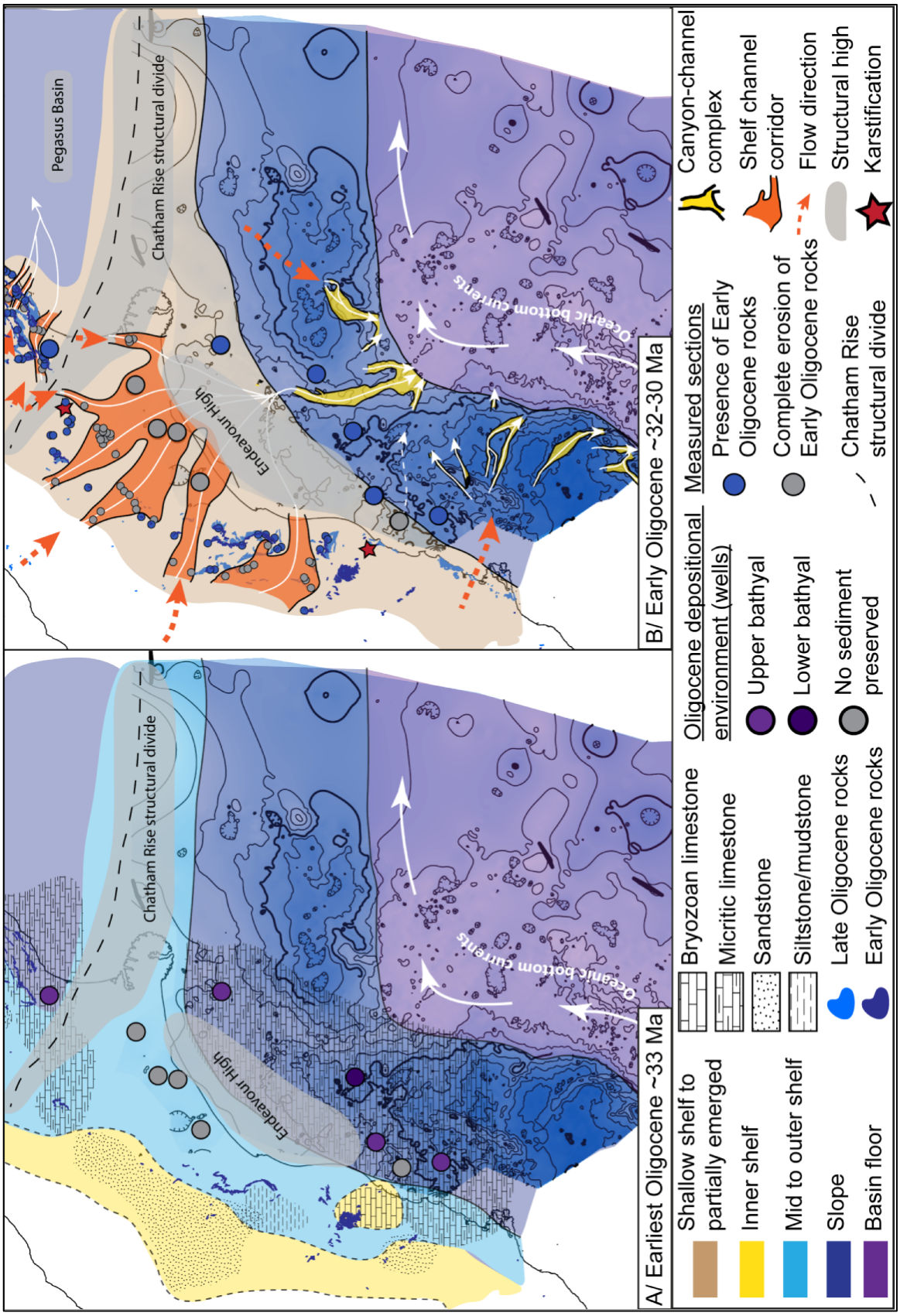

Figure 5.11 Paleogeographic reconstruction of (A) the earliest Oligocene Canterbury Basin showing the maximum inundation of the basin, depositional environment and the area potentially affected by the oceanic bottom currents. (B) Paleogeography during the Early Oligocene ~32 Ma at the time of the sea-level fall that generated a widespread drainage system across the Canterbury Basin. Onshore paleogeography from Field and Browne (1989).

5.7. Discussion

5.7.1 Early Oligocene Erosion

The unconformities of the Oligocene Canterbury Basin, the so-called Marshall Paraconformity, are complex and, as currently defined, were formed in multiple erosional events at different times during the Oligocene (Carter and Landis, 1972; Carter, 1977; Findlay, 1980; Lewis and Belliss, 1984; Gage, 1988; Lever, 2007; Landis et al., 2008). In the Canterbury Basin, the hiatus in sedimentation represented by the unconformity(s) may span a period of as little as ~3.5 Myr to as much as ~15 Myr, with maximum submergence in the basin happening prior to unconformity formation (Figs. 5.4 and 5.5; Fulthorpe et al., 1996; Field and Browne, 1989; Lever 2007; Schiøler and Raine, 2011).

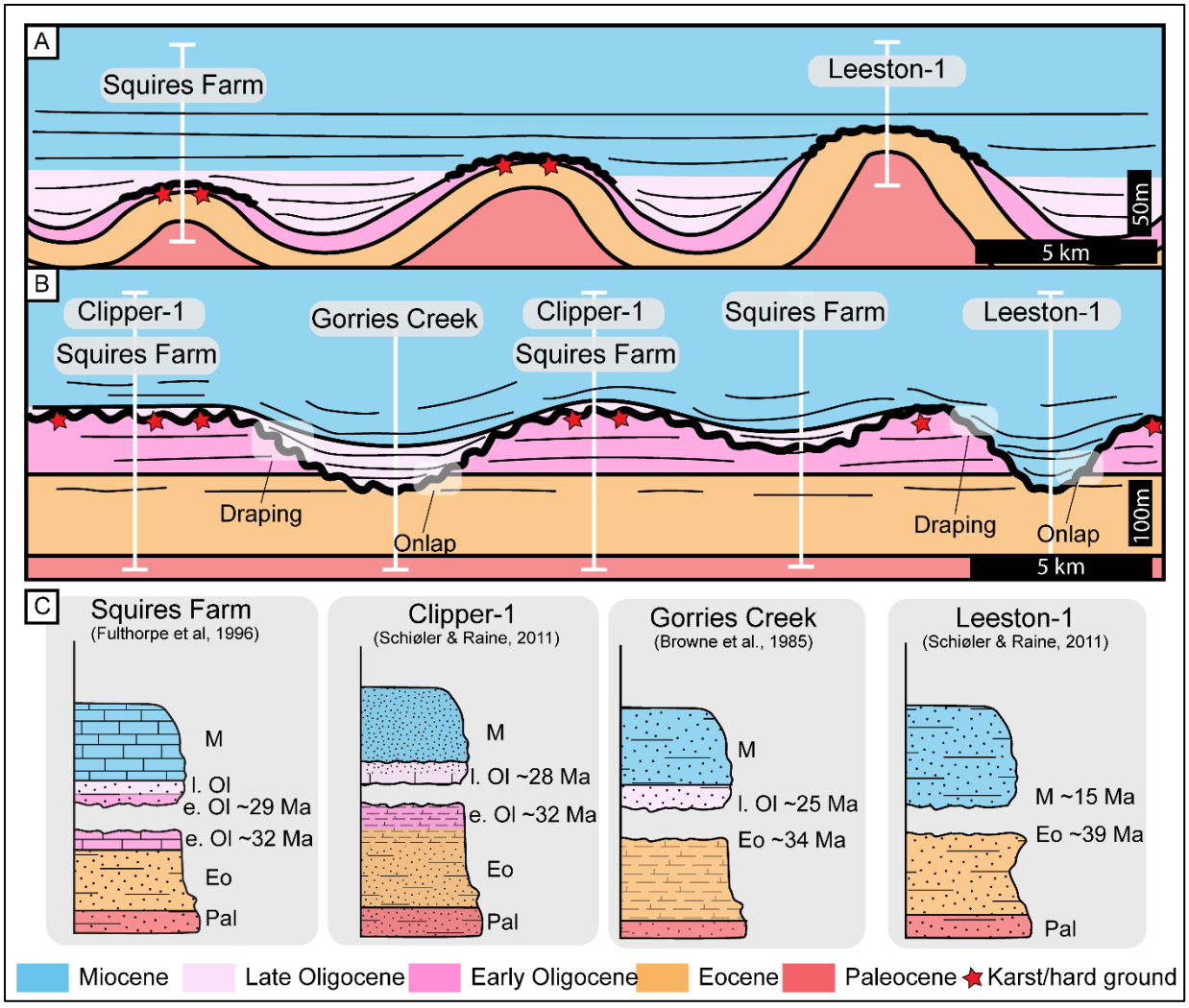

Figure 5.12 Cartoon showing two models for the development of erosion and karstification affecting the top of the Early Oligocene strata: (A) Folding model (Lewis, 1992) and (B) channel model (this study). (C) Shows four schematic stratigraphic sections from the Canterbury Basin with various hiatus surfaces used to illustrate the correlation between their position in model (A) and (B) and the hiatus duration. M: Miocene; l.Ol: Late Oligocene; e.Ol: Early Oligocene; Eo: Eocene; Pal: Paleocene.

The present study addresses and resolves some aspects of the complexity in interpreting unconformities in the Canterbury Basin Oligocene strata. We suggest that some of the contrasting debates that have been proffered for this erosional period could be explained by regional channelization truncating the Oligocene succession. This alternative explanation is based largely on our use and interpretation of an extensive 2D seismic dataset from the offshore region. Neither seismic data nor the offshore portion of the basin has hitherto been considered by previous workers in regard to this question. Together with the use of existing outcrop measured sections and well data, the drainage system mapped here is interpreted to have formed regional corridors of erosion that extended across the Early Oligocene shelf and slope (Fig. 5.11B). Outside each channel, the stratigraphy can be concordant across the unconformity with a ~3 Myr hiatus in sedimentation. Along channel axes, the beds are also parallel but with a larger time gap than outside the channels, whereas the channel margins either display onlap or draping relationships across the unconformity and a hiatus of intermediate duration (Fig. 5.12B).

5.7.2 Causes of Early Oligocene Erosion

We propose that the formation of shelf edge channels and canyon-channel complexes, incising the calcareous shelf and the slope of the Canterbury Basin respectively, was triggered by a sea level fall, which commenced most likely between 29 and 32 Ma. Dating of the oldest strata deposited in the erosive drainage system, indicates that some of these channels remained active until the Early Miocene, with the associated hiatus in sedimentation spanning up to ~15 Myr in some areas during the Oligocene and Early Miocene (Browne and Field, 1985; Field and Browne, 1986; Andrew et al., 1987; Field and Browne, 1989; Schiøler and Raine, 2011). Erosive channels and canyons incising into the shelf and slope of a basin commonly develop when the erosion profile is re-equilibrating to compensate for a fall in sea level, controlled either by eustacy or tectonic uplift (e.g., Schumm, 1993). In the Canterbury Basin during the Oligocene, both mechanisms have been proposed to account for erosion (Lever, 2007). Paleo-water depth, estimated from foraminifera, indicate shallowing of water depths by up to 400 m during the Oligocene (Field and Browne, 1989). Lever (2007) used the eustatic curve from Abreu and Anderson (1998), after Haq et al. (1987) and Mitchum et al. (1993), to suggest a ~100 m sea level fall during the Early Oligocene culminating at between 29 and 28.5 Ma (Fig 2). Changes in water depth are also suggested onshore by the development of paleo-karst topography on the top of the Amuri Limestone in some outcrops, which are interpreted to have formed by sub-aerial exposure of the limestone (Fig. 5.11B - Van der Lingen et al., 1978; Lewis, 1992), but the precise timing of karstification is not known (Carter, 1985; Gage, 1988). Karstification and erosion has previously been attributed to gentle tectonic folding (Fig. 5.12A; e.g., with limb dips of < 5°) of pre-Oligocene strata (e.g., Nicol, 1992; Lewis, 1992). Tectonism at this time has also been inferred from sand diapirs in the basin at various locations (e.g., Lewis 1973; Lewis et al., 1979).

We propose a channel model to account for the differential erosion of the Amuri Limestone and formation of karst and hardground horizons. In our model, karst and hardground horizons are primarily formed on elevated topography and on elevated bathymetry outside the channels. Maximum erosion, which in some cases resulted in complete removal of the Amuri Limestone,

occurred within the channels (Fig. 5.12B). In addition to being consistent with the offshore seismic data, the channel model is favoured over the alternative folding model of Lewis (1992) because it results in spatial separation of karstification and erosion, and promotes the preservation of karst. In the folding model, karst and maximum erosion are coincident with structural highs and areas of karst would be expected to be removed or diminished with erosion of the Amuri Limestone (Fig. 5.12A).

In the offshore Canterbury Basin, oceanic bottom currents could have triggered erosion and reworking of sediments (e.g., Carter et al., 2004; Fulthorpe et al., 2011). These currents may have resulted in the non-preservation of deep-water fans, downdip of the channel-canyon complexes. However, oceanic currents are unlikely to account for the formation of the channel-canyon complexes mapped offshore as these complexes developed perpendicular to the slope, while oceanic bottom currents were primarily flowing sub-parallel to the slope and its toe.

Eustatic sea-level changes have been proposed for the Oligocene in New Zealand by others and could have resulted in changes in the patterns of sedimentation and erosion (e.g., Loutit and Kennet, 1981; Lever, 2007). These changes may have produced fluctuation in sea-level up to ~100 m on time scales of 10s to 100s of thousands of years (e.g., Haq et al., 1987; Mitchum et al., 1993; Abreu and Anderson, 1998). However, foraminifera and sedimentary facies data in the Canterbury Basin suggest changes in sea level of up to hundreds of metres, associated with channelization, that persisted for millions of years (e.g., Fulthorpe et al., 1996; Lever, 2007; Schiøler and Raine, 2011). The temporal and spatial scales of these changes are larger than would be expected for eustatic processes alone and we suggest that regional tectonic uplift may have also played an important role in the formation of both shelf channels and canyon-channel complexes. The channel orientations and their eastward gradients, together with Oligocene sedimentary facies observed in the basin, all suggest that the axis of uplift was primarily west of the Canterbury Basin (Fig. 5.13 - e.g., Gage, 1970; McLennan and Bradshaw 1984; Field and Browne, 1989; Lever, 2007; Thompson et al., 2014; Fordyce and Richards, 2016; this study).

Clues for the location of this Oligocene uplift and topography are provided by data from the Taranaki Basin along its eastern margin. In the Taranaki Basin, western North Island (north of the Alpine Fault), Early Oligocene uplift and erosion has been recorded by proximal fan complexes, imaged by seismic reflection lines and intersected by wells (Fig. 5.13 - King and Thrasher, 1996; Higgs et al., 2004; Strogen et al., 2014; Higgs and King, 2018; Strogen et al., 2019). These fans were shed from the uplifting hanging wall of the Taranaki Fault System, which may also have produced an Early Oligocene regional unconformity, extending southwards into the Marlborough Sounds in the northern South Island (Nicol and Campbell, 1990; Begg et al., 2000). In the Taranaki Basin, Early Oligocene uplift has been attributed to thrusting on the Taranaki Fault System (Holt and Stern, 1994; King and Thrasher, 1996; Stagpoole and Nicol, 2008; Strogen et al., 2014; Reilly et al., 2015; Strogen et al., 2019). This tectonic contraction is supported by folding of Late Eocene strata in the Reinga-Northland Basin (Bache et al., 2012) and may have impacted sedimentation in other parts of northern Zealandia. West of the Taranaki Fault System, deepening of the basin occurred and is indicated by turbidite deposits in the footwall of the fault (Strogen et al., 2014). In the distal Taranaki and New Caledonia basins, Eocene to Early Oligocene anomalous subsidence was recorded (Baur et al., 2014). Similarly, Southland basins west from the Otago region, mainly comprise Early Oligocene turbidite consistent with deep-water at this time (Landis et al., 2008). This

uplift could have covered much of the western North Island and produced deeply incised topography, similar to buried topography beneath the Wanganui Basin (e.g., valleys 1000-2000 m deep) that formed the proto-Marlborough Sounds (Nicol, 2011).

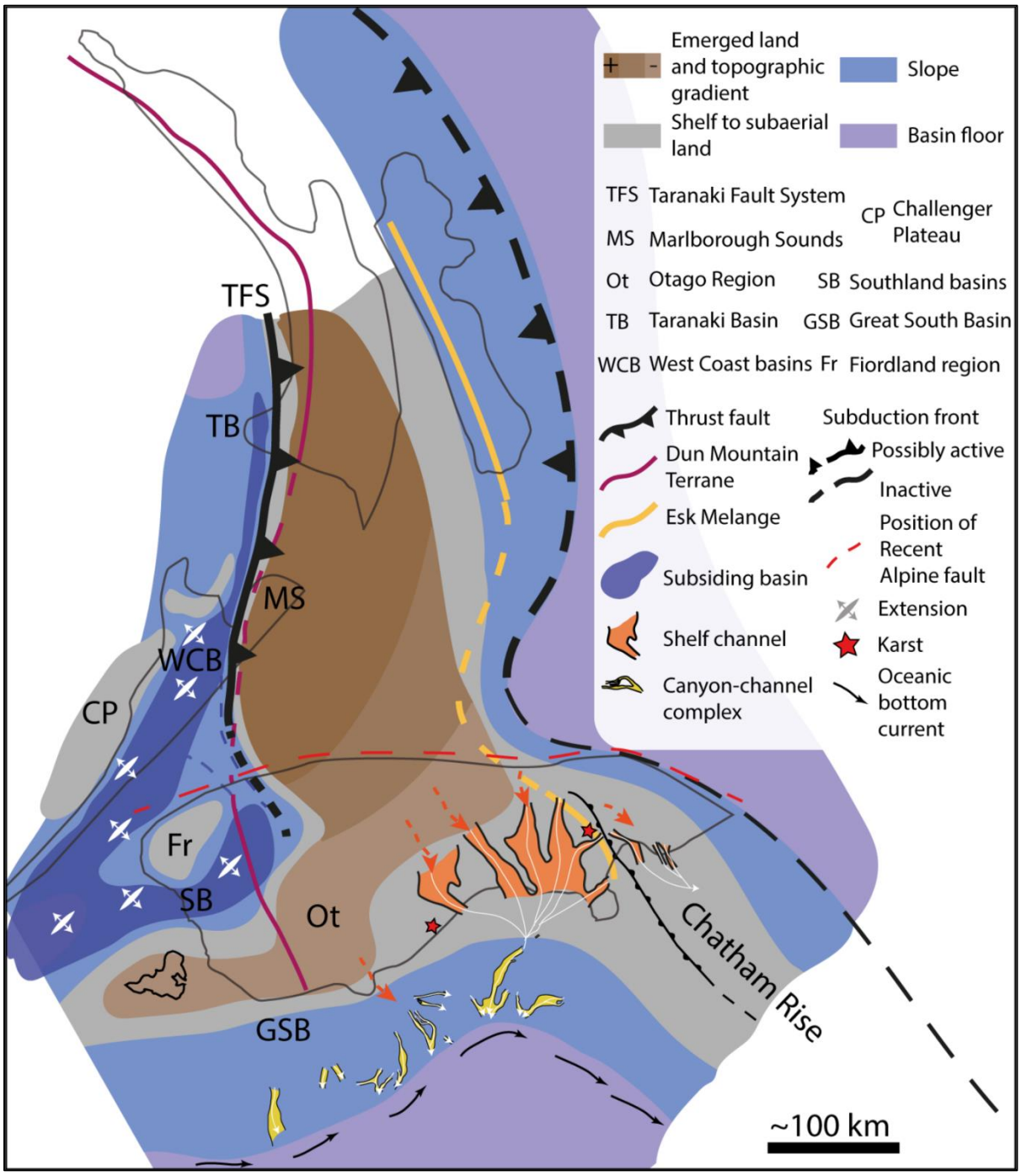

Figure 5.13 Geodynamic and paleogeographic model of Zealandia during the Early Oligocene showing the location of the landmass and the influence of uplift due to tectonic movements in the western North Island on the increase of slope gradient west of the Canterbury Basin leading to the formation of erosive channels. The extent of landmass has been mapped using Landis et al. (2008) and Strogen et al. (2014) adapted to the results of this study. Canyon-channel complexes from the Great South Basin have been interpreted using the Eocene isochron map from Sahoo and Bland (2017).

The region of maximum Early Oligocene uplift appears to have extended to the Wairau/Alpine Fault and, if present, the land to the south of the fault has most likely been displaced ~480 km to the southwest (Fig. 5.13 - e.g., Korsch and Wellman, 1988; Sutherland, 1995). At present day, this Early Oligocene region of maximum uplift south of the Wairau/Alpine fault would correspond to the area west and south-west of the Canterbury Basin (Fig. 5.13). Early Oligocene strata in western Otago supports the notion that this area was either a near-shore or terrestrial environment, thus it may represent the southern extension of uplift postulated for the Wairau/Alpine Fault region (Fig. 5.13). Collectively, the western North Island – Marlborough Sounds – western Otago "high" may have been the source for eastward flowing Early Oligocene channels into the Canterbury Basin.

5.7.3 Longevity of Drainage Systems

The age of the New Zealand landscape is variable and dependent on the rates of surface process which are, in turn, influenced by a range of factors including the age and rate of tectonic deformation, climate, and rock strength (e.g., Newnham et al., 1999; Nicol et al., 2017). The mountain ranges that form the spine of New Zealand are thought by some to be primarily Quaternary in age (e.g., Ghani, 1978; Tippett and Kamp, 1993; Shane et al., 1996). By contrast, in areas characterised by low or no deformation (e.g., Marlborough Sounds, Northwest Nelson, Westland, parts of Otago and eastern Canterbury), the main landscape elements could be Late Miocene (~5-10 Ma) (e.g., Begg et al., 2000; Landis et al., 2008; Nicol, 2011; Craw et al., 2015). In the Canterbury Basin, for example, the topography of Banks Peninsula formed between ~6 and 12 Ma due to a series of volcanic eruptions, and the broad morphology of the volcanoes is still discernible in the landscape (e.g. Hampton et al., 2012).

An older antiquity of the Canterbury landscape is suggested by our interpretation of offshore seismic data and analysis of Oligocene and present-day channel systems. Figure 5.14 compares the locations, trends, and flow directions of Early Oligocene canyon-channel complex drainage and contemporary canyon-channel complex drainage. This figure shows that the approximate locations, flow directions, and geometries of these morphological elements have not changed significantly since ~30 Ma. Both contemporary and Oligocene channel systems form a radial pattern that converges offshore in the direction of flow. The co-location of ancient and modern drainage channels occurs at the intersection of the Chatham Rise and Endeavour High. During the Oligocene, drainage along this intersection flowed SE, similar to the present-day Bounty Channel system. Similarly, on the northern margin of the Chatham Rise, Oligocene channels flowed in a direction similar to present-day channels flowing toward the modern Hikurangi Channel system. Onshore there is insufficient data to compare the location of ancient versus modern drainage channels and valleys, but it seems clear that the paleoflow direction and first-order architecture of the drainage system have not changed significantly. Such an antecedent drainage over ~30 Myr could be consistent with the low rates of tectonic deformation in the offshore Canterbury Basin over the Neogene (e.g., Tippett and Kamp, 1993) and could reflect the apparently stable locations and trends of the Oligocene topographic high and the contemporary Southern Alps. The possible stability of the landscape in the eastern South Island as a whole though is surprising and requires further investigation

given the intense Neogene tectonic deformation in this area that did not seem to have modify the primary trend of the drainage system.

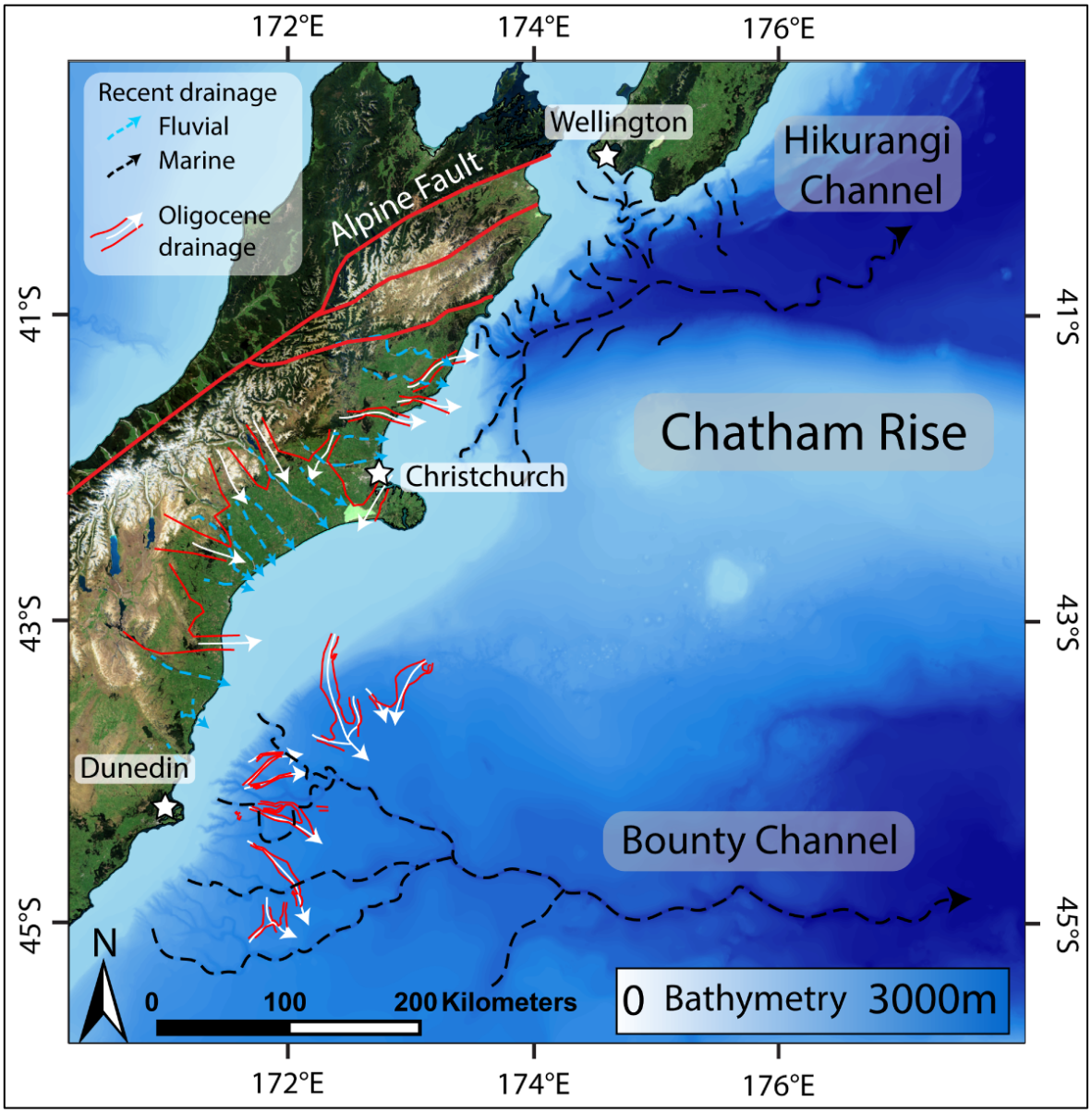

Figure 5.14 Comparison of the Early Oligocene and present-day drainage patterns both onshore and offshore Canterbury basin showing the similarity in trends and locations of these features over time. Satellite image data sourced from LINZ Data Service, Bathymetric data licensed under NIWA Open Data.

5.8. Conclusion

Our study of the offshore Canterbury Basin provides new observations of Early Oligocene erosion through new seismic reflection mapping integrated with drill-hole data and outcrop measured sections for the study region. We have mapped seismic horizons which show that the top Eocene reflector in offshore 2D and 3D seismic data is locally affected by erosional truncations that display channel geometries, and in turn, are overlain by Late Oligocene or Early Miocene reflectors. Mapping of these channels shows a drainage pattern converging

towards the south-east with erosional corridors that, on average, trend E-W to NW-SE, vary in width from 1 to 12 km, are 15 to 90 km long in a down-axis orientation, and are 100 to 200 ms deep (TWT) in the area of the Eocene slope. We interpret these erosive features as canyon-channel complexes. Onshore, we have mapped the geographic distribution of the Amuri Limestone and show regions where it has been completely removed. Although outcrop data are sparse and discontinuous, they appear to define a number of erosional corridors about 5 to 40 km wide which also trend in a NW-SE orientation. We interpret these as erosional shelf channels.

The synchronicity, similar trends, and comparable morphology of the shelf-channels appear to match with the canyon-channel complexes developed in the contemporaneous offshore shelf and suggest they may form part of the same erosive system. These new observations allowed us to propose a paleogeographic map of the earliest Oligocene during a period of major sea level fall. These data, together with data in other regions, provide insights into the processes forming the paleogeography. These insights include:

- The Canterbury Basin formed an amphitheatre shape during the Early Oligocene, being bounded by the Chatham Rise to the north, and by land to the West and in the Otago region to the southwest.
- We propose a model in which erosive channels onshore flow towards the east and south, before merging into canyons that were incising into the slope offshore.
- The present study and our proposed model of a canyon-channel complex provides clarity to how complex Oligocene erosion and some unconformity surfaces formed in the region.
- We propose that a sea level fall at ~ 32-29 Ma triggered erosion of channels incising the calcareous shelf and slope of the Canterbury Basin during the Early Oligocene.
- We suggest that regional tectonic uplift may have played an important role in the sea level fall. Indeed, the temporal (millions vs. hundreds of thousands of years) and spatial scales of the erosive channel-canyon complexes are larger than would be expected for eustatic processes.
- The channel orientations and their eastward gradients, together with Oligocene sedimentary facies observed in outcrop, all suggest that the axis of uplift was primarily west of the Canterbury Basin.
- Tectonic movements collectively affecting the western North Island – Marlborough Sounds – western Otago “high” may have been the source of eastward flowing Early Oligocene channels in the Canterbury Basin.

Both contemporary and Oligocene channel systems form an onshore radial pattern which converges offshore in the direction of flow. In the central, south Canterbury, and northern Otago regions, present-day rivers flow towards the east and the Bounty Trough, similar to the Early Oligocene drainage defined here. In the northern Canterbury region, present-day rivers converge towards the Hikurangi Canyon and the Pegasus Basin, similar to the Oligocene drainage of the northern Canterbury region that flowed along the northern limb of the Chatham Rise. The possible stability of drainage systems in the eastern South Island is a surprising conclusion given the Late Cenozoic tectonic deformation in this area.

5. Acknowledgments

We would like to acknowledge Ewan Fordyce and Marcus Richards from the University of Otago for the organisation of field trips in the south Canterbury and North Otago region to examine several Oligocene sections and ensuing discussions that helped build aspects of this paper. We acknowledge the funding support provided by the Mason Trust from the Department of Geological Sciences, University of Canterbury. GHB acknowledges funding from the NZ government (MBIE) through Strategic Funding to GNS Science and the Sedimentary Basin Research programme.

V. References

ABREU, V.S. & ANDERSON, J.B. (1998) Glacial Eustasy During the Cenozoic: Sequence Stratigraphic Implications. AAPG bulletin, 82, 1385-1400 pp.

ADAMS, J. (1980) Contemporary Uplift and Erosion of the Southern Alps, New Zealand. Geological Society of America Bulletin, 91, 1-114 pp.

ANDREW, P.B., FIELD, B.D., BROWNE, G.H., MCLENNAN, J.M. (1987) Lithostratigraphic Nomenclature for the Upper Cretaceous and Tertiary Sequence of Central Canterbury, New Zealand. New Zealand Geological Survey Record, 24, 40 p.

BACHE, F., SUTHERLAND, R., STAGPOOLE, V., HERZER, R., COLLOT, J. & ROUILLARD, P. (2012) Stratigraphy of the Southern Norfolk Ridge and the Reinga Basin: A Record of Initiation of Tonga–Kermadec–Northland Subduction in the Southwest Pacific. Earth and Planetary Science Letters, 321, 41-53 pp.

BARNES, P.M., GHISETTI, F.C. & GORMAN, A.R. (2016) New Insights into the Tectonic Inversion of North Canterbury and the Regional Structural Context of the 2010–2011 Canterbury Earthquake Sequence, New Zealand. Geochemistry, Geophysics, Geosystems, 17, 324-345 pp.

BAUR, J., SUTHERLAND, R. & STERN, T. (2014) Anomalous Passive Subsidence of Deep-Water Sedimentary Basins: A Prearc Basin Example, Southern New Caledonia Trough and Taranaki Basin, New Zealand. Basin Research, 26, 242-268 pp.

BEGG, J.G. & RATTENBURY, M.S. (2000) Geology of the Wellington Area: Scale 1: 250 000. Institute of Geological & Nuclear Sciences Monograph Geological map, 10.

BRICE, J.C. (1964) Channel Patterns and Terraces of the Loup Rivers in Nebraska. US Geological Survey Professional Paper, 42 p.

BROWNE, G.H. & NAISH, T.R. (2003) Facies Development and Sequence Architecture of a Late Quaternary Fluvial-Marine Transition, Canterbury Plains and Shelf, New Zealand: Implications for Forced Regressive Deposits. Sedimentary Geology, 158, 57-86 pp.

BROWNE, G.H., FIELD, B.D. (1985) The Lithostratigraphy of Late Cretaceous to Early Pleistocene Rocks of Northern Canterbury, New Zealand. New Zealand Geological Survey Record, 6, 63 p.

CARTER, R. (1977). Tour Guide for Queenstown to Dunedin. Field Trip Guides for the 22nd Annual Meeting, Geological Society of New Zealand, Tour A-D, 1-113 pp.

CARTER, R., MCCAVE, I.N. & CARTER, L. (2004). Leg 181 Synthesis: Fronts, Flows, Drifts, Volcanoes, and the Evolution of the Southwestern Gateway to the Pacific Ocean, Eastern New Zealand. Proceedings of the Ocean Drilling Program: scientific results, Texas A & M University.

CARTER, R.M. & LANDIS, C.A. (1972) Correlative Oligocene Unconformities in Southern Australasia. Nature Physical Science, 237, 12 p.

CARTER, R.M., LINDQVIST, J.K. & NORRIS, R.J. (1982) Oligocene Unconformities and Nodular Phosphate — Hardground Horizons in Western Southland and Northern West Coast. Journal of the Royal Society of New Zealand, 12, 11-41 pp.

CARTER, R.M. (1985) The Mid-Oligocene Marshall Paraconformity, New Zealand: Coincidence with Global Eustatic Sea-Level Fall or Rise? Journal of Geology, 93, 359-371 pp.

CATUNEANU, O., GALLOWAY, W.E., KENDALL, C.G.S.C., MIALL, A.D., POSAMENTIER, H.W., STRASSER, A. & TUCKER, M.E. (2011) Sequence Stratigraphy: Methodology and Nomenclature. Newsletters on stratigraphy, 44, 173-245 pp.

CATUNEANU, O. (2017) Chapter One - Sequence Stratigraphy: Guidelines for a Standard Methodology. In: Stratigraphy & Timescales (Ed. by M. Montenari), 2, 1-57 pp. Academic Press.

CONGDON, L.M. (2003) Basin Analysis of the Porter Group, Castle Hill Basin, Canterbury: Implications for Oligocene Tectonics in New Zealand. Unpublished MSc Thesis, University of Canterbury, 197 p.

COOPER, A. & COOPER, R.A. (1995) The Oligocene Bottleneck and New Zealand Biota: Generic Record of a Past Environmental Crisis. Proceedings of the Royal Society of London, 261, 293–302 pp.

COOPER, R.A.E. (2004) The New Zealand Geological Timescale. 22, 284 p.

CRAW, D., UPTON, P., BURRIDGE, C.P., WALLIS, G.P. & WATERS, J.M. (2016) Rapid Biological Speciation Driven by Tectonic Evolution in New Zealand. Nature Geoscience, 9, 140-145 pp.

DAVY, B. (2014) Rotation and Offset of the Gondwana Convergent Margin in the New Zealand Region Following Cretaceous Jamming of Hikurangi Plateau Large Igneous Province Subduction. Tectonics, 33, 1577-1595 pp.

EXON, N.F., KENNETT, J.P. & MALONE, M.J. (2004) Leg 189 Synthesis: Cretaceous–Holocene History of the Tasmanian Gateway. Proceedings of the Ocean Drilling Program, Scientific Results, 189, 1-37 pp.

FIELD, B.D. (1985) Stratigraphic Drillholes at Charteris Bay, Lyttelton Harbour, Christchurch, New Zealand Geological Survey, Department of Scientific and Industrial Research. New Zealand Geological, Survey. SL11.

FIELD, B.D. & BROWNE, G.H. (1989) Cretaceous and Cenozoic Sedimentary Basins and Geological Evolution of the Canterbury Region, South Island, New Zealand. Institute of Geological & Nuclear Sciences Monograph, 2, 94 pp.

FIELD, B.D., BROWNE, G.H. (1986) Lithostratigraphy of Cretaceous and Tertiary Rocks, Southern Canterbury, New Zealand. New Zealand Geological Survey Basin Studies, 14, 55 pp.

FINDLAY, R.H. (1980) The Marshall Paraconformity (Note). New Zealand Journal of Geology and Geophysics, 23, 125-133 pp.

FLEMING, C.A. (1962) New Zealand Biogeography: A Palaeontologists Approach. Tuatara, 10, 53-108 pp.

FORDYCE, R.E. (2009) Field Trip 11. Waitaki/Canterbury Basin. Geological Society of New Zealand Miscellaneous Publications, 128B. Field Trip 11, 19 p.

FORDYCE, R.E. & RICHARDS, M.D. (2016) Fossils and Strata of Central and North Otago-Waitaki Valley. In: Field Trip Guide Volume, Geosciences 2016 Conference. Smillie, R. (compiler). , 28 November - 1 December 2016, Wanaka, New Zealand. Geoscience Society of New Zealand Miscellaneous Publication 145B, 21 p.

FULTHORPE, C.S., CARTER, R.M., MILLER, K.G. & WILSON, J. (1996) Marshall Paraconformity: A Mid-Oligocene Record of Inception of the Antarctic Circumpolar Current and Coeval Glacio-Eustatic Lowstand? Marine and Petroleum Geology, 13, 61-77 pp.

FULTHORPE, C.S., HOYANAGI, K. & BLUM, P. (2011) Iodp Expedition 317: Exploring the Record of Sea-Level Change Off New Zealand. Scientific Drilling, 12, 4-14 pp.

GAGE, M. (1957) The Geology of the Waitaki Subdivision. New Zelaand Geological Survey Bulletin, 55, 135 p.

GAGE, M. (1970) Late Cretaceous and Tertiary Rocks of Broken River, Canterbury. New Zealand Journal of Geology and Geophysics, 13, 507-536 pp.

GAGE, M. (1988) Mid-Tertiary Unconformities in North Otago — a Review and Assessment. Journal of the Royal Society of New Zealand, 18, 119-125 pp.

GHANI, M.A. (1974) Late Cenozoic Vertical Crustal Movements in the Central Part of New Zealand: Thesis Submitted for the Degree of Doctor of Philosophy in Geology at the Victoria University of Wellington, Victoria University of Wellington.

HAMPTON, S., COLE, J. & BELL, D. (2012) Syn-Eruptive Alluvial and Fluvial Volcanogenic Systems within an Eroding Miocene Volcanic Complex, Lyttelton Volcano, Bank Peninsula, New Zealand. New Zealand Journal of Geology and Geophysics, 55, 53-66 pp.

HANSEN, R.J. & KAMP, P.J. (2004) Late Miocene to Early Pliocene Stratigraphic Record in Northern Taranaki Basin: Condensed Sedimentation Ahead of Northern Graben Extension and Progradation of the Modern Continental Margin. New Zealand Journal of Geology and Geophysics, 47, 645-662 pp.

HAQ, B.U., HARDENBOL, J. & VAIL, P.R. (1987) Chronology of Fluctuating Sea Levels since the Triassic. Science, 235, 1156-1167 pp.

HIGGS, K., KING, P., BROWNE, G. & MORGANS, H. (2004) Oligocene Submarine Fan Systems in Taranaki: A Proven Reservoir and an Outcrop Comparison. 2004 New Zealand Petroleum Conference Proceedings, 10 p.

HIGGS, K.E. & KING, P.R. (2018) Sandstone Provenance and Sediment Dispersal in a Complex Tectonic Setting: Taranaki Basin, New Zealand. Sedimentary geology, 372, 112-139 pp.

HOLT, W. & STERN, T. (1994) Subduction, Platform Subsidence, and Foreland Thrust Loading: The Late Tertiary Development of Taranaki Basin, New Zealand. Tectonics, 13, 1068-1092 pp.

KATZ, M.E., CRAMER, B.S., TOGGWEILER, J., ESMAY, G., LIU, C., MILLER, K.G., ROSENTHAL, Y., WADE, B.S. & WRIGHT, J.D. (2011) Impact of Antarctic Circumpolar Current Development on Late Paleogene Ocean Structure. Science, 332, 1076-1079 pp.

KING, P.R. & THRASHER, G.P. (1996) Cretaceous Cenozoic Geology and Petroleum Systems of the Taranaki Basin, New Zealand. Institute of Geological & Nuclear Sciences Monograph 13.

KING, P.R., NAISH, T.R., BROWNE, G.H., FIELD, B.D. & EDBROOKE, S.W. (1999) Cretaceous to Recent Sedimentary Patterns in New Zealand. Institute of Geological and Nuclear Sciences Folio Series 1, 35 p.

KING, P.R. (2000) Tectonic Reconstructions of New Zealand: 40 Ma to the Present. New Zealand Journal of Geology and Geophysics, 43, 611-638 pp.

KORSCH, R. & WELLMAN, H. (1988) The Geological Evolution of New Zealand and the New Zealand Region. In: The Ocean Basins and Margins (Ed. by S. F. G. Nairn A.E.M., Uyeda S.), 7B, 411-482 pp. Plenum Publishing Corporation, New York.

LAIRD, M.G. & BRADSHAW, J.D. (2004) The Break-up of a Long-Term Relationship: The Cretaceous Separation of New Zealand from Gondwana. Gondwana Research, 7, 273-286 pp.

LANDIS, C.A., CAMPBELL, H.J., BEGG, J.G., MILDENHALL, D.C., PATERSON, A.M. & TREWICK, S.A. (2008) The Waipounamu Erosion Surface: Questioning the Antiquity of the New Zealand Land Surface and Terrestrial Fauna and Flora. Geological Magazine, 145, 173-197 pp.

LEVER, H. (2007) Review of Unconformities in the Late Eocene to Early Miocene Successions of the South Island, New Zealand: Ages, Correlations, and Causes. New Zealand Journal of Geology and Geophysics, 50, 245-261 pp.

LEWIS, D., SMALE, D. & VAN DER LINGEN, G.J. (1979) A Sandstone Diapir Cutting the Amuri Limestone, North Canterbury, New Zealand. New Zealand journal of geology and geophysics, 22, 295-305 pp.

LEWIS, D. (1982) Channels across Continental Shelves: Corequisites of Canyon-Fan Systems and Potential Petroleum Conduits. New Zealand journal of geology and geophysics, 25, 209-225.

LEWIS, D.W. (1973) Polyphase Limestone Dikes in the Oamaru Region, New Zealand. Journal of Sedimentary Research, 43, 1031-1045 pp.

LEWIS, D.W. & BELLISS, S.E. (1984) Mid Tertiary Unconformities in the Waitaki Subdivision, North Otago. Journal of the Royal Society of New Zealand, 14, 251-276 pp.

LEWIS, D.W. (1992) Anatomy of an Unconformity on Mid-Oligocene Amuri Limestone, Canterbury, New Zealand. New Zealand Journal of Geology and Geophysics, 35, 463-475 pp.

LIVERMORE, R., HILLENBRAND, C.D., MEREDITH, M. & EAGLES, G. (2007) Drake Passage and Cenozoic Climate: An Open and Shut Case? Geochemistry, Geophysics, Geosystems, 8, 1-11 pp.

LOUTIT, T.S. & KENNETT, J.P. (1981) New Zealand and Australian Cenozoic Sedimentary Cycles and Global Sea-Level Changes. AAPG Bulletin, 65, 1586-1601 pp.

LU, H., FULTHORPE, C.S. & MANN, P. (2003) Three-Dimensional Architecture of Shelf-Building Sediment Drifts in the Offshore Canterbury Basin, New Zealand. Marine Geology, 193, 19-47 pp.

LU, H. & FULTHORPE, C.S. (2004) Controls on Sequence Stratigraphy of a Middle Miocene–Holocene, Current-Swept, Passive Margin: Offshore Canterbury Basin, New Zealand. Geological Society of America Bulletin, 116, 1345-1366 pp.

LU, H., FULTHORPE, C.S., MANN, P. & KOMINZ, M.A. (2005) Miocene-Recent Tectonic and Climatic Controls on Sediment Supply and Sequence Stratigraphy: Canterbury Basin, New Zealand. Basin Research, 17, 311-328 pp.

MARSAGLIA, K.M., BROWNE, G.H., GEORGE, S.C., KEMP, D.B., JAEGER, J.M., CARSON, D. & RICHAUD, M. (2017) The Transformation of Sediment into Rock: Insights from Iodp Site U1352, Canterbury Basin, New Zealand. Journal of Sedimentary Research, 87, 272-287 pp.

MCLENNAN, J.M. & BRADSHAW, J.D. (1984) Angular Unconformity between Oligocene and Older Cenozoic Rocks at Avoca, Canterbury, New Zealand. New Zealand Journal of Geology and Geophysics, 27, 299-303 pp.

MIALL, A.D. (2000) Principles of Sedimentary Basin Analysis (Third Ed.). Springer-Verlag, Heidelberg

MILDENHALL, D., MORTIMER, N., BASSETT, K. & KENNEDY, E. (2014) Oligocene Paleogeography of New Zealand: Maximum Marine Transgression. New Zealand Journal of Geology and Geophysics, 57, 107-109 pp.

MITCHUM, R.M., SANGREE, J.B., VAIL, P.R. & WORNARDT, W.W. (1993) Recognizing Sequences and Systems Tracts from Well Logs, Seismic Data, and Biostratigraphy: Examples from the Late Cenozoic of the Gulf of Mexico: Chapter 7: Recent Applications of Siliciclastic Sequence Stratigraphy in P. Weimer and H. W.

Posamentier, Eds., Siliciclastic Sequence Stratigraphy: Recent Developments and Applications. AAPG Memoir 58, 163-198 pp.

MONTGOMERY, D.R. (2002) Valley Formation by Fluvial and Glacial Erosion. Geology, 30, 1047-1050 pp.

MORTIMER, N. & STRONG, D. (2014) New Zealand Limestone Purity. New Zealand Journal of Geology and Geophysics, 57, 209-218 pp.

MORTIMER, N., CAMPBELL, H.J., TULLOCH, A.J., KING, P.R., STAGPOOLE, V.M., WOOD, R.A., RATTENBURY, M.S., SUTHERLAND, R., ADAMS, C.J., COLLOT, J. & SETON, M. (2017) Zealandia: Earth's Hidden Continent. GSA Today, 27, 27-35 pp.

NELSON, C.S. (1978) Temperate Shelf Carbonate Sediments in the Cenozoic of New Zealand. Sedimentology, 25, 737-771 pp.

NELSON, C.S. & COOKE, P.J. (2001) History of Oceanic Front Development in the New Zealand Sector of the Southern Ocean During the Cenozoic—a Synthesis. New Zealand Journal of geology and geophysics, 44, 535-553 pp.

NEWNHAM, R.M., LOWE, D.J. & WILLIAMS, P.W. (1999) Quaternary Environmental Change in New Zealand: A Review. Progress in Physical Geography, 23, 567-610 pp.

NICOL, A. & CAMPBELL, J. (1990) Late Cenozoic Thrust Tectonics, Picton, New Zealand. New Zealand journal of geology and geophysics, 33, 485-494 pp.

NICOL, A. (1992) Tectonic Structures Developed in Oligocene Limestones: Implications for New Zealand Plate Boundary Deformation in North Canterbury. New Zealand Journal of Geology and Geophysics, 35, 353-362 pp.

NICOL, A., MAZENGARB, C., CHANIER, F., RAIT, G., URUSKI, C. & WALLACE, L. (2007) Tectonic Evolution of the Active Hikurangi Subduction Margin, New Zealand, since the Oligocene. Tectonics, 26, 24 p.

NICOL, A. (2011) Landscape History of the Marlborough Sounds, New Zealand. New Zealand Journal of Geology and Geophysics, 54, 195-208 pp.

NUMMEDAL, D. & SWIFT, D.J. (1987) Transgressive Stratigraphy at Sequence-Bounding Unconformities: Some Principles Derived from Holocene and Cretaceous Examples. In: Sea-Level Fluctuation and Coastal Evolution (Ed. by D. Nummedal, O. H. Pilkey & J. D. Howard), Special Publication 41, 241–260 pp. Society of Economic Paleontologists and Mineralogists.

POCKNALL, D.T. & MILDENHALL, D.C. (1984) Late Oligocene-Early Miocene Spores and Pollen from Southland, New Zealand. New Zealand Geological Survey Paleontological Bulletin, 1-66.

REILLY, C., NICOL, A., WALSH, J.J. & SEEBECK, H. (2015) Evolution of Faulting and Plate Boundary Deformation in the Southern Taranaki Basin, New Zealand. Tectonophysics, 651-652, 1-18 pp.

SAHOO, T., HILL, M. & H. BROWNE, G. (2014) Seismic Attribute Analysis and Depositional Elements in the Canterbury Basin. Advantage NZ : Geotechnical Petroleum Forum, Wellington, New Zealand, 2014.

SAHOO, T., BLAND, K., ARNOT, M., BOYES, A., FUNNELL, R., GRIFFIN, A., KROEGER, K., LAWRENCE, M., O'BRIEN, G. & SCADDEN, P. (2017) Atlas of Petroleum Prospectivity, Southeast Province: Arcgis Geodatabase and Technical Report. GNS Science Data Series 23c, 1.

SAHOO, T.R., KROEGER, K.F., THRASHER, G., MUNDAY, S., MINGARD, H., COZENS, N. & HILL, M. (2015) Facies Distribution and Impact on Petroleum Migration in the Canterbury Basin , New Zealand. In: Eastern Australian Basins Symposium 2015: Publication of Proceedings. Petroleum Exploration Society of Australia, Perth, WA, 187-202 pp.

SCHIØLER, P. & RAINE, J.I., COMPILERS (2011) Revised Biostratigraphy and Well Correlation, Canterbury Basin, New Zealand. Ministry of Economic Development New Zealand Unpublished Petroleum Report PR4365, 142 p.

SCHUMM, S. (1993) River Response to Baselevel Change: Implications for Sequence Stratigraphy. The Journal of Geology, 101, 279-294 pp.

SEVON, W.D. (1969) Stratigraphy and Sedimentology of the Tertiary Rocks of the Mandamus - Dove River Area, North Canterbury, New Zealand. New Zealand Journal of Geology and Geophysics, 12, 283-309 pp.

SHANE, P.A., BLACK, T.M., ALLOWAY, B.V. & WESTGATE, J.A. (1996) Early to Middle Pleistocene Tephrochronology of North Island, New Zealand: Implications for Volcanism, Tectonism, and Paleoenvironments. Geological Society of America Bulletin, 108, 915-925 pp.

SHANMUGAM, G. (1988) Origin, Recognition, and Importance of Erosional Unconformities in Sedimentary Basins. In: New Perspectives in Basin Analysis (Ed. by K. L. Kleinspehn & C. Paola), 83-108 pp. Springer-Verlag, New York.

STAGPOOLE, V. & NICOL, A. (2008) Regional Structure and Kinematic History of a Large Subduction Back Thrust: Taranaki Fault, New Zealand. Journal of Geophysical Research: Solid Earth, 113, 19 p.

STICKLEY, C.E., BRINKHUIS, H., SCHELLENBERG, S.A., SLUIJS, A., RÖHL, U., FULLER, M., GRAUERT, M., HUBER, M., WARNAAR, J. & WILLIAMS, G.L. (2004) Timing and Nature of the Deepening of the Tasmanian Gateway. Paleoceanography, 19, 18 p.

STROGEN, D., P, & KING, P.R. (2014) A New Zealandia-Wide Seismic Horizon Naming Scheme. GNS Science Report, 2014/34, 20 p.

STROGEN, D.P., BLAND, K.J., NICOL, A. & KING, P.R. (2014) Paleogeography of the Taranaki Basin Region During the Latest Eocene–Early Miocene and Implications for the 'Total Drowning'of Zealandia. New Zealand Journal of Geology and Geophysics, 57, 110-127 pp.

STROGEN, D.P., HIGGS, K.E., GRIFFIN, A.G. & MORGANS, H.E.G. (2019) Late Eocene – Early Miocene Facies and Stratigraphic Development, Taranaki Basin, New Zealand: The Transition to Plate Boundary Tectonics During Regional Transgression. Geological Magazine, 1-20 pp.

SUGGATE, R.P., STEVENS, G.R. & TE PUNGA, M.T. (1978) The Geology of New Zealand. Government Printer, Wellington.

SUTHERLAND, R. (1995) The Australia-Pacific Boundary and Cenozoic Plate Motions in the Sw Pacific: Some Constraints from Geosat Data. Tectonics, 14, 819-831 pp.

SWIFT, D.J. (1968) Coastal Erosion and Transgressive Stratigraphy. The Journal of Geology, 76, 444-456 pp.

TALLING, P.J. (1998) How and Where Do Incised Valleys Form If Sea Level Remains above the Shelf Edge? Geology, 26, 87-90 pp.

THOMPSON, N. (2013) Cool-Water Carbonate Sedimentology and Sequence Stratigraphy of the Waitaki Region, South Island, New Zealand. Unpublished PhD thesis, Christchurch. University of Canterbury, 581 p.

THOMPSON, N.K., BASSETT, K.N. & REID, C.M. (2014) The Effect of Volcanism on Cool-Water Carbonate Facies During Maximum Inundation of Zealandia in the Waitaki–Oamaru Region. New Zealand Journal of Geology and Geophysics, 57, 149-169 pp.

TIPPETT, J.M. & KAMP, P.J. (1993) Fission Track Analysis of the Late Cenozoic Vertical Kinematics of Continental Pacific Crust, South Island, New Zealand. Journal of Geophysical Research: Solid Earth, 98, 16119-16148 pp.

VAN DER LINGEN, G.J., SMALE, D. & LEWIS, D. (1978) Alteration of a Pelagic Chalk Below a Paleokarst Surface, Oxford, South Island, New Zealand. Sedimentary geology, 21, 45-66.

VELLA, P. (1967) Eocene and Oligocene Sedimentary Cycles in New Zealand. New Zealand Journal of Geology and Geophysics, 10, 119-145 pp.

WARD, D. & LEWIS, D. (1975) Paleoenvironmental Implications of Storm-Scoured, Ichnofossiliferous Mid-Tertiary Limestones, Waihao District, South Canterbury, New Zealand. New Zealand journal of geology and geophysics, 18, 881-908 pp.

WELLMAN, H. (1953) The Geology of the Geraldine Subdivision. New Zealand Geological Survey Bulletin, 50, 72 p.

WELLMAN, H.W. (1979) An Uplift Map for the South Island of New Zealand and a Model for Uplift of the Southern Alps. In: The Origin of the Southern Alps (Ed. by R. I. Walcott & M. M. Cresswell), 18, 13-20 pp. Royal Society of New Zealand Bulletin.

WOOD, R.A. & HERZER, R.H. (1993) The Chatham Rise, New Zealand. In: South Pacific Sedimentary Basins (Ed. by P. F. Ballance), Sedimentary Basins of the World 2, 329-349 pp. Elsevier Science Publishers, Amsterdam.

WOOD, R.A., ANDREWS, P. B., HERZER, R. H., & COOK, R. A. (1989) Cretaceous and Cenozoic Geology of the Chatham Rise Region, South Island, New Zealand. New Zealand Geological Survey Basin Studies 3, 75 p.

CHAPTER 6) IDENTIFICATION AND MORPHOLOGY OF BURIED VOLCANOES FROM THE CANTERBURY BASIN, NEW ZEALAND

A. Barrier[1], A. Bischoff[1], A. Nicol[1], G.H. Browne[2] and K. Bassett[1]

[1] *University of Canterbury, Department of Geological Science, Christchurch, New Zealand.*

[2]*GNS Science, PO Box 30368, Lower Hutt, New Zealand.*

6. Abstract

Seismic reflection data in the offshore Canterbury Basin has enabled us to identify buried magmatic structures, some of which were previously unknown, ranging in age from mid-Cretaceous to Pleistocene. Buried volcanic edifices of <1 to 20 km diameter have been mapped and are grouped into five geomorphological and chronological categories. 1. Monogenetic to polygenetic volcanoes up to 5 km diameter within the Cretaceous syn-rift succession. 2. Large volcanic complexes with diameters >10 km within the post-breakup Late Cretaceous succession. 3. Monogenetic to polygenetic volcanoes of Paleocene to Middle Miocene age. 4. Large Miocene composite volcanoes of >10 km diameter formed in association with present-day Banks and Otago peninsulas. 5. Eruptive centers along the Chatham Rise that erupted during the Late Neogene. The continuous volcanic activity of the Canterbury Basin from the Late Cretaceous rifting to the Late Neogene was accompanied by widespread sill intrusion but we did not resolve batholiths or plutons which, if present, are at depths of >10 km depth. This study increases the total known surface area of volcanoes in the Canterbury Basin by 300%, and suggests that across Zealandia, more volcanoes can be expected to exist of varying ages. Their mapping could help us to understand better the magmatic evolution of the Zealandia continent and heat flow in our sedimentary basins.

6.1. Introduction:

Rifting and continental breakup caused by lithospheric stretching and magma upwelling are commonly associated with the emplacement of intrusions and eruptions within rift and passive margin basins (e.g., Atlantic, Indian margins, eastern African rift system, Menzies *et al.*, 2002; Roger, 2006; Franke, 2013; Tugend et al., 2018). However, magmatic activity and rifting are not necessarily synchronous; volcanism commonly occurs prior to, during or after the rifting of sedimentary basins (e.g., Planke and Alvestad, 1999; Menzies *et al.*, 2002; Holford *et al.*, 2012).

Rifting and continental breakup can be associated with large volumes of magma emplaced in sedimentary basins, and contemporaneous with sedimentation, in some cases, forming up to 7 km thick volcanic successions (e.g., Africa-South America, Central Atlantic, Deccan Plateau and Greenland, Menzies *et al.*, 2002; Franke, 2013). In such scenarios, the rift

margin is referred to as a magma-rich (magma-dominated) rifted margin (Sawyer *et al.*, 2007; Reston, 2009; Reston and Manatschal, 2011; Doré and Lundin, 2015; Tugend *et al.*, 2018). Over the last decade, continuous improvement in seismic reflection imaging has indicated volcanic activity in rift basins is much more common than previously thought, although characterised by smaller volume than magma rich margins (e.g., Australia, Holford *et al*., 2012; Magee *et al.*, 2013; Reynolds *et al.*, 2016; Mergui Basin, Barrier, 2015; Sautter *et al.*, 2017; New Zealand, Bischoff *et al.*, 2017; Bischoff, 2019). Sedimentary basins can contain distributed volcanoes with a wide range of morphologies and are referred to as a magma-poor (magma-starved) rift margins (Sawyer *et al.*, 2007; Reston, 2009; Reston and Manatschal, 2011; Doré and Lundin, 2015; Tugend *et al.*, 2018).

New Zealand intra-plate volcanism was diffuse during the Late Cretaceous, Cenozoic and Quaternary (Fig. 6.1). This intra-plate volcanism produced a variety of volcano-types with predominately basaltic-alkaline compositions, although rocks originating from tholeiitic, rhyolitic, phonolitic and carbonatitic magmas are also reported in smaller volumes (e.g., Hoernle *et al.*, 2006; Timm *et al.*, 2010; Van der Meer *et al.*, 2016). Products of this volcanism are preserved in sedimentary basins across the Zealandia continent where some of the volcanoes have been buried and remained preserved by sediments (Mortimer *et al.*, 2017a). The origin of Zealandia intra-plate volcanism is controversial. Authors relate it to the presence of a mantle plume that initiated during the final stage of eastern Gondwana breakup (e.g., Hoernle *et al.*, 2006; Van der Meer *et al.*, 2017a) or to the asthenosphere upwelling induced by removal of parts of the subcontinental lithosphere throughout the Cenozoic (e.g., Hoernle *et al.*, 2006; Timm *et al.*, 2010).

The Canterbury Basin, straddling the east coast of the South Island of New Zealand, contains numerous mid-Cretaceous to Pleistocene aged igneous objects emplaced during rift, passive margin, and more recent contractional phases (Figs. 6.1, 6.2 and Table 6.1 - Field and Browne, 1989; Blank, 2013; Bischoff, 2019). Intrusive and extrusive igneous rocks crop-out throughout the onshore Canterbury Basin and range from mafic to felsic in composition. Seismic reflection, well and magnetic data from the offshore Canterbury Basin also show evidence for widespread igneous activity during at least 100 Myr of the basins geological history (Fig. 6.2, Field and Browne, 1989). These volcanic rocks constitute less of the basins rocks than the enclosing strata, and therefore the Canterbury Basin is a magma-poor (magma-starved) rifted margin.

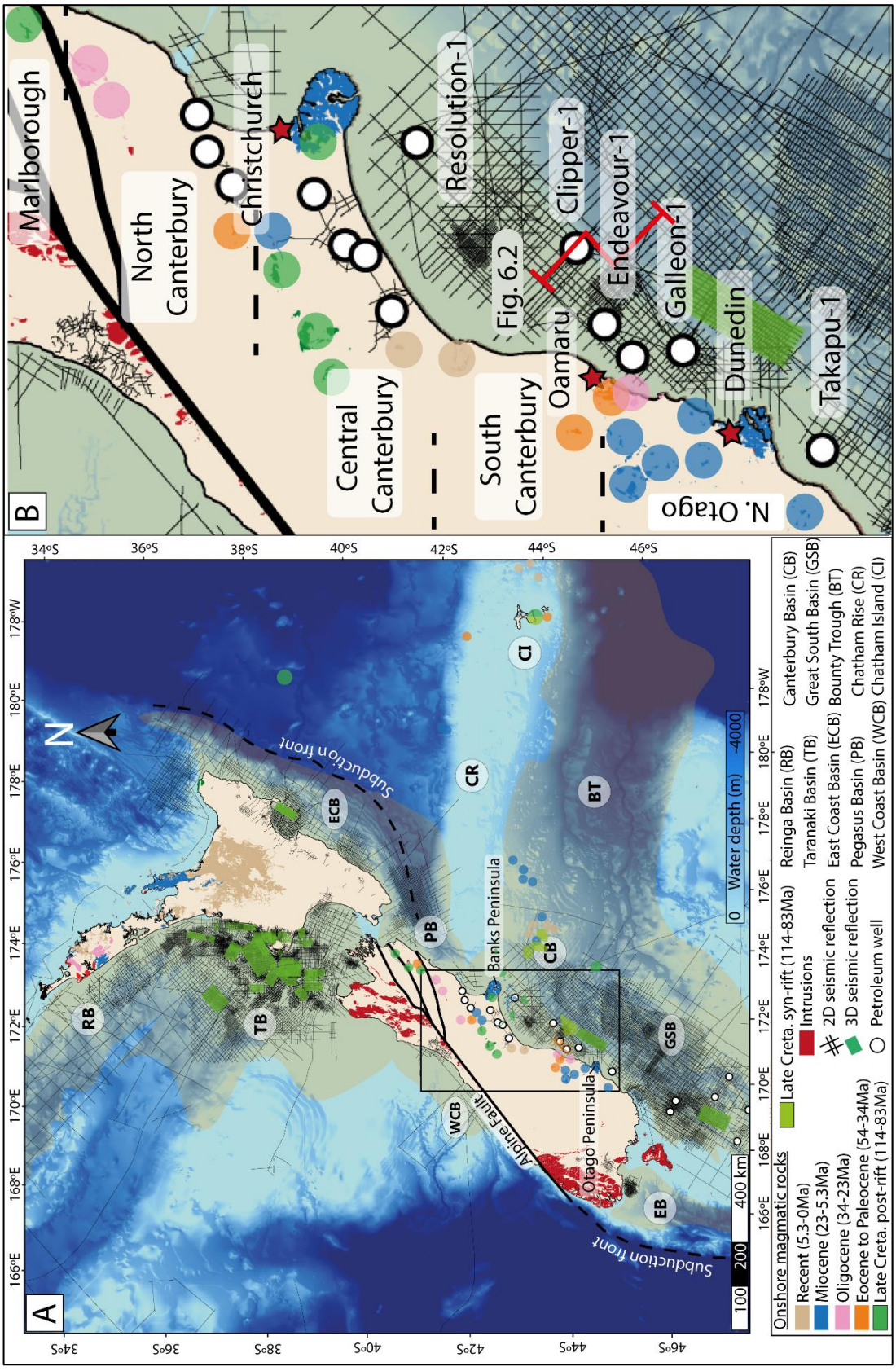

Figure 6.1Map of New Zealand showing onshore volcanic rocks of different age as well as the open file seismic data covering offshore Zealandia sedimentary basins. Offshore potential volcanoes mapped using vintage seismic data and magnetic anomalies was added for the offshore Canterbury Basin (Field and Browne, 1989; Wood et al., 1990).South Zealandia underwater volcanoes identified using dredging are shown (Timm et al., 2010; Mortimer et al., 2019). Wells in the Canterbury and Great South basins are displayed. (B) Detailed map of the Canterbury Basin. Geological map © GNS Science 2014 and bathymetric data licensed under NIWA Open Data Licence v1.0.v

In this paper we use seismic reflection data to map the geometries, size and distribution of buried volcanoes and intrusions across the Canterbury Basin. We present a series of new maps showing the distribution of volcanoes and intrusions that were emplaced within the Canterbury Basin from ~110 Ma and younger. We characterise these igneous systems based on their seismic morphology, location and temporal relationships to major tectonic events in the Canterbury Basin. Our work adds considerably to number of known igneous occurrences in the Canterbury Basin. The characterisation of the type and distribution of igneous bodies adds to our understanding of how igneous-sedimentary systems evolved in New Zealand sedimentary basins and has implications for volcanism elsewhere in Zealandia. Knowledge of the volcanism has implications for heat flow in the basin and the maturity of petroleum systems in Canterbury Basin.

6.2. Regional Geology:

The Canterbury Basin initiated as an intra-continental rift that formed due to widespread extension in Zealandia during the mid-Cretaceous (late Albian, ~110±5 Ma) (Fig. 6.2 - Field and Browne, 1989; Sahoo et al., 2014, 2015). The Canterbury Basin is bounded to the north by the Chatham Rise, an E-W bathymetric high corresponding to the front of the Permian-Early Cretaceous subduction margin and eastern Gondwana plate boundary (Fig. 6.1 - Field and Browne, 1989; Laird and Bradshaw, 2004). To the south of the Chatham Rise, the Canterbury Basin is contiguous with the Great South Basin and the Bounty Trough Rift System, which both formed during eastern Gondwana breakup (Wood et al., 1989; Wood and Herzer, 1993; Sahoo et al., 2015). Onshore, the Canterbury Basin is bounded by the Southern Alps where strong uplift and erosion due to tectonic uplift has removed much of the Late Mesozoic to Early Cenozoic sedimentary cover (Wellman, 1979; Field and Browne, 1989; Browne and Naish, 2003; Marsaglia *et al*., 2017).

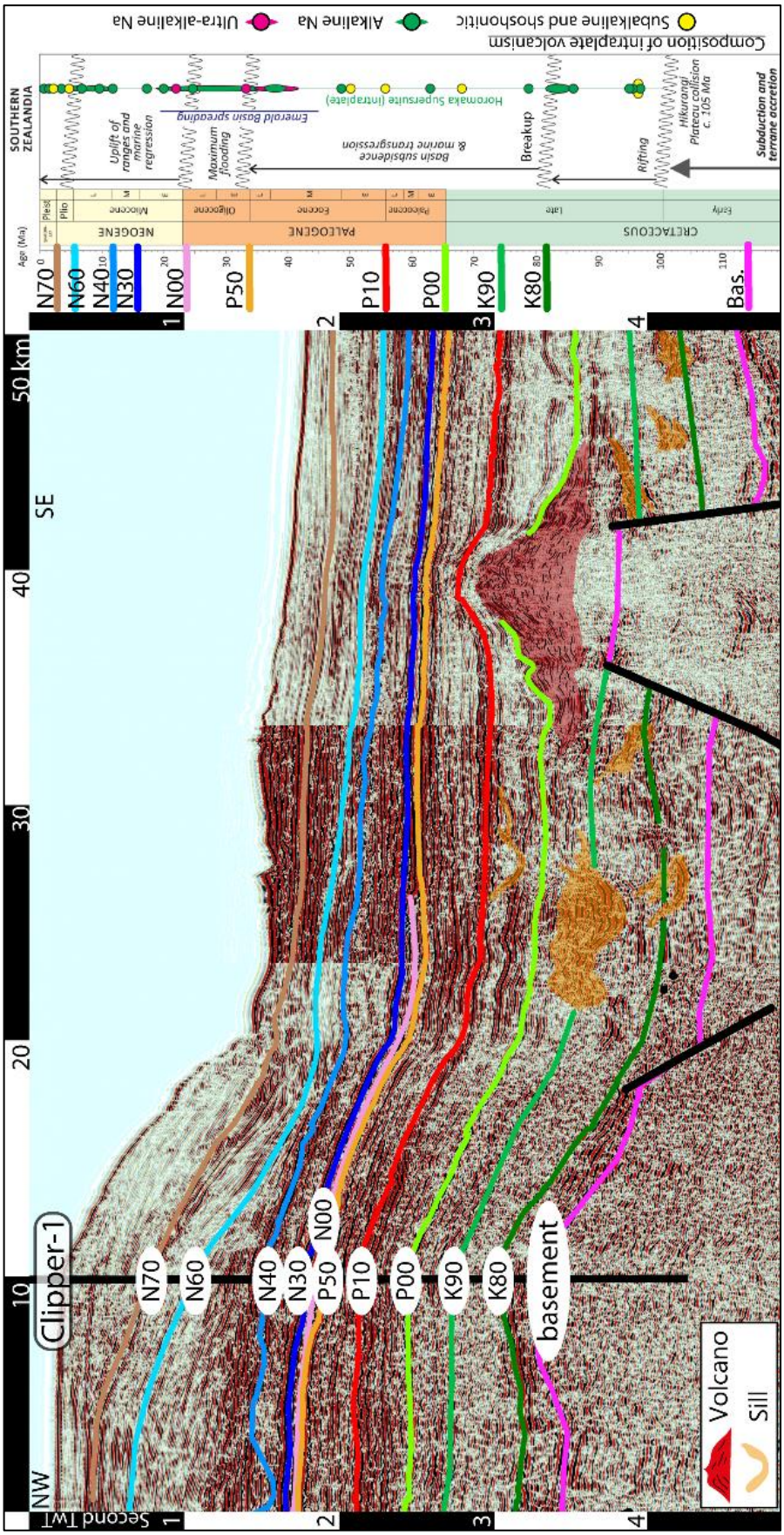

Figure 6.2 Composite seismic profile across the offshore Canterbury Basin tied to Clipper-1 well showing seismic horizon nomenclature. Summary of south Zealandia main tectonic and magmatic events (Mortimer et al., 2017). See figure 6.1 for location of the seismic line.

Table 6.1 Summary of the volcanic activity in the Canterbury Basin.

	Age	Volcanic Unit	Typical volcanic facies	References	Location	
NEOGENE	Late Neogene	Urry Knolls volcanics	Alkali basalts with small cones, flows and probably shallow intrusions	Herzer (1975); Lewis *et al.* (1986)	Chatham Rise	Convergent margin
	Pliocene	Timaru & Geraldine Basalt	Basalt	Duggan and Reay (1986), Sewell and Gibson (1988)	Central Canterbury	
	Late Miocene	Allandale Rhyolite, Lyttleton, Mt Herbert, Akaroa and Diamond Harbour volcanic groups	Basalt, andesites, tarchytes, Rhyolite and Andesite	Barley *et al.* (1988); Sewell (1988); Sewell and Weaver (1990); Shelley (1987); Hampton and Cole (2009)	Banks Peninsula	
	Middle to Late Miocene	Harper Hills Basalt, Oxford basalt, Wairiri volcaniclastite, Bluff Basalt, Sandpit Tuff	Basaltic flow and volcaniclastics	Carlson *et al.* (1980); Browne and Field (1985); Andrews *et al.* (1987); Sewell and Gibson (1988); Field and Browne (1989)	Central and Western Canterbury	
	late Middle Miocene	Waipiata Volcanics, Molehill Basalt	Basalt flow and tuff ring, pumice ignimbrite	Gage (1957); Mutch (1963); Bishop (1979); McMillan (1999)	South Canterbury	
	late Middle Miocene	Dunedin volcanic Group	Basanites to alkalic olivine basalts. Diatremes filled with volcacaniclastics sediments, sills, dikes and plugs.	Benson (1968); Coombs *et al.* (1986); Bishop and Turnbull (1996);	East and Central Otago	
	Early to Middle Miocene	Maahunui volcanic field	Volcanic centres and intrusives complexes	Wood and Herzer (1993); Schiøler and Raine (2011); Bischoff (2019)	Offshore Banks Peninsula; Resolution-1 and Clipper-1	
PALEOGENE	Eocene to Early Oligocene	Cookson volcanics	Basaltic flow and volcaniclastics	Browne and Field (1986); Field and Browne (1989)	North Canterbury	
	Eocene to Early Oligocene	Oamaru volcanics, Waiareka volcanics, Tokarahi Sill, Deborah Volcanics	Shallow marine eruption producing pillow lavas, hyaloclastite breccias ranging in composition from tholeiitic to strongly alkali. Doleritic dikes and sills	Gage (1957); Coombs and Dickey (1965); Coombs *et al.* (1986); Reay and Sipiera (1987); Cas *et al.* (1989); Field and Browne (1989); Maicher (1999)	Oamaru, South Canterbury	Post-rift
	Paleocene to Eocene	Endeavour and View Hill volcanics	Basaltic tuffs	Wilding and Sweetman (1971); Milne, (1975); Schiøler and Raine (2011)	Endeavour-1 and Resolution-1 well, offshore Canterbury Basin	
	Paleocene to Early Oligocene	View Hill volcanics; Thomas formation; Brothers volcanics	Interbedded basaltic flows, pillow lava, tuff and rare volcanic breccia. Dolerite intrusion, basaltic dikes	Gregg (1964); Gage (1970); McLennan (1981); Andrews *et al.* (1987); Field and Browne (1989); Oliver and Keen (1989)	Western, Central Canterbury, North Canterbury and offshore wells	
LATE CRETAECOUS	Haumurian	Barque, Loop and Takapu East volcanic complexes	Volcanic complex identified on 2D and 3D seismic reflection data	BP Shell Todd (1984); Beckman (2012); Beggs *et al.* (2017)	Offshore Canterbury Basin	~break-up
	Haumurian	Galleon Volcanics	Tuff layer in offshore well	Wilson (1985); Schiøler and Raine (2011)	Galleon-1 Offshore Canterbury Basin	
	Haumurian	N/A	Some pebbles of rhyolite have been described by Warren & Speight (1978) in Late Cretaceous post-rift sandstone	Warren and Speden (1978)	Haumuri Bluff in North Canterbury	
	mid-Cretaceous	N/A	Potential volcanic domes recognised on seismic reflection and magnetic data	Field and Browne (1989)	Offhsore Canterbury Basin	Syn-rift
	91±2.6 Ma	McQueens Andesite and Gebbies Rhyolite	Rhyolite	Sewell (1988); Tappenden (2003)	Banks Peninsula	
	97.0±0.5 Ma	Mandamus Igneous Complex	Alkaline suite characterised by basalt, gabbro, syenite, trachyte, phono-tephrite and diatreme with breccia and agglomerates	Field & Browne (1989); Weaver & Pankhurst (1991); Tappenden (2003)	North Canterbury	
	97.0±0.5 Ma	Gridiron Formation and Tapuaenuku Igneous Complex	Basalt and mafic intrusion and dike swarm	Weaver and Pankhurst (1991)	Marlborough	
	99-87 Ma using K-Ar dating 89.3 ±2Ma using Rb-Sr 99.0 Ma ±0.5 Ma to 96.3 Ma ± 0.5 Ma 80.09±1.9 Ma (Banks Peninsula)	Mount Somers Volcanic group	Ignimbrite, rhyolitic domes and dacitic,andesitic to basaltic lava flows	Adams and Oliver (1979); Oliver (1984); Barley (1988); Sewell *et al.*, (1988); Andrews, (1987); Field and Browne (1989); Smith and Cole (1997); Tappenden (2003) (Van Der Meer *et al.* (2017)	Central Canterbury	
	mid-Cretaceous 112.5 ± 0.2 Ma to 114 ±2 Ma	Kyeburn & Shag Point Ignimbrite	Tuffs beds and ignimbrites	Tulloch *et al.* (2009); Adams *et al.* (2017)	Kyeburn & Shag Point (North Otago)	
	mid-Cretaceous ~110.5 to ~83 Ma	Late Cretaceous Campbell Mafic Complex	Mafic granitoids and volcanoes	Tulloch *et al.* (2019)	South-east offshore east coast of South Island, New Zealand	

6.2.1. Late Cretaceous Volcanism

Late Cretaceous volcanism of predominately basaltic-alkaline-rhyolitic composition occurred in most of the onshore Canterbury Basin from ~112 to ~90 Ma and was contemporaneous with rifting (Van Der Meer *et al*, 2017b). Outcropping remnant of the Late Cretaceous eruptive phase correspond to the tuffs and ignimbrites of the Kyeburn Formation in North Otago, the Mount Somers Volcanic Group in south and central Canterbury, the Gridiron Formation, the Mandamus and Tapuaenuku Igneous Complex in North Canterbury (Table 6.1 - e.g., Weaver and Pankhurst, 1981; Barley *et al.*, 1988; Sewell, 1988; Smith and Cole, 1997; Tappenden, 2003; Crampton *et al.*, 2004; Tulloch *et al.*, 2009; Adams *et al.*, 2017; Van Der Meer *et al*, 2017b).

Offshore, mid-Cretaceous volcanism was hypothesised by Weaver and Pankhurst (1991) and Field and Browne (1989), but the poor quality of seismic reflection profiles 30 years ago and a lack of wells penetrating Cretaceous volcanic rocks made distinction between volcanic edifices and basement difficult.

Evidence for Late Cretaceous post-rift volcanism in the onshore Canterbury Basin is scarce but some pebbles of rhyolite have been described by Warren and Speden (1978) in Late Cretaceous sandstone of North Canterbury and could correspond to synchronous volcanic activity or older volcanic rocks eroded from higher lands or within the basin. Offshore, in Galleon-1 well, a Late Cretaceous tuff layer was recovered in cuttings at depths between 2920 and 2929 m within Campanian-Maastrichtian sediments (Wilson, 1985; Schiøler and Raine, 2011).

6.2.2. Paleogene Volcanism

During the Paleocene and Eocene, small volumes of basalt and volcaniclastic rocks were erupted and deposited sporadically across the Canterbury Basin in two main regions; as the View Hill Volcanics in Central Canterbury Basin and as the Waiareka and Deborah Volcanic formations in the Oamaru region (Table 1 – e.g., Gage, 1957; Gregg, 1957; Gage, 1970; McLennan, 1981; Andrew *et al.*, 1987; Field and Browne, 1989; Olivier and Keen, 1989; Thompson *et al.*, 2014). Volcanism continued until the Oligocene in the Oamaru region and in North Canterbury as the Cookson Volcanics, which are also of basaltic composition (Browne and Field, 1985; Field and Browne, 1989).

Offshore, Paleocene basaltic tuffs have been recovered in Endeavour-1 well between 1809 and 1942 m and Clipper-1 well intercalated within the Katiki Formation between 2860.5 and 2980 m. These rocks are referred to as the Endeavour Volcanics (Wilding and Sweetman, 1971; Schiøler and Raine, 2011). In addition, Paleocene volcanic rocks have been recovered in Resolution-1 well between 1476 and 1480 m. They are referred to as the View Hill Volcanics which are basaltic tuffs that crop out in the Central Canterbury Region (Milne, 1975; Schiøler and Raine, 2011).

6.2.3. Neogene Volcanism

Miocene volcanism occurred in four main regions onshore, the Otago Peninsula, Central Otago, western Canterbury and on Banks Peninsula (Figs. 6.1, 6.2 and Table 6.1). This eruptive phase built up two large volcanic complexes of >20-30 km diameter (present-day dimensions), forming Banks Peninsula and Otago Peninsula (e.g., Coombs *et al*., 1986; Bishop and Turnbull, 1996; Hampton and Cole, 2009; Hampton *et al.*, 2012). The volume of magma erupted was ~ 1675 km^3 for the former and 105 km^3 for the latter (Reilly, 1972; Sewell, 1988; Timm et al., 2009). Middle to Late Miocene Harper Hills Basalt erupted at a number of centres in the Central Canterbury Region (Andrew *et al.*, 1987; Field and Browne, 1989). The Harper Hills Basalt was contemporaneous with volcanic rocks drilled in the Resolution 1 well between 1103.5 and 1112 m where they appear to be associated with sill intrusions drilled between 1911.5 and 1963 (Milne, 1975; Schiøler and Raine, 2011). K^{40}/Ar^{40} dating (12±2 Ma) on the sill intrusion indicates that it could relate to the emplacement of the cotemporaneous Maahunui Volcanic Field that is located in the same area (Milne, 1975; Bischoff, 2019; Bischoff *et al*., submitted).

The youngest volcanic eruptive centres in onshore Canterbury Basin are the Timaru and Geraldine basalts of South Canterbury which erupted at about 2.5 Ma (Duggan and Reay, 1986) and the Late Miocene-Pliocene Burnt Hill Group (basaltic formations and volcaniclastic rocks) in central Canterbury (Carlson *et al.*, 1980; Browne, 1983; Andrews *et al.*, 1987). Offshore, dredging of a sea mount recovered latest Miocene to earliest Pleistocene alkali basalts on the Urry Knolls, referred to as the Urry Knolls Volcanics, preserved as small volcanic cones, lava flows deposits and probably shallow intrusions (Herzer, 1975; Herzer *et al.*, 1989).

6.3. Methods and Data:

Buried volcanoes and igneous intrusions were mapped in the Canterbury Basin using seismic reflection data. These data have been used to characterise the geometries and the spatial distribution of the buried volcanic systems within the basin at present-day configuration (e.g., present-day degree of erosion and compaction).

6.3.1. Seismic Data

To study the volcanic systems we have utilised ~26, 000 line kilometre of 2D seismic reflection data and one 3D seismic reflection survey provided by New Zealand Petroleum and Minerals (NZP&M, for details see https://data.nzpam.govt.nz) and issued as part of the 2015 to 2018 Data Pack (Figs. 6.1, and 6.2). Seismic surveys were acquired between 1966 and 2014 with data quality improving towards the present day and areal coverage being variable, with fewer lines available towards the east. Seismic data acquired pre-2000 that have not been reprocessed usually display a poor to medium quality and reduced resolution, which increases the uncertainties associated with interpretation of volcanoes using these lines. The data acquired post-2000 and reprocessed data have a quality that ranges from good to very good, and is the prime seismic data source used to map volcanoes.

6.3.2. Mapping of Igneous Systems Buried in The Canterbury Basin

Igneous systems buried in sedimentary basins can produce similar seismic facies characteristics as sedimentary and structural features (Planke *et al.*, 1999; Jerram *et al.*, 2009; Holford *et al.*, 2012; Klarne and Klarne, 2012; Bischoff *et al.*, 2017; Schofield *et al.*, 2018). The following diagnostic attributes and morphologies have been used to identify volcanoes in seismic data (for discussion see Planke *et al.*, 2005; Reynolds *et al.*, 2016; Bischoff *et al.*, 2017; Bischoff, 2019).

These criteria include:

- Low to high amplitude "dome" shaped reflectors.
- Low amplitude internal reflectivity dipping in opposite directions away from the summit of the dome.
- In plan view, these dome structures should typically show circular or elongated shapes when intersected by several seismic lines.
- Dome structures are typically onlapped by younger reflectors as volcanoes form positive relief until they are buried by sediments.
- Reflectors above the dome structures can show an arcuate geometry in cross section which is typically interpreted to be produced by differential compaction between the volcanic structures and their enclosing sedimentary strata during the burial (e.g., Planke *et al.*, 1999; Bischoff *et al.*, 2017).
- Reflectors below the dome structures display a loss in seismic amplitude and continuity.
- The domes can correspond to positive anomalies on magnetic maps. Here we have used the total magnetic anomaly map provided by FrOG Tech (2011).

Sheet-like intrusions are the only igneous intrusions observed on seismic data in the Canterbury Basin (e.g., Blanke, 2013). Sheet-like intrusions display several geometries: a) Sills are intrusions dominantly concordant with the layering of the host rock and have numerous shapes combining horizontal, inclined and vertical geometries (Galland *et al.*, 2018). b) Laccoliths are flat-lying igneous intrusions with a flat and concordant basal geometry and a dome-like shape deforming overlying strata (Galland *et al.*, 2018). The transition from sills to laccoliths is not based on a robust definition (Galland *et al.*, 2018). In this paper we consider all the sheet-like intrusive bodies concordant to discordant with seismic reflectors as sills that form the following geomorphic features:

- High amplitude reflectors cross-cutting sedimentary reflectors.
- Anomalous high amplitude reflectors present in basement.
- Their geometry varies from "saucer" shape characterized by horizontal inner sill, an inclined sheet and a horizontal outer sill, to strata-concordant, transgressive, step-wise transgressive, v-shaped (Planke et al., 2005; Blank, 2013; Galland et al., 2018; Bischoff, 2019).
- Sills can also form sill complexes corresponding to a cluster of multiple sills (Eide et al., 2017).

The identification of igneous bodies on seismic reflection data can lead to misinterpretation due to their similarity with sedimentary features even on 3D seismic data (e.g., Klarner and

Klarner, 2012; Infante-Paez *et al.*, 2018). Therefore, we acknowledge that the seismic interpretation of both volcanoes and intrusions has limitations, especially when using 2D seismic reflection data. Our 2D seismic data doesn't allow the continuous imaging of the entire basin or the full geometry of many igneous features due to the spacing between the lines, which can be kilometres to tens of kilometres apart, and to limited seismic resolution. We acknowledge the potential to under sample or under represent volcanic edifices and intrusions in the Canterbury Basin especially for small size volcanoes and sills. In addition, the frequency used during seismic acquisition may contribute to poor resolution of some sub-seismic igneous features. Despite these issues the available dataset provides a valuable basis for mapping volcanic systems in the basin.

6.3.3 Characterisation of Buried Volcanoes From Seismic Reflection Data

In this study, we classify buried volcanoes recognised in seismic reflection data using a descriptive terminology based on the geometry, width of their apparent basal diameter and give a minimal value of erupted material for each buried edifice. We have utilised the following parameters to characterise buried volcanoes:

(1) Their geometry, whether they correspond to monogenetic, polygenetic, or volcanic complexes. The nomenclature used to describe the morphology of buried volcanoes is in accordance with the following criteria (Table 2).

Table 6.2 Characteristics used to describe the geomorphology of buried volcanoes in the offshore Canterbury Basin.

Nomenclature	Definition	Volume or diameter characteristics	Reference
Monogenetic volcano	Volcanic edifice with a small cumulative volume that has been built up by one continuous, or many discontinuous, small eruptions fed from one or multiple magma sources	Volume of erupted material <10 km^3 (after Silva and Lindsay, 2015)	Wood, 1979, 1980; Perez-Lopez *et al.*, 2011; Nemeth and Kerezturi, 2015; Silva and Lindsay, 2015; Mordensky and Wallace, 2018
Polygenetic volcano	Discrete volcano formed during several episodic eruptions. The transition from monogenetic to polygenetic volcanoes does not only depends on the width or volume of magma erupted of the volcano and other authors have discussed it (e.g. Nemeth, 2010; Kereszturi and Nemeth, 2013)	Volume of erupted material >10 km^3 (after Silva and Lindsay, 2015)	Silva and Lindsay, 2015
Volcanic complex	Defined in this paper as a volcanic edifice built by the eruptions of a group of polygenetic and monogenetic volcanoes.	N/A	N/A
Volcanic field	Represents an area with a large number of monogenetic or polygenetic volcanoes erupting during the same time interval	N/A	Hildreth, 2007
Fissure eruptions	Elongated fracture of several kilometres from which lava erupts resulting in the alignment of several eruptive centres and lava flows (e.g., Tarawera volcano, New Zealand; Kilauea, Hawaii, fissure swarn, Iceland).	Ratio of minimal and maximal diameter <1	Ashwell *et al.*, 2018; Sigmundsson *et al.*, 2018; Neal *et al.*, 2019

(2) Their distribution in the basin, whether volcanoes are clustered forming volcanic fields, spread-out or aligned.

(3) Their apparent diameter was used to differentiate between whether they are sub-rounded or elongated, with the latter most likely to have formed in fissure eruptions. To this end, we have measured minimum and maximum apparent diameters for each volcanic polygon mapped.
(4) The total surface of mapped volcanoes for each interval of time. For the onshore outcropping volcanoes, we used the area of polygons extracted from the Geological map © GNS Science 2014.

We acknowledge that measurements of volcano diameters can have a high degree of uncertainty when a volcano is intersected by only one or a few seismic reflection profiles. We also acknowledge that older volcanoes buried deeply will be measured with less accuracy than younger equivalents based purely on resolution of the respective features in seismic. The magmatic composition of either an intrusion or a volcano is very difficult to interpret on seismic reflection profiles. Volcanoes display a range of geometries that can be associated with different types of magma, eruptive styles and eruption duration. Therefore, we do not attempt to extrapolate magmatic compositions of the volcanoes in the Canterbury Basin based on their geometries.

6.3.4. Age of Volcanoes and Intrusions

Seismic data has been tied to five petroleum exploration wells in the Canterbury Basin and to the most recent biostratigraphic ages established for these wells (Schiøler and Raine, 2011). From the wells, six seismic horizons have been interpreted across the entire basins using the New Zealand-wide naming convention of GNS Science, the “K” and “P” seismic horizon nomenclature of Strogen and King (2014) (Fig. 6.2). Ages have been assigned to these horizons based on the New Zealand Geological Time Scale (Cooper *et al.*, 2004; Raine *et al.*, 2015) and correlated to the international geological time scale (Table 6.3). From the main horizons, five isochron grids were generated for the syn-rift interval (top basement to K80), the post-rift Late Cretaceous (K80 to P00), the Paleocene (P00 to P10), Eocene (P10 to P50) and the Miocene to Recent (P50 to sea bed) intervals. The isochron grids were then used to show the distribution and evolution of potential volcanoes and intrusions buried in the Canterbury Basin. Due to the condensed and channelized stratigraphic intervals, the lack of well control and the increased spacing between 2D seismic reflection lines a further five horizons, N00 (top Oligocene), N30 (top Early Miocene), N40 (top Middle Miocene), N60 (top Late Miocene) and N70 (Top Pliocene), were interpreted across part of the basin, being especially difficult to correlate towards the east (Fig. 6.1).

Table 6.3 Summary of the seismic horizon nomenclature used in this paper.

Color code	Horizon Name	GNS Science nomenclature (Strogen & King, 2014)	Age (Ma)	NZ Stage	International Stage	Horizon mapped
	Sea Bed	seabed	0	Recent	Recent	yes
	Top Pliocene	N70	2.4	Mangapanian	Piacenzian	no
	Top Late Miocene	N60	5.3	Kapitean	Messinian	no
	Top Middle Miocene	N40	11.6	Waiauan	Serravallian	no
	Top Lower Miocene	N30	16	Altonian	Burdigalian	no
	Top Oligocene	N00	23	Waitakian	Chattian	no
	Top Eocene	P50	34	Runangan	Priabonian	yes
	Top Paleocene	P10	56	Teurian	Thanetian	yes
	Top Late Cretaceous post-rift	P00	66	upper Haumurian	Maastrichtian	yes
	Intra Late Cretaceous post-rift	K90	78	lower Haumurian	intra Campanian	yes
	Top Late Cretaceous syn-rift	K80	84.5±1.5	Piripuan	Santonian	yes
	Top Basement	basement	110±5	Urutawan to Korangan	Aptian-Albian	yes

The mapped horizons were used to estimate the age of potential igneous systems identified on seismic reflection lines. The age of the volcanoes has been determined by assessing how the dome structures are spatially and temporally related with enclosing sedimentary strata. The youngest age of a volcano is estimated by the relative age of the reflector that first onlaps the post-eruptive surface of the dome structure, while the oldest age is estimated by the age of the reflectors that correspond to the pre-eruptive surface beneath the volcanic structure (e.g., Reynolds *et al.*, 2016; Bischoff *et al.*, 2017). Potential volcanoes located on top of basement reflectors were estimated to be formed contemporaneously with the syn-rift phase (~110 Ma to ~85 Ma). Volcanoes were then mapped by age and were associated with the isochron map that represents the time interval during which the volcano formed.

The age of sills can be estimated by analysing the age of deformed horizons overlying the sill or also by the presence of hydrothermal vents that develop on the sea floor at time of sill emplacement (Plank *et al.*, 2005). When neither of these elements are visible a sill is considered to be younger than the sediment it intrudes.

6.4. Results:

The results highlight 185 buried volcanoes and extensive intrusions in the entire sedimentary succession of the offshore Canterbury Basin. The mapping by age of these igneous features and their geometries are illustrated by a series of maps and seismic reflection profiles in the following sections.

6.4.1 Late Cretaceous syn-rift volcanic features

We have mapped 59 syn-rift volcanic complexes that are distributed across much of the offshore Canterbury Basin (Fig. 6.3). These volcanic systems are often within 5 km of rift faults, with 70%, located on horst structures and 30% in depocenters. Most of the horsts of the

Canterbury Basin display a flat top due to erosion (see chapter 3 of this thesis for further details). When a volcano is observed on a horst these uplifted blocks appear to have been associated with limited planation, with the volcano displaying a dome shape characterised by outwards dipping reflectors (Fig. 6.3). Most of the syn-rift volcanoes are located in the south-eastern offshore Canterbury Basin, in the Taiepa Nui Basin and Ruturutu intra-basin High, however this area also has the highest density of seismic coverage and the most recently acquired data (so we are more likely to see volcanoes here if they are present). Late Cretaceous volcanoes mapped in offshore seismic profiles cover an area of 1225 km^2, while the onshore outcrops represent 171 km^2.

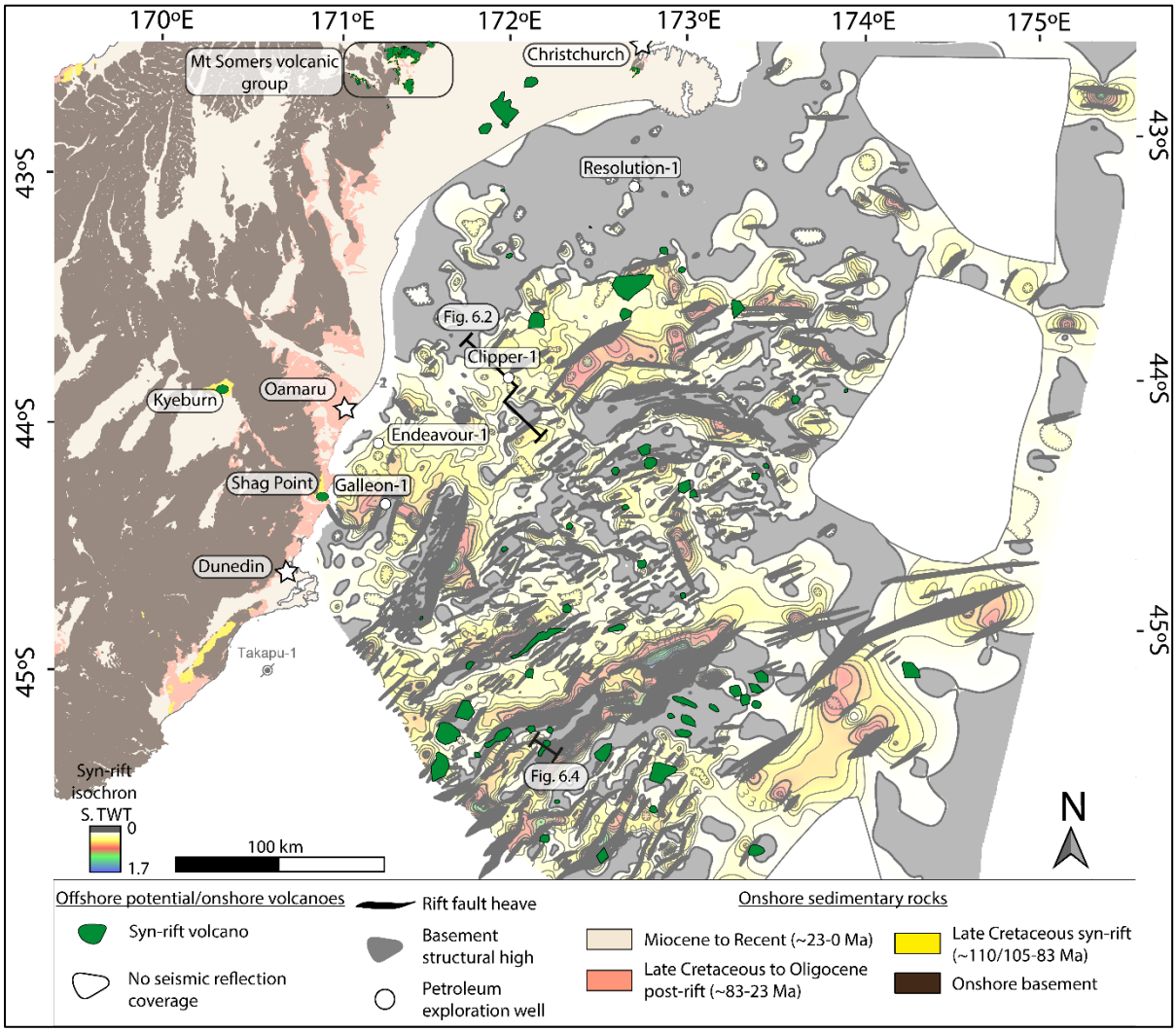

Figure 6.3 Map of the distribution of syn-rift Late Cretaceous buried volcanoes across the Canterbury Basin (~110 to 85 Ma) with the syn-rift isochron map.

Syn-rift volcanic bodies can form monogenetic or polygenetic volcanoes (Figs. 6.4 and 6.5). In the south-east offshore region, where seismic reflection profile coverage is dense (<2 km spacing) and of good quality, syn-rift volcanoes form a ~10 000 km^2 volcanic field. The apparent diameter of syn-rift volcanoes ranges from 0.4 to 11.4 km. Some of these syn-rift volcanoes appear to be elongate along rift faults and display a width-length ratio of 0.15 to 0.46. In Figure 6.5, these elongate volcanoes plot below the 1:1 line. Onshore, in the Central Canterbury area, seismic reflection profiles and petroleum exploration wells show evidence for

mid-Cretaceous volcanic activity of similar size and composition to the Mount Somers Volcanic Group and other contemporaneous onshore syn-rift volcanoes outcropping in the Marlborough region (Indo-Pacific Energy, 2010).

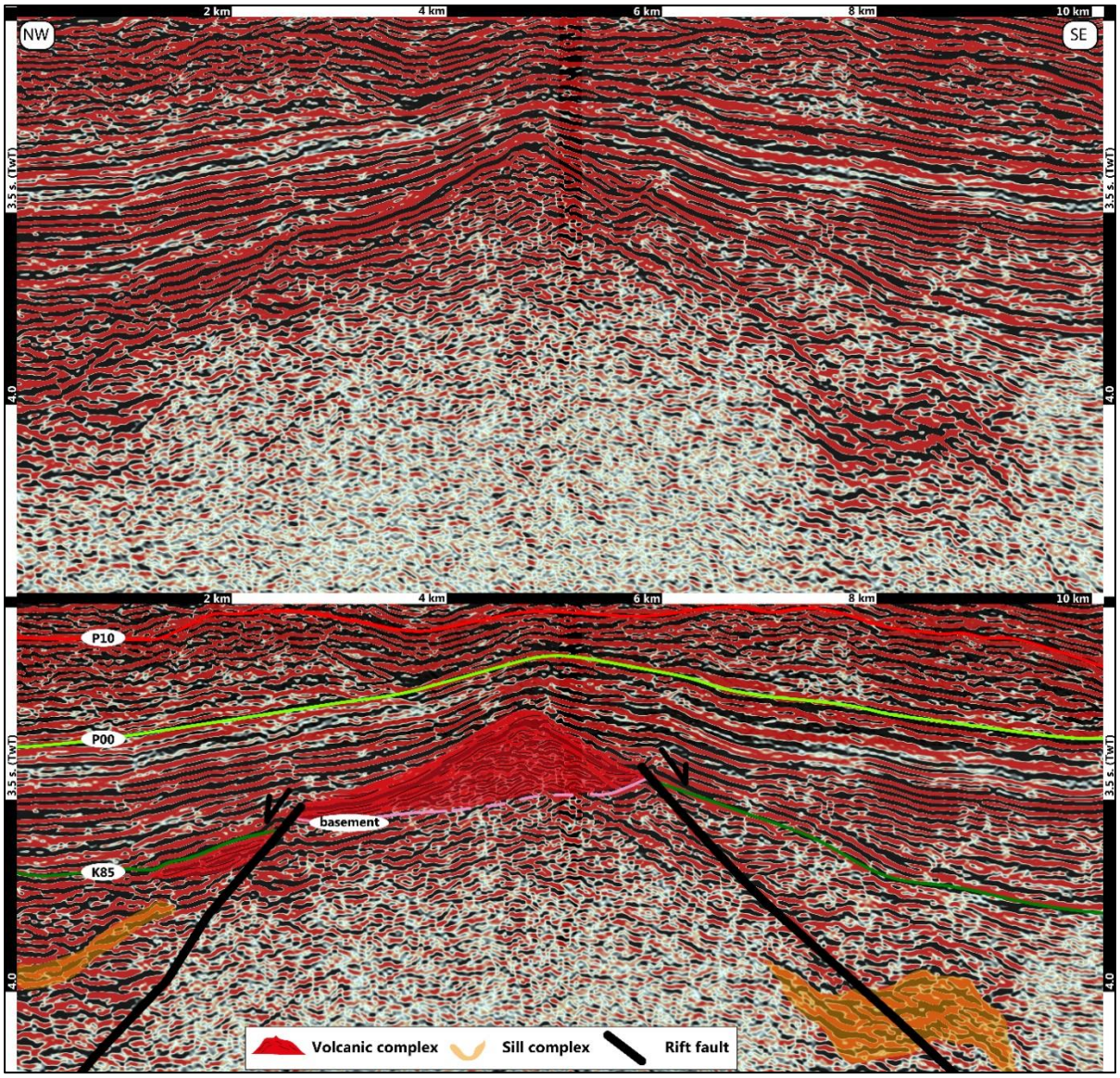

Figure 6.4 Seismic profile across a potential syn-rift Late Cretaceous buried volcano resting on top of a horst. Vertical axis in TwT (secs.) For location of seismic line see Figure 6.3.

Some syn-rift volcanoes immediately south of Banks Peninsula coincide with magnetic anomalies, while volcanoes mapped in the south-eastern offshore Canterbury Basin are not marked by these anomalies (Fig. 6.6).

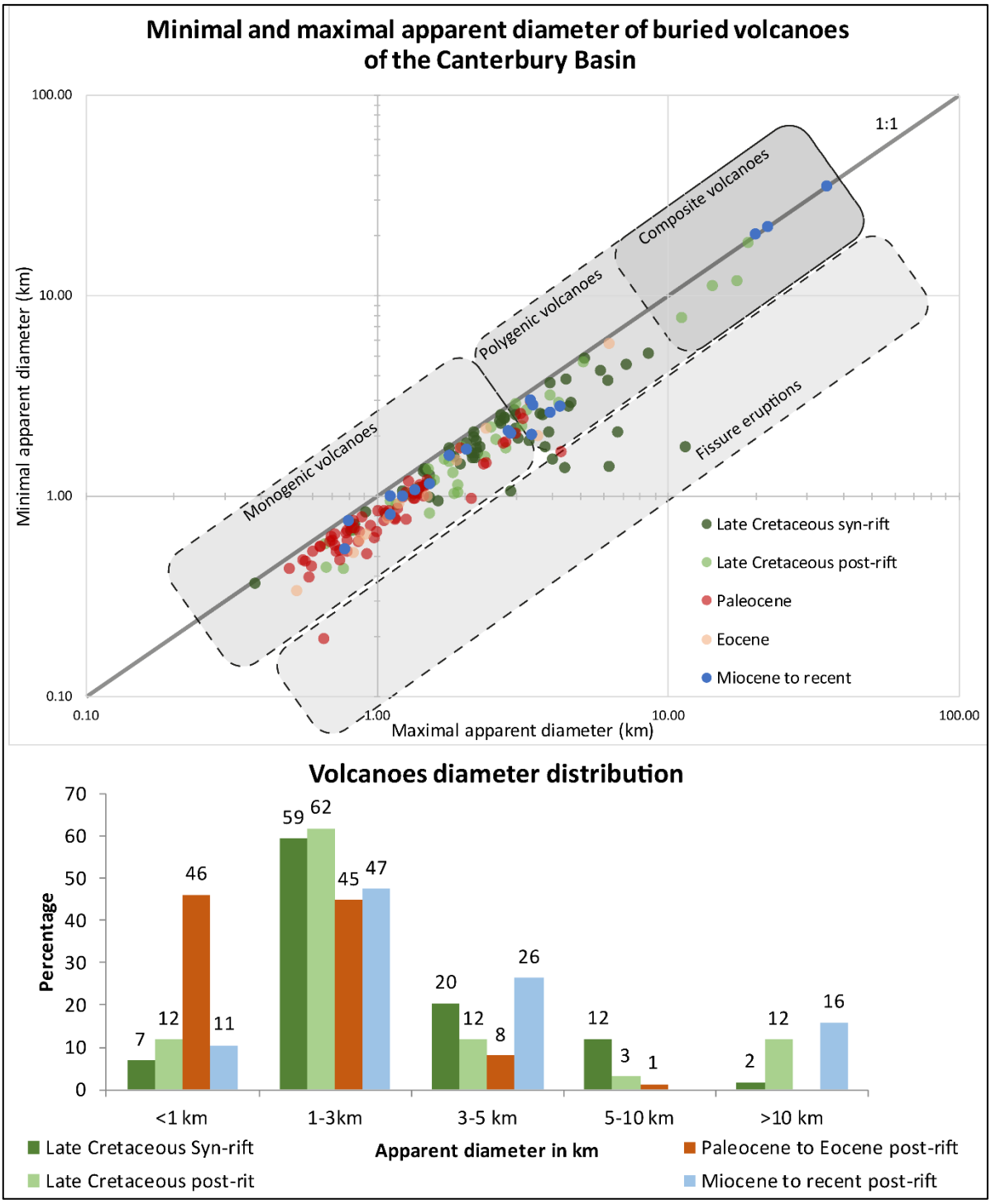

Figure 6.5 Diagram showing the relationships between minimum and maximum apparent diameter from buried volcanoes in the Canterbury Basin.

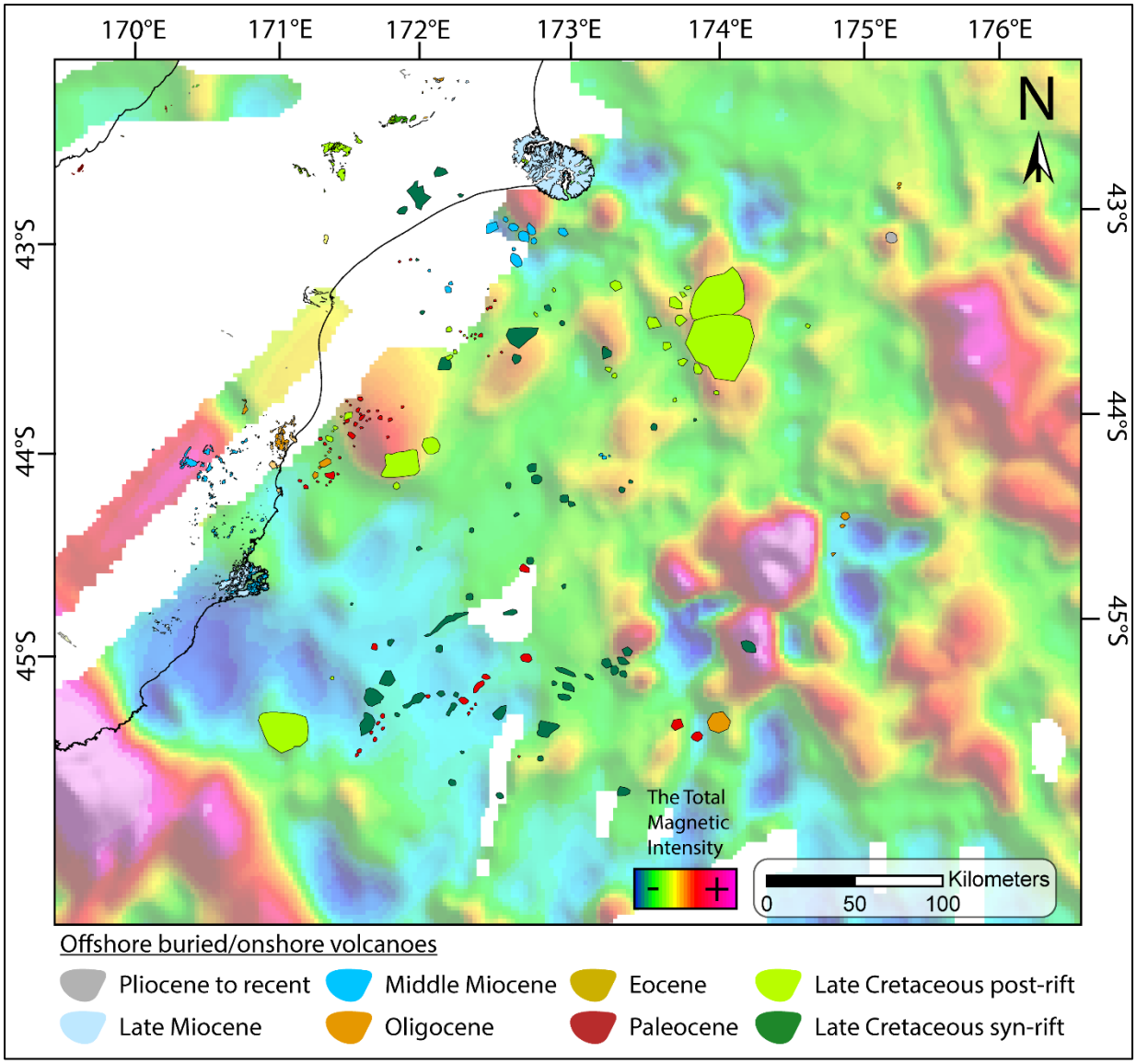

Figure 6.6 Total magnetic intensity map (FrOG Tech, 2011) showing magnetic anomalies across the Canterbury Basin overlain by polygons showing the locations of volcanoes mapped from seismic reflection lines.

6.4.2 Late Cretaceous Post-Rift Volcanic Features

We have mapped 34 post-rift Late Cretaceous volcanoes in the offshore Canterbury Basin. The volcanic activity is clustered in three areas forming large 20 to 40km wide composite volcanic complexes displaying a slightly curved NE-SW alignment (Fig. 6.7). Two of these are in the Clipper Basin and the third is in the south of the Canterbury Basin.
Post-rift Late Cretaceous volcanic geometries have been inferred south-east of Banks Peninsula by BP Shell Todd (1984), Field and Browne (1989) and Wood and Herzer (1993) using seismic reflection data and magnetic anomaly maps. More recently, the Late Cretaceous Sloop Volcanic Complex has been interpreted on seismic reflection data by Beckman (2012) ~100 km southeast from Banks Peninsula. The Sloop Volcanic Complex has an eroded summit and is draped by Eocene reflectors (Fig. 6.8). Thus, the Sloop Volcanic Complex formed a topographic high and remained bathymetric feature on the sea floor until at least the Paleocene. The Late Cretaceous post-rift Barque Volcanic Complex, which is located ~100 km offshore

of Oamaru was interpreted using 3D seismic reflection data by Beggs *et al.* (2016). In addition, a third large volcanic complex, here referred to as the East Tapaku Volcanic Complex, has been recognised in the area and is located offshore, south of the Otago Peninsula (Fig. 6.7).

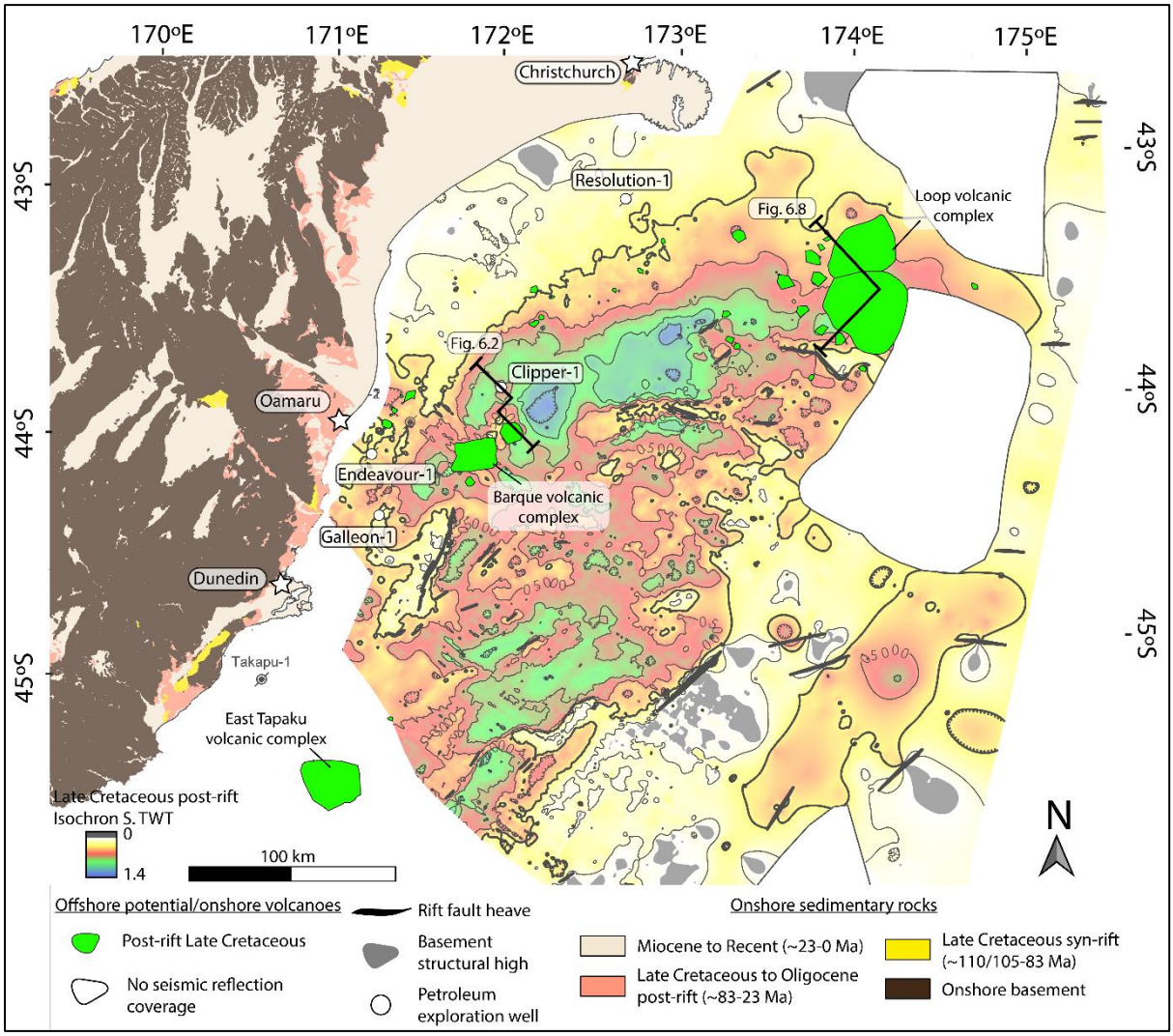

Figure 6.7 Map of the distribution of the post-rift Late Cretaceous buried volcanoes across the Canterbury Basin (~85-66 Ma) plotted along with the Late Cretaceous post-rift isochron map.

On seismic reflection profiles, these composite volcanic complexes display a main central dome structure with numerous satellite vents forming polygenetic volcanic complexes (Figs. 6.2 and 6.8). Beneath the volcanic structures, numerous sill intrusions can be recognised. The total surface of Late Cretaceous post-rift volcanoes mapped on offshore seismic profiles represent 2869 km^2 while onshore, no age-equivalent volcanism is known. The apparent diameter of post-rift composite volcanoes ranges from 11 to 19 km as opposed to <1 to 5 km for more isolated domes. The Sloop Volcanic Complex is composed of two large main vents that combine to form a volcanic complex of around 30 km diameter (Figs. 6.5 and 6.8). Volcanic complexes of this age overlie and downlap onto syn-rift (K80) top basement horizons (Fig. 6.8). The large volcanic complexes are onlapped by Late Cretaceous reflectors and fully draped by Late Cretaceous to Eocene reflectors showing their long-lived presence as structural highs during the post-rift phase of the Canterbury Basin (Fig. 6.8).

The three Late Cretaceous large composite volcanoes coincide with magnetic anomalies (Fig. 6.6).

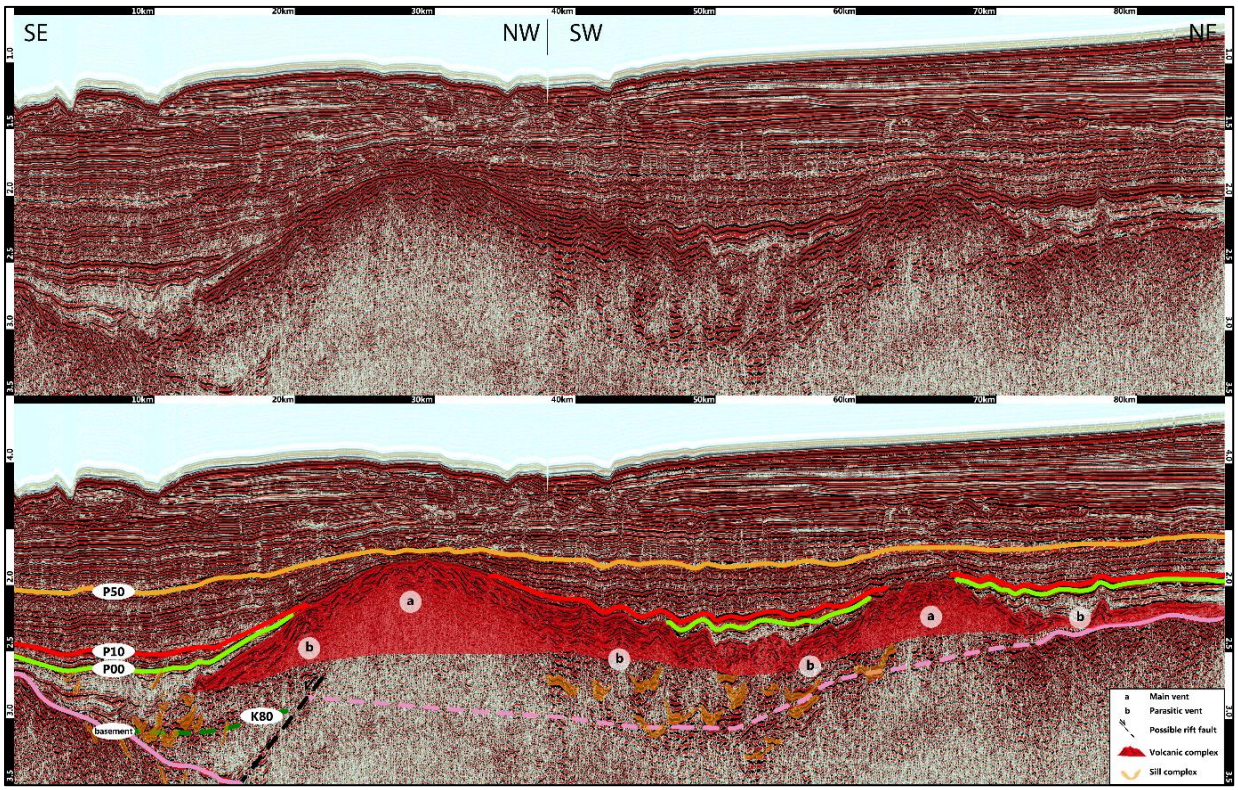

Figure 6.8 Composite seismic profile across the Late Cretaceous post-rift Sloop Volcanic Complex showing the main eruptive centres and the adjacent parasitic vents. Vertical axis in TwT (secs.) For location see Figure 6.7.

6.4.3 Paleocene to Oligocene Volcanic Features

We have mapped 76 post-rift Paleocene to Oligocene volcanoes in the offshore Canterbury Basin. Paleocene to Oligocene volcanism occurred in two areas of the western offshore region and one area in the south-east offshore region, as well as sporadically distributed elsewhere offshore and onshore (Fig. 6.9). The first cluster Paleocene-Eocene volcanic field is located in the offshore Oamaru region where onshore Eocene and Oligocene volcanoes crop out. The second cluster is located between the Resolution-1 and Clipper-1 wells. The south-eastern cluster displays an alignment with rift structures. Other sporadically distributed volcanoes are present east of the Clipper-1 well but here the seismic data is sparse and these features are not well covered by the available line. The total surface area of Paleocene to Oligocene post-rift volcanoes mapped on offshore seismic profiles covers 320 km^2 while the surface area of onshore outcrops represents 130 km^2.

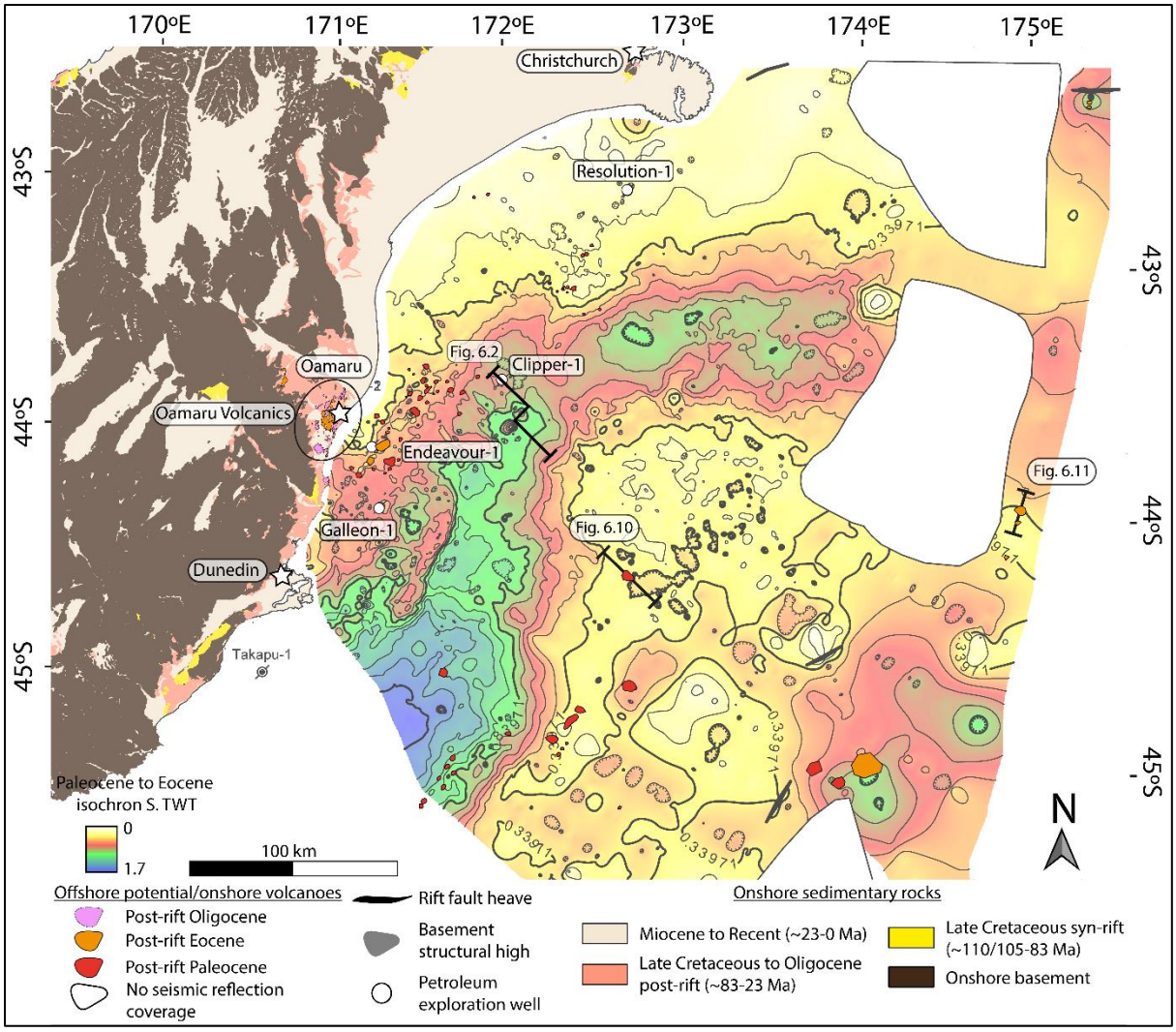

Figure 6.9 Map of the distribution of the post-rift Paleocene, Eocene and Oligocene buried volcanoes across the Canterbury Basin (~66-23 Ma) plotted on the Paleocene to Eocene isochron map.

The Paleocene to Oligocene volcanoes correspond to monogenetic to polygenetic vents forming single cones edifices. They display an apparent diameter ranging from 1 to 2 km (Figs. 6.5, 6.10 and 6.11).

Some of the Paleocene volcanoes offshore Oamaru correspond to magnetic anomalies, but these anomalies could also represent co-located Late Cretaceous post-rift composite volcanoes. The remainder of Paleocene to Oligocene post-rift volcanoes in offshore Canterbury Basin do not correspond to magnetic anomalies (Fig. 6.6).

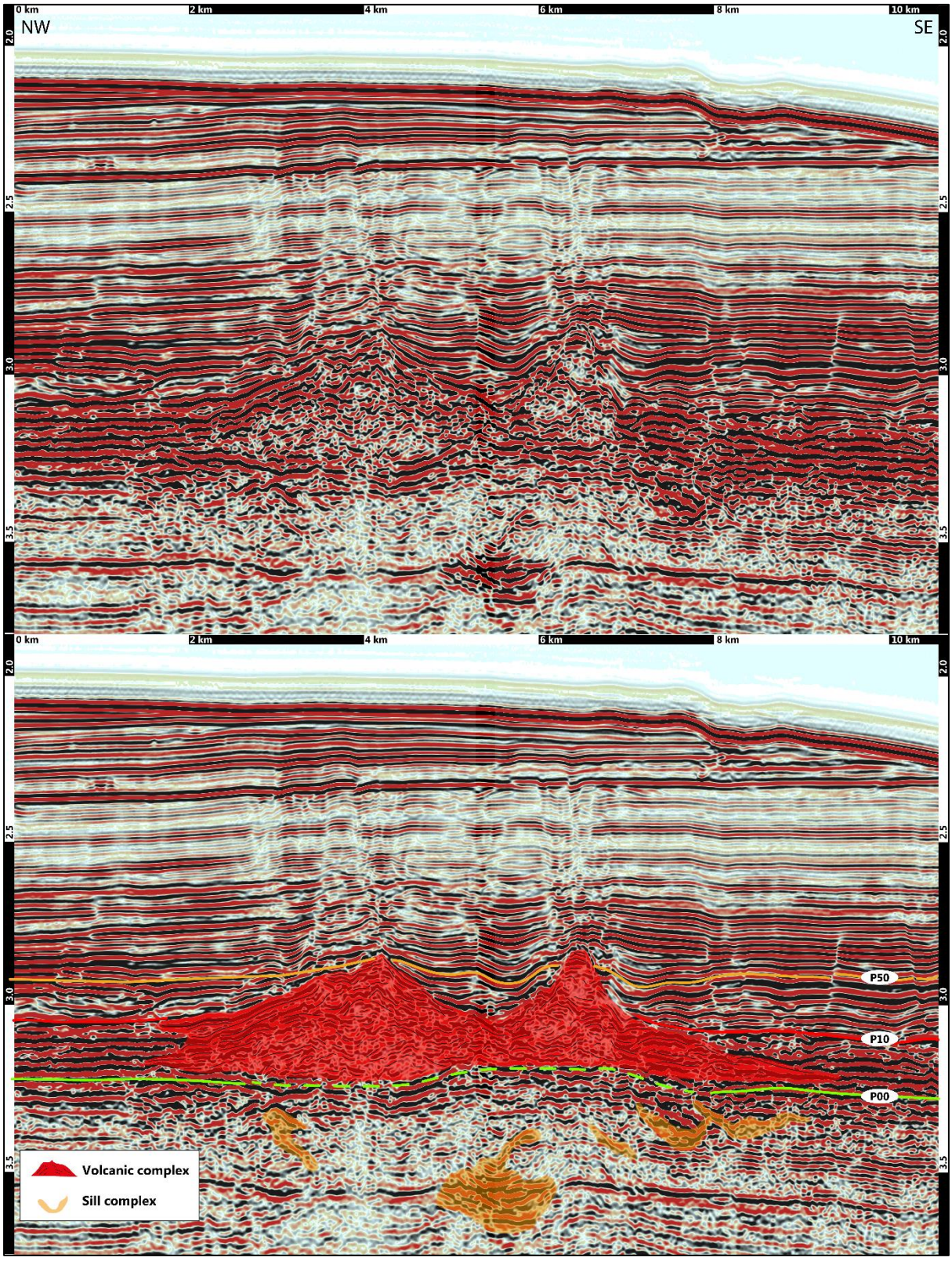

Figure 6.10 Seismic profile showing an example of two Paleocene volcanoes associated with sill intrusions. Vertical axis is in TwT (secs.) For the location of the seismic profile see Figure 6.9.

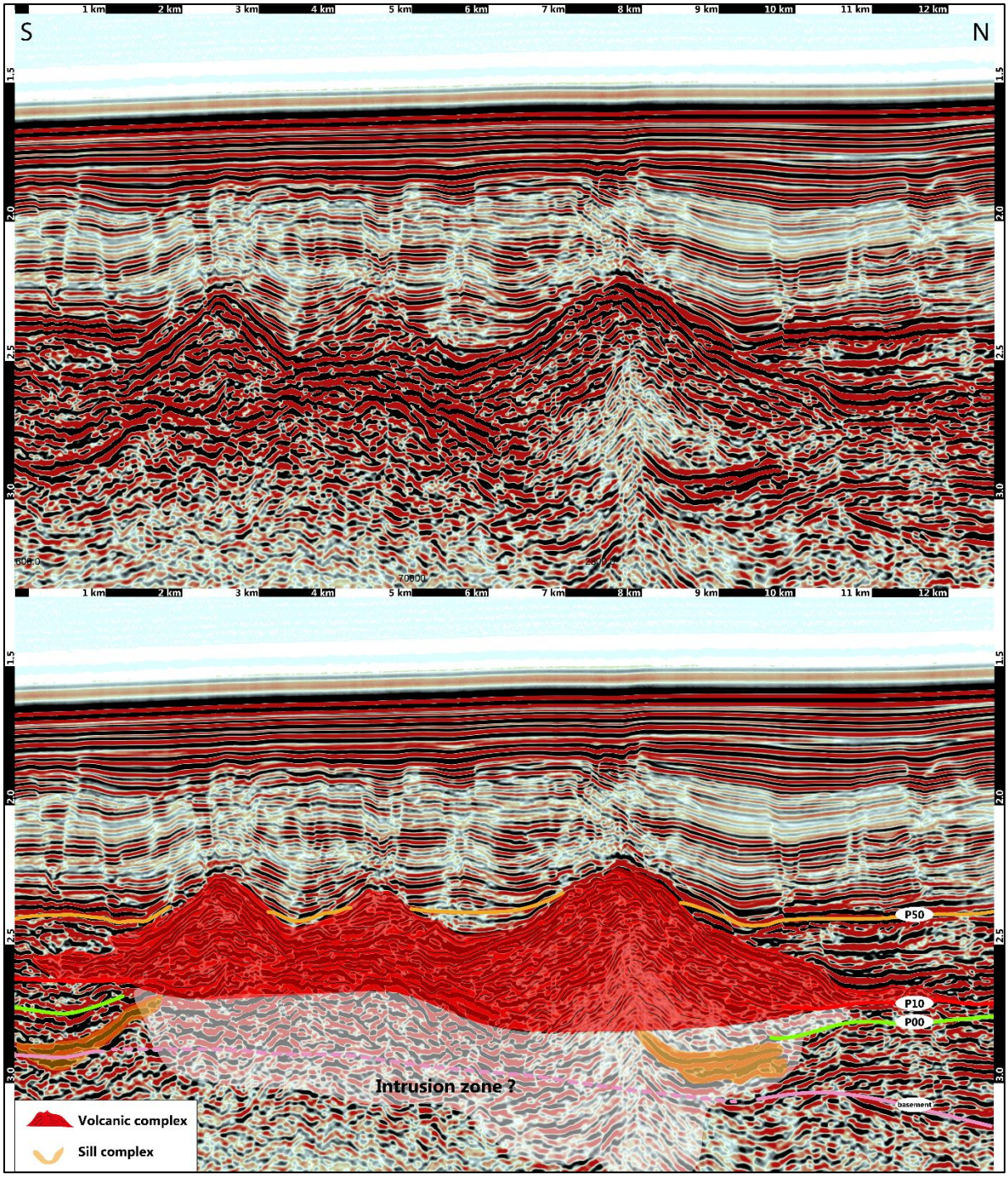

Figure 6.11 Seismic profile showing an example of Eocene volcanoes with associated sill intrusions. Vertical axis in TwT (secs.) For the location of the seismic line see Figure 6.9.

6.4.4 Miocene to Pliocene Volcanic Features

We have mapped 16 post-rift Miocene to Pliocene volcanoes in the offshore Canterbury Basin. The principal Miocene offshore volcanic area is located south of Banks Peninsula while other volcanoes of this age are also located in the eastern offshore. The cluster of volcanoes erupted at least 100km south of Banks Peninsula and have been named the Maahunui volcanic field, which forms ~31 monogenetic volcanoes (Bischoff, 2019). The geometric relationships

between the sedimentary reflectors in the basin and the volcanic cones suggest a Middle Miocene age for the Maahunui volcanic field (Bischoff, 2019). A volcano younger than Banks Peninsula is located east of Banks Peninsula along the Chatham Rise and forms a bathymetric high (Fig. 6.12). No other volcanoes seem to be present around the Dunedin Volcanic Complex in the southern edge of the Canterbury Basin. The total surface area of Miocene to Recent volcanoes mapped on offshore seismic profiles covers 183 km^2, while the surface area of onshore outcrops is 1254 km^2.

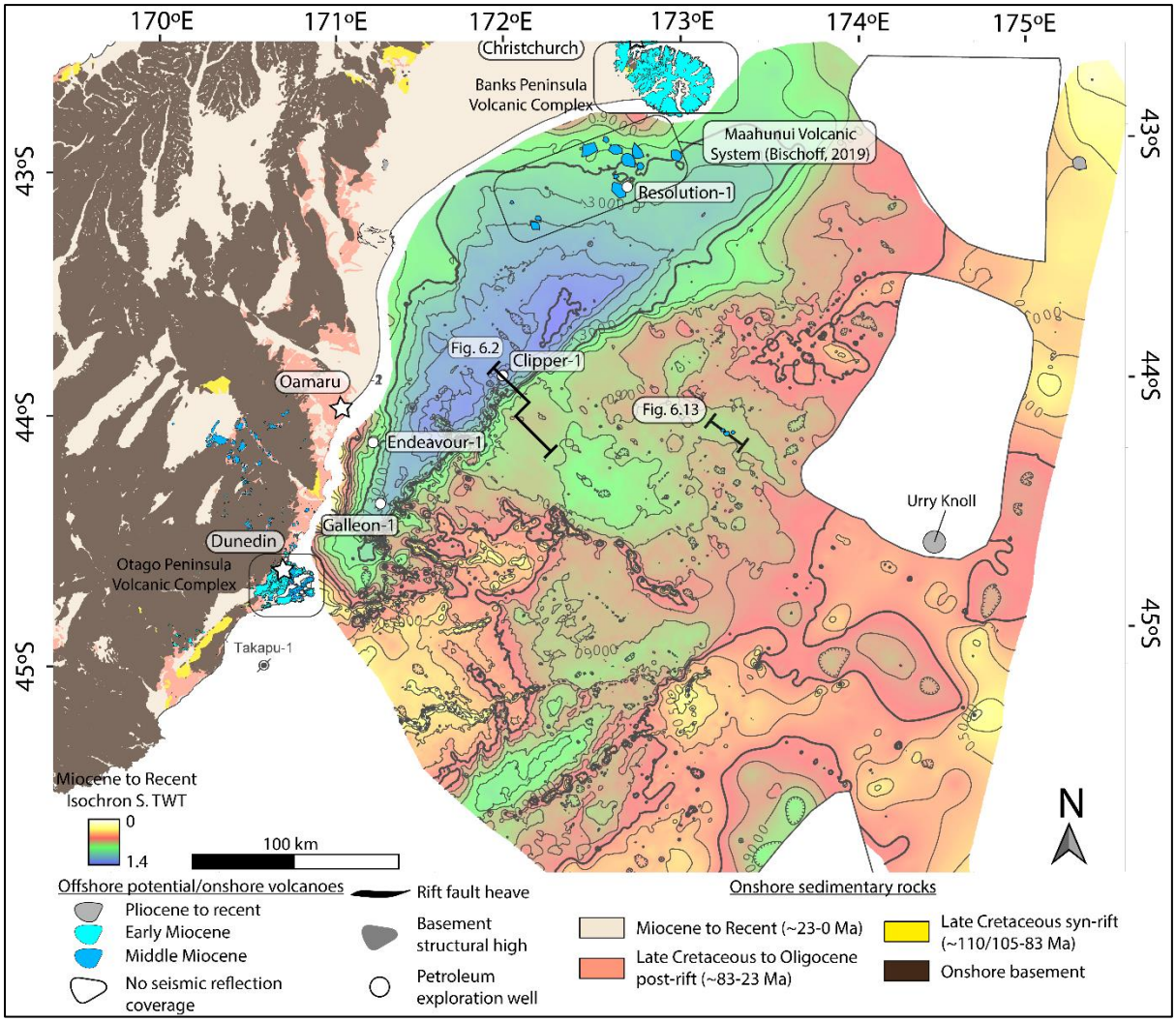

Figure 6.12 Map of the distribution of the Miocene to Recent buried volcanoes across the Canterbury Basin (~23-Recent) plotted on the Miocene to Recent isochron map.

On seismic reflection profiles, monogenetic and polygenetic Miocene volcanoes appear as single cone edifices (Fig. 6.13). The apparent diameter of the offshore Miocene volcanoes varies from >1 to 35 km (Fig. 6.5). The more recent volcanic dome forms a bathymetric high on the sea floor with diameter of up to 3km but is visible only along one seismic profile.

The two Miocene composite volcanoes forming the Banks Peninsula and the Otago Peninsula and the more recent volcanic dome mapped along the Chatham Rise are resolved by magnetic anomalies (Fig. 6.6).

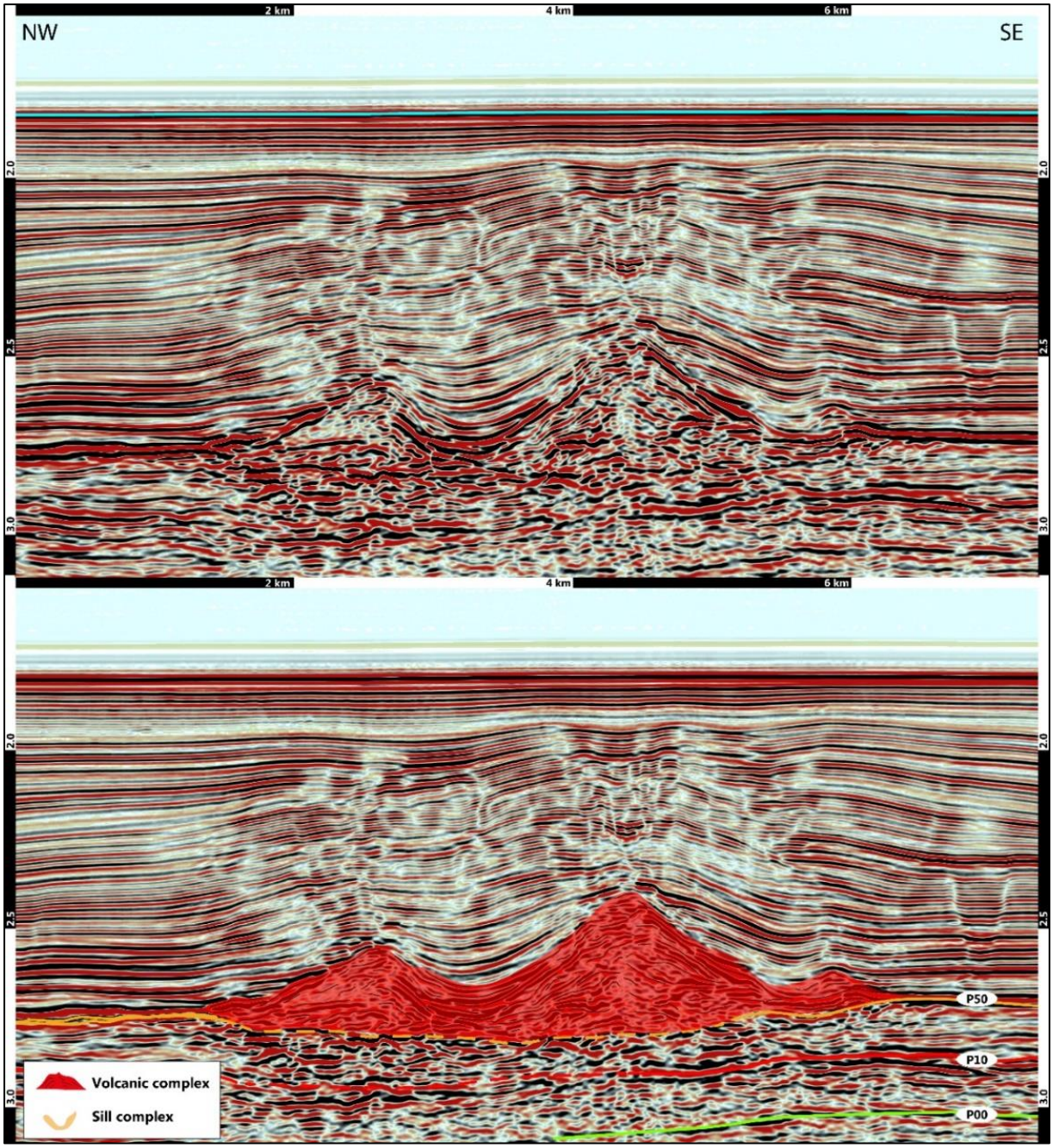

Figure 6.13 Seismic reflection profile showing an example of Miocene volcanoes. Vertical axis in TwT (secs.) For the location of the seismic line see Figure 6.12.

6.4.5 Igneous Intrusions

Igneous intrusions are numerous in the offshore Canterbury Basin and occur both beneath depocenters in the Late Cretaceous to Eocene strata, and on structural highs below the top basement reflector (Fig. 6.14).

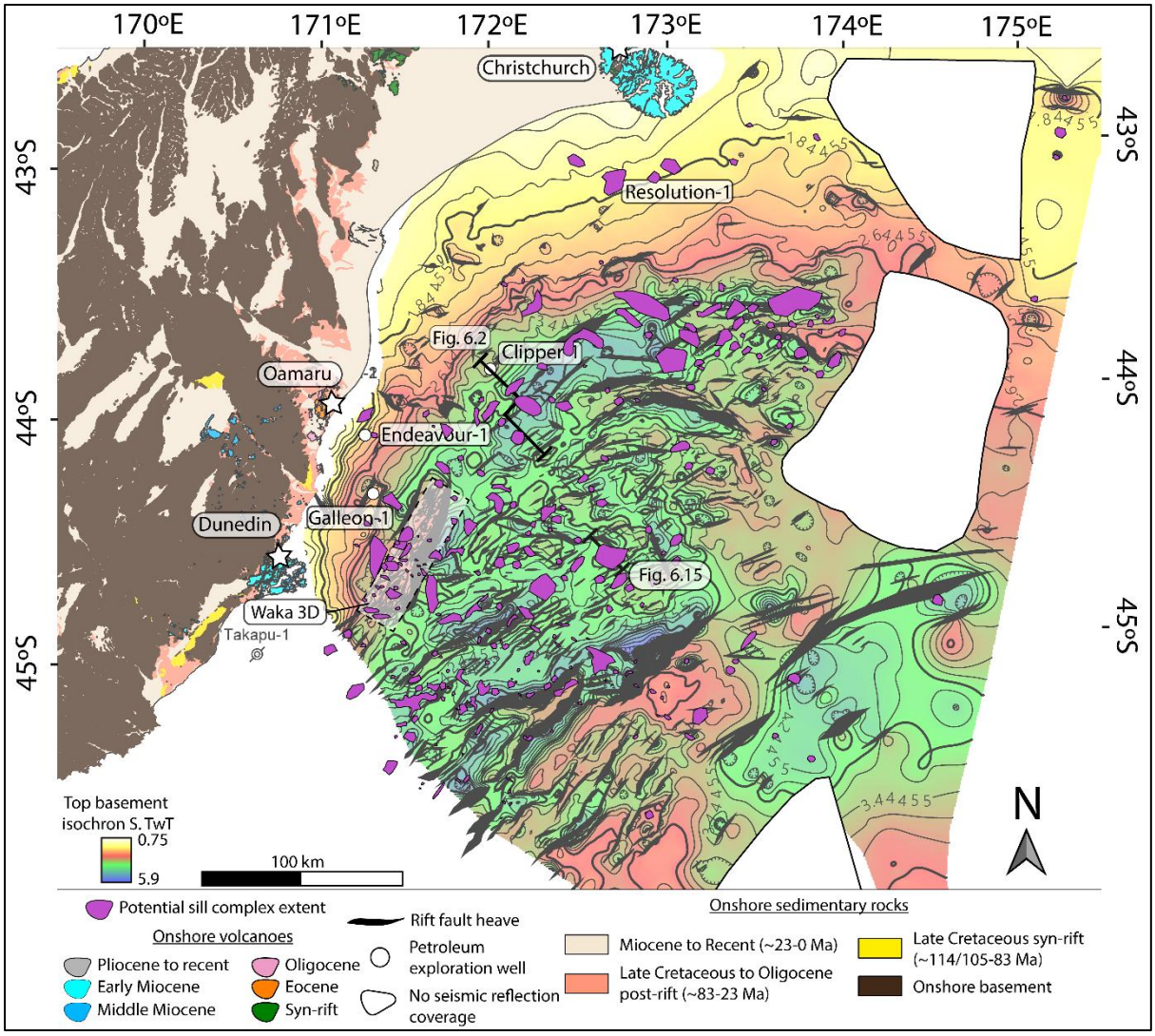

Figure 6.14 Map showing the distribution of sill intrusions which are plotted on the top basement isochron map.

Most of the intrusive features are considered to be sills. Their shape varies from strata-concordant, transgressive, or saucer-shaped (Blanke, 2013). Mapping shows areas of sills occur in swarms rather than as single sills, although it is difficult to define the extent of individual sills using a 2D dataset (Fig. 6.15). In the Canterbury Basin, sills have been previously described by Blanke (2013) using the 3D Waka seismic survey (Fig. 6.14). There they form 24 to 80 km^2 structures. By comparison, sill complexes mapped in 2D seismic reflection lines have surface areas ranging from <5 to 200 km^2. Their age is difficult to determine as most of them do not display forced folding of overlying reflectors. In cases where forced folding is

observed above the sills, such as above the Caravel High and around Resolution-1 well, the fold geometries suggest Early, Middle to Late Miocene age for the emplacement of most sills (Blanke, 2013; Bischoff, 2019). At Resolution-1, the Middle to Late Miocene age is confirmed by K^{40}/Ar^{40} dating (12 ± 2 Ma) on an intrusion drilled at 1911 meters (Milne, 1975; Bischoff, 2019).

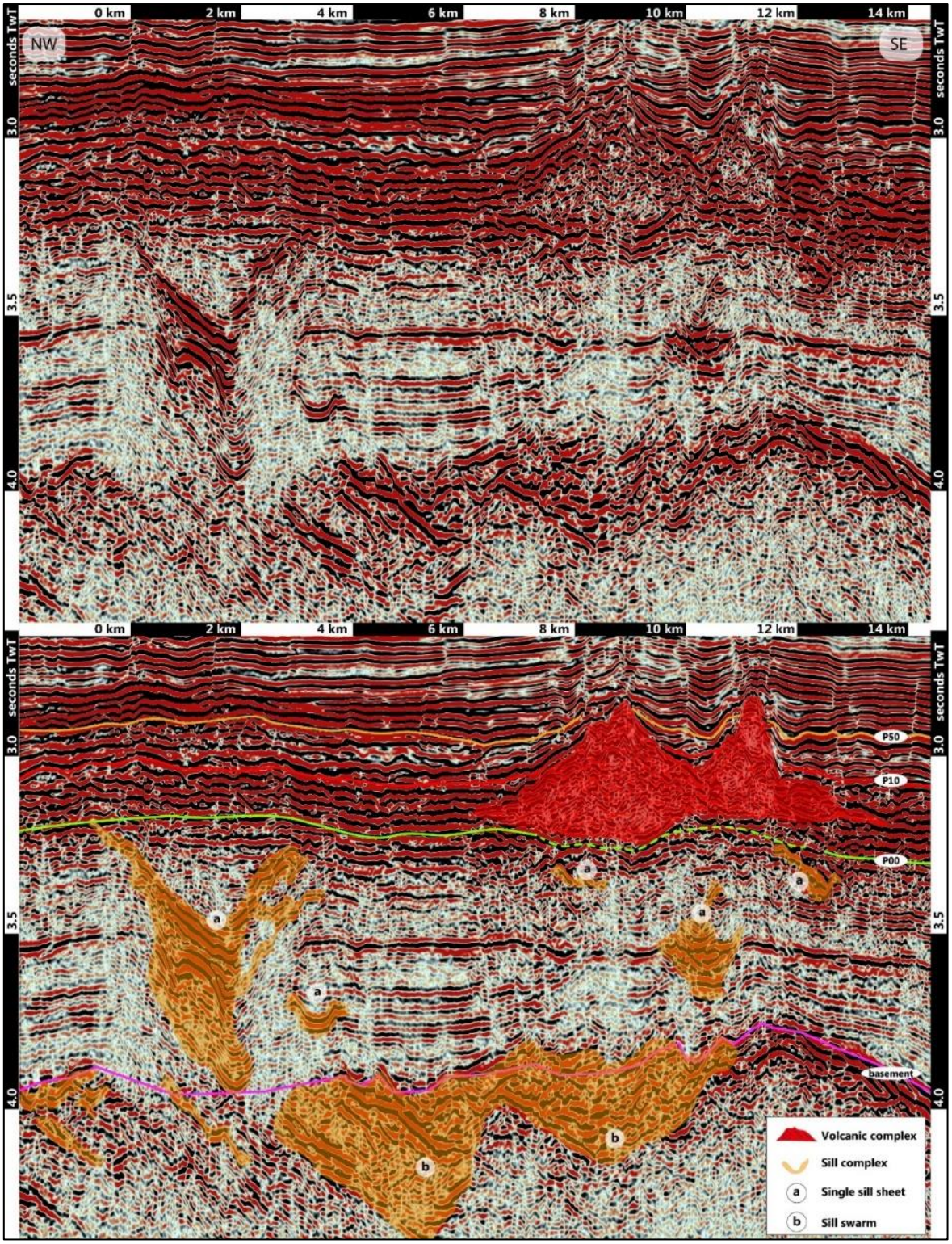

*Figure 6.15 Seismic reflection profile showing examples of different geometries of sill intrusions. Vertical axis in TwT (secs.) For the location of the seismic line see Figure 6.*14

6.5. Discussion:

6.5.1 The Evolution of Magmatism in The Canterbury Basin

The buried volcanoes identified on seismic reflection data suggest five eruptive phases marked by changes in the size of individual volcanoes over time (Fig. 6.5 and Table 6.1). These can be correlated to syn-rift, post-breakup and convergence tectonic phases of Zealandia deformation (Figs. 6.2 and Table 6.1). The five eruptive phases are:

(1) Syn-rift Late Cretaceous subduction/extension related polygenetic volcanoes.
(2) Post-breakup Late Cretaceous large volcanic complexes.
(3) Paleocene to Middle Miocene monogenetic volcanic fields.
(4) Middle to Late Miocene large volcanic complex.
(5) Pliocene to recent monogenetic volcanoes

(1) The syn-rift volcanism present in south-east offshore Canterbury Basin started at the transition from a subduction to a widespread extension during eastern Gondwana breakup. The cessation of the prolonged period of subduction (~105 Ma) that characterised the Paleozoic and Mesozoic eastern margin of Gondwana was partially synchronous with the onset of the period of rifting that started ~110 Ma and continued to ~85 Ma (Laird and Bradshaw, 2004; Davy *et al.*, 2014; see chapter 2 of this thesis for further details). This widespread phase of extension constituted the Late Cretaceous Rift Province of Zealandia and associated rift basins (Figs. 6.2 and Table 6.1 - e.g. Strogen *et al*., 2017; Tulloch *et al.*, 2019; see Chapter 2 and 3 of this thesis for further details). The Canterbury Basin was one of these rift basins, where extension created NE-SW, E-W and NW-SE sets of rift faults forming a series of horsts and half grabens (Field and Browne, 1989; Browne *et al.* 2012; Jongens *et al.*, 2012; see chapter 2 of this thesis for further details). Magmatism occurred contemporaneously with rifting, and produced silicic to intermediate magmas across the Canterbury Basin. The volcanic occurrences mapped in the offshore Canterbury Basin show a correlation between the rift structures where monogenetic to polygenetic volcanoes formed. Their maximum apparent diameter (~11.5 km) is comparable to the estimated diameter of the Mount Somers Volcanic Complex (MSVC) (~12-15 km) that crops out in onshore Canterbury Basin. The MSVC has been inferred to be related to a phase of continental extension (Field *et al.*, 1989; Laird and Bradshaw, 2004; Van der Meer *et al.*, 2016), but was influenced to some degree by subduction processes as it was formed by assimilation of Torlesse metasedimentary rock by a slightly enriched, subduction-modified, mantle-derived melt with a depleted Hf isotopic signature (Van der Meer *et al.*, 2017b). However, the syn-rift volcanoes located in the western offshore Canterbury Basin display a magnetic anomaly unlike the volcanoes located in the eastern offshore Canterbury Basin (Fig. 6.6). This could suggest a difference in magma composition between the eastern and western syn-rift buried volcanoes and therefore a difference in the magma origin. The western Canterbury Basin syn-rift volcanoes could be similar in composition and origin to the Mount Somers Volcanic Group and would have been located ~100km east of the westward subduction interface (Figs. 6.3 and 6.16 – e.g., Cooper and Palin, 2018; see chapter 4 of this thesis for further details). In the eastern Canterbury Basin, volcanism could have been influenced by rifting but remains enigmatic because of the general lack of data.

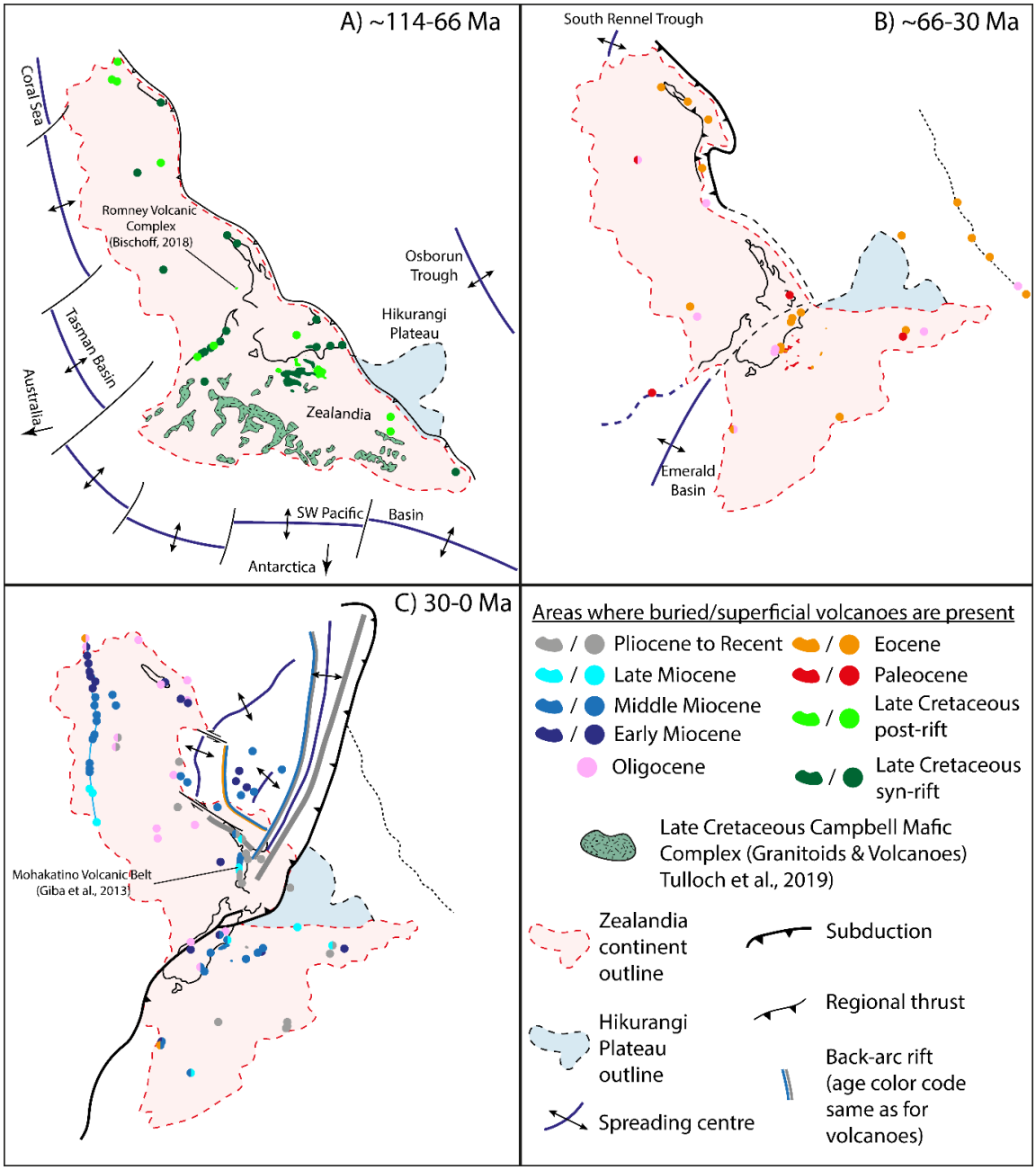

Figure 6.16 Zealandia geodynamic reconstruction showing the position of both buried and surface volcanic systems (modified from Mortimer et al., 2017 and Tulloch et al., 2019). A) Post breakup geodynamic reconstruction showing the Late Cretaceous syn- and large post-rift volcanic complexes as well as the position of the Campbell Plateau Mafic Complex (Tulloch et al., 2019). B) Shows the locations of drift phase small intraplate volcanism across Zealandia. C) Recent setting of Zealandia showing the locations of Miocene to Recent volcanic activity.

(2) Around 83 Ma, the continental crust between southern Zealandia and western Antarctica broke up along a NE-SW (present-day) axis and Zealandia started to drift away from eastern Gondwana with a progressive anti-clockwise rotation (e.g., King *et al.*, 1999). During the Late Cretaceous, post-rift volcanism in the Canterbury Basin was erupting large volumes of magma which formed large volcanic complexes (>10 km diameter) located some 900 km west of the spreading centre (Fig. 6.16). Their alignment displays a trend similar to the spreading centre and has a slight eastward curvature towards the north similar to the

progressive change in orientation of rift faults observed from south to north (Figs. 6.7 and 6.16).

(3) Paleocene to Middle Miocene volcanism marks a drastic reduction in volume of magma with mostly monogenetic volcanic fields erupting offshore. In the Oamaru volcanic field, Paleocene domes were mostly located offshore, whereas the Eocene and Oligocene volcanoes are present both onshore and along the coast. The Paleocene to Oligocene Oamaru volcanic field seems to have moved westward with time (Figs. 6.9 and 6.16). Although other volcanic fields do not suggest a similar evolution, this trend in the Oamaru volcanic field could indicate a westward younging of the volcanoes due to a source of magma that stayed fixed while Zealandia was moving anti-clockwise during its drifting. During the Paleocene, in the south-eastern offshore region, volcanism occurred along a similar trend to the rift structures and erupted in similar locations to earlier-formed syn-rift volcanoes. The onset of the eruptive activity of the Maahunui Middle Miocene volcanic field south of Banks Peninsula predates the large composite volcanoes of Banks and Otago Peninsula. However, due to a lack of dating of the cessation of eruptions, the end of its eruptive cycle could be in part synchronous to Banks Peninsula volcanic complex.

The Middle Miocene marks another change in volcanic style from (3) small eruptive domes of relative short duration to (4) large composite edifices. Banks and Otago peninsula volcanic complexes, the two large Miocene composite volcanoes, are both located over basement structural antiforms. Banks Peninsula is located on the westward extension of the Chatham Rise which formed due to Permian-Early Cretaceous subduction (Field and Browne, 1989; Browne *et al.*, 2012), whereas the Miocene volcanism of the Otago Peninsula is located in the core of the Otago schist belt (Mortimer 1993; Mortimer 2000; Deckert *et al.*, 2002).

(5) The volcanic dome found on the sea floor over the Chatham Rise corresponds to more recent volcanism of smaller magnitude and could be contemporaneous with the Late Neogene Urry Knolls volcano (Herzer, 1975; Herzer *et al.*, 1989). The extent of this volcanism is poorly constrained due to the lack of good resolution seismic data and seismic coverage in the area.

Numerous sills have been recognised on the seismic data within the basement to Eocene succession. Their exact age of emplacement is often difficult to establish due to a lack of seismic imaging, however as the volcanic activity spans the syn-rift Late Cretaceous to Recent, the age of sill emplacement could also span an equivalent period of time. The seismic reflection data do not suggest the presence of large intrusions such as batholiths, laccoliths, plutons or magma chambers, although these features could be present at greater depth than is imaged by seismic profiles and may potentially feed shallower structures such as the volcanoes and sills described here.

6.5.2 Igneous Occurrences Across Zealandia Continent

Recent maps from Mortimer *et al.*, (2017b) summarised all the known occurrences of magmatic activity across Zealandia. They contain data from outcrops and dredging in offshore regions. In this paper we add considerably to geologic coverage in the Canterbury Basin from the analysis of seismic reflection and also highlight that volcanoes in offshore sedimentary basins of Zealandia are little known.

The distribution of both syn- and post-rift Late Cretaceous volcanoes in Zealandia is shown on Figure 6.16A in their reconstructed original locations and orientations. The map shows that Late Cretaceous eruptive edifices are scattered across all of Zealandia with several edifices recognised in the north and east of the North Island, the west coast of the South Island, and the east coast of the South Island. Data from this study suggest extensive Late Cretaceous volcanism offshore Canterbury Basin. Volcanics of this age are absent in onshore Canterbury Basin and are sparse in other basins with only the Romney Volcanic Complex, offshore Taranaki Basin recognised (Rad, 2015; Bischoff, 2019). In addition, the mapping of the Late Cretaceous Campbell Mafic Complex based on magnetic anomaly data (Tulloch *et al.*, 2019) suggests an extensive Late Cretaceous area influenced by magmatism in south Zealandia where seismic coverage is absent.

The widespread Paleocene to Oligocene volcanic activity across Zealandia and the offshore Canterbury Basin data is less extensive than the Late Cretaceous one (Figure 6.16B). However, the mapping offshore Canterbury Basin considerably increases the extent of known Paleocene-Oligocene volcanic activity (Figure 6.16B). Paleocene to Oligocene volcanoes mapped across Zealandia do not show a westward migration over time as suggested by the Oamaru Volcanic Field. Very little Paleocene to Eocene volcanic activity has been described in the western region of the North Island of New Zealand and the West Coast of the South Island (e.g., Sewell and Nathan, 1987; Hoernle *et al.*, 2006).

Miocene to Recent volcanic activity is widespread across Zealandia (Figure 6.16C). In the offshore Taranaki Basin, the Mohakatino Volcanic Belt corresponds to a series of volcanoes younging towards the south (Giba *et al.*, 2013) and indicates that some buried volcanoes are present.

The buried volcanoes recognised in offshore Canterbury Basin using seismic reflection data as well as other similar features recognised in the Taranaki Basin indicate the potential for many more volcanic centres to be discovered in Zealandia sedimentary basins. Seismic data is a valuable tool for determining the extent of buried magmatic objects and improve the knowledge of what is known to date. The volcanoes mapped from onshore outcrop data probably under represent the full extent of magmatic features in Zealandia.

6.6. Conclusion

Buried volcanoes and intrusions are present in most of the Canterbury Basin, erupting intermittently from the Late Cretaceous to Pleistocene time. Seismic reflection data presented here permitted the mapping of 185 volcanoes forming a total surface area of ~4775 km^2 and is approximately a factor of three greater than the surface area of 1555 km^2 for onshore volcanoes. Their size and distribution vary in time and space and they can be grouped into 5 volcanic phases:

- (1) Widespread volcanic activity related to subduction-extension processes from ~110 to 85 Ma. This phase corresponds to monogenetic to polygenetic volcanoes of up to 5 km diameter where the majority is located in the south-eastern Canterbury Basin along rift faults. They are synchronous with the Mount Somers Volcanic Complex and with the Kyeburn and Shag Point Ignimbrites that are related to subduction processes. However, the mid-Cretaceous volcanoes located in the south-eastern offshore, >200km away from the western subduction interface, display a close relation to the rifting. Therefore, they could have a different composition than the MSVC.

- (2) Large composite volcanoes formed in the Late Cretaceous during the post breakup phase of basin evolution. These volcanoes are not observed onshore, but offshore, large composite volcanoes are aligned along a NE-SW trend parallel rift faults. Three main volcanic complexes of >10 km apparent diameter erupted during the post rift Late Cretaceous. They are named, from north to south, the Sloop, Barque and East Takapu volcanic complexes. They were accompanied by other monogenetic to polygenetic volcanic edifices of a few kilometres apparent diameter in their surroundings.
- (3) Paleogene to Middle Miocene emplacement of small monogenetic domes with apparent diameters of kilometres. They were forming volcanic fields that were mostly located around the Oamaru region (Paleocene to Oligocene) both onshore and offshore, as well as offshore, south of Banks Peninsula (Early Miocene). Volcanoes formed monogenetic domes. Other Paleocene volcanoes were present in the south-east offshore Canterbury Basin still showing some alignment with rift structures.
- (4) Middle to Late Miocene eruption of large composite volcanoes produced large volumes of magma located onshore forming both Banks and Otago peninsulas.
- (5) Pliocene to Quaternary sporadic small domes erupting offshore along the Chatham Rise.

Our mapping in the offshore areas has increased the known aerial extent of volcanism in the Canterbury Basin by 300%. Numerous intrusions are also present in the Canterbury Basin as sills. Seismic data doesn't allow imaging batholiths or plutons which, if present, are below the seismic data (e.g., >10 km depth). Buried volcanoes are known to be locally present offshore in other Late Cretaceous rift basins of Zealandia, and detailed mapping using seismic reflection data could provide new insights into the magmatic evolution of the Zealandia continent.

6. Acknowledgments

We acknowledge the funding support provided by the Mason Trust from the Department of Geological Sciences, University of Canterbury. GHB acknowledges funding from the NZ government (MBIE) through Strategic Funding to GNS Science and the Sedimentary Basin Research programme.

6. References

ADAMS, C. & OLIVER, P. (1979) Potassium-Argon Dating of Mt Somers Volcanics, South Island, New Zealand: Limitations in Dating Mesozoic Volcanic Rocks. New Zealand Journal of Geology and Geophysics, 22, 455-463 pp.

ADAMS, C.J., CAMPBELL, H.J., MORTIMER, N. & GRIFFIN, W.L. (2017) Perspectives on Cretaceous Gondwana Break-up from Detrital Zircon Provenance of Southern Zealandia Sandstones. Geological Magazine, 154, 661-682 pp.

ANDREW, P.B., FIELD, B.D., BROWNE, G.H., MCLENNAN, J.M., (1987) Lithostratigraphic Nomenclature for the Upper Cretaceous and Tertiary Sequence of Central Canterbury, New Zealand. New Zealand geological Survey record, 24, 40p.

ASHWELL, P., KENNEDY, B., EDWARDS, M. & COLE, J. (2018) Characteristics and Consequences of Lava Dome Collapse at Ruawahia, Taupo Volcanic Zone, New Zealand. Bulletin of Volcanology, 80, 43p.

BARLEY, M.E., WEAVER, S.D. & DE LAETER, J.R. (1988) Strontium Isotope Composition and Geochronology of Intermediate—Silicic Volcanics, Mt Somers and Banks Peninsula, New Zealand. New Zealand Journal of Geology and Geophysics, 31, 197-206.

BARRIER, A. (2015) Impact of the Tectonic on the Oligocene Ranong Delta Distribution and Regional Sedimentological Characterization (Andaman Sea, East Indian Ocean). Internal report Institut Polytechnique LaSalle Beauvais.

BECKMAN, D.W. (2012) Final Interpretation Report for Acb11, Offshore Canterbury, New Zealand. Ministry of Economic Development Petroleum Report Series, PR4492, 50p.

BEGGS, M. (2016) Barque Prospect, Offshore Canterbury Basin: Impact of 3d Seismic on Evaluation of a Giant Structural Prospect. Petroleum New Zealand Conference 2016, Auckland.

BENSON, W.N. (1968) Dunedin District, 1:50 000 New Zealand Geological Survey Miscellaneous Series Map 1. . Wellington, New Zealand. Department of Scientific and Industrial Research.

BISCHOFF, A. (2019) Architectural Elements of Buried Volcanic Systems and Their Impact on Geoenergy Resources, Ph.D. Thesis, Canterbury University, New Zealand. Pre-print.

BISCHOFF, A.P., NICOL, A. & BEGGS, M. (2017) Stratigraphy of Architectural Elements in a Buried Volcanic System and Implications for Hydrocarbon Exploration. Interpretation, 5, 141-159 pp.

BISHOP, D. (1979) Sheet S135 Ranfurly.“Geological Map of New Zealand 1: 63 360”. Map (1 sheet) and notes (20 p.). New Zealand Department of Scientific and Industrial Research, Wellington.

BISHOP, D.G., TURNBULL, I.M., COMPILERS (1996) Geology of the Dunedin Area. Institute of Geological and Nuclear Sciences, 1:250 000 Geological map 21, 1-52 pp.

BLANKE, S.J. (2013) "Saucer Sills" of the Offshore Canterbury Basin. Advantage NZ Petroleum Conference, Auckland.

BOILLOT, G. & COULON, C. (1998) La Déchirure Continentale Et L'ouverture Océanique: Géologie Des Marges Passives. G & B Pub, 208p.

BP, AQUITAINE, S. & TODD (1984) Interpretation and Prospectivity of Ppl 38203 Canterbury Basin, New Zealand. New Zealand Geological Survey Library, Petroleum Report 1046.

BROWNE, G. (1983) A New Interpretation of Brecciation in the Sandpit Tuff, Harper Hills, Canterbury. New Zealand Journal of Geology and Geophysics, 26, 429-434 pp.

BROWNE, G.H. & NAISH, T.R. (2003) Facies Development and Sequence Architecture of a Late Quaternary Fluvial-Marine Transition, Canterbury Plains and Shelf, New Zealand: Implications for Forced Regressive Deposits. Sedimentary Geology, 158, 57-86 pp.

BROWNE, G.H., FIELD, B.D., BARRELL, D.J.A., JONGENS, R., BASSETT, K.N. & WOOD, R.A. (2012) The Geological Setting of the Darfield and Christchurch Earthquakes. New Zealand Journal of Geology and Geophysics, 55, 193-197 pp.

BROWNE, G.H., FIELD, B.D. (1985) The Lithostratigraphy of Late Cretaceous to Early Pleistocene Rocks of Northern Canterbury, New Zealand. New Zealand Geological Survey Record, 6, 63p.

CARLSON, J., GRANT-MACKIE, J. & RODGERS, K. (1980) Stratigraphy and Sedimentology of the Coalgate Area, Canterbury, New Zealand. New Zealand journal of geology and geophysics, 23, 179-192 pp.

CAS, R., LANDIS, C. & FORDYCE, R. (1989) A Monogenetic, Surtla-Type, Surtseyan Volcano from the Eocene-Oligocene Waiareka-Deborah Volcanics, Otago, New Zealand: A Model. Bulletin of Volcanology, 51, 281-298 pp.

COOMBS, D. & DICKEY, J. (1965) The Early Tertiary Petrographic Province of North-East Otago: Waiareka and Deborah Volcanic Formations. NZ Dept. Scientific and Industrial Research, Information Series, 51, 38-54 pp.

COOMBS, D.S., CAS, R., KAWACHI, Y., LANDIS, C., MCDONOUGH, W. & REAY, A. (1986) Cenozoic Volcanism in North, East and Central Otago. Royal Society of New Zealand Bulletin, 23, 278-312 pp.

COOPER, A.F. & PALIN, J.M. (2018) Two-Sided Accretion and Polyphase Metamorphism in the Haast Schist Belt, New Zealand: Constraints from Detrital Zircon Geochronology. GSA Bulletin, 130, 1501-1518 pp.

COOPER, R., AGTERBERG, F.P., ALLOWAY, B., BEU, A., CAMPBELL, H., CRAMPTON, J.S., CROUCH, E., CRUNDWELL, M., GRAHAM, I.J., HOLLIS, C., JONES, C., KAMP, P.,

MILDENHALL, D.C., MORGANS, H., NAISH, T.R., RAINE, J.I., RONCAGLIA, L., SADLER, P.M., SCHIØLER, P. & WILSON, G. (2004) The New Zealand Geological Timescale. 22, 284p.

CRAMPTON, J.S.H., C.J.; RAINE, J.I.; RONCAGLIA, L.; SCHIOLER, P.; STRONG, C.P.; WILSON, G.J. (2004) Cretaceous (Taitai, Clarence, Raukumara and Mata Series). In: The New Zealand Geological Timescale (Ed. Cooper, R.A.) Institute of Geological & Nuclear Sciences monograph, 22, 102-122 pp.

DAVY, B. (2014) Rotation and Offset of the Gondwana Convergent Margin in the New Zealand Region Following Cretaceous Jamming of Hikurangi Plateau Large Igneous Province Subduction. Tectonics, 33, 1577-1595 pp.

DE SILVA, S. & LINDSAY, J.M. (2015) Primary Volcanic Landforms. The Encyclopedia of Volcanoes (Second Edition), 273-297 pp.

DECKERT, H., RING, U. & MORTIMER, N. (2002) Tectonic Significance of Cretaceous Bivergent Extensional Shear Zones in the Torlesse Accretionary Wedge, Central Otago Schist, New Zealand. New Zealand Journal of Geology and Geophysics, 45, 537-547 pp.

DORÉ, T. & LUNDIN, E. (2015) Research Focus: Hyperextended Continental Margins—Knowns and Unknowns. Geology, 43, 95-96 pp.

DUGGAN, M. & REAY, A. (1986) The Timaru Basalt. Royal Society of New Zealand Bulletin, 23, 246-277 pp.

EIDE, C.H., SCHOFIELD, N., LECOMTE, I., BUCKLEY, S.J. & HOWELL, J.A. (2018) Seismic Interpretation of Sill Complexes in Sedimentary Basins: Implications for the Sub-Sill Imaging Problem. Journal of the Geological Society, 175, 193-209 pp.

ENERGY, I.-P. (2000) Ealing-1 Well Completion Report. Ministry of Economic Development New Zelanad Unpublished Petroleum Report, PR 2559, 280p.

FIELD, B.D. & BROWNE, G.H. (1989) Cretaceous and Cenozoic Sedimentary Basins and Geological Evolution of the Canterbury Region, South Island, New Zealand. Institute of Geological & Nuclear Sciences monograph, 2, 94p.

FIELD, B.D., BROWNE, G.H. (1986) Lithostratigraphy of Cretaceous and Tertiary Rocks, Southern Canterbury, New Zealand. New Zealand Geological Survey basin studies, 14, 55p.

FRANKE, D. (2013) Rifting, Lithosphere Breakup and Volcanism: Comparison of Magma-Poor and Volcanic Rifted Margins. Marine and Petroleum Geology, 43, 63-87 pp.

GAGE, M. (1957) The Geology of the Waitaki Subdivision. New Zelaand Geological Survey Bulletin, 55, 135p.

GAGE, M. (1970) Late Cretaceous and Tertiary Rocks of Broken River, Canterbury. New Zealand journal of geology and geophysics, 13, 507-536 pp.

GALLAND, O., BERTELSEN, H., EIDE, C., GULDSTRAND, F., HAUG, Ø., LEANZA, H.A., MAIR, K., PALMA, O., PLANKE, S. & RABBEL, O. (2018) Storage and Transport of Magma in the Layered Crust—Formation of Sills and Related Flat-Lying Intrusions. In: Volcanic and Igneous Plumbing Systems, 113-138 pp.

GIBA, M., WALSH, J., NICOL, A., MOUSLOPOULOU, V. & SEEBECK, H. (2013) Investigation of the Spatio-Temporal Relationship between Normal Faulting and Arc Volcanism on Million-Year Time Scales. Journal of the Geological Society, 170, 951-962 pp.

GREGG, D. (1964) Sheet 18—Hurunui Geological Map of New Zealand 1:250,000 Wellington: N.Z. Department of Scientific and Industrial Research.

HAMPTON, S. & COLE, J. (2009) Lyttelton Volcano, Banks Peninsula, New Zealand: Primary Volcanic Landforms and Eruptive Centre Identification. Geomorphology, 104, 284-298 pp.

HAMPTON, S., COLE, J. & BELL, D. (2012) Syn-Eruptive Alluvial and Fluvial Volcanogenic Systems within an Eroding Miocene Volcanic Complex, Lyttelton Volcano, Bank Peninsula, New Zealand. New Zealand Journal of Geology and Geophysics, 55, 53-66.

HERZER, R. (1975) Uneven Submarine Topography South of Mernoo Gap—the Result of Volcanism and Submarine Sliding. New Zealand Journal of Geology and Geophysics, 18, 183-188 pp.

HERZER, R., CHALLIS, G., CHRISTIE, R., SCOTT, G. & WATTERS, W. (1989) The Urry Knolls, Late Neogene Alkaline Basalt Extrusives, Southwestern Chatham Rise. Journal of the Royal Society of New Zealand, 19, 181-193 pp.

HIGGS, K.E., BROWNE, G.H. & SAHOO, T.R. (2019) Reservoir Characterisation of Syn-Rift and Post-Rift Sandstones in Frontier Basins: An Example from the Cretaceous of Canterbury and Great South Basins, New Zealand. Marine and Petroleum Geology, 101, 1-29 pp.

HILDRETH, W. (2007) Quaternary Magmatism in the Cascades: Geologic Perspectives. US Geological Survey, 1744, 125p.

HOERNLE, K., WHITE, J.V., VAN DEN BOGAARD, P., HAUFF, F., COOMBS, D., WERNER, R., TIMM, C., GARBE-SCHÖNBERG, D., REAY, A. & COOPER, A. (2006) Cenozoic

Intraplate Volcanism on New Zealand: Upwelling Induced by Lithospheric Removal. Earth and Planetary Science Letters, 248, 350-367 pp.

HOLFORD, S., SCHOFIELD, N., MACDONALD, J., DUDDY, I. & GREEN, P. (2012) Seismic Analysis of Igneous Systems in Sedimentary Basins and Their Impacts on Hydrocarbon Prospectivity: Examples from the Southern Australian Margin. The APPEA Journal, 52, 229-252 pp.

INFANTE-PAEZ, L., MARFURT, K.J. & WALLET, B. (2018) Igneous Bodies That Look Like Sedimentary Features in Seismic Data: A Way to Avoid Pitfalls in Seismic Interpretation. SEG Technical Program Expanded Abstracts 2018, Society of Exploration Geophysicists, 1613-1617 pp.

JERRAM, D.A., SINGLE, R.T., HOBBS, R.W. & NELSON, C.E. (2009) Understanding the Offshore Flood Basalt Sequence Using Onshore Volcanic Facies Analogues: An Example from the Faroe–Shetland Basin. Geological Magazine, 146, 353-367 pp.

JONGENS, R., BARRELL, D.J.A., CAMPBELL, J.K. & PETTINGA, J.R. (2012) Faulting and Folding beneath the Canterbury Plains Identified Prior to the 2010 Emergence of the Greendale Fault. New Zealand Journal of Geology and Geophysics, 55, 169-176 pp.

KERESZTURI, G. & NÉMETH, K. (2012) Monogenetic Basaltic Volcanoes: Genetic Classification, Growth, Geomorphology and Degradation. In: Updates in Volcanology-New Advances in Understanding Volcanic Systems, InTech, 3-88 pp.

KING, P.R., NAISH, T.R., BROWNE, G.H., FIELD, B.D. & EDBROOKE, S.W. (1999) Cretaceous to Recent Sedimentary Patterns in New Zealand. Institute of Geological and Nuclear Sciences Folio Series 1, 35p.

KLARNER, S. & KLARNER, O. (2012) Identification of Paleo-Volcanic Rocks on Seismic Data. In: Updates in Volcanology-A Comprehensive Approach to Volcanological Problems, IntechOpen, 181–206 pp.

LAIRD, M.G. & BRADSHAW, J.D. (2004) The Break-up of a Long-Term Relationship: The Cretaceous Separation of New Zealand from Gondwana. Gondwana Research, 7, 273-286 pp.

LEWIS, K., BENNETT, D., HERZER, R. & VONDERBORCH, C. (1986) Seismic Stratigraphy and Structure Adjacent to an Evolving Plate Boundary, Western Chatham Rise, New-Zealand. in Blakeslee, J.H., Initial reports of the Deep Sea Drilling Project, Leg 90, Sites 587–594 90, 1325-1338 pp.

MAGEE, C., HUNT-STEWART, E. & JACKSON, C.A.-L. (2013) Volcano Growth Mechanisms and the Role of Sub-Volcanic Intrusions: Insights from 2d Seismic Reflection Data. Earth and Planetary Science Letters, 373, 41-53 pp.

MAICHER, D. (1999) Hyaloclastite Beds of Shelf and Seamount: Roles of Exsolution, Entrapment and Entrainment. Unpublished PhD dissertation Thesis, University of Otago, Dunedin, New Zealand, 272p.

MARSAGLIA, K.M., BROWNE, G.H., GEORGE, S.C., KEMP, D.B., JAEGER, J.M., CARSON, D. & RICHAUD, M. (2017) The Transformation of Sediment into Rock: Insights from Iodp Site U1352, Canterbury Basin, New Zealand. Journal of Sedimentary Research, 87, 272-287 pp.

MCLENNAN, J. (1981) The Cretaceous – Tertiary Rocks of Avoca, Oxford and Burnt Hill, Northwestern Canterbury, University of Canterbury MSc Thesis, 234p.

MCMILLAN, S.G. (1999) Geology of Northeast Otago: Hampden (J42) and Palmerston (J43). Institute of Geological & Nuclear Sciences.

MENZIES, M.A., KLEMPERER, S.L., EBINGER, C.J. & BAKER, J. (2002) Characteristics of Volcanic Rifted Margins. Special Papers-Geological Society of America, 1-14 pp.

MILNE, A.D. (1975) Well Completion Report Resolution. Todd Canterbury Service Limited. New Zealand Geological Survey Open-file Petroleum Report PR648, 149p.

MORDENSKY, S.P. & WALLACE, P.J. (2018) Magma Storage Below Cascades Shield Volcanoes as Inferred from Melt Inclusion Data: A Comparison of Long-Lived and Short-Lived Magma Plumbing Systems. Journal of Volcanology and Geothermal Research, 368, 1-12 pp.

MORTIMER, N. (1993) Geology of the Otago Schist and Adjacent Rocks. Scale 1:500 000. Lower Hutt: Institute of Geological & Nuclear Sciences. Institute of Geological & Nuclear Sciences geological map 7.

MORTIMER, N. (2000) Metamorphic Discontinuities in Orogenic Belts: Example of the Garnet–Biotite–Albite Zone in the Otago Schist, New Zealand. International Journal of Earth Sciences, 89, 295-306 pp.

MORTIMER, N., RATTENBURY, M.S., KING, P.R., BLAND, K.J., BARRELL, D.J.A., BACHE, F., BEGG, J.G., CAMPBELL, H.J., COX, S.C., CRAMPTON, J.S., EDBROOKE, S.W., FORSYTH, P.J., JOHNSTON, M.R., JONGENS, R., LEE, J.M., LEONARD, G.S., RAINE, J.I., SKINNER, D.N.B., TIMM, C., TOWNSEND, D.B., TULLOCH, A.J., TURNBULL, I.M. & TURNBULL, R.E. (2014) High-Level Stratigraphic Scheme for New Zealand Rocks. New Zealand Journal of Geology and Geophysics, 57, 402-419 pp.

MORTIMER, N., CAMPBELL, H.J., TULLOCH, A.J., KING, P.R., STAGPOOLE, V.M., WOOD, R.A., RATTENBURY, M.S., SUTHERLAND, R., ADAMS, C.J., COLLOT, J. & SETON, M. (2017a) Zealandia: Earth's Hidden Continent. GSA Today, 27, 27-35 pp.

MORTIMER, N., GANS, P.B., MEFFRE, S., MARTIN, C.E., SETON, M., WILLIAMS, S., TURNBULL, R.E., QUILTY, P.G., MICKLETHWAITE, S., TIMM, C., SUTHERLAND, R., BACHE, F., Collot, J., Maurizot, P., Rouillard, P. & Rollet, N. (2017b) Regional Volcanism of Northern Zealandia: Post-Gondwana Break-up Magmatism on an Extended, Submerged Continent. Geological Society, London, Special Publications, 463, 28p.

Mortimer, N., van den Bogaard, P., Hoernle, K., Timm, C., Gans, P., Werner, R. & Riefstahl, F. (2019) Late Cretaceous Oceanic Plate Reorganization and the Breakup of Zealandia and Gondwana. Gondwana Research, 65, 31-42.

Mutch, A. (1963) Sheet 23 Oamaru (1st Edition) Geological Map of New Zealand 1: 250 000. . Department of scientific and Industrial Research, Wellington, New Zealand.

NEAL, C., BRANTLEY, S., ANTOLIK, L., BABB, J., BURGESS, M., CALLES, K., CAPPOS, M., CHANG, J., CONWAY, S. & DESMITHER, L. (2019) The 2018 Rift Eruption and Summit Collapse of Kīlauea Volcano. Science, 363, 367-374 pp.

NEMETH, K. (2010) Monogenetic Volcanic Fields: Origin, Sedimentary Record, and Relationship with Polygenetic Volcanism. The Geological Society of America Special Paper, 470, 43-66 pp.

NÉMETH, K. & KERESZTURI, G. (2015) Monogenetic Volcanism: Personal Views and Discussion. International Journal of Earth Sciences, 104, 2131-2146 pp.

OLIVER, P.J. (1984). The Mid-Cretaceous Volcanic Rocks of Rakaia Gorge and Malvern Hills Area, Canterbury. New Zealand Geological Survey Record, 3, 86-91 pp.

OLIVER, P.J. & KEENE, H.W. (1989) Sheet K36 Ac & Part Sheet K35 Mount Somers. Geological Map of New Zealand 1:50 000. Map (One Sheet) and Notes. . Wellington, New Zealand. Department of Scientific and Industrial Research.

PÉREZ-LÓPEZ, R., LEGRAND, D., GARDUÑO-MONROY, V., RODRÍGUEZ-PASCUA, M. & GINER-ROBLES, J. (2011) Scaling Laws of the Size-Distribution of Monogenetic Volcanoes within the Michoacán-Guanajuato Volcanic Field (Mexico). Journal of Volcanology and Geothermal Research, 201, 65-72 pp.

PLANKE, S. & ALVESTAD, E. (1999) Seismic Volcanostratigraphy of the Extrusive Breakup Complexes in the Northeast Atlantic: Implications from Odp/Dsdp Drilling. Proceedings of the Ocean Drilling Program, Scientific Results, Ocean Drilling Program College Station, Tex, 163, 3-16 pp.

PLANKE, S., ALVESTAD, E. & ELDHOLM, O. (1999) Seismic Characteristics of Basaltic Extrusive and Intrusive Rocks. The Leading Edge, 18, 342-348 pp.

PLANKE, S., RASMUSSEN, T., REY, S.S. & MYKLEBUST, R. (2005) Seismic Characteristics and Distribution of Volcanic Intrusions and Hydrothermal Vent Complexes in the Vøring and Møre Basins. Geological Society, London, Petroleum Geology Conference series, 6, 833-844 pp.

RAD, F. (2015) Pep 38451 Romney-1 Well Completion Report. NZP&M, Ministry of Business, Innovation & Employment (MBIE), New Zealand, Unpublished Petroleum Report PR4951, 980p.

RAINE, J.I., BEU, A.G., BOYES, A.F., CAMPBELL, H.J., COOPER, R.A., CRAMPTON, J.S., CRUNDWELL, M.P., HOLLIS, C.J., MORGANS, H.E.G. & MORTIMER, N. (2015) New Zealand Geological Timescale Nzgt 2015. New Zealand Journal of Geology and Geophysics, 58, 398-403 pp.

REAY, A. & SIPIERA, P. (1987) Mantle Xenoliths from the New Zealand Region. Mantle xenoliths: Chichester, UK, John Wiley and Sons, 347-358 pp.

RESTON, T. (2009) The Structure, Evolution and Symmetry of the Magma-Poor Rifted Margins of the North and Central Atlantic: A Synthesis. Tectonophysics, 468, 6-27 pp.

RESTON, T. & MANATSCHAL, G. (2011) Rifted Margins: Building Blocks of Later Collision. In: Arc-continent collision, Springer, Berlin, Heidelberg, 3-21 pp.

REYNOLDS, P., HOLFORD, S. & SCHOFIELD, N. (2016) The Facies Architecture of Submarine Basaltic Volcanoes and Their Effects on Fluid Flow. ASEG Extended Abstracts, 2016, 1-6 pp.

ROGERS, N. (2006) Basaltic Magmatism and the Geodynamics of the East African Rift System. Geological Society, London, Special Publications, 259, 77-93 pp.

SAHOO, T.R., KROEGER, K.F., THRASHER, G., MUNDAY, S., MINGARD, H., COZENS, N. & HILL, M. (2015) Facies Distribution and Impact on Petroleum Migration in the Canterbury Basin, New Zealand. In: Eastern Australian Basins Symposium 2015: Publication of Proceedings. Petroleum Exploration Society of Australia, Perth, WA, 187-202 pp.

SAUTTER, B., PUBELLIER, M., JOUSSELIN, P., DATTILO, P., KERDRAON, Y., CHOONG, C.M. & MENIER, D. (2017) Late Paleogene Rifting Along the Malay Peninsula Thickened Crust. Tectonophysics, 710, 205-224 pp.

SAWYER, D.S., COFFIN, M.F., RESTON, T.J., STOCK, J.M. & HOPPER, J.R. (2007) Cobboom: The Continental Breakup and Birth of Oceans Mission. Scientific Drilling, 5, 13-25 pp.

SCHIØLER, P.R., J.I., COMPILERS (2011) Revised Biostratigraphy and Well Correlation, Canterbury Basin, New Zealand. GNS Science Consultancy Report 2011/12, PR4365, 142p.

SCHOFIELD, N., JERRAM, D.A., HOLFORD, S., ARCHER, S., MARK, N., HARTLEY, A., HOWELL, J., MUIRHEAD, D., GREEN, P., HUTTON, D. & STEVENSON, C. (2018) Sills in Sedimentary Basins and Petroleum Systems. In: Physical Geology of Shallow Magmatic Systems: Dykes, Sills and Laccoliths, Springer International Publishing, 273-294 pp.

SEWELL, R. & NATHAN, S. (1987) Geochemistry of Late Cretaceous an Early Tertiary Basalts from South Westland. New Zealand Geological Survey Record, 18, 87-94 pp.

SEWELL, R. (1988) Late Miocene Volcanic Stratigraphy of Central Banks Peninsula, Canterbury, New Zealand. New Zealand Journal of Geology and Geophysics, 31, 41-64 pp.

SEWELL, R. & GIBSON, I. (1988) Petrology and Geochemistry of Tertiary Volcanic Rocks from Inland Central and South Canterbury, South Island, New Zealand. New Zealand Journal of Geology and Geophysics, 31, 477-492 pp.

SEWELL, R.J. & WEAVER, S.D. (1990) Sheet N36ac—Akaroa Harbour. 1:50 000 map sheet and notes. Wellington, New Zealand.Department of Scientific and Industrial Research.

SHELLEY, D. (1987) Lyttelton 1 and Lyttelton 2, the Two Centres of Lyttelton Volcano. New Zealand journal of geology and geophysics, 30, 159-168 pp.

SIGMUNDSSON, F., EINARSSON, P., HJARTARDÓTTIR, Á.R., DROUIN, V., JÓNSDÓTTIR, K., ÁRNADÓTTIR, T., GEIRSSON, H., HREINSDÓTTIR, S., LI, S. & ÓFEIGSSON, B.G. (2018) Geodynamics of Iceland and the Signatures of Plate Spreading. Journal of Volcanology and Geothermal Research, In Press.

SMITH, T. & COLE, J. (1997) Somers Ignimbrite Formation: Cretaceous High-Grade Ignimbrites from South Island, New Zealand. Journal of volcanology and geothermal research, 75, 39-57 pp.

STROGEN, D.P., SEEBECK, H., NICOL, A. & KING, P.R. (2017) Two-Phase Cretaceous – Paleocene Rifting in the Taranaki Basin Region, New Zealand; Implications for Gondwana Break-Up. Journal of the Geological Society, 174, 929-946 pp.

STROGEN, D.P.K., P.R. (2014) A New Zealandia-Wide Seismic Horizon Naming Scheme. GNS Science Report, 2014/34, 20p.

TAPPENDEN, V.E. (2003) Magmatic Response to the Evolving New Zealand Margin of Gondwana During the Mid-Late Cretaceous. PhD thesis, University of Canterbury, 376p.

THOMPSON, N.K., BASSETT, K.N. & REID, C.M. (2014) The Effect of Volcanism on Cool-Water Carbonate Facies During Maximum Inundation of Zealandia in the Waitaki–Oamaru Region. New Zealand Journal of Geology and Geophysics, 57, 149-169 pp.

TIMM, C., HOERNLE, K., WERNER, R., HAUFF, F., VAN DEN BOGAARD, P., WHITE, J., MORTIMER, N. & GARBE-SCHÖNBERG, D. (2010) Temporal and Geochemical Evolution of the Cenozoic Intraplate Volcanism of Zealandia. Earth-Science Reviews, 98, 38-64 pp.

TUGEND, J., GILLARD, M., MANATSCHAL, G., NIRRENGARTEN, M., HARKIN, C., EPIN, M.-E., SAUTER, D., AUTIN, J., KUSZNIR, N. & MCDERMOTT, K. (2018) Reappraisal of the Magma-Rich Versus Magma-Poor Rifted Margin Archetypes. Geological Society, London, Special Publications, 476, SP476. 479p.

TULLOCH, A., MORTIMER, N., IRELAND, T., WAIGHT, T., MAAS, R., PALIN, M., SAHOO, T., SEEBECK, H., SAGAR, M., BARRIER, A. & TURNBULL, R. (2019) Reconnaissance Basement Geology and Tectonics of South Zealandia. Tectonics, 38, 516-551 pp.

TULLOCH, A.J., RAMEZANI, J., MORTIMER, N., MORTENSEN, J., VAN DEN BOGAARD, P. & MAAS, R. (2009) Cretaceous Felsic Volcanism in New Zealand and Lord Howe Rise (Zealandia) as a Precursor to Final Gondwana Break-Up. Geological Society, London, Special Publications, 321, 89-118 pp.

VAN DER MEER, Q., WAIGHT, T.E., WHITEHOUSE, M.J. & ANDERSEN, T. (2017) Age and Petrogenetic Constraints on the Lower Glassy Ignimbrite of the Mount Somers Volcanic Group, New Zealand. New Zealand Journal of Geology and Geophysics, 60, 209-219 pp.

VAN DER MEER, Q., WAIGHT, T.E., TULLOCH, A., WHITEHOUSE, M.J. & ANDERSEN, T. (2018) Magmatic Evolution During the Cretaceous Transition from Subduction to Continental Break-up of the Eastern Gondwana Margin (New Zealand) Documented by in-Situ Zircon O–Hf Isotopes and Bulk-Rock Sr–Nd Isotopes. Journal of Petrology, 59, 849-880 pp.

VAN DER MEER, Q.H., STOREY, M., SCOTT, J.M. & WAIGHT, T.E. (2016) Abrupt Spatial and Geochemical Changes in Lamprophyre Magmatism Related to Gondwana

Fragmentation Prior, During and after Opening of the Tasman Sea. Gondwana Research, 36, 142-156 pp.

VAN DER MEER, Q.H.A., WAIGHT, T.E., SCOTT, J.M. & MÜNKER, C. (2017) Variable Sources for Cretaceous to Recent Himu and Himu-Like Intraplate Magmatism in New Zealand. Earth and Planetary Science Letters, 469, 27-41 pp.

WARREN, G. & SPEDEN, I.G. (1978) The Piripauan and Haumurian Stratotypes (Mata Series, Upper Cretaceous) and Correlative Sequences in the Haumurian Bluff District, South Marlborough (S56). . New Zealand Geological Survey bulletin 92, 60p.

WEAVER, S. & PANKHURST, R. (1991) A Precise Rb-Sr Age for the Mandamus Igneous Complex, North Canterbury, and Regional Tectonic Implications. New Zealand journal of geology and geophysics, 34, 341-345 pp.

WELLMAN, H.W. (1979) An Uplift Map for the South Island of New Zealand and a Model for Uplift of the Southern Alps. In: The Origin of the Southern Alps (Ed. Walcott, R.I. & Cresswell, M.M.). Royal Society of New Zealand Bulletin, 18, 13-20 pp.

WILDING, A.S., L.A.D (1971) Endeavour-1 Well Completion Report. Ministry of Economic Development New Zelanad Unpublished Petroleum Report, PR 303, 186p.

WOOD, C.A. (1978) Morphometric Evolution of Composite Volcanoes. Geophysical Research Letters, 5, 437-439 pp.

WOOD, C.A. (1980) Morphometric Evolution of Cinder Cones. Journal of Volcanology and Geothermal Research, 7, 387-413 pp.

WOOD, R.A. & HERZER, R.H. (1993) The Chatham Rise, New Zealand. In: Ballance, P.F. (ed.) South Pacific sedimentary basins. Amsterdam: Elsevier Science Publishers. Sedimentary basins of the world 2, 329-349 pp.

WOOD, R.A., P.B.; HERZER, R.H.; COOK, R.A.; HORNIBROOK, N. DE B.; HOSKINS, R.H.; BEU, A.G.; MAXWELL, P.A.; KEYES. I.W.; RAINE, J.I.; MILDENHALL, D.C.; WILSON, G.J.; SMALE, D.; SOONG, C.W.R.; WATTERS, W.A. (1989) Cretaceous and Cenozoic Geology of the Chatham Rise Region, South Island, New Zealand. New Zealand Geological Survey basin studies 3, 75p.

CHAPTER 7) CONCLUSIONS AND FURTHER WORK

7.1 Conclusions

This PhD thesis aimed to answer the five key questions addressed in Chapter 1 by assessing a basin analysis of the structures and tectonics of the Canterbury Basin to understand their impacts on sediment distribution. Conclusions of Chapters 2 to 6 are presented below, and address the key questions posed in Chapter 1.

7.1.1 What information does the Late Cretaceous-Eocene sedimentary fill of the Canterbury Basin provide on the tectonic and paleogeographic evolution of the basin and its surrounding landmass?

The Canterbury Basin contains mid Cretaceous (~110 Ma) to Recent strata up to 8 km thick. The basin initiated during eastern Gondwana breakup at ~110-85 Ma which resulted in the formation of depocenters that were under-filled by sediments at the end of rifting. The basin and range topography produced by normal faulting, persisted for a protracted period of time until its complete burial and draping during the Paleocene to Eocene. From the syn-rift to the post-rift phase, the interplay of rift structures and sedimentation impacted sedimentary records giving insights on the evolution of the Zealandia landmass. Several key conclusions are drawn from our study:

- Early syn-rift sedimentation (~110 Ma to 85 Ma) occurred in association with transverse and axial drainage systems, with alluvial fans developing along fault scarps into braided rivers flowing along rift valleys. Downstream, they were possibly connected either to lakes or to the sea, which progressively transgressed inland over time.
- After the Santonian (85 Ma; Late Cretaceous) following eastern Gondwana breakup, the rifting and crustal extension decreased significantly. Post-Gondwana breakup reflectors progressively draped the paleo-relief, as fan deltas formed along paleo-fault scarps and deltas were developed on top of horsts. When marine transgression covered the structural highs, horsts ceased to provide sediments to nearby areas and instead, pelagic sedimentation dominated when horsts were transgressed. Further offshore to the south-east, an accretionary shelf-edge clinoform developed along the eastern margin of the Taiepa Nui NE-SW rift depocenter.
- By the Paleocene and Eocene, shelf-edge clinoforms parallel to the present-day coast line and to the Chatham Rise, started to develop in the basin with deep-water fans accumulating at the toe of the shelf slope. These fans were depositing along the topographic depressions adjacent to the buried Taiepa Nui horst but not further east. Eocene shelf-edge clinoforms display an increase in thickness which could highlight basin subsidence or uplift in the western part of the basin.
- We suggest that whether the Canterbury Basin filled with sediment depended on potentially number of factors such as the availability of sediment, the duration of the rifting, the lack of surrounding paleo-topography, the type of drainage systems, the nature of the basement rocks providing source for detrital sedimentation, and paleo-climate. Of these, the more likely causes for the low sediment supply includes the

postulated long transportation distance to bring sediment into the basin, the likelihood that the greywacke and schist source areas would produce little sand relative to other basins of Zealandia, and the overall small landmass feeding Zealandia rift basins for which Canterbury Basin was the furthest away from.

- The variable degree of preservation of rift structures and changes in the timing of the marine transgression between Northern. and Southern Zealandia, during the Late Cretaceous, suggests differences in regional-scale tectonic behaviors between the north and south of Zealandia. Such differences could either be related to Late Cretaceous uplift of Northern Zealandia associated with a continuation of subduction, or the presence of a structural boundary between the north and south of Zealandia since the Late Cretaceous.
- There are similarities in the pre-rift and rift structural orientations with Late Cretaceous-Eocene and Recent paleogeographic features, such as the western position of highlands and the orientation of both coastline and shelf-edge clinoforms. The persistent western position of the topography, as a sediment source for the Canterbury Basin, supports the hypothesis that the first-order topography of Zealandia could have existed since at least the Late Cretaceous.

7.1.2 What processes controlled the multi-directional stretching of the Canterbury Basin?

The Canterbury Basin in eastern Gondwana was deformed by rift faults from ~110 to ~85 Ma with trends of NE-SW, E-W and NW-SE. These fault sets are present throughout the basin, although E-W and NE-SW trending structures dominate along the Chatham Rise and in the southern Canterbury Basin, respectively. Each of these fault sets is characterised by segmentation and relay ramps consistent with normal faulting. The normal-faulting hypothesis is further supported by horizontal separation diagrams and displacement analysis which indicate that all fault sets primarily accrued normal dip-slip, with displacement lows at segment boundaries (there is presently no evidence that segment boundaries have the pop-up or pull-apart basin geometries expected for strike-slip faults). Analysis of growth strata indicates that the three fault sets accrued displacements synchronously. The available data support the view that the Canterbury Basin accommodated multiple directions of extension coevally during the Cretaceous. The three fault sets are each parallel to spreading centres that define the present margins of Zealandia, with NE-SW trending faults in the southern basin being parallel to the mid-ocean ridge separating southern Zealandia and western Antarctica. The parallelism between spreading centres and rift faulting suggests that the multi-directional extension in the Canterbury Basin records the early stages of Gondwana breakup. The mantle convection processes or changes in plate tectonic forces responsible for Gondwana breakup produced distributed extension across much of Zealand and influenced its continental crust for about 25 Myr prior to breakup. With the onset of breakup, extension was focused along the spreading centres and distributed stretching of Zealandia ceased or continued at much diminished rates.

7.1.3 How to quantify syn-rift sediment fill in rift basins after rift cessation?

Rift systems are generally sites of sediment deposition which occurs in depocenters produced by faulting. The degree of rift basin infill after rift cessation is here defined using the

Sediment Fill Ratio (SFR), which the ratio of syn-rift maximum sedimentation to syn-rift fault throw. The parameters are measured in the immediate hangingwall of each fault using seismic reflection lines. Rift basins are defined as being starved (SFR $\leq$0.2), under-filled (0.2<SFR$\leq$0.9, balanced-filled (0.9<SFR$\leq$1.1) and over-filled (SFR>1.1). The fill geometry of the seven rift systems studied here range from being under-filled to over-filled. Within each basin the degree of filling of depocenters in the immediate hangingwall of each fault is dependent on fault size. Curves of SFR vs fault throw typically show a non-linear negative relationship with smaller faults (e.g., throws <0.5 seconds TwT) most likely to be over-filled. This over-filling may reflect the lower displacement rates on smaller faults. Under-filling is most common proximal to large faults (e.g., throws >1 seconds TwT) and in rift systems dominated by large faults. Rift systems comprising entirely over-filled depocenters may have received a significant supply of sediment from outside the rift system.

7.1.4 What mechanisms triggered Early Oligocene channels incision of the Canterbury Basin shelf and slope?

Our study of the offshore Canterbury Basin provides new observations of Early Oligocene erosion through new seismic mapping from drill hole data for the study region. We have mapped seismic horizons which show that the top Eocene reflector in offshore 2D and 3D seismic data is locally affected by erosional truncations that display channel geometries, and in turn, are overlain by Late Oligocene or Early Miocene reflectors. Mapping of these channels shows a drainage pattern converging towards the south-east with erosional corridors that, on average, trend E-W to NE-SW, vary in width from 1 to 12 km, are 15 to 90 km long, and are 100 to 200 ms deep in the area of the Eocene slope. We interpret these erosive features as canyon-channel complexes. Onshore, we have mapped the geographic distribution of the Amuri Limestone and show regions where it has been completely removed. Although outcrop data are sparse and discontinuous, they appear to define a number of erosional corridors about 5 to 40 km wide which trend NW-SE. We interpret these as erosional shelf channels.

The synchronicity, similar trends, and comparable morphology of the shelf-channels appear to match with the canyon-channel complexes developed in the contemporaneous offshore shelf, and suggest they may form part of the same erosive system. These new observations allowed us to propose a paleogeographic map of the earliest Oligocene during the major sea level fall. This data, together with data in other regions, provides insights on the processes controlling the Early Oligocene sea-level fall. These insights include:

- The Canterbury Basin formed an amphitheatre shape during the Early Oligocene, being bounded by the Chatham Rise to the north, by the shelf to the west, and by land in the Otago region to the south.
- We propose a model in which erosive channels onshore flow towards the east, south, and north-east before merging into canyons that were incising into the slope offshore.
- The present study provides additional support for the idea that Oligocene erosion and unconformity development is complex and that some of this complexity could locally arise due to channelization.
- We propose that erosive channels incising the calcareous shelf and slope of the Canterbury Basin during the Early Oligocene, was triggered by a sea level fall most likely in the period 32-29 Ma.
- The temporal (millions vs. hundreds of thousands of years) and spatial scales of these changes are larger than would be expected for eustatic processes and we suggest that regional tectonic uplift may have played an important role in the formation of channels.

- The channel orientations and their eastward gradients, together with Oligocene sedimentary facies observed in outcrop, all suggest that the axis of uplift was primarily west of the Canterbury Basin.
- Tectonic movements collectively affecting the western North Island – Marlborough Sounds – western Otago high may have been the source for eastward flowing Early Oligocene channels in the Canterbury Basin.

Both contemporary and Oligocene channel systems form an onshore radial pattern which converges offshore in the direction of flow. In the central, south Canterbury, and northern Otago regions, present-day rivers flow towards the east and the Bounty Trough, similar to the Early Oligocene drainage in central, south, and offshore Canterbury Basin. In the northern Canterbury region, present-day rivers converged towards the Hikurangi Canyon and the Pegasus Basin, similarly to the drainage of the northern Canterbury region that flowed along the northern limb of the Chatham Rise. The possible stability of drainage systems in the eastern South Island is a surprising conclusion given the Late Cenozoic tectonic deformation in this area, and requires further testing.

7.1.5 What was the evolution of the magmatic activity in the offshore Canterbury Basin?

Buried volcanoes and intrusions are present in most of the Canterbury Basin, erupting intermittently from the Late Cretaceous to Pleistocene time. Seismic reflection data presented here permitted the mapping of 185 volcanoes forming a total surface area of ~4775 km^2 and is approximately a factor of three greater than the surface area of 1555 km^2 for onshore volcanoes. Their size and distribution vary in time and space and they can be grouped into 5 volcanic phases:

- (1) Widespread volcanic activity related to subduction-extension processes from ~110 to 85 Ma. This phase corresponds to monogenetic to polygenetic volcanoes of up to 5 km diameter where the majority is located in the south-eastern Canterbury Basin along rift faults. They are synchronous with the Mount Somers Volcanic Complex and with the Kyeburn and Shag Point Ignimbrites that are related to subduction processes. However, the mid-Cretaceous volcanoes located in the south-eastern offshore, >200km away from the western subduction interface, display a close relation to the rifting. Therefore, they could have a different composition than the MSVC.
- (2) Large composite volcanoes formed in the Late Cretaceous during the post breakup phase of basin evolution. These volcanoes are not observed onshore, but offshore, large composite volcanoes are aligned along a NE-SW trend parallel rift faults. Three main volcanic complexes of >10 km apparent diameter erupted during the post rift Late Cretaceous. They are named, from north to south, the Sloop, Barque and East Takapu volcanic complexes. They were accompanied by other monogenetic to polygenetic volcanic edifices of a few kilometres apparent diameter in their surroundings.
- (3) Paleogene to Middle Miocene emplacement of small monogenetic domes with apparent diameters of kilometres. They were forming volcanic fields that were mostly located around the Oamaru region (Paleocene to Oligocene) both onshore and offshore, as well as offshore, south of Banks Peninsula (Early Miocene). Volcanoes formed monogenetic domes. Other Paleocene volcanoes were present in the south-east offshore Canterbury Basin still showing some alignment with rift structures.

- (4) Middle to Late Miocene eruption of large composite volcanoes produced large volumes of magma located onshore forming both Banks and Otago peninsulas.
- (5) Pliocene to Quaternary sporadic small domes erupting offshore along the Chatham Rise.

Our mapping in the offshore areas has increased the known aerial extent of volcanism in the Canterbury Basin by 300%. Numerous intrusions are also present in the Canterbury Basin as sills. Seismic data doesn't allow imaging batholiths or plutons which, if present, are below the seismic data (e.g., >10 km depth). Buried volcanoes are known to be locally present offshore in other Late Cretaceous rift basins of Zealandia, and detailed mapping using seismic reflection data could provide new insights into the magmatic evolution of the Zealandia continent.

7.2 Further Work

This PhD project has contributed to an improved understanding of the sedimentological, paleogeographic and tectonic evolution of the Canterbury Basin, Zealandia and eastern Gondwana geology. A PhD is necessarily a finite piece of work and many geological problems associated with the Canterbury Basin remain unresolved. In particular, some of the findings are preliminary and have highlighted interesting aspects of the geology that require more investigation to improve our knowledge of sedimentological, tectonic and plate boundary processes.

7.2.1 Basement reflectors in the offshore Canterbury Basin and in other offshore sedimentary basins of Zealandia.

During the course of the interpretation of seismic reflection lines in the Canterbury Basin it has become clear that interpreted basement rocks contain reflectivity. The structural analysis of basement reflectors using seismic data could improve our understanding of the spatial distribution of basement reflectors in the offshore Canterbury Basin and of the structures that deform these reflectors. Mapping of basement reflectors may place constraints on the distribution of basement terranes offshore and could give new input for the understanding of pre-rift geological history of the Canterbury Basin (e.g., Fig. 7.1). There is potential that detailed analysis of basement reflectors will impart knowledge of the Permian-Early Cretaceous accretionary wedge and associated fold and thrust belt along the southern margin of the Chatham Rise. In addition, in the Otago Schist offshore of the Otago Peninsula, detachments surfaces mapped onshore by Deckert *et al.* (2002) may be visible in seismic data (Fig. 7.1b and 7.1c). Analyse of basement fabric will be aided by detailed examination of 3D seismic reflection surveys. In particular, the Wherry 3D seismic survey, which is currently not in open file access, is located over basement reflectors in the north offshore Canterbury Basin and is likely to provide a rich dataset for future studies of basement (Fig. 7.2)

Velocity analysis of basement reflectors has been attempted using velocity data from the New Zealand Petroleum and Mineral database. The hypothesis being that the data would display: (1) a progressive increase in velocity between Late Cretaceous and basement reflectors if their lithology are similar (e.g. sediments). (2) A sharp increase in velocity in between Late Cretaceous and basement reflectors if both have different lithologies (e.g. meta-sediments vs. sediments). However, data from NZPAM does not permit velocity analysis of the basement as the velocities only display variation parallel to shallow reflectors but not at the top basement

and basin fill contact. We conclude then the data provided by the New Zealand Petroleum and Mineral database could have been processed only for shallow reflectors and therefore is not suitable for the analysis of basement velocity. Despite the limited results so far, more detailed analysis of the velocity data may prove fruitful and could be used to test the hypotheses listed above.

Lastly, regional scale mapping of basement reflectors across Zealandia could be conducted in offshore sedimentary basins where basement reflectivity has been observed (e.g. Bache *et al.*, 2014, Tulloch *et al.*, 2019). Regional maps of basement reflectors and structure may help map basement terranes offshore and augment existing knowledge of pre-~110 Ma basement deformation.

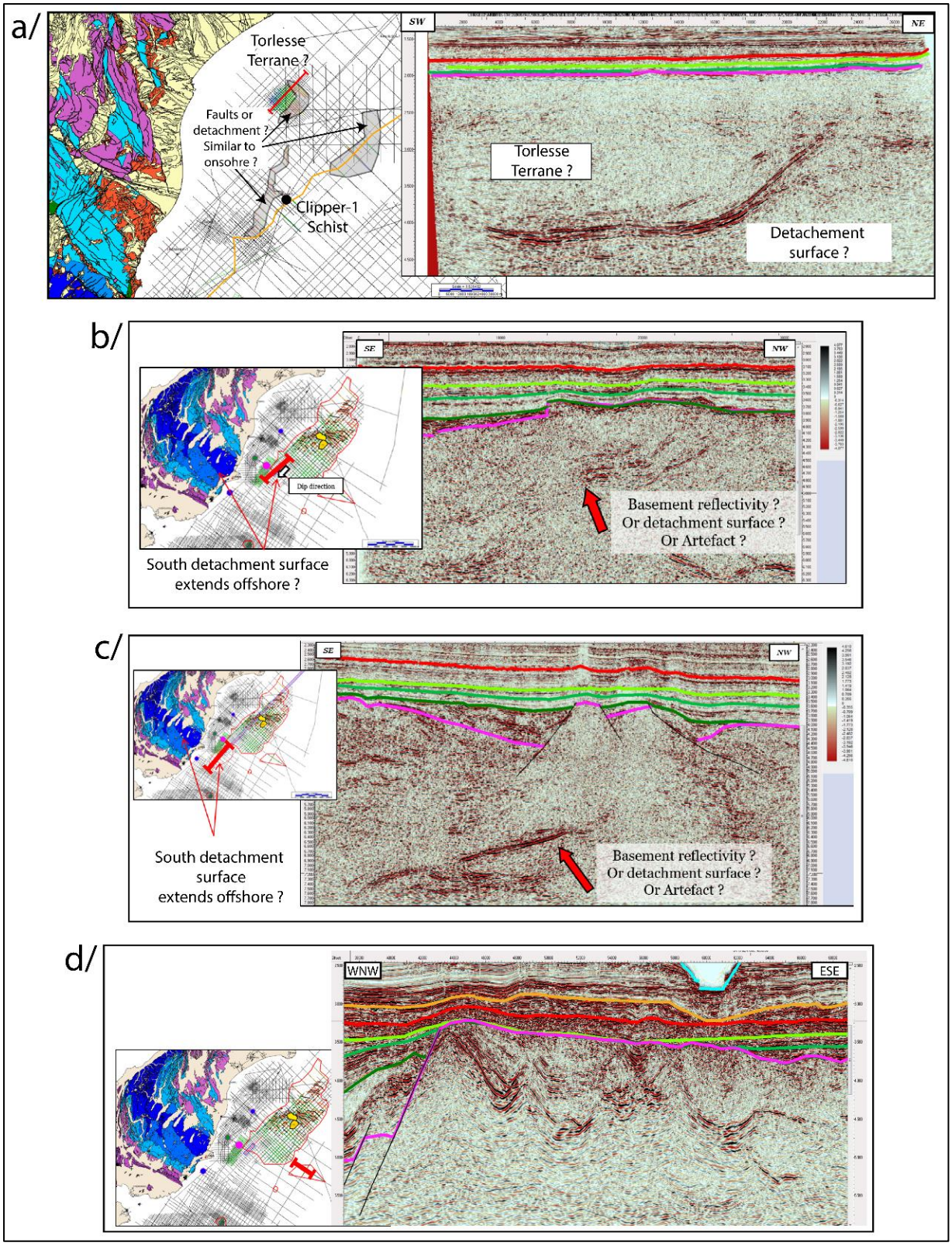

Figure 7.7.1 Seismic profiles across the offshore Canterbury Basin showing basement reflectivity. (a) Seismic reflection profile showing possible detachment surface between Torlesse and Schist basement potentially similar to what crops out onshore. (b-c) Seismic reflection profiles showing a southward dipping basement reflectivity in the axe of the southern detachment surface bounding the Otago Schist Belt. (d) Seismic reflection profile showing basement reflectivity in the Taiepa Nui High.

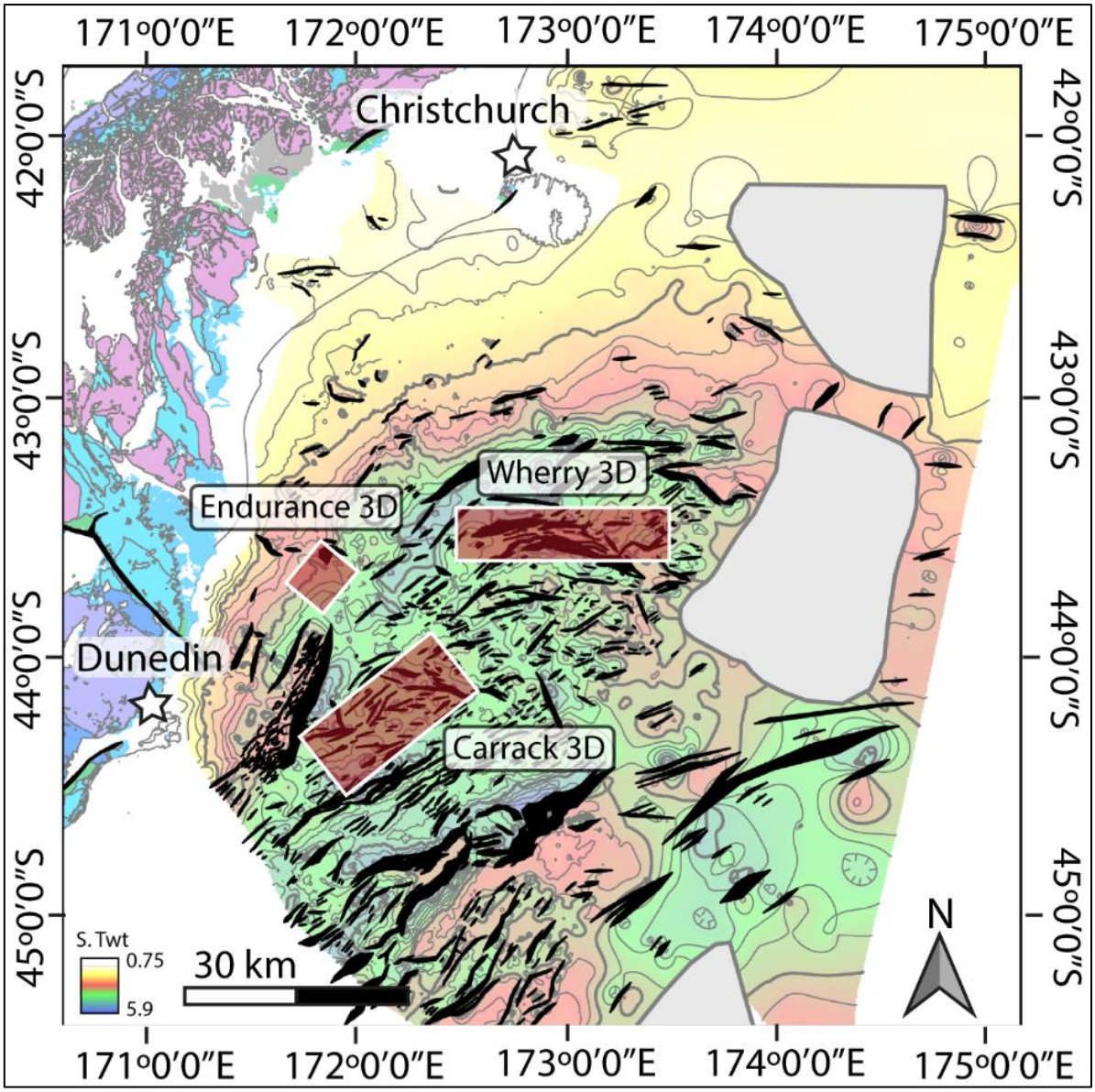

Figure 7.7.2 Top basement isochron map showing the location of Wherry, Carrack and Endurance 3D seismic surveys represented by red squares, correspond to data in private-access own by Oil and Gas companies.

7.2.2 Detailed fault kinematics analysis using 3D seismic data along the Wherry High and the Puke intra basin

Three additional 3D seismic surveys exist in the Canterbury Basin and will become open file in the next few years (Fig. 7.2). Two of them, the Carrack and Wherry 3D, could give important insights into fault kinematics. These surveys will provide high resolution 3D data on faults with orientation from NE-SW, to E-W and to WNW-ESE trends. These 3D data (including time-slices and similarity attribute mapping) of different rift fault trends will provide detailed on fault displacements and slip sense (i.e. dip-slip vs strike-slip). In addition, the Wherry 3D survey could bring valuable insight into the evolution of displacement along a rift fault displaying changes in the trend of its segments.

7.2.3 Late Cretaceous to Eocene shelf-edge progradation around Zealandia

Chapter 2 highlights the presence of shelf-edge prograding clinoforms within Late Cretaceous post-rift strata as well as draping shelf-edge clinoforms within Paleocene-Eocene post-rift strata. A detailed analysis of the evolution and succession of such clinoform using sequence stratigraphy or quantitative seismic stratigraphy techniques will constrain the evolution of these shelf-edge clinoforms. Such information could help us to understand better the evolution of the landmass around the Canterbury Basin. Clinoform progradation provides a distal record of hinterland uplift and deformation that is often difficult to retrieve from the hinterland itself. For example, pulses of sediment input into the basin likely record the timing and magnitude of regional or plate boundary events.

Detailed analysis of the clinoform evolution is likely to be of great value if conducted at a Zealandia scale. Other prograding shelf are known to have developed around Zealandia (e.g., the Late Cretaceous Taranaki Delta, Strogen *et al.*, 2017). A calendar of the pulse of sedimentation across sedimentary basin surrounding Zealandia could help us to understand better the evolution of sediment input into the basins across the entire Zealandia region, which may help constrain the topography and tectonic uplift across the entire continent.

7.2.4 Shelf to basin floor analysis of Miocene to Recent Canterbury Basin sediments

This PhD thesis emphasized the similarity between paleogeographic trends from the Late Cretaceous to the Oligocene with present-day geomorphology (e.g., location of topographic highs, drainage patterns, trend of shelf-edge clinoforms). The isochron map of reflectors between the top Eocene (P50) and the sea floor shows that some rift structures influenced sediment thicknesses post-Eocene (Fig. 7.3). The degree to which rift structures influence Neogene sedimentation and the associated processes could be elucidated by detailed analysis of the Miocene, Pliocene and Pleistocene intervals using the most-recent seismic data available is necessary.

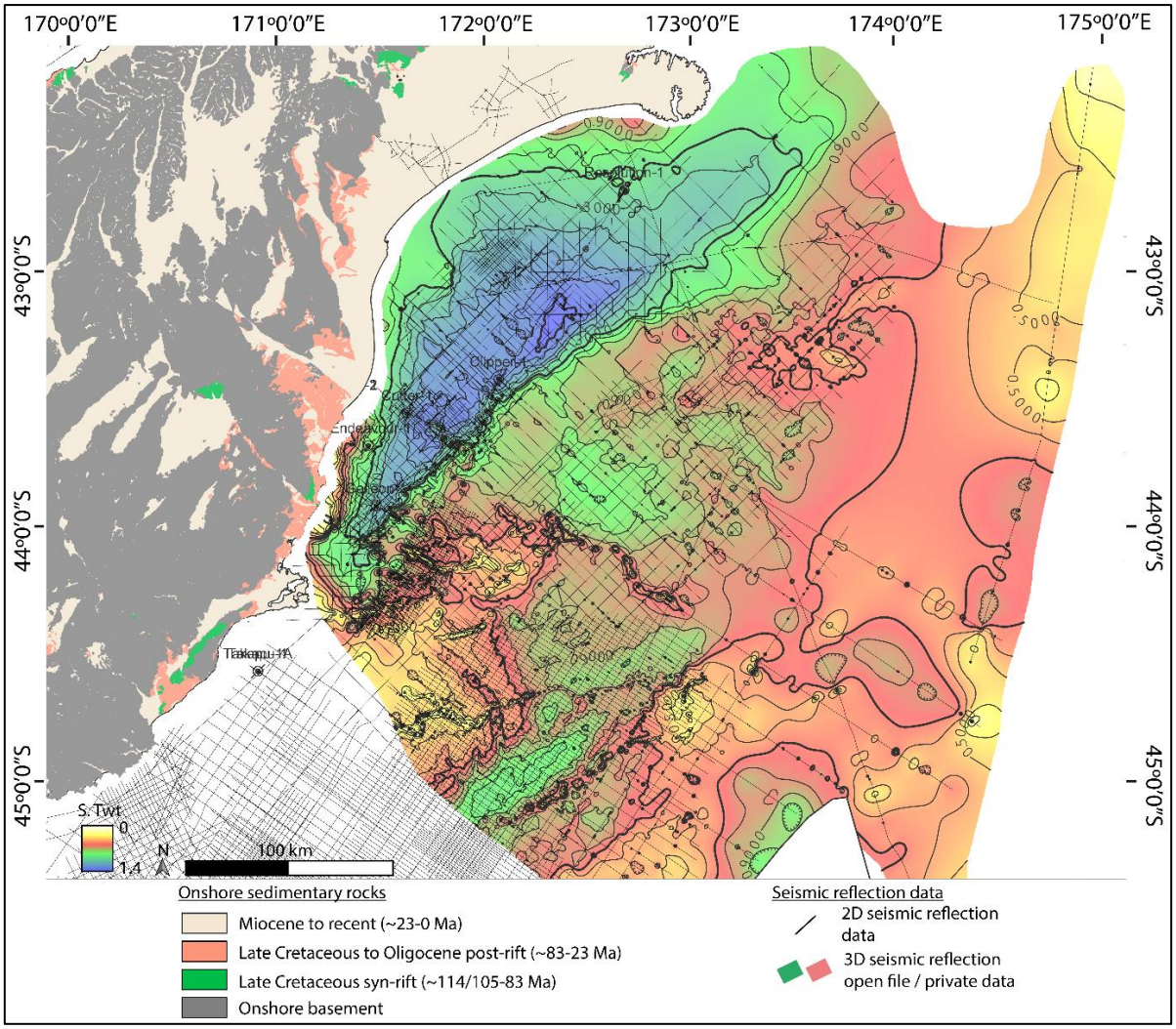

Figure 7.7.3 ***Miocene to Recent isochron map showing the thickness variations of Miocene to Recent strata with potential influence of buried rift structures towards the south-east of the Canterbury basin. Recent data towards the south-east offshore could give a new overview of the evolution of deep-water sediment in the offshore Canterbury Basin, a period of time not covered in this PHD thesis.***

7.2.5 Testing of the Subduction front embayment model

The model of the embayment of the subduction front during the mid-Cretaceous has been included in our plate reconstructions based on the available literature and geological maps of basement terranes. The embayment model requires bending and pinching of the Murihiku and Brook Street terranes across the area approximately occupied by the Alpine Fault, possibly in response to partial subduction of the Hikurangi Plateau indenter. The embayment model may account for some aspects on the basement terrane geometries, and by structural analysis of the Southland Syncline from which it can be suggested that rotations of basement terranes in this area were pre-Eocene (Fig. 7.4 - Lamb *et al.*, 2016). The geological map of the Southland region suggest that little strike-slip occurred along the northern NE-SW trending Moonlight fault and the N-S fault separating the Median Batholith and the Southland Syncline (Figs. 7.4a and 7.4b). If contraction occurred in the area during the mid-Cretaceous then these faults could have acted as thrusts at this time, which resulted in pinching of the Brook-Street and Murihiku terranes, overthrust by the Median Batholith (Fig. 7.4b and 7.4c). Although the embayment

model has been proposed, it has not been fully tested in this thesis with all of the available datasets. Cross section balancing, fault kinematic and unconformities analysis within basement terranes and Cretaceous-Cenozoic cover rocks may help differentiate Cenozoic from Mesozoic deformation and constrain the mid-Cretaceous spatial extent of contraction.

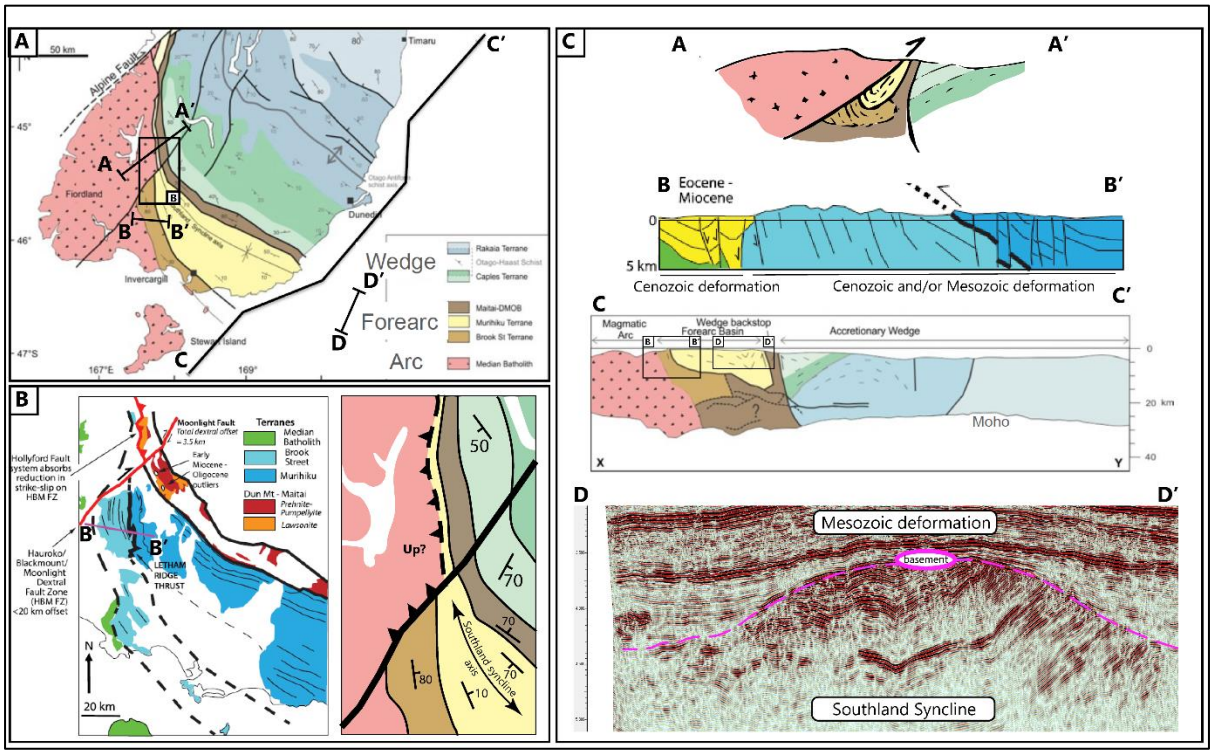

Figure 7.7.4 Summary of basement terrane geometries in the southern South Island, New Zealand, and the relation between Mesozoic versus Cenozoic deformation. A) Map of basement terrane of the south of New Zealand South Island (Mortimer, 2000). B) Detailed map of the pinching of the Brook-Street and Murihiku terranes showing possible strike-slip (left map from Lamb et al., 2016) or thrusting of the Median Batholith over the Brook-Street and Murihiku terranes (modified from Mortimer, 2000). C) Cross section across Zealandia basement terranes from NW onshore to SE offshore: AA' Schematic cross section showing possible thrust geometry of the Median Batholith over the Brook-Street and Murihiku terranes as the process resulting in the pinching of both basement terranes towards the NE. BB' section shows both Cenozoic deformation affecting Eocene-Miocene strata as well as Brook-Street and Murihiku terranes deformation of either Mesozoic and/or Cenozoic ages (from Lamb et al., 2016). CC' cross section showing offshore basement terrane geometries interpreted from the SESI profile where the Southland Syncline extends offshore were little or no Cenozoic deformation occurred (Mortimer et al., 2000). Seismic reflection profile offshore Great South Basin showing folded basement reflectors of a geometry similar to the one of the Southland Syncline indicating Mesozoic deformation of this terrane.

7.2.6 Buried volcanoes around Zealandia sedimentary basins

Many volcanoes and volcanic systems were identified in the Canterbury Basin during the course of seismic reflection mapping in this thesis. Due to time constraints the detailed geometries of these volcanoes and their relations to the enclosing basin strata has not been conducted as part of this thesis. We believe that there is significant scope to study many of the volcanoes in the Canterbury Basin in significantly more detail than has been possible here. In particular, the Endurance 3D seismic survey, which is not yet open file, is located over one of the Large Late Cretaceous Volcanic Complexes of the Canterbury Basin (Fig. 7.2). These data

could give important information to understand better the eruptive style of one of these large volcanoes. In addition, the mapping of igneous complexes on seismic reflection data could be done in other sedimentary basins across Zealandia in order to produce a regional map of buried igneous features in its sedimentary basins. Such a synthesis could bring new information on the igneous evolution of Zealandia from its breakup to the present day. We believe that a Zealandia-wide study of buried volcanoes will reveal many more volcanoes than was previously known to exist and may provide key information about the igneous and tectonic evolution of the continental that New Zealand is part of.

7. References

BACHE, F., MORTIMER, N., SUTHERLAND, R., COLLOT, J., ROUILLARD, P., STAGPOOLE, V. & NICOL, A. (2014) Seismic Stratigraphic Record of Transition from Mesozoic Subduction to Continental Breakup in the Zealandia Sector of Eastern Gondwana. Gondwana Research, 26, 1060-1078 pp.

COOPER, A.F. & IRELAND, T.R. (2015) The Pounamu Terrane, a New Cretaceous Exotic Terrane within the Alpine Schist, New Zealand; Tectonically Emplaced, Deformed and Metamorphosed During Collision of the Lip Hikurangi Plateau with Zealandia. Gondwana Research, 27, 1255-1269 pp.

COOPER, A.F. & PALIN, J.M. (2018) Two-Sided Accretion and Polyphase Metamorphism in the Haast Schist Belt, New Zealand: Constraints from Detrital Zircon Geochronology. GSA Bulletin, 130, 1501-1518 pp.

DECKERT, H., RING, U. & MORTIMER, N. (2002) Tectonic Significance of Cretaceous Bivergent Extensional Shear Zones in the Torlesse Accretionary Wedge, Central Otago Schist, New Zealand. New Zealand Journal of Geology and Geophysics, 45, 537-547 pp.

LAMB, S., MORTIMER, N., SMITH, E. & TURNER, G. (2016) Focusing of Relative Plate Motion at a Continental Transform Fault: Cenozoic Dextral Displacement> 700 Km on New Zealand's Alpine Fault, Reversing> 225 Km of Late Cretaceous Sinistral Motion. Geochemistry, Geophysics, Geosystems, 17, 1197-1213 pp.

MORTIMER, N. (2000) Metamorphic Discontinuities in Orogenic Belts: Example of the Garnet–Biotite–Albite Zone in the Otago Schist, New Zealand. International Journal of Earth Sciences, 89, 295-306 pp.

REYNERS, M., EBERHART-PHILLIPS, D., UPTON, P. & GUBBINS, D. (2017) Three-Dimensional Imaging of Impact of a Large Igneous Province with a Subduction Zone. Earth and Planetary Science Letters, 460, 143-151 pp.

STROGEN, D.P., SEEBECK, H., NICOL, A. & KING, P.R. (2017) Two-Phase Cretaceous – Paleocene Rifting in the Taranaki Basin Region, New Zealand; Implications for Gondwana Break-Up. Journal of the Geological Society, 174, 929-946 pp.

TULLOCH, A., MORTIMER, N., IRELAND, T., WAIGHT, T., MAAS, R., PALIN, M., SAHOO, T., SEEBECK, H., SAGAR, M., BARRIER, A. & TURNBULL, R. (2019) Reconnaissance Basement Geology and Tectonics of South Zealandia. Tectonics, 38, 516-551 pp.

APPENDIX 1: Isochron structural maps

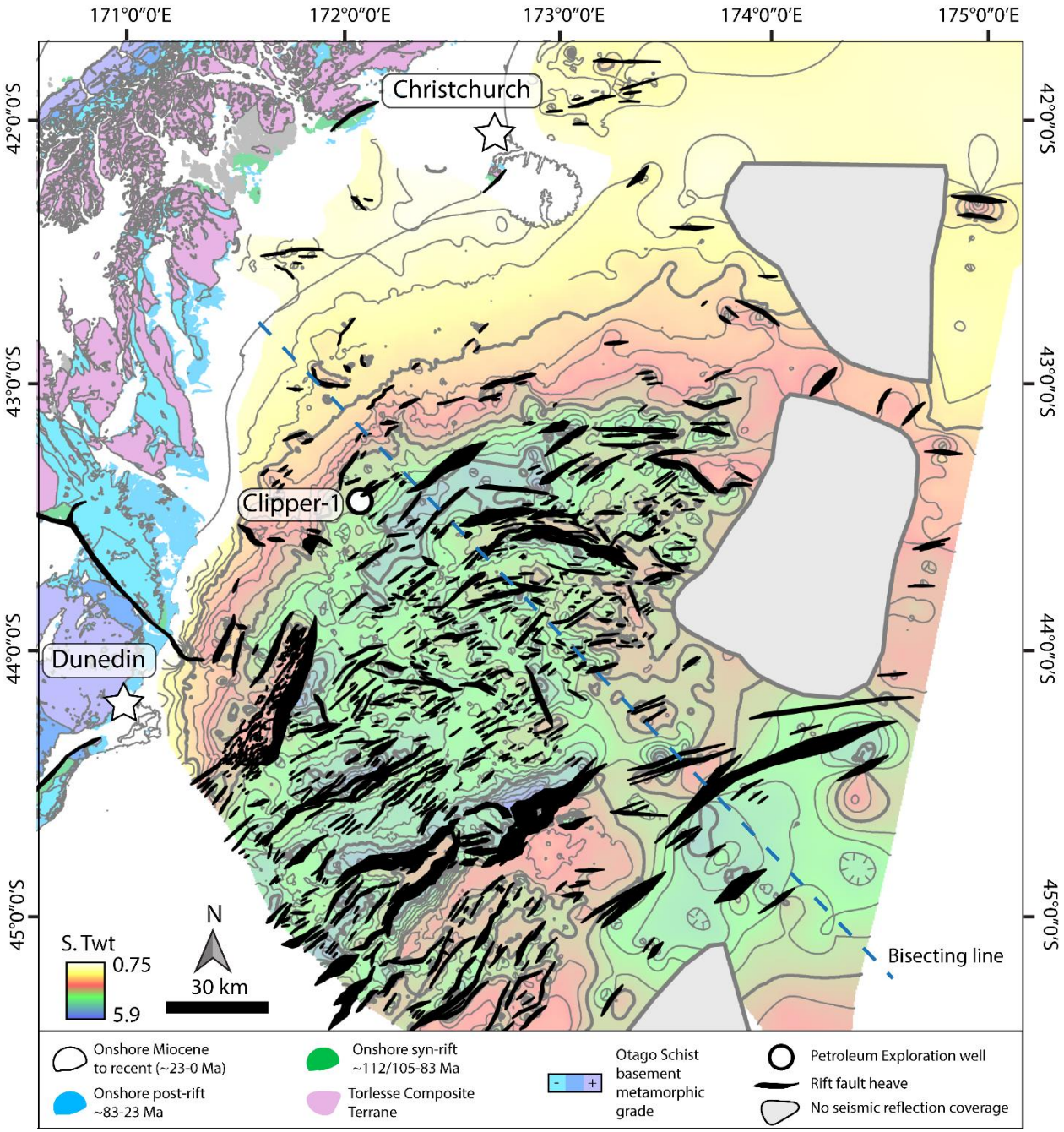

Top basement isochron map generated from seismic interpretation.

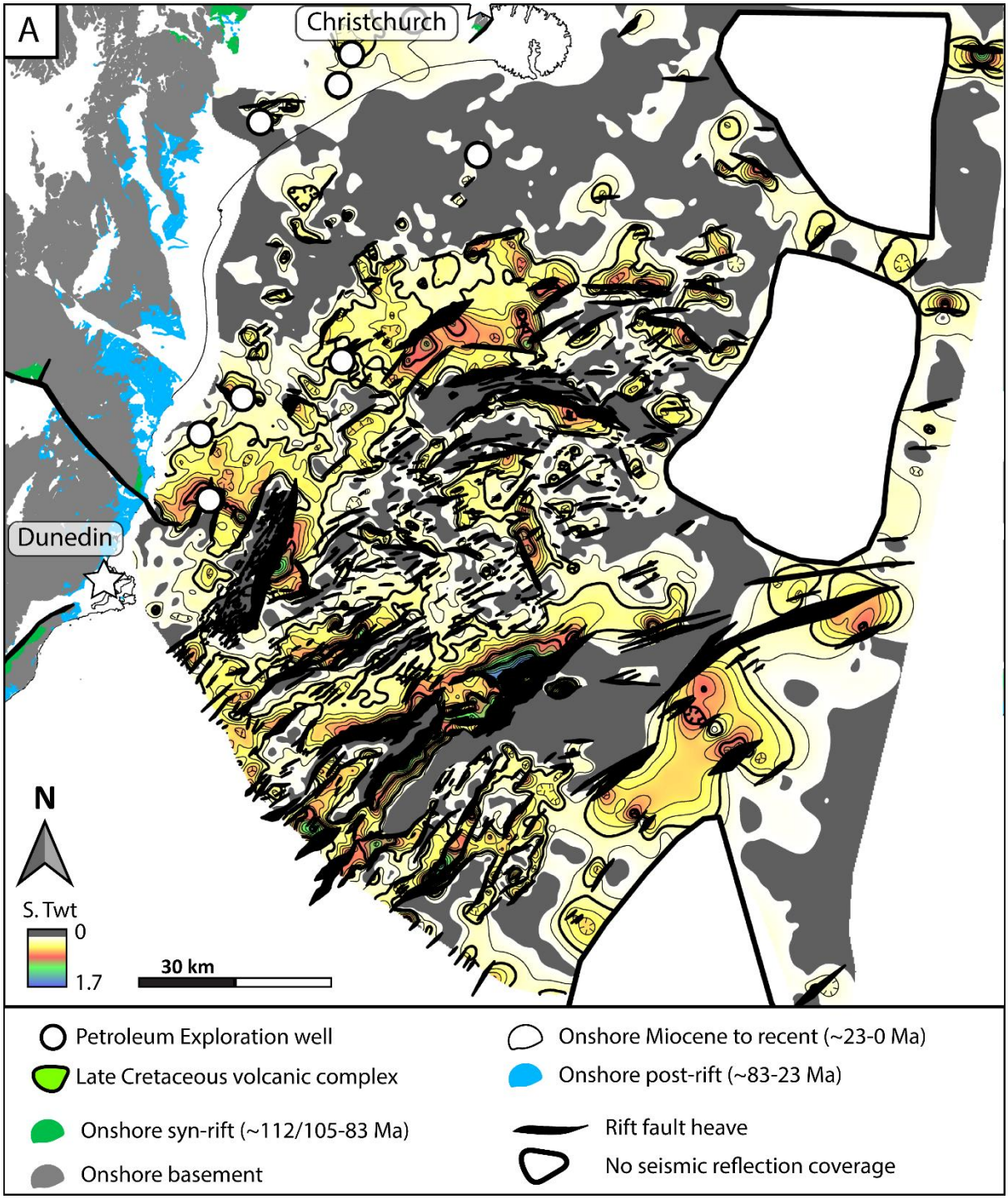

Late Cretaceous syn-rift isochron map (top basement to top K80) generated from seismic horizon mapping.

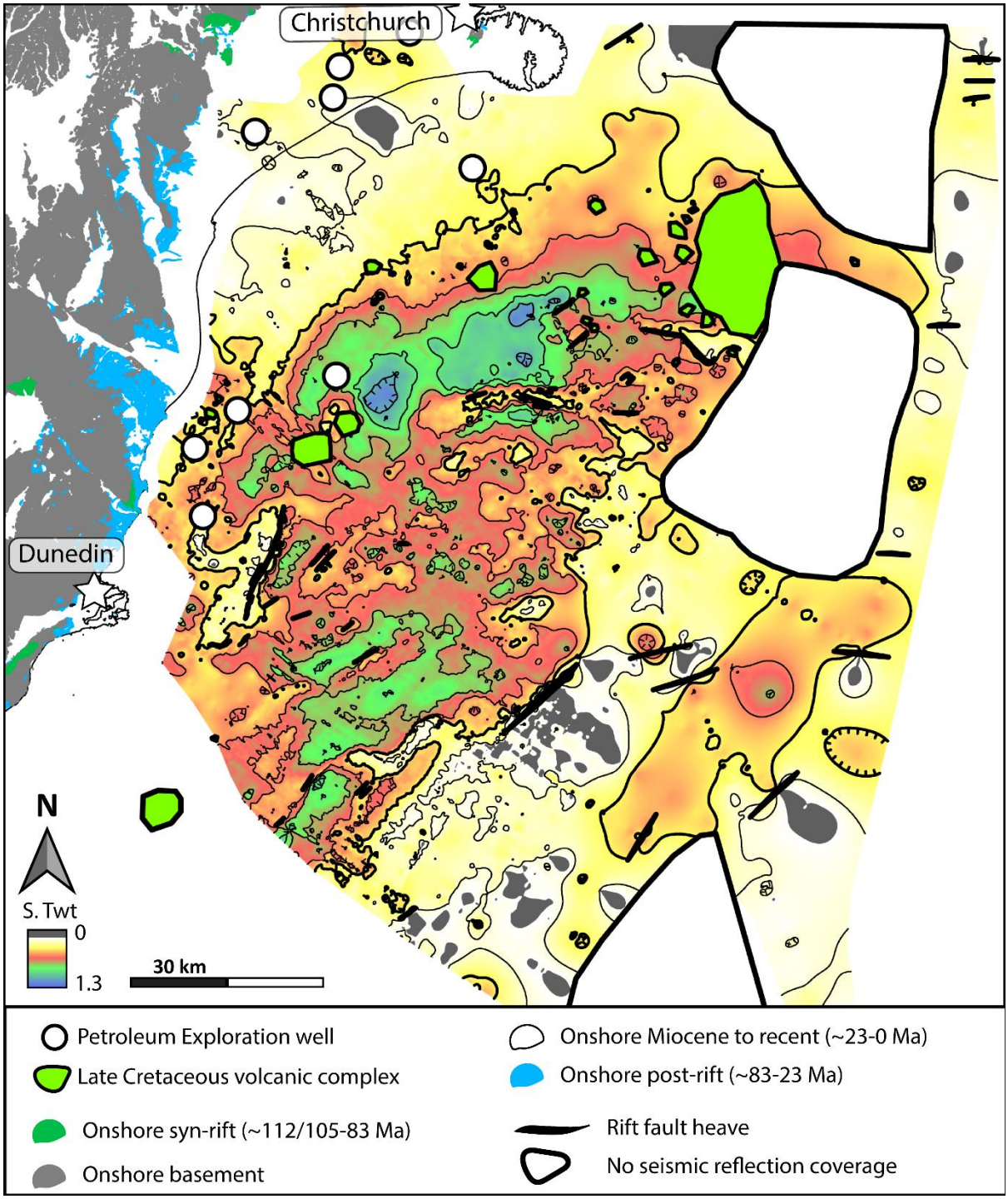

Late Cretaceous post-rift isochron map (Top K80 to P00) generated from seismic horizon mapping.

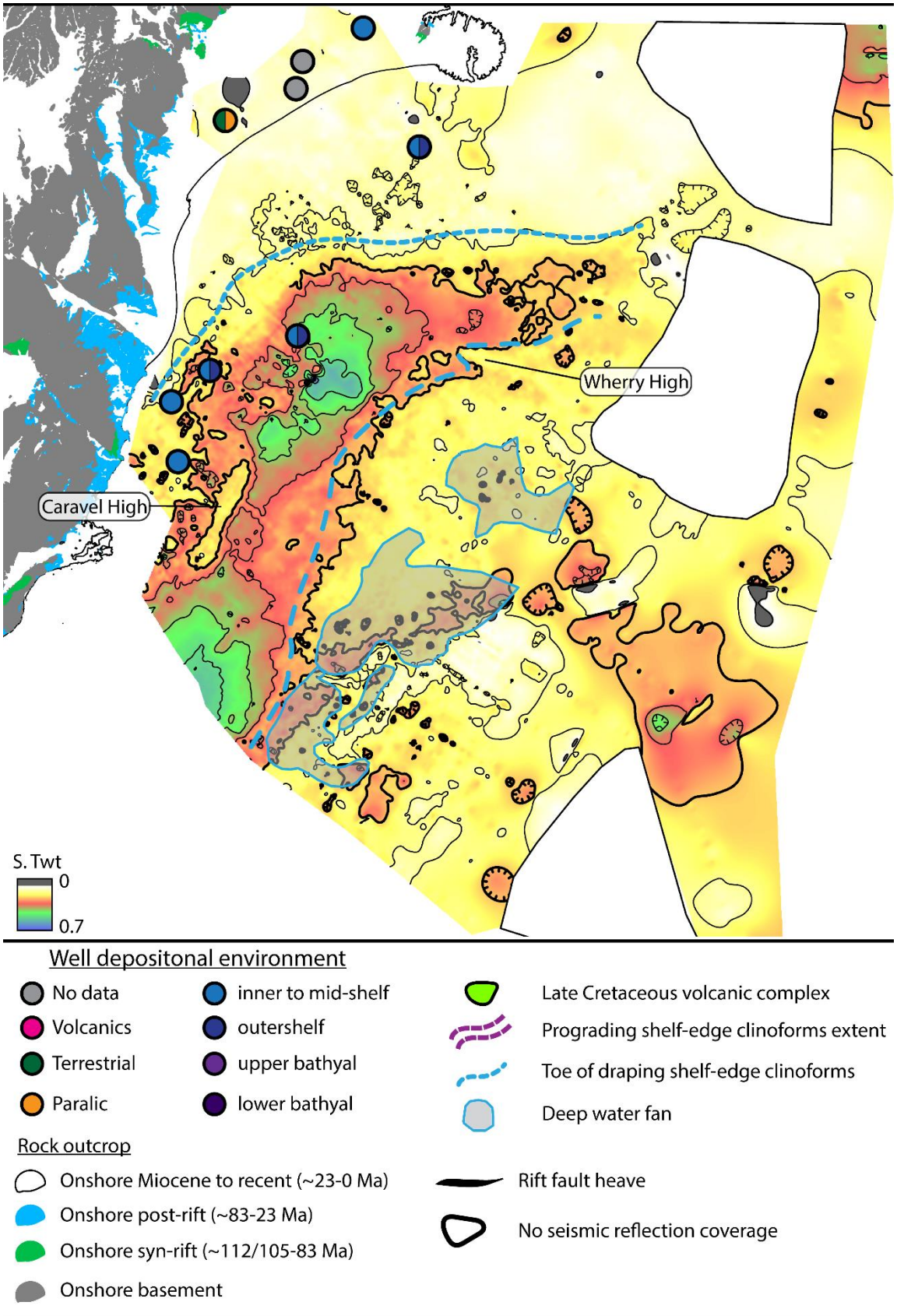

Paleocene post-rift isochron map (Top P00 to P10) generated from seismic horizon mapping.

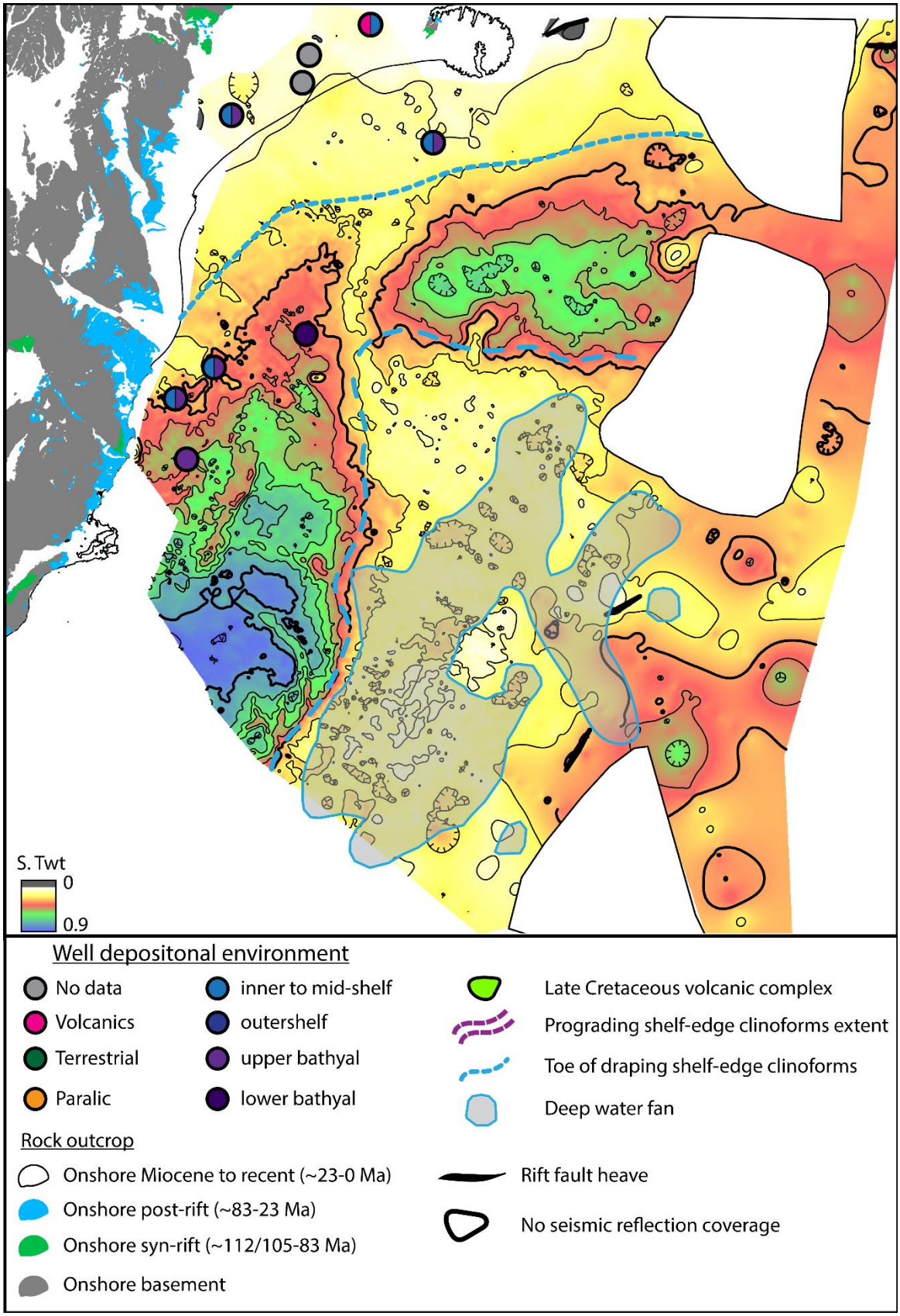

Eocene post-rift isochron map (Top P10 to P50) generated from seismic horizon mapping.

APPENDIX 2: Clipper-1 well stratigraphy

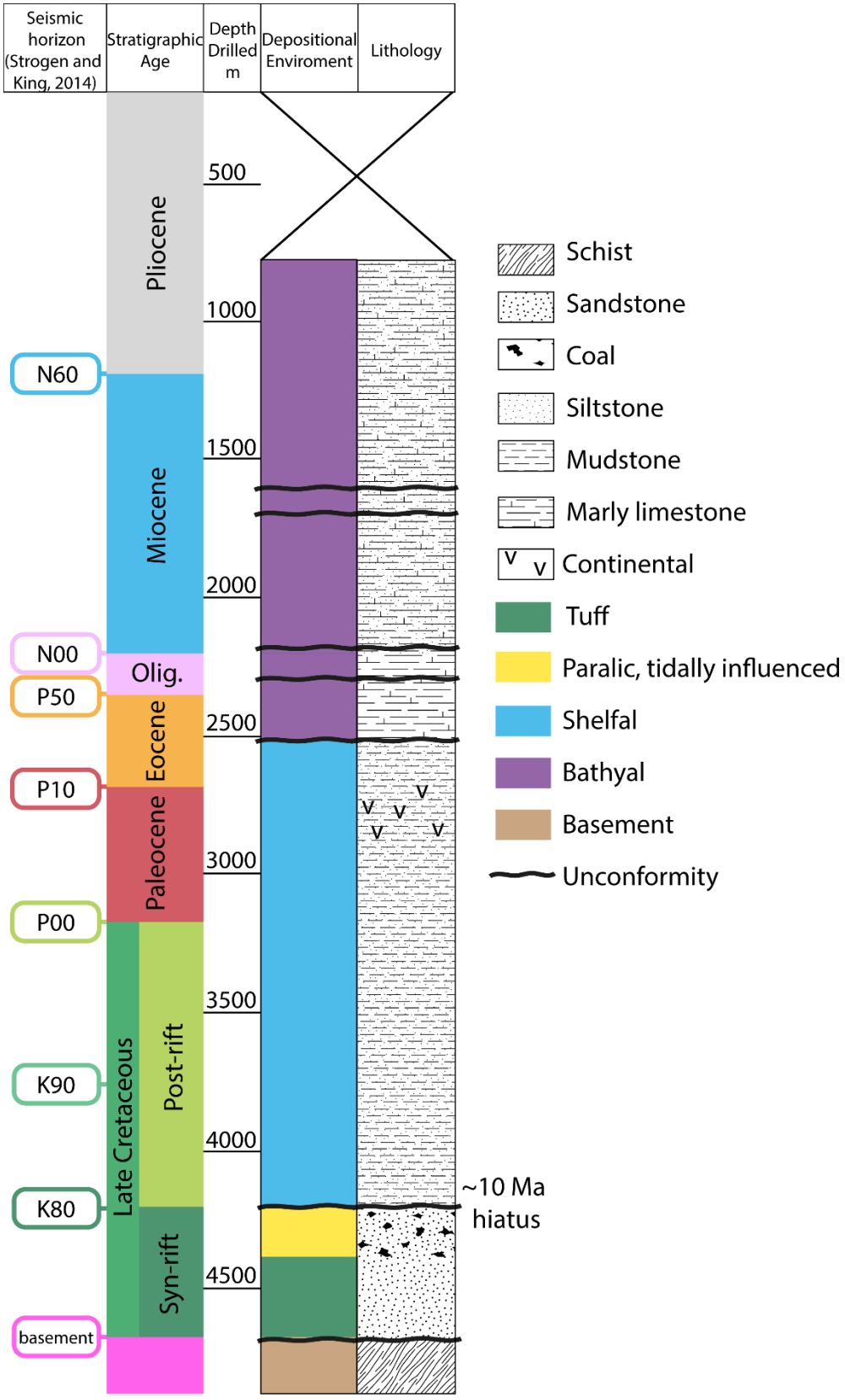

APPENDIX 3: Supplementary Material Chapter 4

Supplementary Material 1:

(A) Evolution of the velocity with depth was derived from Clipper-1 well. The graph shows an increase of velocity with depth. Therefore, for a same time measurement, time/depth conversion for deep measurements will result in a higher metric value (b1<b2).

(B-C) Table showing the impact of time depth conversion on measurements made in time and SFR values.
For under filled half graben: Time depth conversion on measurements along large faults (~2.5 second TwT) decreases slightly SFR values by maximum of 15%. Time depth conversion on measurements along small faults (~500 ms TwT) decreases SFR values by less than 5%. For over filled half grabens: Time depth conversion on measurements along large faults (~2.5 second TwT) increases slightly SFR values by maximum 10%. Time depth conversion on measurements along small faults (~500 ms TwT) decreases SFR values by less than 5%. For over filled half grabens: Time depth conversion has no influence on the SFR values.

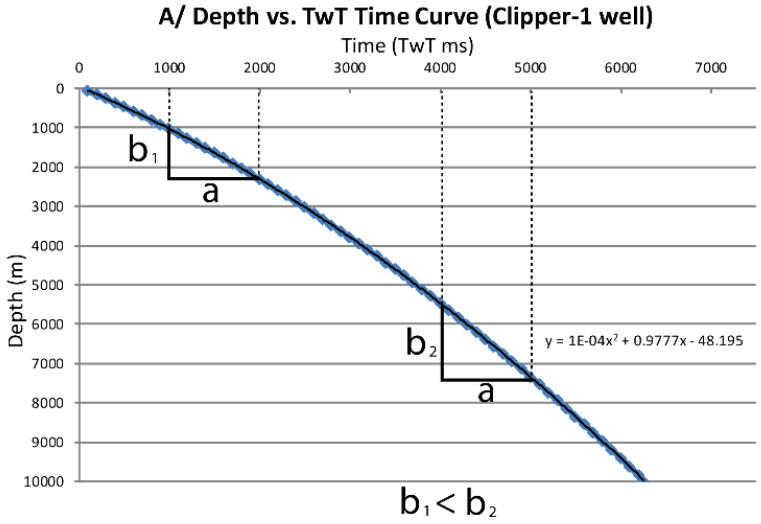

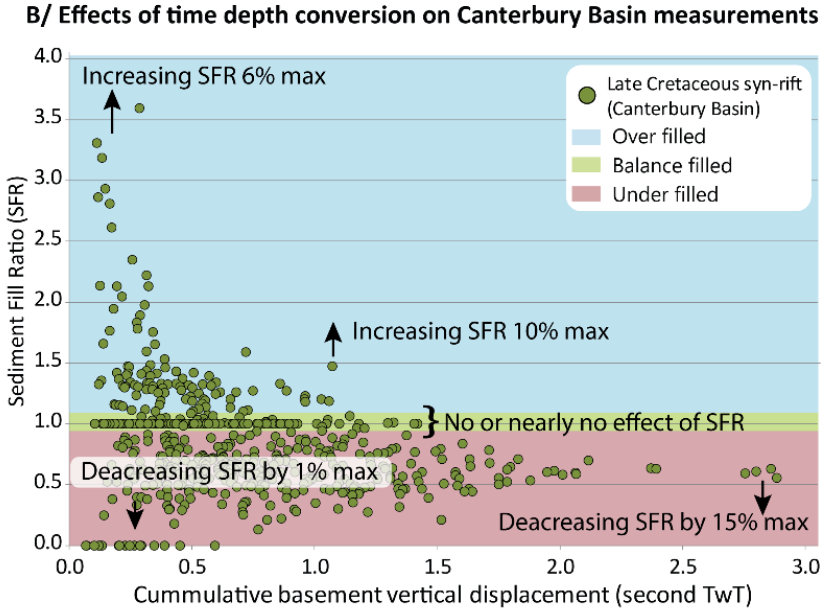

C/

	Small fault shallow measurements (Shallowest measurement 500 ms)						
	Time			Depth			SFR's Similarity
	Fault throw (ms)	Syn-rift Thickness (ms)	SFR time	Fault throw (m)	Syn-rift Thickness (m)	SFR depth	(T/D)
SFR under-filled	250.00	100.00	0.40	275.68	108.77	0.39	1.01
	250.00	125.00	0.50	275.68	136.28	0.49	1.01
	250.00	150.00	0.60	275.68	163.91	0.59	1.01
	250.00	175.00	0.70	275.68	191.66	0.70	1.01
	250.00	200.00	0.80	275.68	219.54	0.80	1.00
SFR balance d-filled	250.00	225.00	0.90	275.68	247.55	0.90	1.00
	250.00	250.00	1.00	275.68	275.68	1.00	1.00
	250.00	275.00	1.10	275.68	303.93	1.10	1.00
SFR over-filled	250.00	375.00	1.50	275.68	418.20	1.52	0.99
	250.00	500.00	2.00	275.68	563.85	2.05	0.98
	250.00	1000.00	4.00	275.68	1177.70	4.27	0.94
	250.00	1500.00	6.00	275.68	1841.55	6.68	0.90

	Small fault deep measurements (Shallowest measurement 2500 ms)						
	Time			Depth			SFR's Similarity
	Fault throw (ms)	Syn-rift Thickness (ms)	SFR time	Fault throw (m)	Syn-rift Thickness (m)	SFR depth	(T/D)
SFR Under-filled	250.00	100.00	0.40	375.68	148.77	0.40	1.01
	250.00	125.00	0.50	375.68	186.28	0.50	1.01
	250.00	150.00	0.60	375.68	223.91	0.60	1.01
	250.00	175.00	0.70	375.68	261.66	0.70	1.01
	250.00	200.00	0.80	375.68	299.54	0.80	1.00
SFR balance d-filled	250.00	225.00	0.90	375.68	337.55	0.90	1.00
	250.00	250.00	1.00	375.68	375.68	1.00	1.00
	250.00	275.00	1.10	375.68	413.93	1.10	1.00
SFR over-filled	250.00	375.00	1.50	375.68	568.20	1.51	0.99
	250.00	500.00	2.00	375.68	763.85	2.03	0.98
	250.00	1000.00	4.00	375.68	1577.70	4.20	0.95
	250.00	1500.00	6.00	375.68	2441.55	6.50	0.92

	Large fault shallow measurements (Shallowest measurement 500 ms)						
	Time			Depth			SFR's Similarity
	Fault throw (ms)	Syn-rift Thickness (ms)	SFR time	Fault throw (m)	Syn-rift Thickness	SFR depth	(T/D)
SFR Under-filled	3000.00	1200.00	0.40	4133.10	1437.24	0.35	1.15
	3000.00	1500.00	0.50	4133.10	1841.55	0.45	1.12
	3000.00	1800.00	0.60	4133.10	2263.86	0.55	1.10
	3000.00	2100.00	0.70	4133.10	2704.17	0.65	1.07
	3000.00	2400.00	0.80	4133.10	3162.48	0.77	1.05
SFR balance d-filled	3000.00	2700.00	0.90	4133.10	3638.79	0.88	1.02
	3000.00	3000.00	1.00	4133.10	4133.10	1.00	1.00
	3000.00	3300.00	1.10	4133.10	4645.41	1.12	0.98
SFR over-filled	3000.00	4500.00	1.50	4133.10	6874.65	1.66	0.90
	3000.00	6000.00	2.00	4133.10	10066.20	2.44	0.82
	3000.00	12000.00	4.00	4133.10	27332.40	6.61	0.60
	3000.00	18000.00	6.00	4133.10	51798.60	12.53	0.48

	Large fault deep measurements (Shallowest measurement 2500 ms)						
	Time			Depth			SFR's Similarity
	Fault throw (ms)	Syn-rift Thickness (ms)	SFR time	Fault throw (m)	Syn-rift Thickness (m)	SFR depth	(T/D)
SFR Under-filled	3000.00	1200.00	0.40	5333.10	1917.24	0.36	1.11
	3000.00	1500.00	0.50	5333.10	2441.55	0.46	1.09
	3000.00	1800.00	0.60	5333.10	2983.86	0.56	1.07
	3000.00	2100.00	0.70	5333.10	3544.17	0.66	1.05
	3000.00	2400.00	0.80	5333.10	4122.48	0.77	1.03
SFR balance d-filled	3000.00	2700.00	0.90	5333.10	4718.79	0.88	1.02
	3000.00	3000.00	1.00	5333.10	5333.10	1.00	1.00
	3000.00	3300.00	1.10	5333.10	5965.41	1.12	0.98
SFR over-filled	3000.00	4500.00	1.50	5333.10	8674.65	1.63	0.92
	3000.00	6000.00	2.00	5333.10	12466.20	2.34	0.86
	3000.00	12000.00	4.00	5333.10	32132.40	6.03	0.66
	3000.00	18000.00	6.00	5333.10	58998.60	11.06	0.54

Supplementary Material 2:

Modelling of the volume created by rift fault of different throw magnitude. We used Schlische *et al*. (1996) to calculate the relation between faults throw and fault length such as $T=0.03L^{1.06}$. An increase of one order of magnitude fault throw increases the accommodation by ~2.9 order of magnitude (2A). In addition, for a similar total fault throw but different fault magnitude, the smaller the fault is, the less accommodation is formed. Therefore, for different fault throw, the amount of small fault required to generate as much accommodation as for a large fault is by far higher than the number of fault required to produce the same amount of vertical displacement (2B-2C-2D-2E). This is independent on the geometric model used to model the geometry of a half graben (2C-2D-2E)

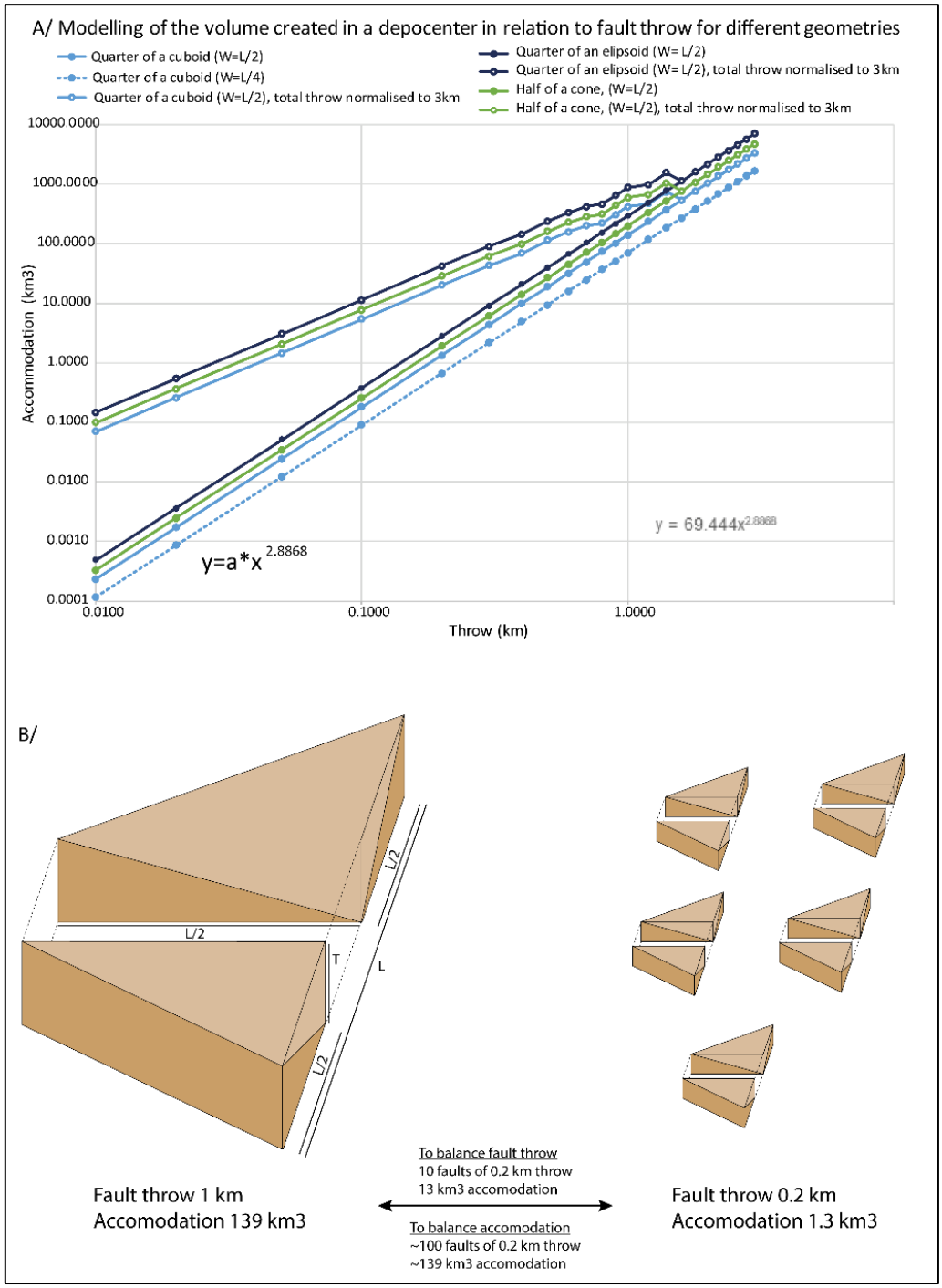

C/ Quarter of a cuboid shape

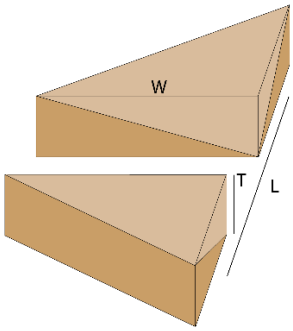

Fault throw (km)	Length (km)	A Width=L/2 (km)	B Width=L/4 (km)	A Accom Space (km3)	B Accom Space (km3)	Nb faults ~3 km throw	A Accom Space for 3 km throw	B Accom Space for 3 km throw	A Ratio 3km throw	B Ratio 3km throw
0.0100	0.4326	0.2163	0.1081	0.0002	0.0001	300	0.0702	0.0351	47186	47186
0.0200	0.8319	0.4160	0.2080	0.0017	0.0009	150	0.2595	0.1298	12759	12759
0.0500	1.9747	0.9873	0.4937	0.0244	0.0122	60	1.4622	0.7311	2265	2265
0.1000	3.7974	1.8987	0.9493	0.1802	0.0901	30	5.4075	2.7037	612	612
0.2000	7.3025	3.6513	1.8256	1.3332	0.6666	15	19.9976	9.9988	166	166
0.3000	10.7053	5.3526	2.6763	4.2976	2.1488	10	42.9759	21.4880	77	77
0.4000	14.0431	7.0216	3.5108	9.8605	4.9302	7	69.0232	34.5116	48	48
0.5000	17.3336	8.6668	4.3334	18.7783	9.3892	6	112.6698	56.3349	29	29
0.6000	20.5867	10.2934	5.1467	31.7860	15.8930	5	158.9301	79.4651	21	21
0.7000	23.8092	11.9046	5.9523	49.6018	24.8009	4	198.4073	99.2037	17	17
0.8000	27.0056	13.5028	6.7514	72.9304	36.4652	3	218.7911	109.3956	15	15
0.9000	30.1794	15.0897	7.5449	102.4649	51.2325	3	307.3947	153.6974	11	11
1.0000	33.3333	16.6667	8.3333	138.8889	69.4444	3	416.6667	208.3333	8	8
1.2000	39.5893	19.7947	9.8973	235.0971	117.5486	2	470.1943	235.0971	7	7
1.4000	45.7863	22.8931	11.4466	366.8671	183.4336	2	733.7343	366.8671	5	5
1.6000	51.9332	25.9666	12.9833	539.4107	269.7053	1	539.4107	269.7053	6	6
1.8000	58.0366	29.0183	14.5091	757.8552	378.9276	1	757.8552	378.9276	4	4
2.0000	64.1017	32.0508	16.0254	1027.2558	513.6279	1	1027.2558	513.6279	3	3
2.2000	70.1324	35.0662	17.5331	1352.6041	676.3021	1	1352.6041	676.3021	2	2
2.4000	76.1322	38.0661	19.0331	1738.8353	869.4176	1	1738.8353	869.4176	2	2
2.6000	82.1038	41.0519	20.5259	2190.8338	1095.4169	1	2190.8338	1095.4169	2	2
2.8000	88.0493	44.0247	22.0123	2713.4382	1356.7191	1	2713.4382	1356.7191	1	1
3.0000	93.9708	46.9854	23.4927	3311.4450	1655.7225	1	3311.4450	1655.7225	1	1

D/ Half of a cone

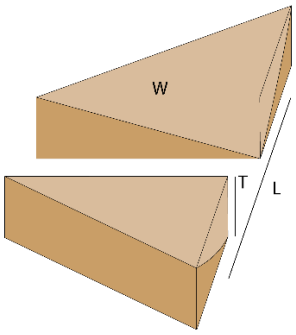

Fault throw (km)	Length (km)	A Width=L/2 (km)	B Width=L/4 (km)	A Accom Space (km3)	B Accom Space (km3)	Nb faults ~3 km throw	A Accom Space for 3 km throw	B Accom Space for 3 km throw	A Ratio 3km throw	B Ratio 3km throw
0.0100	0.4326	0.2163	0.1081	0.0005	0.0002	300	0.1470	0.0735	47186	47186
0.0200	0.8319	0.4160	0.2080	0.0036	0.0018	150	0.5438	0.2719	12759	12759
0.0500	1.9747	0.9873	0.4937	0.0511	0.0255	60	3.0637	1.5319	2265	2265
0.1000	3.7974	1.8987	0.9493	0.3777	0.1888	30	11.3300	5.6650	612	612
0.2000	7.3025	3.6513	1.8256	2.7933	1.3967	15	41.8997	20.9498	166	166
0.3000	10.7053	5.3526	2.6763	9.0045	4.5022	10	90.0448	45.0224	77	77
0.4000	14.0431	7.0216	3.5108	20.6600	10.3300	7	144.6201	72.3101	48	48
0.5000	17.3336	8.6668	4.3334	39.3450	19.6725	6	236.0701	118.0351	29	29
0.6000	20.5867	10.2934	5.1467	66.5993	33.2996	5	332.9964	166.4982	21	21
0.7000	23.8092	11.9046	5.9523	103.9276	51.9638	4	415.7106	207.8553	17	17
0.8000	27.0056	13.5028	6.7514	152.8065	76.4032	3	458.4195	229.2097	15	15
0.9000	30.1794	15.0897	7.5449	214.6884	107.3442	3	644.0651	322.0325	11	11
1.0000	33.3333	16.6667	8.3333	291.0053	145.5026	3	873.0159	436.5079	8	8
1.2000	39.5893	19.7947	9.8973	492.5845	246.2922	2	985.1689	492.5845	7	7
1.4000	45.7863	22.8931	11.4466	768.6740	384.3370	2	1537.3480	768.6740	5	5
1.6000	51.9332	25.9666	12.9833	1130.1938	565.0969	1	1130.1938	565.0969	6	6
1.8000	58.0366	29.0183	14.5091	1587.8871	793.9436	1	1587.8871	793.9436	4	4
2.0000	64.1017	32.0508	16.0254	2152.3456	1076.1728	1	2152.3456	1076.1728	3	3
2.2000	70.1324	35.0662	17.5331	2834.0277	1417.0139	1	2834.0277	1417.0139	2	2
2.4000	76.1322	38.0661	19.0331	3643.2739	1821.6370	1	3643.2739	1821.6370	2	2
2.6000	82.1038	41.0519	20.5259	4590.3184	2295.1592	1	4590.3184	2295.1592	2	2
2.8000	88.0493	44.0247	22.0123	5685.2991	2842.6495	1	5685.2991	2842.6495	1	1
3.0000	93.9708	46.9854	23.4927	6938.2656	3469.1328	1	6938.2656	3469.1328	1	1

E/ Quarter of an elispoid

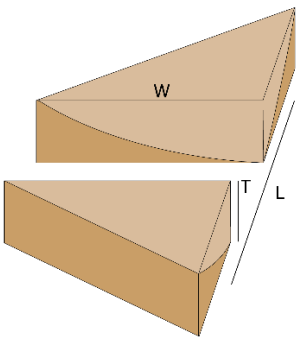

Fault throw (km)	Length (km)	A Width=L/2 (km)	B Width=L/4 (km)	A Accom Space (km3)	B Accom Space (km3)	Nb faults ~3 km throw	A Accom Space for 3 km throw	B Accom Space for 3 km throw	A Ratio 3km throw	B Ratio 3km throw
0.0100	0.4326	0.2163	0.1081	0.0003	0.0002	300	0.0997	0.0498	47186	47186
0.0200	0.8319	0.4160	0.2080	0.0025	0.0012	150	0.3686	0.1843	12759	12759
0.0500	1.9747	0.9873	0.4937	0.0346	0.0173	60	2.0767	1.0383	2265	2265
0.1000	3.7974	1.8987	0.9493	0.2560	0.1280	30	7.6797	3.8399	612	612
0.2000	7.3025	3.6513	1.8256	1.8934	0.9467	15	28.4006	14.2003	166	166
0.3000	10.7053	5.3526	2.6763	6.1034	3.0517	10	61.0344	30.5172	77	77
0.4000	14.0431	7.0216	3.5108	14.0038	7.0019	7	98.0268	49.0134	48	48
0.5000	17.3336	8.6668	4.3334	26.6689	13.3345	6	160.0137	80.0068	29	29
0.6000	20.5867	10.2934	5.1467	45.1425	22.5713	5	225.7126	112.8563	21	21
0.7000	23.8092	11.9046	5.9523	70.4445	35.2223	4	281.7781	140.8890	17	17
0.8000	27.0056	13.5028	6.7514	103.5757	51.7879	3	310.7271	155.3636	15	15
0.9000	30.1794	15.0897	7.5449	145.5207	72.7603	3	436.5620	218.2810	11	11
1.0000	33.3333	16.6667	8.3333	197.2500	98.6250	3	591.7500	295.8750	8	8
1.2000	39.5893	19.7947	9.8973	333.8849	166.9425	2	667.7699	333.8849	7	7
1.4000	45.7863	22.8931	11.4466	521.0247	260.5124	2	1042.0494	521.0247	5	5
1.6000	51.9332	25.9666	12.9833	766.0710	383.0355	1	766.0710	383.0355	6	6
1.8000	58.0366	29.0183	14.5091	1076.3060	538.1530	1	1076.3060	538.1530	4	4
2.0000	64.1017	32.0508	16.0254	1458.9088	729.4544	1	1458.9088	729.4544	3	3
2.2000	70.1324	35.0662	17.5331	1920.9684	960.4842	1	1920.9684	960.4842	2	2
2.4000	76.1322	38.0661	19.0331	2469.4939	1234.7469	1	2469.4939	1234.7469	2	2
2.6000	82.1038	41.0519	20.5259	3111.4222	1555.7111	1	3111.4222	1555.7111	2	2
2.8000	88.0493	44.0247	22.0123	3853.6249	1926.8125	1	3853.6249	1926.8125	1	1
3.0000	93.9708	46.9854	23.4927	4702.9141	2351.4571	1	4702.9141	2351.4571	1	1

Supplementary Material 3: Examples of seismic profiles and cross sections from rift basins used in this study

(A) North Carnarvon Basin (Western Australia) (Pink, basement; Green, syn-rift and Yellow, post-rift)

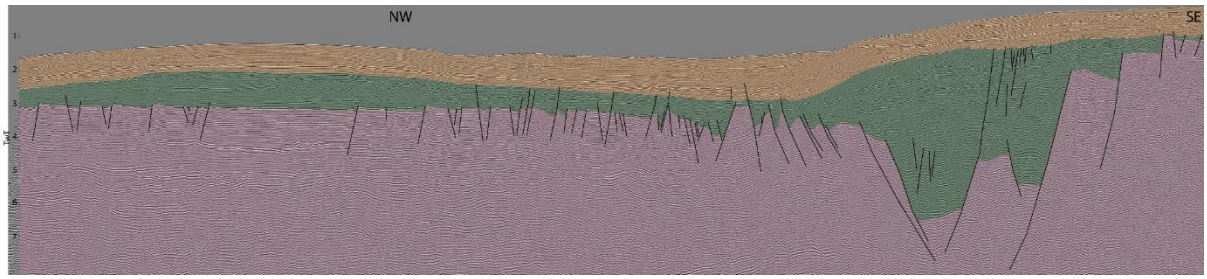

(B) Northern Taupo Rift (New Zealand, active rift system) (Mousopoulou et al., 2008)

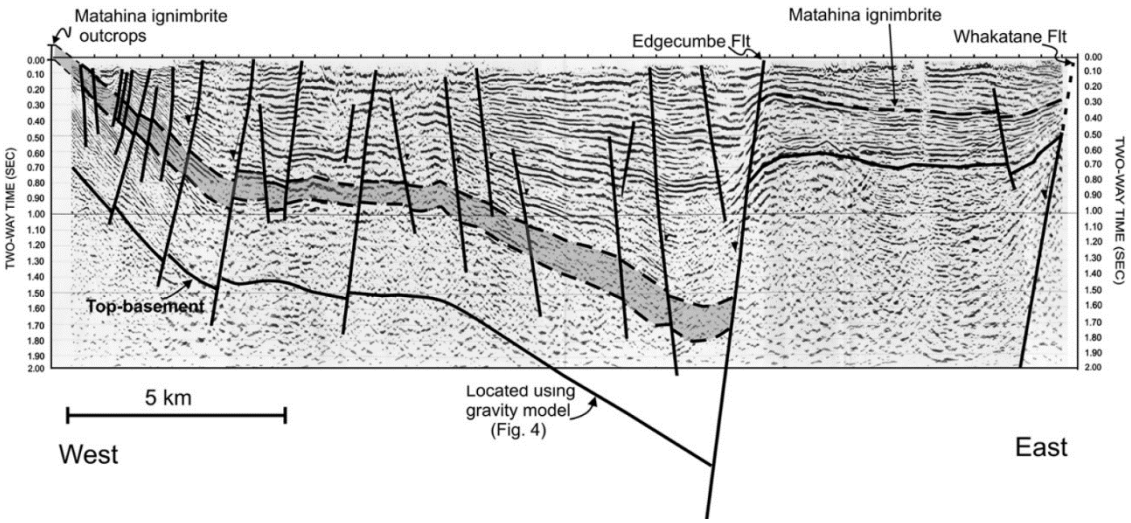

(C) Corinth Gulf Rift (Greece, active rift system) (Taylor et al., 2011)

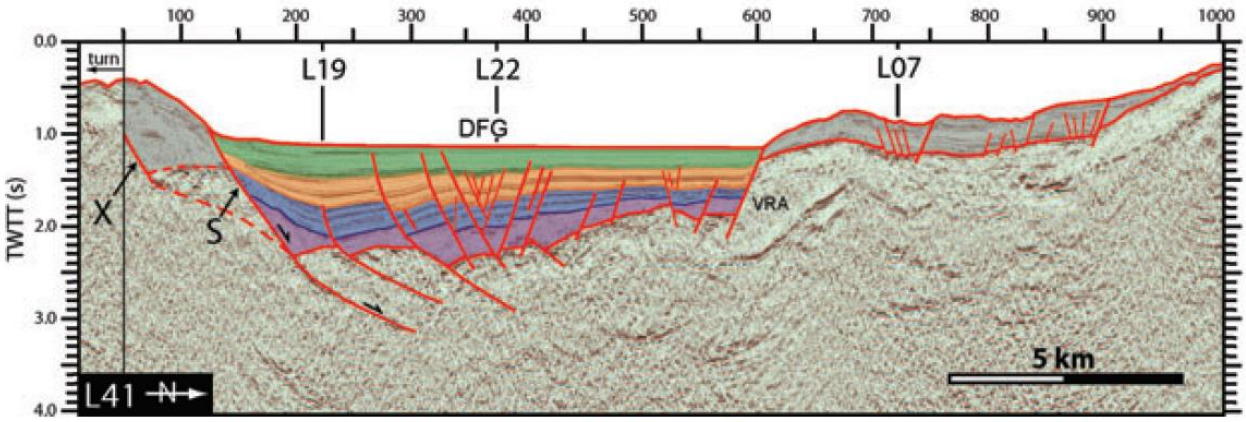

(D) Pannonian Basin (Central Europe) (Balazs et al., 2016)

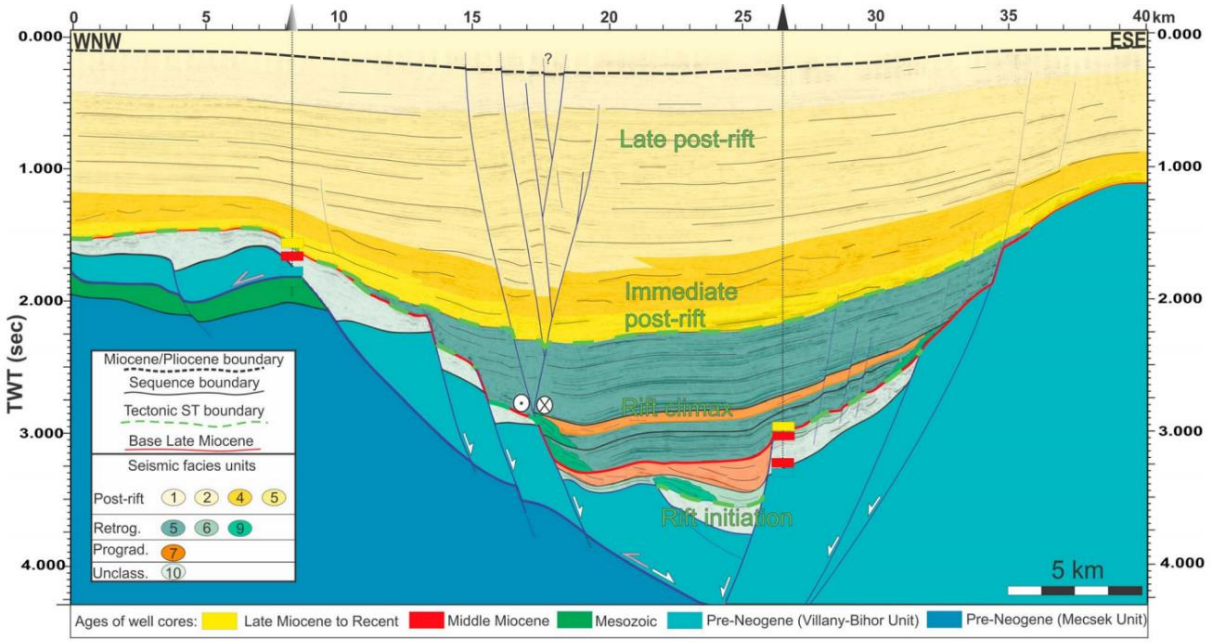

(E) Punta del Este and Pelotas basins (Offhsore Uruguay) (Morales et al., 2017)

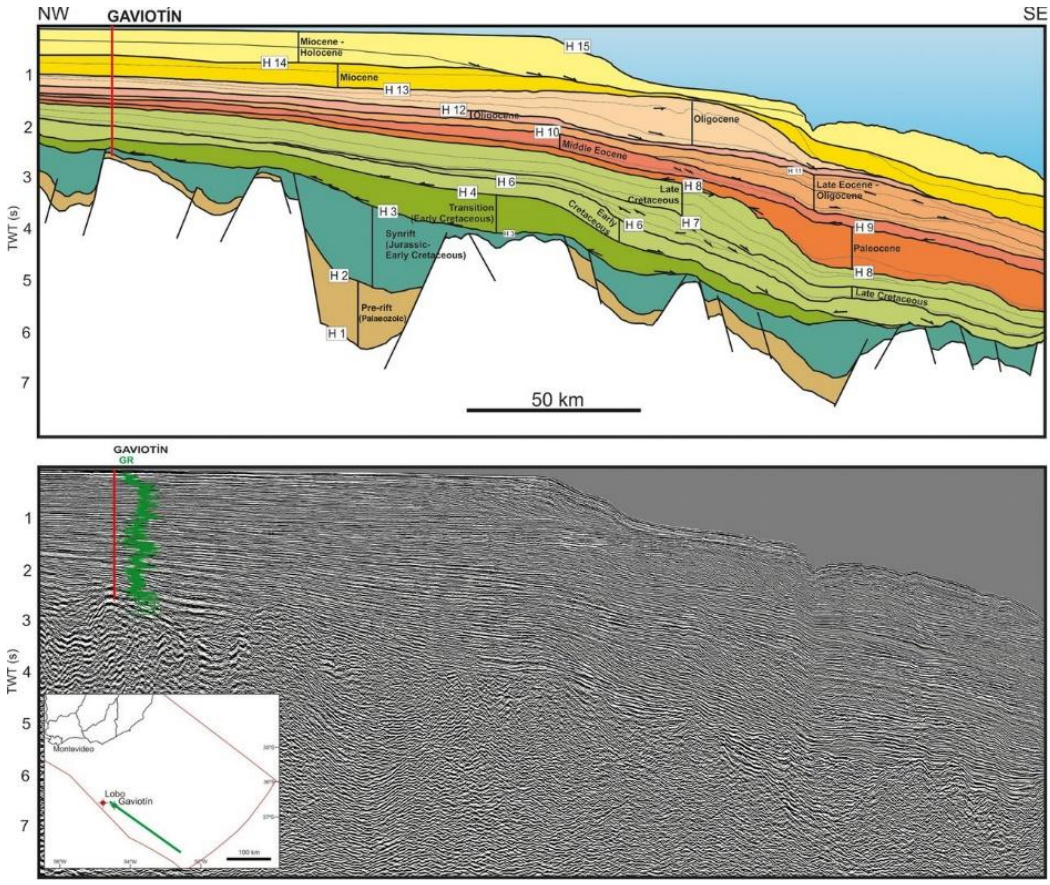

(F) Mergui Basin (Andaman Sea) (Morley et al., 2011) (Oligocene to lowermost Miocene represents the syn-rift interval)

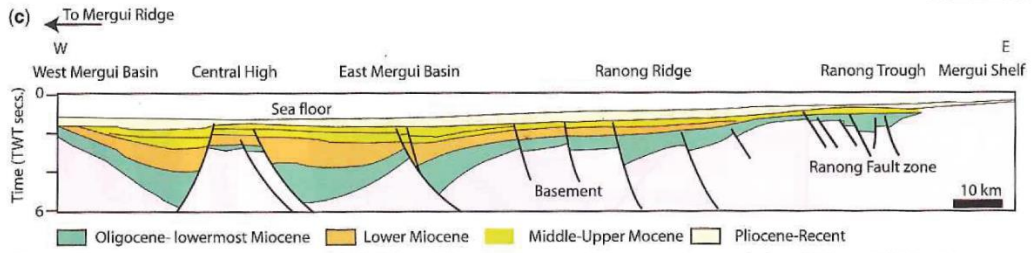

Fig. 10.32. Stratigraphy and cross-section through the Mergui Basin, Andaman Sea, based on data in Polachan & Racey (1994) and Andreason *et al.* (1997). (**a**) Oligocene–Recent stratigraphy of the Mergui Basin; (**b**) stratigraphy of the syn-rift section (Oligocene–early Miocene) schematically illustrating the east–west variation in stratigraphy across the basin and the effect of rift-basin highs (e.g. Central High horst block) on large-scale distribution of sedimentary facies, modified from Andreason *et al.* (1997); (**c**) east–west cross-section through the Mergui Basin illustrating the typical half-graben geometries of the basin (modified from Polachan & Racey 1994).

APPENDIX 4: Scientific communications

List of publications

Tulloch, A., Mortimer, N., Ireland, T., Waight, T., Maas, R., Palin, M., Sahoo, T., Seebeck, H., Sagar, M., Barrier, A., Turnbull, R., 2019. Reconnaissance basement geology and tectonics of South Zealandia. Tectonics (in press).

List of conferences and public talks

During the duration of the PhD project from November 2015 to December 2018, 13 conferences/workshops were attended and 4 public talks were given. Among the 11 conferences, 3 were international conferences where the PhD project was presented throughout 2 posters and 2 oral presentations. 5 petroleum industry related conferences and workshops were attended with 4 posters and 1 oral presentation.

Oral presentations:

- (1) Mid-Oligocene paleogeography of the Canterbury Basin: insights from onshore and offshore data**. GSNZ annual geology conference**, December 2016 (Wanaka, New Zealand).
- (2) Pre-rift reflectors within North Offshore Canterbury Basin, the western edge of the Chatham Rise. **Workshop at GNS**, August 2017 (Lower Hutt, New Zealand).
- (3) Late Mesozoic to Neogene geological history of the Canterbury Basin, new insights from offshore industry seismic reflection data. **Seminar at the geology department of the University of Otago**, September 2017 (Dunedin, New Zealand).
- (4) Impact of faulting on the late Mesozoic and younger sedimentary fill of the Canterbury Basin. **IMS and ASF conference**, October 2017 (Toulouse, France).
- (5) Late Cretaceous rifting of the Canterbury Basin during Zealandia intra-continental extension. **GSNZ annual geology conference**, November 2017 (Auckland, New Zealand).
- (6) Buried volcanoes in sedimentary basins, a tour of Zealandia. **University of Canterbury Workshop**, March 2018 (Christchurch, New Zealand).
- (7) Basin analysis, a multidisciplinary approach: The geological evolution of the Canterbury Basin. **Class talk, geology 300 level courses**, University of Canterbury, April 2018 (Christchurch, New Zealand).
- (8) Eastern Gondwana Late Cretaceous breakup: insights from the structure and kinematics of the Canterbury Rifting. **Geology Department Seminar, University of Canterbury**, June 2018 (Christchurch, New Zealand).
- (9) Eastern Gondwana Late Cretaceous breakup: insights from the structure and kinematics of the Canterbury Rifting. **3rd New Zealand Petroleum Geoscience Workshop,** September 2018 (GNS Science, Lower Hutt, New Zealand).
- (10) An under filled rift basin: source, reservoir, and seal distribution within the Canterbury Basin, New Zealand. **ICE petroleum conference**, November 2018 (Cape Town, South Africa).

- (11) The sedimentary fill of an under filled syn-rift basin: The example of the Late Cretaceous Canterbury Basin, New Zealand. **Talk at CSIRO**, November 2018 (Perth, Australia).
- (12) Late Cretaceous-Eocene under filling of the Canterbury Basin: What does it tell us about eastern Gondwana Landmass Evolution? **GSNZ Conference annual geology conference**, November 2018 (Napier, New Zealand).

Poster presentations:

- (1) Magmatic occurrences in the Canterbury Basin. **AAPG Asia Pacific Region GTW**, influence of Volcanism and Associated Magmatic Processes on Petroleum System, March 2017 (Oamaru, New Zealand). **[Poster-Award]**
- (2) Late Mesozoic and Early Cenozoic tectonics of the Canterbury Basin. **PEPANZ New Zealand annual petroleum conference**, March 2017 (New Plymouth, New Zealand).
- (3) Impact of volcanism on carbonate sedimentation in the Canterbury Basin, using onshore volcanic structures as analogues for buried volcanoes offshore New Zealand. **IMS and ASF conference**, October 2017 (Toulouse, France).
- (4) Impact of late Mesozoic and younger tectonic on half-graben filling and petroleum potential of the Canterbury Basin. **ICE petroleum conference**, October 2017 (London, England).
- (5) Pre-rift reflectors in the Canterbury Basin, impact petroleum system potential**. PEPANZ New Zealand annual petroleum conference**, March 2018 (Wellington, New Zealand).